Looking Beyond Genetic Alterations in Metastatic Uveal Melanoma

Kyra Noëlle Smit

The work presented in this thesis was conducted at the Department of Clinical Genetics and Ophthalmology, Erasmus MC, Rotterdam, The Netherlands and was financially supported by Combined Ophthalmic Research Rotterdam, Prof. Dr. Henkes stichting, Nelly Reef Fonds, Stichting Erasmus Trustfonds and Donders Fonds

Financial support for the printing of this thesis was kindly provided by Landelijke Stichting voor Blinden en Slechtzienden, Rotterdamse Blindenbelangen and Stichting Blindenhulp.

ISBN: 978-94-6402-181-3
Author: Kyra N Smit
Cover: Ricky Dul
Layout: Kyra N Smit
Printed by: Gildeprint

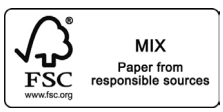

Looking Beyond Genetic Alterations in Metastatic Uveal Melanoma

Epigenetische en transcriptionele modificaties in gemetastaseerde oogmelanomen

Proefschrift
Ter verkrijging van de graad van doctor aan de

Erasmus Universiteit Rotterdam
Op gezag van de Rector Magnificus

Prof.dr. F.A. van der Duijn Schouten

en volgens besluit van het College voor Promoties.
De openbare verdediging zal plaatsvinden op

dinsdag 20 april 2021 om 15.30 uur

door

Kyra Noëlle Smit

geboren op 8 mei 1990 te Capelle aan den IJssel

Erasmus University Rotterdam

Promoter
Dr. J.E.M.M. de Klein

Overige leden
Prof.dr. R.M.W. Hofstra
Prof.dr. J.W.M. Martens
Dr. J.F. Kiilgaard

Copromoteren
Dr. E. Kiliç
Dr. H.W. Mensink

Voor mijn ouders

Table of contents

Chapter 1. Introduction
1.1 General introduction 11
1.2 Outline and scope of this thesis 23

Chapter 2. Risk stratification in UM patients
2.1 Combined mutation and CNV detection 33
2.2 Correlation gene mutation status with CNV profile 49

Chapter 3. Epigenetic and transcriptional regulation in metastatic UM
3.1 Aberrant microRNA expression 57
3.2 Hypermethylated tumor suppressor genes in UM 77

Chapter 4. Potential biomarkers and therapeutics
4.1 Exosomes as a non-invasive biomarker 101
4.2 Uveal melanoma: towards a molecular understanding 117

Chapter 5. Discussion and summary
5.1 General discussion 147
5.2 Summary 159
5.3 Samenvatting 165

Chapter 6. Epilogue
6.1 List of abbreviations 173
6.2 About the author 179
6.3 PhD portfolio 183
6.4 List of publications 189
6.5 Acknowledgements 193

Chapter 1
Introduction

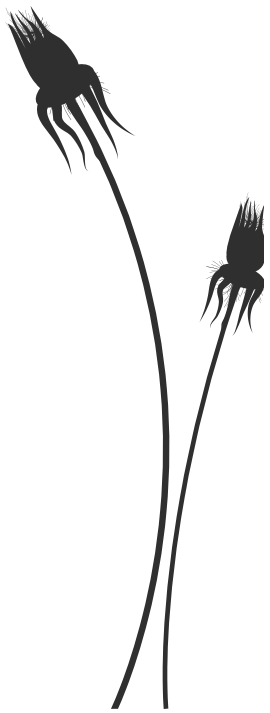

Chapter 1.1
General introduction

Cancer

Almost one third of all annual deaths in the Netherlands is caused by cancer[1]. Carcinogenesis is a process in which several subsequential alterations in a cell drive the progression of normal human cells into cancer cells. Cancer cells break the most basic rules of cell behavior. Whereas normal cells carefully control cell growth to maintain normal tissue architecture and function, cancer cells become masters of their own destiny and proliferate continuously[2]. This abnormal growth will give rise to a neoplasm; the tumor. Tumors usually acquire (epi)genetic alterations, which can increase the ability of cancer cells to invade and colonize distant environments that are normally reserved for other cells[3-5]. Once cancer cells show these characteristics, they are considered to be malignant. Secondary tumors at other sites in the body, called metastases, are hard to eradicate and generally kill the patient.

Uveal melanoma

Uveal melanoma (UM) is a malignant neoplasm arising from melanocytes in the eye. During embryogenesis, neural crest cells migrate not only to the skin to develop into pigment-producing melanocytes, but also to the uveal tract of the eye. The uveal tract is a pigmented tissue located between the outer layer of the eye (cornea and sclera) and the inner layer (retina). It has several functions, such as improving the contrast of the retinal image by absorbing excessive light and allowing nutrition and gas exchange via the blood vessel[6]. Since the sclera and lens lack any intrinsic blood supply, the uveal tract also indirectly supplies diffusible nutrients to these structures. UM can arise in every part of the uveal tract, but the choroid is the most common location (72%), followed by the ciliary body (23%) and iris (5%) (Figure 1). The iris is a thin circular structure that controls the amount of light entering the eye by controlling the size of the pupil. Whereas the ciliary body holds and controls the shape of the lens, in order to focus light on the retina.

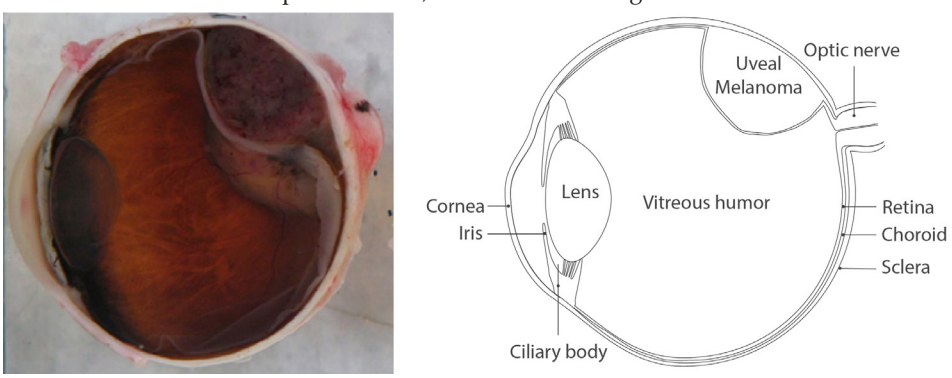

Figure 1. Cross section of an eye containing an UM (left) and a schematic representation of the different ocular structures (right).

Approximately 80% of the primary ocular tumors in adults are UM. The incidence of UM has remained stable over the last years and ranges from 4.3 to 10.9 per million in the Western World, with the highest incidence in Scandinavia[7, 8]. The diagnosis of UM is based on the clinical appearance of the tumor. Techniques such as fundoscopy, optical coherence tomography and ultrasonography can detect the unusual mass inside the eye. Whenever tumor tissue is available, the diagnosis can be confirmed by histopathological examination as well.

Primary UM can be successfully treated by surgery or radiotherapy. The type of treatment depends on multiple factors, such as tumor size and tumor location. In case of a large tu-

mor or a tumor located closely to the optic nerve, total removal of the eye - enucleation- is preferred. Smaller tumors can be successfully treated by irradiation, which induces lethal chromosomal injury and damage to blood vessels in the tumor. Despite successful treatment of the primary tumor, approximately 50% of the UM patients will die due to metastatic disease, often within 2 years after enucleation[8]. Interestingly, the metastatic risk is the same for all treatment options[9, 10]. Since metastasis can still occur years after complete removal of the eye, it is hypothesized that micrometastases are already present at time of diagnosis, but can remain dormant for many years[11, 12]. Several clinical features have been shown to associate with increased metastatic risk, such as large tumor size and high age. Additionally, histopathological features can predict metastatic risk. Hematoxylin and eosin (H&E) staining can be used to differentiate between spindle and epithelioid cell type, with the latter being more frequent in high metastatic risk UM (Figure 2)[13, 14]. Other histopathological features, such as mitotic activity, presence of necrosis, extraocular extension and inflammation also show an association with metastatic risk[15-17].

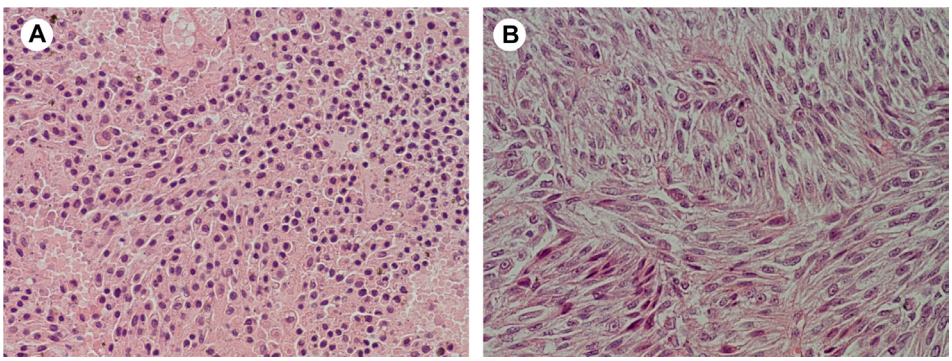

Figure 2. HE staining of UM cells shows **A)** epitheloid cells with larger nuclei and **B)** spindle cells with elongated nuclei (200x).

At this moment there are no standardized treatments for metastatic UM. In case of a local, single metastatic lesion, partial liver resection can extend the lifespan of a metastatic UM patient[18]. Whereas multiple local metastatic lesions can be treated by isolated hepatic perfusion (IHP). With IHP the liver is isolated from the systemic circulation, thereby allowing a much higher concentration of chemotherapeutic agent to be used. In case of multiple, diffuse metastatic lesions experimental therapies are offered to the patient. Unfortunately, all of these treatments can only postpone death by several months; no curative treatment options are present at this time for metastatic UM[19, 20].

Genetics

The human body consists of approximately 100 trillion cells that, even though they are very different from each other, contain exactly the same genetic information. This genetic information is stored as deoxyribonucleic acid (DNA) and packaged into 23 chromosome-pairs in the nucleus of the cell. DNA consists of a double-stranded structure formed by bases attached to a deoxyribose sugar-phosphate backbone[21, 22]. The genetic information is stored as a code made up of four bases; adenine, thymine, guanine and cytosine. Human genes consist of a unique sequence of bases and can code for a specific protein. Each gene has two copies in each cell, positioned on paired chromosomes (except for the genes located on the X and Y-chromosome). Once activated, a gene is first transcribed into messengerRNA (mRNA)[23]. This mRNA can then be translated into a string of amino acids which folds into a specific protein, the functional unit of a cell[24, 25].

The expression of genes is controlled at many levels. A gene can be turned on or off via binding of activating or inhibitory proteins. Gene expression can also be influenced by permanent alterations in the DNA sequence, called mutations. In cancer cells, the presence of specific mutations alter the expression of genes[2]. These mutations can be silent, missense or nonsense mutations. Silent mutations do not encode for a different amino acid and therefore do not change the protein. Missense mutations cause a change in amino acid, that produces a changed protein and non-sense mutations cause a premature stop-codon and thereby results in a truncated protein (Figure 3). Furthermore, larger regions of a gene can be altered by deletion of several nucleotides. Hence, DNA mutations can impact the cells' functioning by changing the amount of protein or the proteins' structure, which can enhance or impair the specific function carried out by the protein. In cancer cells, inactivating mutations are generally found in tumor suppressor genes; genes that protect a cell from becoming carcinogenic by regulating processes such as apoptosis, DNA repair or cell cycle. DNA mutations that activate the proteins function are frequently found in oncogenes, genes that are involved in cell growth, proliferation and inhibition of apoptosis[3].

Point mutations		
No mutation	THE FAT CAT ATE THE RAT	
Silent mutation	THE FAT KAT ATE THE RAT	Substitution
Missense mutation	THE FAT HAT ATE THE RAT	Substitution
Nonsense mutation	THE FAT MCA TAT ETH ERA T	Insertion
Nonsense mutation	THE FAT ATA TET HER AT	Deletion

Figure 3. The effect of silent, missense and nonsense mutations on the DNA sequence. Every three-letter word represents an amino acid. Silent mutations do not result in a different sentence/protein, missense mutations result in a different but correct sentence, whereas nonsense mutations result in a completely wrong sentence.

Genetics of UM

Of all cancer types UM has one of the lowest mutational burdens[26, 27]. Only few genes are known to be frequently mutated in UM. The first gene that was found to be mutated in UM, was the guanine nucleotide-binding protein α Q (*GNAQ*). It is hypothesized that melanocytes become pre-malignant by mutations in *GNAQ* or its paralogue guanine nucleotide-binding protein α 11 (*GNA11*)[28,29]. Mutations in these genes result in an overactivation of the Gα11/Q pathway, that stimulates cell growth and proliferation by initiating several downstream pathways in the cell. More than 95% of the UM harbor a mutually exclusive mutation in amino acid residues Q209 and R183 of *GNAQ* or *GNA11*, which suggests that these mutations are initiating mutations in the tumorigenesis of UM. UM that do not show mutated *GNAQ* or *GNA11*, usually have a mutation in the cysteinyl leukotriene receptor 2 (*CYSTLR2*) or phospholipase C beta 4 (*PCLB4*); two proteins that act respectively upstream and downstream of GNAQ and GNA11[30, 31]. Hence, mutations in these two genes cause activation of the same signaling pathways as mutations in *GNAQ* and *GNA11*. Mutations in these genes do not correlate with metastatic risk[32, 33]. The aggressiveness of UM is determined by secondary driver mutations in the *BAP1*, *SF3B1* and *EIF1AX* genes (Figure 4).

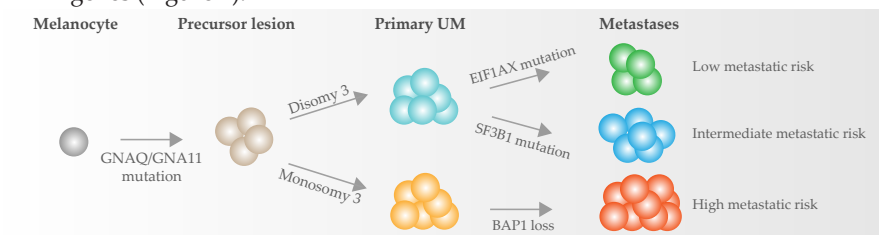

Figure 4. Genetic progression model for (metastatic) uveal melanoma.

The majority of the metastatic UM show loss of the BAP1 protein. Mutations in the *BAP1* gene, located on chromosome 3, can be found through the entire gene and can range from a single basepair mutation to large deletions involving several exons. Since loss of function mutations require the loss of both wildtype alleles, most *BAP1*-mutated UM also show loss of one chromosome 3 (monosomy 3). Loss of BAP1 protein can be detected by immunohistochemical staining (IHC) and is a strong indicator for risk of metastatic disease (Figure 5) [34-36]. BAP1 is a deubiquitinating enzyme (DUB), which are critical regulators of ubiquitin signaling. It has been shown that BAP1 interacts with many different proteins, such as the DNA repair protein BRCA1 and transcription-factors such as YY1[37, 38]. Unfortunately, it is not clear yet how exactly loss of BAP1 protein contributes to UM metastasis.

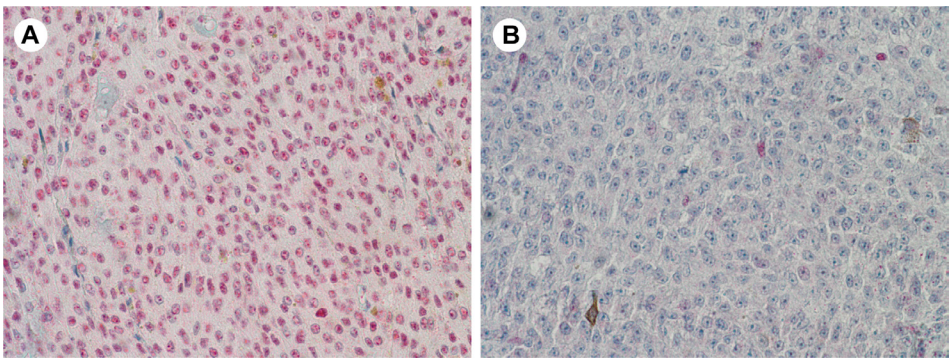

Figure 5. BAP1 IHC in UM shows A) positive nuclear BAP1 staining and B) negative BAP1 staining.

In a quarter of the UM a mutation in the gene *SF3B1* is observed[39-41]. *SF3B1* encodes for subunit 1 of the splicing factor 3b, a protein that is involved in pre-mRNA splicing. Genes are transcribed into pre-mRNA which still contains introns and subsequently the spliceosome-complex removes these introns in order to produce mature mRNA. Correct splicing of pre-mRNA is crucial for cell survival[42]. Dysregulated splicing can produce aberrantly spliced mRNA, resulting in a loss of protein-expression or they can be translated into unique, aberrant proteins[43]. Mutations in spliceosome genes have also been observed in other cancers, such as breast and hematologic cancers, suggesting that dysregulated splicing could be advantageous for cancer cells[44-46]. *SF3B1* is the most frequently mutated spliceosome gene in UM, but mutations in *U2AF1* and *SRSF2* have been described as well[47]. Most UM patients harboring an *SF3B1*-mutated UM will develop metastases eventually, however they do show a longer disease-free survival than patients with a monosomy 3, *BAP1*-mutated UM[48]. The disease-free survival can vary greatly between patients with an *SF3B1*-mutated UM, as some develop metastases within 5 years while others after 15 years.

Another frequently mutated gene in disomy 3 tumors is *EIF1AX* (eukaryotic translation initiation factor 1A, X-linked)[41]. EIF1AX is involved in translation, a process where the ribosome converts the mRNA into a protein[49]. When the ribosome is scanning the mRNA for the startcodon EIF1AX stabilizes the ribosome and thereby facilitates proper translation of the mRNA[50, 51]. *EIF1AX* mutations occur in ~20% of the UM and do not result in loss of the protein but rather a change of function. *EIF1AX*-mutated UM hardly metastasize. Indicating that mutations in the *EIF1AX* gene might make melanocytes more malignant, but it is not enough to initiate metastasis.

Chromosomal anomalies in UM

Besides mutations in the DNA, other alterations can also occur in cancer, such as variations in the copy number of chromosomes (CNV)[3]. During UM progression several non-

random chromosomal aberrations can occur on either the short (p) or long (q) arm of chromosomes 1, 3, 6 and 8 (Figure 6)[52]. As described previously, monosomy 3 is most significantly associated with metastatic disease[53]. It is observed in approximately 50% of the UM. Since monosomy 3 is often observed with other chromosomal aberrations, it is thought to be an early event in UM tumorigenesis[54]. Some tumors duplicate the remaining chromosome 3, thereby causing isodisomy of chromosome 3 which results in loss of heterozygosity (LOH)[55]. It is thought that the monosomy 3 not only reduces the expression of *BAP1*, but also that of other chromosome 3 genes. By duplicating chromosome 3, a cell can compensate for this reduced expression and thereby stimulate UM progression.

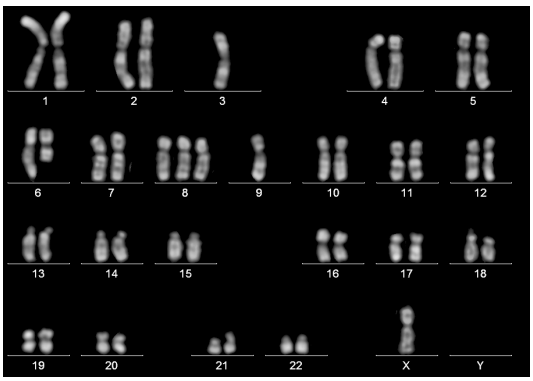

Figure 6. Karyotype of an UM showing several chromosomal anomalies, such as loss of chromosome 3, loss of chromosome 6q and gain of chromosome 8 (courtesy of the Department of Clinical Genetics, Erasmus MC).

Another chromosomal anomaly often found in metastatic UM is gain of chromosome 8 [56]. This gain can occur by either entire chromosome 8 gain, formation of isochromosome 8q of by partial amplification of 8q. The latter is mainly observed in disomy 3 UM, while isochromosome 8q is frequently found in monosomy 3 UM[57, 58]. Given the high prevalence of increased copies of 8q in metastatic UM, the chromosome 8q region probably contains genes that contribute to UM metastasis. Several oncogenes have been identified on chromosome 8q, such as *MYC*, *PVT1* and *DDEF*[27, 59]. However, the exact underlying genetic mechanism of 8q gain is yet to be elucidated.

UM can show rearrangements on both arms of chromosome 6. Gain of chromosome 6p have been observed, as well as deletion of chromosome 6q[57, 60]. However, both CNVs do not show an association with survival. Thirty percent of UM patients also show deletion of chromosome 1p, which is associated with high metastatic risk. Chromosome 1p loss is often observed together with monosomy 3, in which monosomy with loss of chromosome 1p has a worse prognosis than monosomy without chromosome 1p loss[61]. Abnormalities on other chromosomes in UM have been described, such as chromosome 9p and 16q, but do not occur frequently and show no correlation to metastatic risk. Around 17% of the UM show polyploidy, meaning that their genome contains more than the normal two copies of each chromosome. It is in general associated with worse prognosis; however in UM it has been shown that polyploidy does not significantly affect survival[62].

Epigenetics in UM

Gene expression can also be affected by alterations that do not affect the DNA sequence itself, these are called epigenetic modifications. Numerous epigenetic modifications exist, however the most studied one is DNA methylation. DNA methylation involves the transfer of a methyl-group (CH_3-group) to the C-5 position of the cytosine ring of DNA by the enzyme DNA-methyltransferase. Methylation of the DNA is dynamic and can occur at

any cytosine in the genome, however more than 98% of the DNA methylation occurs at cytosines in the CG-sequence. The human genome contains around 28 million of these CpG-dinucleotides and they often cluster in very CG-rich regions, which are called CpG islands [63]. Most, if not all, CpG islands are situated in regions that are involved in transcription initiation. How exactly DNA methylation helps to control gene expression is not fully understood. It is suggested that DNA methylation interferes directly with the binding of proteins necessary for transcription initiation. Additionally, several proteins are known to specifically bind methylated DNA and could thereby prevent transcription-proteins from binding the DNA. DNA methylation aids in the process of repressing unneeded eukaryotic genes to very high degree. The importance of DNA methylation is shown by the widespread involvement of errors in this mechanism in carcinogenesis[64-66]. Several studies indicate a large amount of changes in DNA methylation during tumor progression. Regarding UM, several studies show increased methylation in the promoters of *p16*, *PRAME*, *TIMP3* and *RASSF1*[67-70]. A change in methylation can contribute to UM development, progression and metastasis by downregulating genes that suppress these processes.

Another way to control the expression of a gene is by microRNA (miRNAs) expression. These small non-protein-coding RNA molecules are incorporated into a protein complex termed RNA-induced silencing complex (RISC). A miRNA-loaded RISC can control gene expression by binding to complementary mRNA[71, 72]. Depending on the degree of complementarity, miRNAs can silence genes by cleavage and degradation of the mRNA or by translational repression. Currently 1872 annotated precursor-miRNA genes have been identified that can produce ~2578 mature miRNAs. Over the past decade it has been shown that miRNA expression is heavily dysregulated in cancer cells[73]. A few pilot studies have investigated miRNA expression in UM and identified upregulation of several miRNAs in metastatic UM, such as miRNA-32, miRNA-146b, miRNA143, miRNA-34b/c and miRNA-137[74-78]. Which (oncogenic) pathways could be influenced by differential miRNA expression is often difficult to determine, since one miRNA can bind many different mRNAs. Interestingly, miRNAs are very stable in tissues and body fluids, indicating that they could serve as non-invasive metastatic-biomarkers.

A plethora of mechanisms contributes to altered gene function and malignant transformation of a cell (Figure 7). The majority of UM research has focused on identifying UM-specific copy number variations and mutations, since these alterations can result in an up or downregulation of a specific protein in a cell. But epigenetic alterations may be just as important in the development and metastasis of UM, or even more important. It has been shown that loss of gene expression occurs about 10 times more frequently by transcription silencing, than by mutations in the DNA[79]. Therefore, it could be beneficial to shift our focus more towards the epigenetic alterations that drive UM development and metastasis.

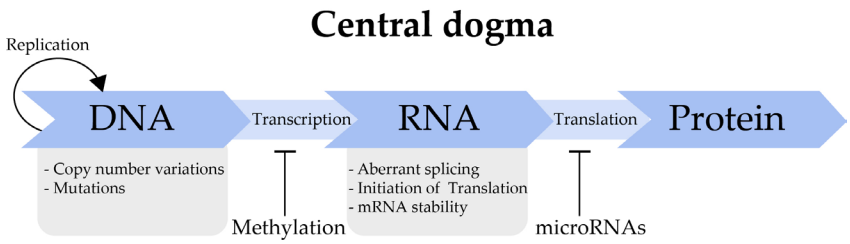

Figure 7. The central dogma describes the flow of genetic information within a cell. DNA is transcribed into RNA, which is then translated into the bioactive molecule: the protein. The protein level can be affected by many mechanisms, such as copy number variations, mutations, methylation of the DNA, aberrant splicing, initiation of translation, mRNA stability and microRNAs.

Non-invasive biomarkers

As previously described in this chapter, UM patients at risk for metastases can be identified by different methods with the mutation profile being the most reliable method. Most UM patients are treated by eye conserving therapies, such as radiotherapy or proton therapy, meaning that there is no tumor tissue available for prognostication unless an invasive biopsy is taken. Therefore many UM patients would profit from the development of a non-invasive biomarker that can predict metastatic risk. As mentioned before, detecting oncogenic miRNAs in the circulation of patients could be a promising non- invasive biomarker. Another non-invasive biomarker that is often used in cancer screening is cell-free DNA (cfDNA); small fragments of DNA that are released into the bloodstream by apoptotic and necrotic cells. Detecting mutated cfDNA or an increase in oncogenic miRNAs has been shown to be useful for diagnostic applications in several cancer types[80]. However, the studies investigating the presence of cfDNA and oncogenic miRs in the circulation of UM patients show variable results and are not conclusive. Since genetic material is released into the blood by all cells, it could be that UM are too small to secrete a detectable level of oncogenic miRs or mutant cfDNA into the blood.

A potentially more promising non-invasive biomarker for UM are extracellular vesicles (EVs). It has been shown that cancer patients show an increased level of EVs in their blood. EVs function in cell-to-cell communication by transporting bioactive molecules such as miRNA, mRNA, DNA and proteins. They allow cells to communicate with each other even if they are located far apart from each other[81]. Many cell types release EVs, which can be found in most body fluids, including blood, saliva, urine breast milk and plasma[82-84]. Vesicles derived from various tissues differ in their molecular composition. Depending on their cellular origin, EVs can be classified as apoptotic bodies (ABs), microvesicles (MVs) and exosomes. ABs are the biggest vesicles (1000-5000 nm) and are released by apoptotic cells. MVs have a size of 100-1000 nm and are shed from the plasma membrane. Exosomes are derived from multivesicular endosome and are the smallest vesicles (30-100 nm)[85]. They are the product of a process called endocytosis, in which invagination of the cells' plasma membrane and membrane fission results in the formation of vesicles into an early endosome. As the early endosome matures into a multivesicular endosome, intraluminal vesicles are formed inside the endosome. Multivesicular endosomes can fuse with lysosomes, thereby degrading the contents of the vesicles, or they can fuse with the plasma membrane which releases the vesicles into the extracellular environment (Figure 8)[86].

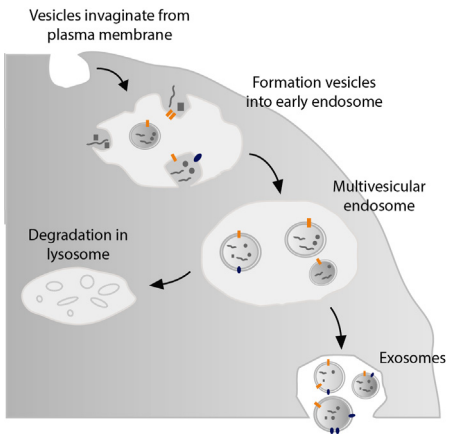

Figure 8. Biogenesis of exosomes starts with invagination of the plasma membrane, resulting in the formation of an early endosome. The early endosome matures into a multivesicular endosome containing vesicles. The multivesicular endosome can fuse with the lysosome, which results in degradation of the vescicles or it can fuse with the plasma membrane leading to the release of vesicles, called exosomes.

The last years exosome research has received substantial interest with the discovery that they contain mRNA and miRNAs[87]. Additionally, tumor cells secrete an increased amount of exosomes and these vesicles often exhibit unique cargo making them a promising prognostic marker [88]. The exact mechanism of how exosomes interact with recipient cells is unknown. However, it has been shown in numerous studies that exosomes are involved in many processes that contribute to tumorigenesis, including angiogenesis[89], drug resistance mechanisms [90], immune-suppression[91], epithelial to mesenchymal transition[92, 93] and educating the pre-metastatic niche[94-96]. This shows the importance of secreted exosomes in the development and metastatic progression of cancer besides their potential as a biomarker.

Chapter 1.2
Scope of this thesis

Scope of this thesis

This thesis aims to elucidate the (epi)genetic and transcriptional mechanisms contributing to metastatic spread of UM. The research performed is outlined in the following parts;

Chapter 2 describes the development of two methods that facilitate metastatic risk prediction in UM patients. As previously described in chapter 1, there are several factors that can predict metastatic risk in UM. If tissue is available, CNVs, expression profiles and mutations in DNA can be identified. The choice for these methods depends largely on the available material. In **chapter 2.1** we describe a method that we developed that allows simultaneous detection of UM-specific mutations and CNVs in small amounts of DNA. In **chapter 2.2** we discuss CNV patterns that are associated with specific secondary driver mutations in *EIF1AX*, *SF3B1* and *BAP1*.

With the development of next generation sequencing techniques, the genetic aberrancies driving UM progression have been described extensively. However, the changes on the epigenetic level have been discussed to lesser extent. Recent studies have shown that abnormal epigenetic silencing of genes is no less important than mutations in DNA sequences for the development of most cancers. The aim of **chapter 3** is to elucidate how epigenetic mechanisms contribute to UM metastasis. In **chapter 3.1** we compare the miRNA expression between low, intermediate and high metastatic risk UM by performing RNA sequencing. We investigate up and downregulation of several miRNAs in high metastatic risk UM and integrate the miRNA data with mRNA data in order to identify the downstream effects of aberrant miRNA expression. In **chapter 3.2** we describe methylation-patterns that show association with metastatic disease by making use of a new genome-wide methylation analysis technique.

Even though extensive research regarding UM metastasis has been done, up until now no effective treatment is available for metastatic UM. In **chapter 4** we describe how UM surveillance and therapy could be improved in the future. **Chapter 4.1** describes our first steps towards a possible new non-invasive biomarker; exosomes. We characterize exosomes secreted by cultured UM cells, analyze the genetic content and make suggestions about how these exosomes could be used in the future as liquid biomarker to predict metastatic risk. In **chapter 4.2** we review what is already known about the aberrant mechanisms behind UM development. In this review we discuss which mechanisms could be targeted in metastatic UM treatment and hypothesize about promising future treatment options.

Finally, in **chapter 5** the main findings are summarized and, where possible, overall conclusions are drawn. Additionally, challenges for the research field and future prospects are discussed.

References

1. CBS. Doodsoorzakenstatistiek. 2018.
2. Weinberg RA. The biology of Cancer. 2013(2nd Edition).
3. Hanahan D, Weinberg RA. The hallmarks of cancer. Cell. 2000;100(1):57-70.
4. Evan GI, Vousden KH. Proliferation, cell cycle and apoptosis in cancer. Nature. 2001;411(6835):342-8.
5. Loeb LA, Loeb KR, Anderson JP. Multiple mutations and cancer. Proc Natl Acad Sci U S A. 2003;100(3):776-81.
6. Hong L, Simon JD, Sarna T. Melanin structure and the potential functions of uveal mela nosomes. Pigment Cell Res. 2006;19(5):465-6.
7. Virgili G, Gatta G, Ciccolallo L, Capocaccia R, Biggeri A, Crocetti E, et al. Incidence of uveal melanoma in Europe. Ophthalmology. 2007;114(12):2309-15.
8. Singh AD, Turell ME, Topham AK. Uveal melanoma: trends in incidence, treatment, and survival. Ophthalmology. 2011;118(9):1881-5.
9. Damato B. Does ocular treatment of uveal melanoma influence survival? Br J Cancer. 2010;103(3):285-90.
10. Seddon JM, Gragoudas ES, Albert DM, Hsieh CC, Polivogianis L, Friedenberg GR. Comparison of survival rates for patients with uveal melanoma after treatment with proton beam irradiation or enucleation. Am J Ophthalmol. 1985;99(3):282-90.
11. Eskelin S, Pyrhonen S, Summanen P, Hahka-Kemppinen M, Kivela T. Tumor doubling times in metastatic malignant melanoma of the uvea: tumor progression before and after treatment. Ophthalmology. 2000;107(8):1443-9.
12. Zimmerman LE, McLean IW, Foster WD. Does enucleation of the eye containing a malignant melanoma prevent or accelerate the dissemination of tumour cells. Br J Oph thalmol. 1978;62(6):420-5.
13. Gill HS, Char DH. Uveal melanoma prognostication: from lesion size and cell type to molecular class. Can J Ophthalmol. 2012;47(3):246-53.
14. McLean IW, Foster WD, Zimmerman LE. Uveal melanoma: location, size, cell type, and enucleation as risk factors in metastasis. Hum Pathol. 1982;13(2):123-32.
15. Coupland SE, Campbell I, Damato B. Routes of extraocular extension of uveal melanoma: risk factors and influence on survival probability. Ophthalmology. 2008;115(10):1778-85.
16. Folberg R, Rummelt V, Parys-Van Ginderdeuren R, Hwang T, Woolson RF, Pe'er J, et al. The prognostic value of tumor blood vessel morphology in primary uveal melanoma. Ophthalmology. 1993;100(9):1389-98.
17. Mooy CM, Luyten GP, de Jong PT, Luider TM, Stijnen T, van de Ham F, et al. Immunohis tochemical and prognostic analysis of apoptosis and proliferation in uveal melanoma. Am J Pathol. 1995;147(4):1097-104.
18. Mariani P, Piperno-Neumann S, Servois V, Berry MG, Dorval T, Plancher C, et al. Surgical management of liver metastases from uveal melanoma: 16 years' experience at the Institut Curie. Eur J Surg Oncol. 2009;35(11):1192-7.
19. Augsburger JJ, Correa ZM, Shaikh AH. Effectiveness of treatments for metastatic uveal melanoma. Am J Ophthalmol. 2009;148(1):119-27.
20. Damato B, Eleuteri A, Taktak AF, Coupland SE. Estimating prognosis for survival after treatment of choroidal melanoma. Prog Retin Eye Res. 2011;30(5):285-95.
21. Alberts B, Johnson A, Lewis J, Raff M, Roberts K, Walter P. Molecular Biology of the Cell. Garland Science. 2008;5th edition.
22. Watson JD, Crick FH. Molecular structure of nucleic acids; a structure for deoxyribose nucleic acid. Nature. 1953;171(4356):737-8.
23. Brenner S, Jacob F, Meselson M. An unstable intermediate carrying information from genes to ribosomes for protein synthesis. Nature. 1961;190:576-81.
24. Alberts B. The cell as a collection of protein machines: preparing the next generation of molecular biologists. Cell. 1998;92(3):291-4.
25. Chakalova L, Debrand E, Mitchell JA, Osborne CS, Fraser P. Replication and transcrip tion: shaping the landscape of the genome. Nat Rev Genet. 2005;6(9):669-77.
26. Shain AH, Bagger MM, Yu R, Chang D, Liu S, Vemula S, et al. The genetic evolution of metastatic uveal melanoma. Nat Genet. 2019;51(7):1123-30.
27. Robertson AG, Shih J, Yau C, Gibb EA, Oba J, Mungall KL, et al. Integrative Analysis Identifies Four Molecular and Clinical Subsets in Uveal Melanoma. Cancer Cell. 2017;32(2):204-20 e15.

28. Van Raamsdonk CD, Griewank KG, Crosby MB, Garrido MC, Vemula S, Wiesner T, et al. Mutations in GNA11 in uveal melanoma. N Engl J Med. 2010;363(23):2191-9.
29. Van Raamsdonk CD, Bezrookove V, Green G, Bauer J, Gaugler L, O'Brien JM, et al. Fre quent somatic mutations of GNAQ in uveal melanoma and blue naevi. Nature. 2009;457(7229):599-602.
30. Johansson P, Aoude LG, Wadt K, Glasson WJ, Warrier SK, Hewitt AW, et al. Deep se quencing of uveal melanoma identifies a recurrent mutation in PLCB4. Oncotarget. 2016;7(4):4624-31.
31. Moore AR, Ceraudo E, Sher JJ, Guan Y, Shoushtari AN, Chang MT, et al. Recurrent activating mutations of G-protein-coupled receptor CYSLTR2 in uveal melanoma. Nat Genet. 2016;48(6):675-80.
32. Bauer J, Kilic E, Vaarwater J, Bastian BC, Garbe C, de Klein A. Oncogenic GNAQ muta tions are not correlated with disease-free survival in uveal melanoma. Br J Cancer. 2009;101(5):813-5.
33. Koopmans AE, Vaarwater J, Paridaens D, Naus NC, Kilic E, de Klein A, et al. Patient sur vival in uveal melanoma is not affected by oncogenic mutations in GNAQ and GNA11. Br J Cancer. 2013;109(2):493-6.
34. Farquhar N, Thornton S, Coupland SE, Coulson JM, Sacco JJ, Krishna Y, et al. Patterns of BAP1 protein expression provide insights into prognostic significance and the biology of uveal melanoma. J Pathol Clin Res. 2018;4(1):26-38.
35. Kalirai H, Dodson A, Faqir S, Damato BE, Coupland SE. Lack of BAP1 protein expression in uveal melanoma is associated with increased metastatic risk and has utility in routine prognostic testing. Br J Cancer. 2014;111(7):1373-80.
36. Koopmans AE, Verdijk RM, Brouwer RW, van den Bosch TP, van den Berg MM, Vaarwa ter J, et al. Clinical significance of immunohistochemistry for detection of BAP1 mutations in uveal melanoma. Mod Pathol. 2014;27(10):1321-30.
37. Nishikawa H, Wu W, Koike A, Kojima R, Gomi H, Fukuda M, et al. BRCA1-associated protein 1 interferes with BRCA1/BARD1 RING heterodimer activity. Cancer Res. 2009;69(1):111-9.
38. Yu H, Mashtalir N, Daou S, Hammond-Martel I, Ross J, Sui G, et al. The ubiquitin car boxyl hydrolase BAP1 forms a ternary complex with YY1 and HCF-1 and is a critical regulator of gene expression. Mol Cell Biol. 2010;30(21):5071-85.
39. Furney SJ, Pedersen M, Gentien D, Dumont AG, Rapinat A, Desjardins L, et al. SF3B1 mu tations are associated with alternative splicing in uveal melanoma. Cancer Discov. 2013;3(10):1122-9.
40. Harbour JW, Roberson ED, Anbunathan H, Onken MD, Worley LA, Bowcock AM. Recurrent mutations at codon 625 of the splicing factor SF3B1 in uveal melanoma. Nat Genet. 2013;45(2):133-5.
41. Martin M, Masshofer L, Temming P, Rahmann S, Metz C, Bornfeld N, et al. Exome sequencing identifies recurrent somatic mutations in EIF1AX and SF3B1 in uveal mela noma with disomy 3. Nat Genet. 2013;45(8):933-6.
42. Wahl MC, Will CL, Luhrmann R. The spliceosome: design principles of a dynamic RNP machine. Cell. 2009;136(4):701-18.
43. Darman RB, Seiler M, Agrawal AA, Lim KH, Peng S, Aird D, et al. Cancer-Associated SF3B1 Hotspot Mutations Induce Cryptic 3' Splice Site Selection through Use of a Differ ent Branch Point. Cell Rep. 2015;13(5):1033-45.
44. Read A, Natrajan R. Splicing dysregulation as a driver of breast cancer. Endocr Relat Cancer. 2018;25(9):R467-R78.
45. Seiler M, Peng S, Agrawal AA, Palacino J, Teng T, Zhu P, et al. Somatic Mutational Land scape of Splicing Factor Genes and Their Functional Consequences across 33 Cancer Types. Cell Rep. 2018;23(1):282-96 e4.
46. Wang L, Lawrence MS, Wan Y, Stojanov P, Sougnez C, Stevenson K, et al. SF3B1 and other novel cancer genes in chronic lymphocytic leukemia. N Engl J Med. 2011;365(26):2497-506.
47. van Poppelen NM, Drabarek W, Smit KN, Vaarwater J, Brands T, Paridaens D, et al. SRSF2 Mutations in Uveal Melanoma: A Preference for In-Frame Deletions? Cancers (Basel). 2019;11(8).
48. Yavuzyigitoglu S, Koopmans AE, Verdijk RM, Vaarwater J, Eussen B, van Bodegom A, et al. Uveal Melanomas with SF3B1 Mutations: A Distinct Subclass Associated with Late-Onset Metastases. Ophthalmology. 2016;123(5):1118-28.

49. Chaudhuri J, Si K, Maitra U. Function of eukaryotic translation initiation factor 1A (eIF1A) (formerly called eIF-4C) in initiation of protein synthesis. J Biol Chem. 1997;272(12):7883-91.
50. Kozak M. Regulation of translation in eukaryotic systems. Annu Rev Cell Biol. 1992;8:197-225.
51. Martin-Marcos P, Zhou F, Karunasiri C, Zhang F, Dong J, Nanda J, et al. eIF1A residues implicated in cancer stabilize translation preinitiation complexes and favor suboptimal initiation sites in yeast. Elife. 2017;6.
52. Prescher G, Bornfeld N, Becher R. Nonrandom chromosomal abnormalities in primary uveal melanoma. J Natl Cancer Inst. 1990;82(22):1765-9.
53. Ewens KG, Kanetsky PA, Richards-Yutz J, Purrazzella J, Shields CL, Ganguly T, et al. Chromosome 3 status combined with BAP1 and EIF1AX mutation profiles are associated with metastasis in uveal melanoma. Invest Ophthalmol Vis Sci. 2014;55(8):5160-7.
54. Prescher G, Bornfeld N, Hirche H, Horsthemke B, Jockel KH, Becher R. Prognostic impli cations of monosomy 3 in uveal melanoma. Lancet. 1996;347(9010):1222-5.
55. White VA, McNeil BK, Horsman DE. Acquired homozygosity (isodisomy) of chromosome 3 in uveal melanoma. Cancer Genet Cytogenet. 1998;102(1):40-5.
56. van den Bosch T, van Beek JG, Vaarwater J, Verdijk RM, Naus NC, Paridaens D, et al. Higher percentage of FISH-determined monosomy 3 and 8q amplification in uveal mela noma cells relate to poor patient prognosis. Invest Ophthalmol Vis Sci. 2012;53(6):2668-74.
57. Aalto Y, Eriksson L, Seregard S, Larsson O, Knuutila S. Concomitant loss of chromosome 3 and whole arm losses and gains of chromosome 1, 6, or 8 in metastasizing primary uveal melanoma. Invest Ophthalmol Vis Sci. 2001;42(2):313-7.
58. Horsman DE, Sroka H, Rootman J, White VA. Monosomy 3 and isochromosome 8q in a uveal melanoma. Cancer Genet Cytogenet. 1990;45(2):249-53.
59. Ehlers JP, Worley L, Onken MD, Harbour JW. DDEF1 is located in an amplified region of chromosome 8q and is overexpressed in uveal melanoma. Clin Cancer Res. 2005;11(10):3609-13.
60. Metzelaar-Blok JA, Jager MJ, Moghaddam PH, van der Slik AR, Giphart MJ. Frequent loss of heterozygosity on chromosome 6p in uveal melanoma. Hum Immunol. 1999;60(10):962-9.
61. Kilic E, Naus NC, van Gils W, Klaver CC, van Til ME, Verbiest MM, et al. Concurrent loss of chromosome arm 1p and chromosome 3 predicts a decreased disease-free survival in uveal melanoma patients. Invest Ophthalmol Vis Sci. 2005;46(7):2253-7.
62. Yavuzyigitoglu S, Mensink HW, Smit KN, Vaarwater J, Verdijk RM, Beverloo B, et al. Metastatic Disease in Polyploid Uveal Melanoma Patients Is Associated With BAP1 Muta tions. Invest Ophthalmol Vis Sci. 2016;57(4):2232-9.
63. Jin B, Li Y, Robertson KD. DNA methylation: superior or subordinate in the epigenetic hierarchy? Genes Cancer. 2011;2(6):607-17.
64. Esteller M, Corn PG, Baylin SB, Herman JG. A gene hypermethylation profile of human cancer. Cancer Res. 2001;61(8):3225-9.
65. Herman JG, Baylin SB. Gene silencing in cancer in association with promoter hypermeth ylation. N Engl J Med. 2003;349(21):2042-54.
66. Jones PA, Baylin SB. The fundamental role of epigenetic events in cancer. Nat Rev Genet. 2002;3(6):415-28.
67. Field MG, Durante MA, Decatur CL, Tarlan B, Oelschlager KM, Stone JF, et al. Epigenetic reprogramming and aberrant expression of PRAME are associated with increased meta static risk in Class 1 and Class 2 uveal melanomas. Oncotarget. 2016;7(37):59209-19.
68. Maat W, van der Velden PA, Out-Luiting C, Plug M, Dirks-Mulder A, Jager MJ, et al. Epi genetic inactivation of RASSF1a in uveal melanoma. Invest Ophthalmol Vis Sci. 2007;48(2):486-90.
69. Moulin AP, Clement G, Bosman FT, Zografos L, Benhattar J. Methylation of CpG island promoters in uveal melanoma. Br J Ophthalmol. 2008;92(2):281-5.
70. van der Velden PA, Zuidervaart W, Hurks MH, Pavey S, Ksander BR, Krijgsman E, et al. Expression profiling reveals that methylation of TIMP3 is involved in uveal melanoma development. Int J Cancer. 2003;106(4):472-9.
71. Bartel DP. MicroRNAs: target recognition and regulatory functions. Cell. 2009;136(2):215-33.
72. Brennecke J, Stark A, Russell RB, Cohen SM. Principles of microRNA-target recognition.

PLoS Biol. 2005;3(3):e85.
73. Esquela-Kerscher A, Slack FJ. Oncomirs - microRNAs with a role in cancer. Nat Rev Can cer. 2006;6(4):259-69.
74. Chen X, Wang J, Shen H, Lu J, Li C, Hu DN, et al. Epigenetics, microRNAs, and car cinogenesis: functional role of microRNA-137 in uveal melanoma. Invest Ophthalmol Vis Sci. 2011;52(3):1193-9.
75. Dong F, Lou D. MicroRNA-34b/c suppresses uveal melanoma cell proliferation and mi gration through multiple targets. Mol Vis. 2012;18:537-46.
76. Li Z, Yu X, Shen J, Jiang Y. MicroRNA dysregulation in uveal melanoma: a new player enters the game. Oncotarget. 2015;6(7):4562-8.
77. Ma YB, Song DW, Nie RH, Mu GY. MicroRNA-32 functions as a tumor suppressor and directly targets EZH2 in uveal melanoma. Genet Mol Res. 2016;15(2).
78. Worley LA, Long MD, Onken MD, Harbour JW. Micro-RNAs associated with metastasis in uveal melanoma identified by multiplexed microarray profiling. Melanoma Res. 2008;18(3):184-90.
79. Vogelstein B, Papadopoulos N, Velculescu VE, Zhou S, Diaz LA, Jr., Kinzler KW. Cancer genome landscapes. Science. 2013;339(6127):1546-58.
80. Schwarzenbach H, Hoon DS, Pantel K. Cell-free nucleic acids as biomarkers in cancer patients. Nat Rev Cancer. 2011;11(6):426-37.
81. Simons M, Raposo G. Exosomes--vesicular carriers for intercellular communication. Curr Opin Cell Biol. 2009;21(4):575-81.
82. Caby MP, Lankar D, Vincendeau-Scherrer C, Raposo G, Bonnerot C. Exosomal-like vesicles are present in human blood plasma. Int Immunol. 2005;17(7):879-87.
83. Lasser C, Alikhani VS, Ekstrom K, Eldh M, Paredes PT, Bossios A, et al. Human saliva, plasma and breast milk exosomes contain RNA: uptake by macrophages. J Transl Med. 2011;9:9.
84. Pisitkun T, Shen RF, Knepper MA. Identification and proteomic profiling of exosomes in human urine. Proc Natl Acad Sci U S A. 2004;101(36):13368-73.
85. Abels ER, Breakefield XO. Introduction to Extracellular Vesicles: Biogenesis, RNA Cargo Selection, Content, Release, and Uptake. Cell Mol Neurobiol. 2016;36(3):301-12.
86. Huotari J, Helenius A. Endosome maturation. EMBO J. 2011;30(17):3481-500.
87. Crescitelli R, Lasser C, Szabo TG, Kittel A, Eldh M, Dianzani I, et al. Distinct RNA profiles in subpopulations of extracellular vesicles: apoptotic bodies, microvesicles and exosomes. J Extracell Vesicles. 2013;2.
88. Skog J, Wurdinger T, van Rijn S, Meijer DH, Gainche L, Sena-Esteves M, et al. Glioblasto ma microvesicles transport RNA and proteins that promote tumour growth and provide diagnostic biomarkers. Nat Cell Biol. 2008;10(12):1470-6.
89. Anderson JD, Johansson HJ, Graham CS, Vesterlund M, Pham MT, Bramlett CS, et al. Comprehensive Proteomic Analysis of Mesenchymal Stem Cell Exosomes Reveals Modu lation of Angiogenesis via Nuclear Factor-KappaB Signaling. Stem Cells. 2016;34(3):601-13.
90. Ji R, Zhang B, Zhang X, Xue J, Yuan X, Yan Y, et al. Exosomes derived from human mes enchymal stem cells confer drug resistance in gastric cancer. Cell Cycle. 2015;14(15):2473-83.
91. Karlsson M, Lundin S, Dahlgren U, Kahu H, Pettersson I, Telemo E. "Tolerosomes" are produced by intestinal epithelial cells. Eur J Immunol. 2001;31(10):2892-900.
92. Greening DW, Gopal SK, Mathias RA, Liu L, Sheng J, Zhu HJ, et al. Emerging roles of exosomes during epithelial-mesenchymal transition and cancer progression. Semin Cell Dev Biol. 2015;40:60-71.
93. Azmi AS, Bao B, Sarkar FH. Exosomes in cancer development, metastasis, and drug resis tance: a comprehensive review. Cancer Metastasis Rev. 2013;32(3-4):623-42.
94. Peinado H, Aleckovic M, Lavotshkin S, Matei I, Costa-Silva B, Moreno-Bueno G, et al. Melanoma exosomes educate bone marrow progenitor cells toward a pro-metastatic phenotype through MET. Nat Med. 2012;18(6):883-91.
95. Hoshino A, Costa-Silva B, Shen TL, Rodrigues G, Hashimoto A, Tesic Mark M, et al. Tumour exosome integrins determine organotropic metastasis. Nature. 2015;527(7578):329-35.
96. Costa-Silva B, Aiello NM, Ocean AJ, Singh S, Zhang H, Thakur BK, et al. Pancreatic cancer exosomes initiate pre-metastatic niche formation in the liver. Nat Cell Biol. 2015;17:816-26

Chapter 2

Risk stratification in uveal melanoma patients

Chapter 2.1

Combined mutation and copy-number variation detection by targeted NGS in uveal melanoma.

Kyra N Smit, Natasha M van Poppelen, Jolanda Vaarwater, Robert Verdijk, Ronald van Marion, Helen Kalirai, Sarah E Coupland, Sophie Thornton, Neil Farquhar, Hendrikus-Jan Dubbink, Dion Paridaens, Annelies de Klein, Emine Kiliç

Modern Pathology. 2018 May;31(5):763-771

Abstract

Uveal melanoma is a highly aggressive cancer of the eye, in which nearly 50% of the patients die from metastasis. It is the most common type of primary eye cancer in adults. Chromosome and mutation status have been shown to correlate with the disease free survival. Loss of chromosome 3 and inactivating mutations in *BAP1*, which is located on chromosome 3, are strongly associated with 'high risk' tumors that metastasize early. Other genes often involved in uveal melanoma are *SF3B1* and *EIF1AX*, which are found to be mutated in intermediate- and low risk tumors, respectively. To obtain genetic information of all genes in one test we developed a targeted sequencing method that can detect mutations in uveal melanoma genes and chromosomal anomalies in chromosome 1,3 and 8. With as little as 10ng DNA we obtained enough coverage on all genes to detect mutations, such as substitutions, deletions and insertions. These results were validated with Sanger sequencing in 28 samples. In more than 90% of the cases, the *BAP1* mutation status corresponded to the BAP1 immunohistochemistry. The results obtained in the Ion Torrent single nucleotide polymorphism assay were confirmed with several other techniques, such as fluorescence in situ hybridisation, multiplex ligation-dependent probe amplification and Illumina SNP-array. By validating our assay in 27 formalin-fixed paraffin-embedded and 43 fresh uveal melanomas, we show that mutations and chromosome status can reliably be obtained using targeted next-generation sequencing. Implementing this technique as a diagnostic pathology application for uveal melanoma will allow prediction of the patients' metastatic risk and potentially assess eligibility for new therapies.

Introduction

Uveal melanoma is the most common primary intraocular malignancy in adults with a worldwide annual incidence in Caucasians of 5-7 per million per year[1]. Despite successful treatment of the primary tumor, nearly 50% of the patients develop liver metastasis within 5 years. Once metastatic disease is diagnosed, survival is between 2 and 9 months[2]. Approximately 40% of uveal melanoma patients developed metastases within 4 years, but dissemination can occur even up to 4 decades after diagnosis[3]. This demonstrates that the prognosis for uveal melanoma patients can strongly vary between patients, and is dependent on a number of factors, including clinical and histological parameters, as well as the underlying genetic 'make up' of the tumor cells[4].

Chromosomal anomalies are often found in solid tumors, but previous work has shown that most of the chromosomal anomalies in uveal melanoma are limited to chromosome 1, 3, 6 and 8. Some of these chromosomal variations correlated with metastasis, such as loss of chromosome 3[5]. Monosomy 3 is observed in half of the patients and is strongly associated with poor survival. Loss of chromosome 3 is thought to be an early event, since it is present in the majority of the cells and often accompanies other chromosomal anomalies, such as gain of chromosome 8q[6,7,8]. Another common anomaly in metastasizing uveal melanoma with monosomy 3 is loss of chromosome 1p[9]. Chromosome 6 shows frequent rearrangements in both p- and q-arm in uveal melanoma; yet, deletion of 6q or gain of 6p are not associated with metastatic disease[10].

Uveal melanoma are genetically well-characterized tumors. Recent research using genome-wide sequencing led to the discovery of several genetic alterations, which correlate to a distinct survival pattern. Activating mutations in guanine-nucleotide binding protein-Q (*GNAQ*) and -alpha 11 (*GNA11*) were found in the majority of uveal melanoma patients (83-93%), and are therefore thought to be initiating mutations[11,12,13]. Inactivating mutations in the BRCA-associated protein 1 (*BAP1*), located on chromosome 3p, were found in the early metastasizing patients[14]. Recently two other genes have been reported that play a role in uveal melanoma biogenesis. Mutations in the eukaryotic translation initiation factor 1A (*EIF1AX*) were observed in non-metastasizing tumors[15] and a hotspot mutation in the splicing factor 3 subunit 1 (*SF3B1*)-gene was detected in late metastasizing tumors[16,17]. Both of these genes are known to be mutually exclusive.

Current clinical diagnostics for uveal melanoma include several techniques, such as expression profiling[18], copy number analysis by Illumina single nucleotide polymorphism (SNP)-array[19], multiplex ligation-dependent probe amplification[20] or fluorescence in situ hybridisation[21], immunohistochemistry of the BAP1 protein[22,23] and Sanger sequencing of *EIF1AX*, *SF3B1* and *BAP1*. In some cases, whole-genome sequencing or whole-exome sequencing is used to identify the somatic mutations present in the tumor[15,24]. In this study we performed Ion Torrent next-generation sequencing with a custom made panel on 70 uveal melanomas to determine if targeted sequencing can be implemented in the routine uveal melanoma-diagnostics. This panel has been designed specifically for uveal melanoma, covering all major hotspot mutations in the five relevant genes and several single nucleotide polymorphisms on chromosome 1, 3 and 8 to allow analysis of clinically relevant chromosomal anomalies.

Material and Methods

Uveal melanoma samples

Sixty-five uveal melanoma samples were selected from our Rotterdam Ocular Melanoma Study Group-database and 5 were external samples from patients who underwent enucleation, received for diagnostics from the Liverpool Ocular Oncology Research Group. Samples included in this study were diagnosed as uveal melanoma, collected between 1988 and 2016, and include formalin-fixed paraffin-embedded and fresh specimens. A written informed consent was obtained before treatment, the study was performed according to the guidelines of the Declaration of Helsinki and was approved by the local ethics committee.

DNA extraction

Targeted next-generation sequencing was performed on DNA extracted from fresh- and formalin-fixed paraffin-embedded samples. For all tumor samples, an ophthalmic pathologist reviewed and selected tumor areas with an estimated minimal tumor cell percentage of 85%. DNA isolation from fresh tissue was carried out using the QIAmp DNA mini kit (Qiagen, Hilden, Germany), according to the manufacturer's instructions. For formalin-fixed paraffin-embedded samples, depending on the size of the tumor, 2-6 5µm sections were de-paraffinized and hematoxylin stained prior to isolation of the DNA. Formalin-fixed paraffin-embedded tumor tissue was micro-dissected by scraping the cells manually from hematoxylin-stained sections. DNA was then extracted by incubation of the tissues overnight at 56°C in lysis buffer (Promega, Madison, WI, USA), containing 5% Chelex (Bio-Rad, Berkley, CA, USA) and Proteinase K (Qiagen). Proteinase K was inactivated by incubating the sample for 10 minutes at 95°C and cell debris was pelleted down together with the Chelex by centrifugation in a micro-centrifuge at maximum speed. DNA concentrations were measured with the Quant-iT Picogreen assay kit (Thermofisher Scientific, Grand Island, NY, USA), as described by the manufacturer. All DNA samples were stored at -20°C. The DNAs provided by the Liverpool Ocular Oncology Research Group had been extracted as previously described using the Qiagen DNeasy Blood and Tissue kit[25].

Targeted Next-Generation Sequencing

A custom primer panel covering the five uveal melanoma genes and several single nucleotide polymorphisms located on chromosomes 1, 3 and 8, was designed using Ion Ampliseq Designer 2.0 (ThermoFisher Scientific). This resulted in an 11.5 kb amplicon panel, containing 98 amplicons. Amplicons designed for *GNAQ*, *GNA11*, *EIF1AX* and *SF3B1* covered only the exons containing the known mutation hotspots. All exons of the *BAP1* gene were covered by amplicons. On chromosome 1 and 8, seventeen amplicons were designed to cover highly polymorphic regions in the entire chromosome (Supplementary table 1). These highly polymorphic regions with a global minor allele frequency of at least 45% were selected based on data found in the NCBI SNP database26. For chromosome 3 twenty-one amplicons were designed, due to the clinical relevance. The DNA input varied between 3 and 10 ng, depending on the amount of DNA available per sample. Library construction was performed using the AmpliSeq Library Kit 2.0. Next-Generation amplicon sequencing of the libraries was performed by semiconductor sequencing with the Ion Torrent Personal Genome Machine (Thermofisher Scientific) on an Ion Chip, according to the manufacturer's protocol.

Mutation Analysis

Adapter trimming and filtering of poor quality reads was performed on raw Ion Torrent sequence data by using the platform specific Torrent Suite Software V4.4.3 (Thermofish-

er Scientific). The generated sequence reads were analysed with Coverage Analysis and Variant Caller v3.6 plugins to perform sequence coverage analysis and identify variants, respectively. Variants identified as a common polymorphism in the 1000 Genomes-database and variants that were present in >90% of the samples were excluded. If variants were present in a frequency higher than 15% and if they had a minimum read depth of 100 reads, they were called as mutations. Analysis of the detected mutations was done by visualizing the reads in Integrative Genomics Viewer software (Broad Institute, Cambridge, MA, USA) and comparing them to the Ensemble genome database (NM_002072; NM_002067; NM_004656; NM_012433; NM_001412).

Sanger sequencing

DNA from 28 tumor samples was sequenced using the Sanger method to confirm results found by next-generation sequencing. Selected regions of the genes of interest were amplified by polymerase chain reaction (PCR). Subsequently, sequencing of the PCR products and mutation analysis of *GNAQ*, *GNA11*, *BAP1* and *SF3B1* and *EIF1AX* was done as reported previously[13,16,22]. Alignment of the sequence reads was done with reference sequence Hg19 from the Ensemble genome database.

Immunohistochemical staining

To detect loss of the BAP1 protein in tumors, immunohistochemical staining of BAP1 was performed on 4μm formalin-fixed paraffin-embedded sections of tumors. Staining was done by an automated immunohistochemistry staining system (Ventana Medical Systems Inc, Tucson, AZ, USA) as described before[22]. BAP1 protein expression data were also available for the cases received from Liverpool Ocular Oncology Research Group, which were stained as previously described[27]. Sections were evaluated by the ophthalmic pathologists in Rotterdam and Liverpool (RV and SEC, respectively).

Copy number variation analysis

Validation of the copy number status of the chromosomes was performed by SNP-array, multiplex ligation-dependent probe amplification and fluorescence in situ hybridisation analysis. Two hundred nanograms of fresh tumor DNA was used for the Illuminia 610Q SNP-array (Illumina, San Diego, CA, USA). Results were analyzed with Nexus Software (BioDiscovery, El Segundo, CA, USA). One hundred nanograms of DNA from each formalin-fixed paraffin-embedded uveal melanoma was used for multiplex ligation-dependent probe amplification analysis of chromosomes 1p, 3, 6 and 8 as previously described[20]. Fluorescence in situ hybridisation analysis was performed on directly fixed tumor material, with probes for chromosome 1, 3 and 8 as reported previously[21]

Results

Coverage of uveal melanoma genes

To detect mutations in the *GNAQ*-, *GNA11*-, *EIF1AX*-, *SF3B1*- and *BAP1* gene, 43 amplicons were used to sequence these genes reliably. Samples with a minimum total read count of 40.000 were analyzed for mutations in the five uveal melanoma genes. The total amount of read counts for fresh samples was on average slightly higher than those of formalin-fixed paraffin-embedded samples (Figure 1A). Most of the amplicons covering the five uveal melanoma genes consisted of 1 – 2% of the total read count, which corresponds to a minimum of 400 reads (Figure 1B). The median read count of all amplicons was 1.1%. Several amplicons obtained a coverage of less than 1% of the total read count, such as *EIF1AX* exon 1 and BAP1 exon 1 and 3. By adding extra amplicons in the primer mix for these areas, we compensated for these lower read counts.

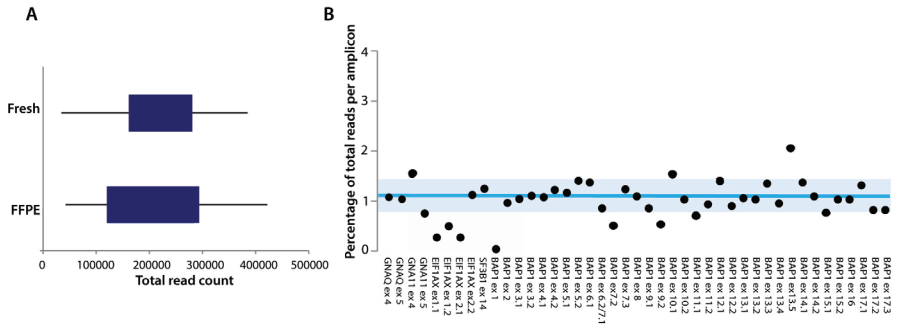

Figure 1. Sequencing efficiency of formalin-fixed, paraffin-embedded and fresh uveal melanoma specimens
A) Boxplots showing the total read count for all fresh- (top plot) and formalin-fixed, paraffin-embedded (FFPE) samples (bottom plot) **B)** Percentage of total reads visualized for all amplicons covering the five uveal melanoma genes. Solid line indicates median for all amplicons and light grey area shows second- and third quartile.

Mutation analysis

Seventy uveal melanoma samples were sequenced with our targeted panel. DNA was isolated from fresh specimens (n=43) and from formalin-fixed paraffin-embedded material (n=27). From all 70 samples sufficient DNA was extracted for sequencing. Forty-one percent of the samples harbored a *GNAQ* exon 5 c.626A>C or c.626A>T mutation, 3% a *GNAQ* exon 4 c.548G>A mutation, 41% a *GNA11* exon 5 c.626A>T mutation, 1% a GNA11 exon 4 c.547C>T mutation and in the remaining samples no mutations in either of these two genes were detected (Table 1). Mutations in the *BAP1* gene were found in 41% of the cases, mutations in *SF3B1* in 16% and *EIF1AX* in 20% of the samples (Supplementary Table 2). From 28 samples we extracted enough DNA from fresh tissue to perform Sanger sequencing as well. All the mutations found by next-generation sequencing in these samples were validated by Sanger sequencing and no new mutations were identified.

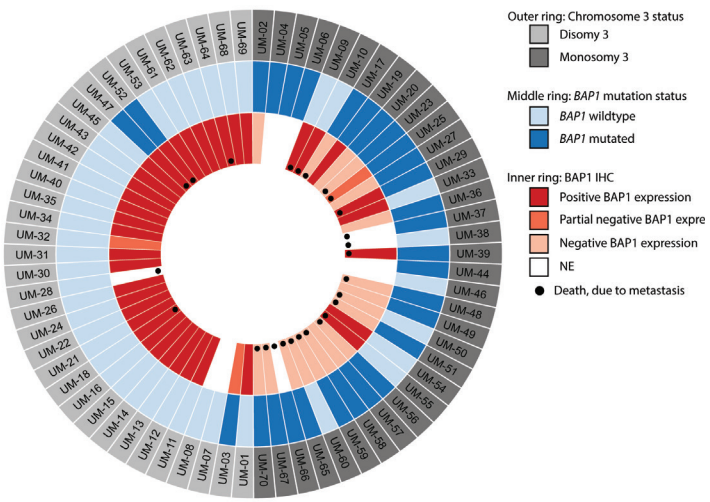

Figure 2. The overlap between the chromosome 3 status, *BAP1* mutation status and BAP1 expression
A doughnut chart visualizing the chromosome 3 status (outer ring), *BAP1* mutation status (middle ring) and BAP1 immunohistochemistry (IHC) (inner ring) for all 70 uveal melanoma samples.

Detection of loss of BAP1 protein expression

Absence of the BAP1 protein is often associated with monosomy 3 uveal melanoma. The loss of nuclear BAP1 expression can be immunohistochemically assessed, which is routinely performed in a diagnostic setting. Uveal melanoma samples were sequenced and analysed for *BAP1* mutations. Half of all the samples showed loss of chromosome 3. 74% of these monosomy 3 samples harbored a *BAP1* mutation and 26% did not. BAP1 immunohistochemistry was carried out for 59 samples, since we did not have tissue available for immunohistochemistry in all samples. In the *BAP1*-mutated samples of which we obtained BAP1 immunohistochemistry data, 80% showed a negative BAP1 immunohistochemistry (-), 5% showed a mixture of positive and negative BAP1 cells in the tumor (+/-) and 15% showed a positive BAP1 immunohistochemistry (+) (Figure 2 and Supplementary table 2). The results obtained from three samples are depicted in figure 3. Hematoxylin and eosin staining indicated a high presence of tumor cells in all three samples (Figure 3A). BAP1 staining was positive for the upper sample and negative for both the middle and lower sample (Figure 3B). Ion Torrent sequencing of the *BAP1* gene revealed no mutations in the top sample but did show a mutation in the other two samples (Figure 3C), confirming the presence of *BAP1* mutations in the immunohistochemistry BAP1 negative tumors.

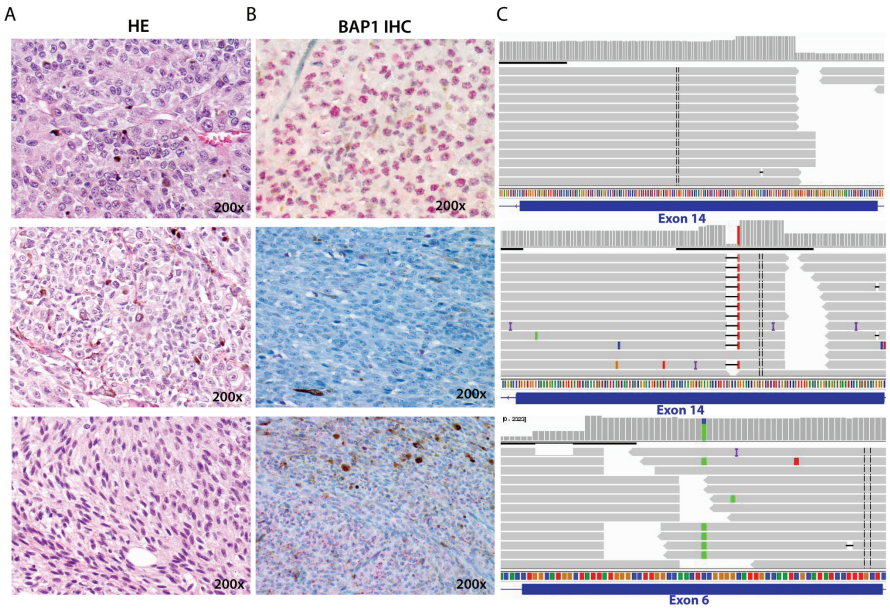

Figure 3. Histopathological and genetic aspects of three uveal melanoma specimens
A) Hematoxylin and eosin-staining (HE) of three uveal melanoma samples (200x) **B)** Immunohistochemistry (IHC) staining of BAP1 protein showing strong nuclear BAP1 expression in the top sample and loss of BAP1 expression in middle and bottom sample (200x) **C)** From top to bottom: no mutation observed in the *BAP1*-gene, a 5-basepair deletion and insertion in exon 14 resulting in a frameshift (c.175_179delinsA) and a point mutation in exon 6 which changes a Glutamate into a STOP-codon (c.406G>T).

Copy number analysis

SNP-array, multiplex ligation-dependent probe amplification and fluorescence in situ hybridisation analyses are commonly used to identify chromosomal changes in tissues. To determine whether the Ion Torrent uveal melanoma custom panel allows a reliable detection of allelic imbalances caused by (partial) losses and gains of chromosome 1, 3 and 8, we compared results obtained by fluorescence in situ hybridisation and SNP-array with the copy number variation results from our custom panel. Single nucleotide polymorphism covering amplicons were evenly distributed over the entire chromosome (Figure 4A),

which allowed us to observe partial aberrations as well. Fluorescence in situ hybridisation results showed disomy 3 for the top sample and monosomy 3 for the lower sample (Figure 4B). This was confirmed with the SNP-array, where the Log R Ratio and B-allele frequency shows no loss of heterozygosity for chromosome 3 in the upper sample and monosomy 3 for the lower sample (Figure 4C). The same pattern of allelic distribution was seen with the Ion Torrent single nucleotide polymorphism-analysis of chromosome 3 (Figure 4D). The B-allele frequencies for chromosome 1 and 8 were confirmed as well, as shown in supplementary figure 1. Across all samples we found that 50% showed monosomy 3, 30% loss of chromosome 1p and 57% gain of chromosome 8q. These percentages overlapped with the percentages found by other copy number variation-techniques. Thirty-four samples were validated with only an Illumina SNP-array, 15 with SNP-array and fluorescence in situ hybridisation, 7 with only fluorescence in situ hybridisation and 5 samples with multiplex ligation-dependent probe amplification (Supplementary table 3).

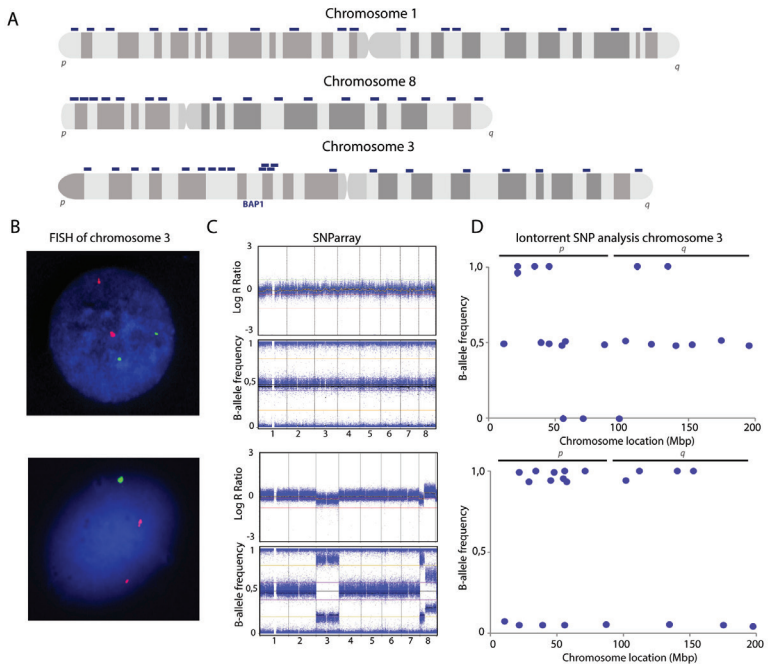

Figure 4. Copy number analysis of chromosome 3
A) Visualization of the evenly spread amplicons covering highly polymorphic single nucleotide polymorphisms on chromosome 1,3 and 8. **B)** Fluorescence in situ hybridisation (FISH) of chromosome 5 (red) and chromosome 3 (green) shows no loss for chromosome 3 in the top sample and loss of chromosome 3 in the bottom sample **C)** Top SNP-array visualizes chromosome status for chromosome 1 to 8. Both Log R Ratio and B-allele frequency indicate disomy 3, whereas the SNP-array for the bottom panel shows loss of chromosome 3 **D)** Single nucleotide polymorphism (SNP) analysis performed by the targeted uveal melanoma panel visualizes the B-allele frequency for chromosome 3. Top single nucleotide polymorphism analysis shows heterozygosity for the single nucleotide polymorphisms, indicating disomy 3, while bottom sample shows no heterozygous variants indicating loss of heterozygosity of chromosome 3.

Discussion

Uveal melanoma is characterized by recurrent mutated genes and chromosomal anomalies. In this study we present a novel custom-designed next-generation sequencing assay for uveal melanoma, which can be used to predict uveal melanoma patients' prognoses based on mutation status and chromosome status of chromosome 1,3 and 8. The assay can be conducted with using either freshly isolated DNA or DNA obtained from formalin-

fixed paraffin-embedded material. This is the first study that establishes a method that can be used for uveal melanoma diagnostics on both formalin-fixed paraffin-embedded and fresh material. Our assay is cost-effective, since one method can replace techniques, such as fluorescence in situ hybridisation, SNP-array and Sanger sequencing and it can be considered as a good alternative for BAP1 immunohistochemistry. Other important advantages are the low amount of DNA (10 ng) necessary for sequencing, which makes the technique suitable for transvitreal fine needle aspirations biopsies and the small amplicon-size, allows sequencing of partially degraded DNA from formalin-fixed paraffin-embedded tissue. Our assay could be performed on other next-generation sequencing platforms than Ion Torrent sequencing as well, if these two characteristics are taken into account. Furthermore, compared to other techniques that only identify the high risk patients that metastasize early, this technique also allows us to identify the potentially late metastasizing patients that often harbor a *SF3B1* mutation.

Prognostication of uveal melanoma patients can be achieved by analyzing mutation status. Currently, this is usually performed by Sanger sequencing. Mutations in *GNAQ*, *GNA11* and *SF3B1*, all gain of function mutations, occur almost exclusively in hotspot locations, therefore only these locations have to be sequenced. Since mutations can occur throughout the entire *BAP1* gene, large amounts of DNA are needed for the sequencing of multiple exons. Whole-exome sequencing is a reliable and easy method to obtain mutation status as well. However, since only a few genes are involved in the oncogenesis of uveal melanoma, many irrelevant reads will be produced. Whole-exome sequencing is less cost-effective for the diagnostic setting, compared to targeted Ion Torrent sequencing.

Several regions of the human genome are difficult to cover with next-generation sequencing. As shown in figure 1B, a few exons, such as *BAP1* exon 1 and the first two exons of *EIF1AX*, show a relatively low read count. Due to this low read count, it is more difficult to detect mutations in this particular exon. These findings are not only observed in our targeted uveal melanoma panel, but also in whole-genome sequencing data of uveal melanoma[17,28]. Since exon 1 of the *BAP1* gene is located in the non-translated region, the effect of a mutation in this UTR region is not always clear. Another region, which is sensitive for sequencing errors is exon 1 of *EIF1AX*, caused by a pseudogene on chromosome 1. Amplicons covering only exon 1 may also produce reads derived from chromosome 1. By adding a second set of reads generated by a different amplicon for *EIF1AX*, we now cover not only exon 1 but also a part of the 3'UTR, which will obtain longer reads that can only be derived from *EIF1AX* exon 1.

In our cohort we observed mutations in all of the major uveal melanoma genes. Eighty-six percent of the samples showed a mutation in *GNAQ* or *GNA11*. Mutations in *EIF1AX* were found in 20%, mutations in *SF3B1* in 16% and mutations in *BAP1* were detected in 41% of the cases. The obtained results do not exactly overlap with the mutation rates for uveal melanoma that we previously reported[16], but those differences can be explained by the bias in our sample population. Samples selected for this study were not randomly chosen, but rather selected based on follow-up length and tissue availability. Figure 2 shows that only 74% of the monosomy samples harbor a *BAP1* mutation, which can be explained by studies showing that *BAP1* mutations arise after loss of chromosome 3[29]. Most of the *BAP1*-mutated samples showed a negative BAP1 immunohistochemistry, but some had positive and negative BAP1 immunohistochemistry cells, which possibly indicates that not all of the cells in the tumor have acquired the mutation yet. However, we also observed *BAP1*-mutated samples that showed a positive BAP1 immunohistochemistry. For the disomy 3 samples, this can be explained by the presence of a *BAP1* wildtype gene, but this is not the case for the monosomy 3 samples. In these samples we hypothesize that

the mutated mRNA is not degraded by nonsense mediated decay and could thereby still be translated into a partially functional or non-functional protein. If the antibody binds at a different location as where the mutation is found, it will show a positive immunohistochemistry. However, for the majority (91.6%) of the samples the uveal melanoma panel can correctly detect mutations corresponding to the observed loss of BAP1-expression.

Besides mutation status-analysis, our panel also provides information about the copy number status. Techniques such as fluorescence in situ hybridisation, multiplex ligation-dependent probe amplification and SNP-array can provide information about the chromosomal change of one or several chromosomes in the tumor in most cases, but these techniques also have their disadvantages. The probes used for fluorescence in situ hybridisation are specific for a certain region, i.e. fluorescence in situ hybridisation testing does not screen the entire chromosome. It is also a relatively laborious technique, which can take up to several days. Performing a SNP-array requires less time, but the amount of DNA necessary (200 ng) is significantly higher than other techniques. Furthermore, standard SNP-array is less successful on DNA extracted from formalin-fixed paraffin-embedded tissue compared to freshly obtained DNA. With our uveal melanoma panel, we reliably detect copy number variations by sequencing of highly polymorphic single nucleotide polymorphisms. Since this assay requires less DNA than conventional SNP-arrays and less time than fluorescence in situ hybridisation, it is a promising method for routine uveal melanoma diagnostics. Copy number analysis by next-generation sequencing can be challenging in case of low tumor percentages, but since uveal melanoma typically tend to have a high tumor cell content and little heterogeneity for chromosome 3 we do not expect this will pose a problem in our assay[30]. Chromosome 1 and 8 might have more heterogeneity, thus in case of low tumor cell content and non-conclusive Ion Torrent single nucleotide polymorphisms array results, additional experiments might be necessary. The single nucleotide polymorphism analysis performed with this uveal melanoma panel does not allow detection of polyploidy in samples. However, recently it has been shown that polyploidy in uveal melanoma does not change the mutation prevalence, which means that detecting polyploidy in uveal melanoma patients has little impact in this method since it does not affect the prognosis[31].

Our Ion Torrent uveal melanoma panel is in the current state already suitable for implementation in uveal melanoma prognostication, with the advantage that it can easily be expanded by adding the more recently discovered genes into our panel. Recently, it has been reported that a small percentage of the uveal melanoma samples contain mutations in other spliceosome components, *SR2F2* and *U2AF1*. It is thought that these tumors act in the same way as *SF3B1*-mutated tumors[32]. Other rare alterations in uveal melanoma are mutations in *PCLB4* and *CYSTLR2*, which are downstream targets of GNA11 and GNAQ and are thereby thought to be less suitable for prognostication[33].

In summary, we present a next-generation sequencing based assay that can readily be implemented as a diagnostic pathology application for uveal melanoma. Mutation and copy number variation data can be obtained by one technique, which can reliably predict the patients' outcome and potentially assess eligibility for new therapies. At present there is no successful treatment for metastasized uveal melanoma; however, with the development of new therapies, identification of high-risk patients will be very important, particularly in adjuvant therapy trials. Our custom-designed uveal melanoma panel will make a valuable contribution to the rapid stratification of uveal melanoma patients.

Acknowledgements
We thank Quincy van den Bosch for his assistance with imaging and Tom Brands and Tom

de Vries-Lentsch for helping with the figures. This study was supported by a grant of the Combined Ophthalmic Research Rotterdam.

Disclosure/Conflict of interest
The authors declare no conflict of interest.

References

1. Singh A, Turell M, Topham A. Uveal melanoma: trends in incidence, treatment and survival. Ophthalmology 2011; 118:1881-1885
2. Woodman S. Metastatic uveal melanoma: biology and emerging treatments. Cancer J 2012 ;18:148-152
3. Coupland S, Sidiki S, Clark B. Metastatic choroidal melanoma to the contralateral orbit 40 years after enucleation. Arch Ophthalmol 1996;114:751-756
4. Damato B, Eleuteri A, Taktak A, et al.Estimating prognosis for survival after treatment of choroidal melanoma. Prog Retin Eye Res 2011;30:285-295
5. Prescher G, Bornfeld N, Becher R. Nonrandom chromosomal abnormalities in primary uveal melanoma. J Natl Cancer Institute 1990; 82:1765-1769
6. van den Bosch T, van Beek J, Vaarwater J, et al. Higher percentage of FISH-determined monosomy 3 and 8q amplification in uveal melanoma cells relate to poor patient progno sis. Invest Ophthalmol Vis Sci 2012;15:2668-2674
7. de Lange M, van Pelt S, Versluis M, et al. Heterogeneity revealed by integrated genomic analysis uncovers a molecular switch in malignant uveal melanoma. Oncotarget 2015; 6: 37824-37835
8. Dogrusöz M, Bagger M, van Duinen S, et al. The prognostic value of AJCC staging in uveal melanoma is enhanced by adding chromosome 3 and 8q status. Invest Ophthalmol Vis Sci 2017;58:833-842
9. Kilic E, Naus N, van Gils W, et al. Concurrent loss of chromosome arm 1p and chromosome 3 predicts a decreased disease-free survival in uveal melanoma patients. Invest Ophthalmol Vis Sci 2005; 46:2253-2257
10. White V, Chambers J, Courtright P, et al. Correlation of cytogenetic abnormalities with the outcome of patients with uveal melanoma. Cancer 1998; 83:354-359
11. van Raamsdonk C, Bezrookove V, Green G, et al. Frequent somatic mutations of GNAQ in uveal melanoma and blue naevi. Nature 2009; 457:599-602
12. van Raamsdonk C, Griewank K, Crosby M, et al. Mutations in GNA11 in uveal melanoma. N Eng J Med 2010; 363:2191-2199
13. Koopmans A, Vaarwater J, Paridaens D, et al. Patient survival in uveal melanoma is not affected by oncogenic mutations in GNAQ and GNA11. Br J Cancer 2013; 109:493-496
14. Harbour J, Onken M, Roberson E, et al. Frequent mutations of BAP1 in metastasising uveal melanomas. Science 2006; 330:1410-1413
15. Martin M, Masshöfer L, Temming P, et al. Exosome sequencing identifies recurrent somatic mutations in EIF1AX and SF3B1 in uveal melanoma with disomy 3. Nature genet ics 2013; 45:933-936
16. Yavuzyigitoglu S, Koopmans A, Verdijk R, et al. Uveal melanomas with SF3B1 mutations: A distinct subclass associated with late-onset metastases. Ophthalmology 2016; 123: 1118-1128
17. Furney S, Pedersen M, Gentien D, et al. SF3B1 mutations are associated with alternative splicing in uveal melanoma. Cancer Discovery 2013; 3:1122-1129
18. Onken M, Worley L, Ehlers J, et al. Gene expression profiling in uveal melanoma reveals two molecular classes and predicts metastatic death. Cancer Res 2004; 64:7205-7209
19. Ewens K, Kanetsky P,Richards-Yutz J, et al. Genomic profile of 320 uveal melanoma cases: Chromosome 8p-loss and metastatic outcome. Invest Ophthalmol Vis Sci 2013; 54:5721-5729
20. Damato B, Dopierala J, Coupland S. Genotypic profiling of 452 choroidal melanomas with multiplex ligation-dependent probe amplification. Clinical Cancer Research 2010; 16:6083-6092
21. Vaarwater J, van den Bosch T, Mensink H, et al. Multiplex ligation-dependent probe amplification equals fluorescence in-situ hybridization for the identification of patients at risk for metastasic disease in uveal melanoma. Melanoma Research 2012; 22:30-37

22. Koopmans A, Verdijk R, Brouwer R, et al. Clinical Significance of immunohistochemistry for detection of BAP1 mutations in uveal melanoma. Modern Pathology 2014: 27(10):1321-1330
23. van den Nes J, Nelles J, Kreis S, et al. Comparing the prognostic value of BAP1 mutation pattern, chromosome 3 status and BAP1 immunohistochemistry in uveal melanoma. Am J Surg Pathol 2016; 40:796-805
24. Royer-Bertrand B, Torsello M, Rimoldi D, et al. Comprehensive genetic landscape of uveal melanoma by Whole-Genome Sequencing. Am J Hum Genet 2016; 99:1190-1198
25. Lake S, Kalirai H, Dopierala J, et al. Comparison of formalin-fixed and snap-frozen samples analysed by multiplex ligation-dependent probe amplification for prognostic testing in uveal melanoma. Invest Ophthalmol Vis Sci 2012;53:2647-2652
26. Dubbink HJ, Atmodimedjo P, van Marion R, et al. Diagnostic detection of allelic losses and imbalances by next-generation sequencing 1p/19q co-deletion analysis of gliomas. J Mol Diagn 2016;18:775-786
27. Kalirai H, Dodson A, Faqir S, et al. Lack of BAP1 protein expression in uveal melanoma is associated with increased metastatic risk and has utility in routine prognostic testing. Br J Cancer 2014;111:1373-1380
28. Johansson P, Aoude L, Wadt K, et al. Deep sequencing of uveal melanoma identifies a recurrent mutation in PLCB4. Oncotarget 2016; 7:4624-4631
29. Robertson A, Shih J, Yau C, et al. Integrative analysis identifies four molecular and clinical subsets in uveal melanoma. Cancer Cell 2017; 32:204-220
30. Mensink HW, Vaarwater J, Kiliç, et al. Chromosome 3 intratumor heterogeneity in uveal melanoma. Invest Ophthalmol Vis Sci 2009; 50:500-504
31. Yavuzyigitoglu S, Mensink H, Smit K, et al. Metastatic disease in polyploid uveal mela noma is associated with BAP1 mutations. Invest Ophthalmol Vis Sci 2016; 27: 2232-2239
32. Ilagan J, Ramakrishnan A, Hayes B, et al. U2AF1 mutations alter splice site recognition in hematological malignancies. Genome Res 2015; 25:14-26
33. Moore A, Ceraudo E, Sher J, et al. Recurrent activating mutations of G-protein-coupled receptor CYSLTR2 in uveal melanoma. Nature Genetics 2016; 48:675-680

Supplementary Table 1. List of the highly polymorphic single nucleotide polymorphisms (SNP) covered by the uveal melanoma panel

	SNP-number	Position (bp)
Chromosome 1	rs7418256	4,084,304
	rs7412149	9,579,964
	rs12048851	16,382,718
	rs10907287	18,497,478
	rs6425861	34,372,503
	rs639298	42,001,530
	rs11209106	68,001,206
	rs480304	82,123,485
	rs10493903	98,900,818
	rs17258467	120,323,058
	rs1752380	151,347,746
	rs3856201	163,736,341
	rs10753786	169,288,770
	rs2072040	175,096,333
	rs138685314	188,228,295
	rs6681013	215,154,797
	rs592197	234,817,283
Chromosome 3	rs1601368	10,829,535
	rs1549356	21,528,837
	rs7612272	28,816,226
	rs7648156	34,497,918
	rs1274960	39,192,542
	rs267218	45,633,834
	rs9311387	46,115,590
	rs295449	47,375,955
	rs3821659	54,987,923
	rs2702143	55,738,509
	rs9868630	56,012,096
	rs62259027	57,747,389
	rs9310190	70,420,837
	rs12497448	86,741,603
	rs1151334	102,257,506
	rs3749299	111,673,147
	rs4045771	121,962,478
	rs975149	134,666,475
	rs1004009	152,754,481
	rs9866779	175,021,665
	rs11717776	197,569,559
Chromosome 8	rs2405488	2,141,263
	rs4498602	10,180,242
	rs17577614	15,470,729
	rs13275706	19,327,151
	rs6557699	23,602,610
	rs1882928	31,023,822
	rs10095600	36,911,156
	rs4147426	47,909,945
	rs10107875	60,526,565
	rs6995640	68,904,187
	rs2120410	79,844,006
	rs13261311	87,705,504
	rs4735258	94,935,937
	rs4734993	108,686,209
	rs2142250	117,093,062
	rs6415522	131,905,690
	rs7008457	145,536,593

Supplementary Table 2. Mutation status, BAP1 immunohistochemistry and chromosome 3 status of all 70 samples

	Tissue	*GNAQ* ex 4	*GNAQ* ex 5	*GNA11* ex 4	*GNA11* ex 5	*EIF1AX* ex 1/2	*SF3B1* ex 14	*BAP1*	BAP1 IHC	Monosomy 3
UM-1	FFPE		●^{s}			●^{s}			+	
UM-2	FFPE		●					●	-	●
UM-3	FFPE		●					●	+/-	
UM-4	FFPE				●			●	ne	●
UM-5	FFPE		●					●	ne	●
UM-6	FFPE		●					●	ne	●
UM-7	FFPE				●		●		ne	
UM-8	FFPE		●			●			ne	
UM-9	FFPE								+	●
UM-10	FFPE				●				+	●
UM-11	FFPE				●		●		+	
UM-12	FFPE				●		●		+	
UM-13	FFPE				●		●		+	
UM-14	FFPE				●				+	
UM-15	FFPE				●				+	
UM-16	FFPE				●				+	
UM-17	FFPE				●			●	-	●
UM-18	FFPE		●			●			+	
UM-19	FFPE				●			●	+	●
UM-20	FFPE							●	-	●
UM-21	FFPE				●		●		+	
UM-22	FFPE				●		●		+	
UM-23	FFPE		●					●	-	●
UM-24	FFPE				●		●		+	
UM-25	FFPE				●^{s}			●^{s}	+/-	●
UM-26	FFPE		●^{s}						+	
UM-27	FFPE				●^{s}			●^{s}	-	●
UM-28	Fresh								ne	
UM-29	Fresh		●^{s}					●^{s}	+	●
UM-30	Fresh					●			+	
UM-31	Fresh				●	●			+	
UM-32	Fresh								+/-	
UM-33	Fresh		●			●			+	●
UM-34	Fresh								+	
UM-35	Fresh				●^{s}	●^{s}			+	
UM-36	Fresh		●					●	-	●
UM-37	Fresh		●					●	ne	●
UM-38	Fresh				●^{s}				ne	●
UM-39	Fresh				●^{s}			●^{s}	+	●
UM-40	Fresh		●^{s}			●^{s}			+	
UM-41	Fresh								+	
UM-42	Fresh				●^{s}	●^{s}			+	
UM-43	Fresh				●	●			+	
UM-44	Fresh		●^{s}					●^{s}	ne	●
UM-45	Fresh		●			●			+	
UM-46	Fresh				●				ne	●
UM-47	Fresh	●						●	+	
UM-48	Fresh			●^{s}				●^{s}	-	●
UM-49	Fresh	●						●	-	●
UM-50	Fresh		●^{s}						-	●
UM-51	Fresh				●^{s}			●^{s}	-	●
UM-52	Fresh				●^{s}			●^{s}	+	
UM-53	Fresh		●^{s}				●^{s}		+	
UM-54	Fresh		●^{s}			●^{s}			+	●
UM-55	Fresh								+	●
UM-56	Fresh		●^{s}					●^{s}	-	●
UM-57	Fresh				●^{s}			●^{s}	-	●
UM-58	Fresh		●					●	-	●
UM-59	Fresh		●^{s}					●^{s}	-	●
UM-60	Fresh		●^{s}						-	●
UM-61	Fresh		●^{s}			●^{s}			+	
UM-62	Fresh				●^{s}		●^{s}		+	
UM-63	Fresh		●^{s}			●^{s}			+	
UM-64	Fresh		●^{s}				●^{s}		+	
UM-65	Fresh		●^{s}					●^{s}	-	●
UM-66	Fresh		●					●	ne	●
UM-67	Fresh		●^{s}					●^{s}	-	●
UM-68	Fresh				●^{s}		●^{s}		+	
UM-69	Fresh								+	
UM 70	Fresh				●			●	-	●

Mutation status:

●: mutation observed ●s: mutation validated by sanger sequencing

BAP1 immunohistochemistry:

+: positive BAP1 staining +/-: mixed positive and negative BAP1 staining in tumor -: negative BAP1 staining NE: not evaluated

Copy number status:

●: monosomy 3 obsererved

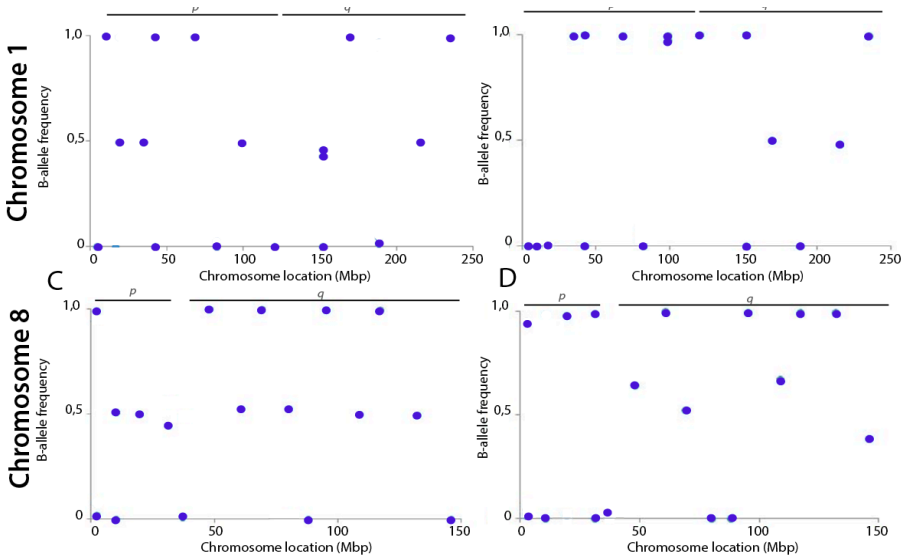

Supplementary Figure 1. Copy number analysis of chromosome 1 and 8
A) Single nucleotide polymorphism analysis indicates no loss of the entire chromosome 1 **B)** The absence of heterozygous variants in the B-allele frequency in the 1p arm of chromosome 1, indicates loss of 1p and normal 1q **C)** Single nucleotide polymorphism analysis shows two copies of chromosome 8 **D)** Loss of the p-arm of chromosome 8 and allelic imbalance of the 8q arm.

Supplementary Table 3. Chromosome status of chromosome 1p, 3 and 8q determined by Iontorrent single nucleotide polymorphism (SNP) assay or other copy number variation analysis techniques

	Loss of chromosome 1p	Loss of chromosome 3	Gain of chromosome 8q
Iontorrent SNP assay	30% *(19/63)*	52% *(33/63)*	57% *(36/63)*
Other*	33% (20/61)	48% (29/61)	61% (37/61)

** SNP-array, multiplex ligation-dependent probe amplification and/or fluorescence in situ hybridisation analysis*

Chapter 2.2

Correlation of gene mutation status with copy number profile in uveal melanoma

Serdar Yavuzyigitoglu*, Wojtek Drabarek*, **Kyra N. Smit**, Natasha van Poppelen, Anna E. Koopmans, Jolanda Vaarwater, Tom Brands, Bert Eussen, Hendrikus J. Dubbink, Job van Riet, Harmen van de Werken, Berna Beverloo, Robert M. Verdijk, Nicole Naus, Dion Paridaens, Emine Kiliç, Annelies de Klein
* These authors contributed equally to this work

Ophthalmology. 2017 April;124(4): 573-575

Report

Copy number variations (CNV) , gene expression profiling but also the recurrent gene mutations in *BAP1*, *SF3B1*, or *EIF1AX*, can be used to stratify uveal melanoma (UM) patients [1-4]. Recently, Decatur et al described an association between specific gene mutations and gene expression profiles[5]. In this report we describe the relationship between mutational status of *BAP1*, *SF3B1* and *EIF1AX* and CNV patterns using conventional karyotyping data to explore the nature of these CNVs.

In total, 277 patients from the Rotterdam Ocular Melanoma Study Group (ROMS) were included in this study. Details of the patient population and methods are described in the Supplementary Methods (available at www.aaojournals.org). For 207 samples, single nucleotide polymorphism array data and mutational status were available. These patients were divided into 4 subgroups: patients with (1) immunohistochemically BAP1-negative tumors (BAP1neg); (2) *SF3B1*-mutated tumors (*SF3B1*mut) and (3) *EIF1AX*-mutated tumors (*EIF1AX*mut). Patients in which the tumors were immunohistochemically BAP1 positive and contained no *SF3B1* or *EIF1AX* mutations were classified as (4) no recurrent mutations (NRM) tumors. This group was further split into subgroups with and without the loss of heterozygosity (LOH) of the BAP1 locus (NRMLOH+ and NRMLOH-, respectively).

We visualized sample distribution of the single nucleotide polymorphism array data across the predefined groups to obtain chromosomal patterns (Fig 1A) and found that BAP1neg tumors (n = 84) were characterized by loss of chromosome 3 (95% of the cases) and gain of the entire long (q) arm of chromosome 8 (80%). Gain of chromosome 8q was often accompanied by loss of chromosome 8p (26%). Loss of chromosome 1p, 6q and 16q was also observed frequently (25%, 19% and 20%, respectively). SF3B1mut tumors (n = 42) were characterized by gain of chromosome 6p (85%) and 8q (73%), and loss of chromosome 6q (52%) and 11q (45%). In addition, loss of chromosome 1p (36%) and gain of chromosome 9q (24%) were present in *SF3B1*mut tumors.

BAP1neg UMs showed gains or losses of entire chromosomes or chromosome arms , whereas *SF3B1*mut UMs were characterized by structural variants of the distal ends of the chromosomes (e.g. gain of chromosome 8q23qter, 8q13qter, 6p12.3pter or loss of 6q16.1qter and 11q22qter). *EIF1AX*mut tumors (n = 26) showed gain of chromosome 6p (often 6p21.33pter) in 65% of the cases. No other recurrent CNVs were observed in *EIF1AX*mut UMs. NRMLOH- tumors (n = 28) were characterized by gains of the distal ends of chromosome 6p (53%) and 8q (28%). NRMLOH+ UMs (n = 19) were characterized by monosomy 3, because we stratified for LOH of BAP1. These samples showed a very similar CNV profile as the BAP1neg UMs because these tumors also contained the typical gain of the entire arm of chromosome 8q, often accompanied by loss of chromosome 8p, and gain of the entire arm of chromosome 6p with loss of chromosome 6q.

To substantiate the finding that BAP1neg UMs contain mainly entire chromosome or chromosome arm CNVs, and *SF3B1*mut UMs smaller, partial chromosome CNVs, we calculated the percentages of aneuploidy and the number of CN events for all groups. These results (Fig 1B) showed significant greater percentages of aneuploidy in BAP1neg tumors compared with SF3B1mut tumors (11.8% and 9.3%, respectively; P = 0.024). *EIF1AX*mut tumors and NRMLOH- UMs harbored the least percentage of aneuploidy (1.7% and 4.3%, respectively), which were significantly lower than in BAP1neg and SF3B1mut tumors (P < 0.001 for all). As for CN events, *SF3B1*mut UMs harbored the most CN events, although this was not significantly higher than BAP1neg UMs (P = 0.074) in the single nucleotide polymorphism array data when corrected for multiple testing. However, both groups har-

bored more CN events than *EIF1AX*mut and NRMLOH- UMs (P ≤ 0.01 for all; Fig 1C).

Furthermore, cytogenetic data and mutational status of 70 patients were used for analysis of the different types of chromosomal anomalies. Translocations or partial chromosome arm CNVs were categorized as chromosomal structural variants (CSVs) and were numerated manually. Although cases were limited, *SF3B1*mut UMs strongly associated with >3 CSVs per tumor compared to BAP1neg (P = 0.002; Fig 1D). Moreover, 70% (7 of 10) of the UMs with >3 harbored an *SF3B1* mutation, showing that tumors with multiple CSVs are most likely to be *SF3B1*-mutated.

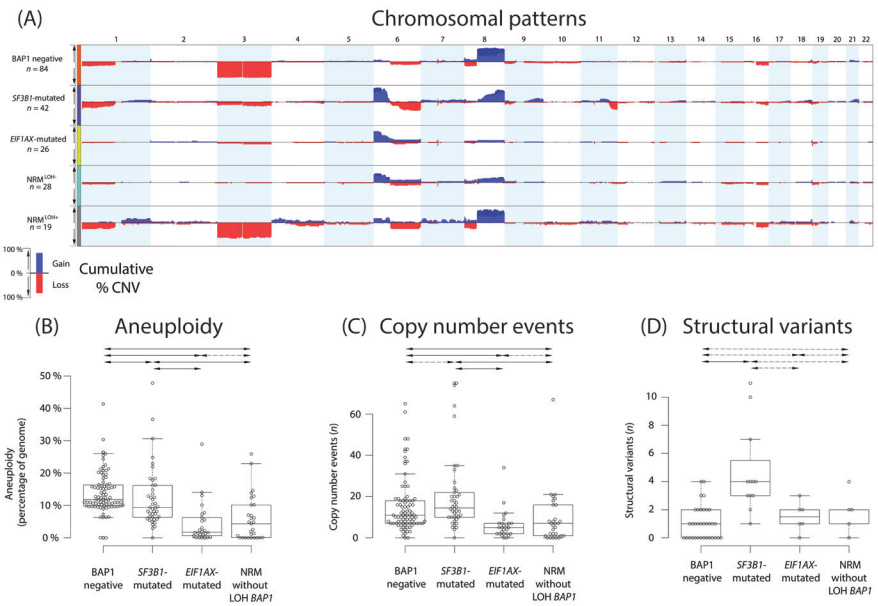

Figure 1. A) Summary plots showing the chromosomal patterns for the different groups of uveal melanomas (UMs). The chromosomes are depicted on the x-axis. The Y-axis shows the cumulative percentage of copy number variation per group. Dark blue indicates gain of chromosome and red indicated loss of chromosome. The sex-chromosomes are excluded. **B)** Statistical comparisons of the percentage of aneuploidy between the groups and **C)** the total number of copy number (CN) events. **D)** Comparison of the number of chromosomal structural variants obtained from cytogenetic data. The continuous lines between the groups are statistically significant differences (P < 0.05) between the groups. The dashed line depicts no significant difference between the groups.

Another type of chromosomal anomaly found in UMs were isochromosomes. These were observed in 74% (25/34) of all BAP1neg tumors (Supplementary Table, available at www.aaojournals.org), whereas both *SF3B1*mut and *EIF1AX*mut UMs harbored no isochromosomes. Remarkably, besides isochromosomes 8q, also isochromosome 6p was recurrent in BAP1neg UMs. Other chromosomal changes in BAPneg UMs were almost exclusively translocations with breakpoints in the centromeric regions (and thus entire chromosome arms) whereas *SF3B1*mut tumors contained more structural aberrations with recurrent distal breakpoints on chromosome 6 and 8, suggesting that different mechanisms play a role in causing these anomalies.

These novel insights in the chromosomal patterns and different types of chromosomal anomalies show that UMs with different mutated genes represent distinct molecular classes. We and others have shown that stratification based on *BAP1*, *SF3B1* and *EIF1AX* mutations reveal that patients with these mutated genes have a high, intermediate or low risk of developing metastases, respectively[4, 5].

A limitation in this study was the use of BAP1 immunohistochemistry to replace –in part - *BAP1* sequencing. For example, we expect *BAP1* mutations in the NRMLOH+ group, because these tumors revealed similar CNVs as the BAP1neg UMs. We are currently investigating this using deep sequencing and Western blotting. Furthermore, in this study all except 2 tumors were obtained from enucleated eyes; therefore, the tumor population is skewed towards larger tumors. These tumors tend to have a worse prognosis than eyes that undergo eye-conserving therapy. Nevertheless, this limitation does not affect the clinical significance of our observations that UMs have different molecular classes.

In conclusion, in this report we show that patients with UMs harbor mutation-specific chromosomal patterns in the tumor. These chromosomal patterns are characterized by different types of chromosomal anomalies, thus illustrating that distinct biological mechanisms underlie uveal melanoma pathogenesis. These pathways could possibly be specifically targeted with future diagnostics and types of treatment.

References

1. Harbour JW, Onken MD, Roberson ED, et al. Frequent mutation of BAP1 in metastasizing uveal melanomas. Science 2010;330:1410-3.
2. Koopmans AE, Verdijk RM, Brouwer RW, et al. Clinical significance of immunohisto chemistry for detection of BAP1 mutations in uveal melanoma. Mod Pathol 2014;27:1321-30.
3. Martin M, Masshofer L, Temming P, et al. Exome sequencing identifies recurrent somatic mutations in EIF1AX and SF3B1 in uveal melanoma with disomy 3. Nat Genet 2013;45: 933-6.
4. Yavuzyigitoglu S, Koopmans AE, Verdijk RM, et al. Uveal Melanomas with SF3B1 Mutations: A Distinct Subclass Associated with Late-Onset Metastases. Ophthalmology 2016; 123:1118-28.
5. Decatur CL, Ong E, Garg N, et al. Driver Mutations in Uveal Melanoma: Associations With Gene Expression Profile and Patient Outcomes. JAMA Ophthalmol 2016.

Chapter 3

Epigenetic and transcriptional regulation in metastatic UM

Chapter 3.1

Aberrant microRNA expression and its implications for uveal melanoma metastasis

Kyra N Smit, Jiang Chang, Kasper Derks, Jolanda Vaarwater, Tom Brands, Rob M Verdijk, Erik AC Wiemer, Hanneke W Mensink, Joris Pothof, Annelies de Klein and Emine Kiliç

Cancers (Basel). 2019;11(6)

Abstract

Uveal melanoma (UM) is the most frequently found primary intra-ocular tumor in adults. It is a highly aggressive cancer that causes metastasis-related mortality in up to half of the patients. Many independent studies have reported somatic genetic changes associated with high metastatic risk, such as monosomy of chromosome 3 and mutations in *BAP1*. Still, the mechanisms that drive metastatic spread are largely unknown. This study aimed to elucidate the potential role of microRNAs in the metastasis of UM. Using a next-generation sequencing approach in 26 UM samples we identified thirteen differentially expressed microRNAs between high-risk UM and low/intermediate-risk UM, including the known oncomirs microRNA-17-5p, microRNA-21-5p, and miR-151a-3p. Integration of the differentially expressed microRNAs with expression data of predicted target genes revealed 106 genes likely to be affected by aberrant microRNA expression. These genes were involved in pathways such as cell cycle regulation, EGF signaling and EIF2 signaling. Our findings demonstrate that aberrant microRNA expression in UM may affect the expression of genes in a variety of cancer-related pathways. This implies that some microRNAs can be responsible for UM metastasis and are promising potential targets for future treatment.

Introduction

Uveal melanoma (UM) is an aggressive cancer that arises from melanocytes located in the uveal tract of the eye. Although treatment of primary tumors has a high success rate, up to half of the patients develop metastasis which often results in death within several months[1]. UM display chromosomal aberrations and genetic abnormalities that underlie both the development and metastasis of UM tumors. Most tumors carry a *GNAQ* or *GNA11* mutation. These mutations are considered to be tumor-initiating mutations and do not increase the risk of metastasis[2–4]. UM patients can be stratified into three different metastatic risk groups; those who have a low-, intermediate-, or high-risk of developing metastasis[5].

High-risk UM harbor a mutation in the tumor suppressor gene BRCA-associated protein (*BAP1*), located on chromosome 3[6]. Mutations in this gene often coincide with monosomy 3, resulting in loss of expression of the BAP1 protein. BAP1 is a deubiquitinating enzyme known to be active in several cellular processes such as DNA damage response, apoptosis, and chromatin remodeling[7–9]. Intermediate-risk tumors carry a mutation in the gene-encoding splicing factor 3 subunit 1 (*SF3B1*), which is part of a protein complex involved in pre-mRNA splicing[5,10,11]. *SF3B1* mutations in UM are known to result in aberrantly spliced transcripts that can either be degraded by nonsense-mediated decay or translated into unique, aberrant proteins. Low-risk UM often harbor a mutation in the eukaryotic translation initiation factor 1A (*EIF1AX*) gene, which is involved in the transfer of methionyl initiator tRNA to the small ribosomal subunit during translation[10.]
Besides the classification of UM into different metastatic risk groups based on gene mutations, the disease can also be separated into two subclasses based on mRNA expression analysis. Each subclass has a distinct gene expression profile. Class 2 tumors, which include high-risk UM, have a stem cell-like expression pattern; whereas class 1 tumors, which include low- and intermediate-risk UM, have the transcriptome of a differentiated melanocyte[12].

Another mechanism that is thought to be essential in the development and metastatic progression of a tumor is aberrant expression of microRNAs. MicroRNAs (miRNAs) are small, single-stranded, non-coding RNAs that can regulate gene expression by binding to mRNA[13,14]. Although limited studies of miRNA expression in UM have been done [15–24], the miRNA profiles of the three risk groups and the downstream effects of any aberrant miRNA expression remains unclear. In this study we; therefore, performed small RNA sequencing in UM tissue. Additionally, mRNA sequencing of all UM samples allowed us to determine associations between miRNAs that were differentially expressed and the expression of their putative downstream mRNA-targets. Our aim was to identify miRNAs that might contribute to the invasive and metastatic potential of UM.

Materials and Methods

Tissue Samples

26 patients diagnosed with UM were selected from our Rotterdam Ocular Melanoma Study-group (ROMS) database. The specimens were collected from enucleated eyes between 1995 and 2010 at the Erasmus University Medical Centre and the Rotterdam Eye Hospital (Rotterdam, The Netherlands). Shortly after surgery, half of the tumor was snap-frozen in liquid nitrogen to allow for DNA and RNA extraction. The other half of the eye was formalin-fixed paraffin-embedded and stained with hematoxylin and eosin for routine histological examination by an ophthalmic pathologist to verify neoplastic nature. This study was performed according to the guidelines of the Declaration of Helsinki (MEC-2009-375, 12 November 2009) and informed consents were obtained at the time of diagnosis.

Mutational Analysis

DNA was extracted from fresh tumor tissue using the QIAmp DNA-mini kit (Qiagen, Hilden, Germany) according to the manufacturer's instructions. Mutation analysis of *EIF1AX*, *SF3B1* and *BAP1* was carried out using Sanger sequencing as reported in previous publications[4,25].

Isolation and Sequencing of Small RNA and mRNA

Total RNA was isolated from sections of snap-frozen tumor samples, using the Qiagen miRNeasy isolation kit (Qiagen) according to the manufacturer's manual. The quantity and purity of the RNA was determined using Bioanalyzer (Agilent Genomics, Santa Clara, CA, USA). A total amount of 4 μg RNA (RIN > 7.0) was used for the preparation of the small RNA and larger RNA libraries using the Ion Total RNA-seq kit (Thermofisher Scientific, Waltham, MA, USA) following the manufacturer's protocol. Both RNA libraries were subsequently sequenced with the Ion Proton sequencer (Thermofisher Scientific).

Analysis of the Sequencing Data

Adapter sequences, low quality reads, and reads containing poly-N were removed from the generated RNA sequenced data using the Torrent Suite Software V 4.4.3 (Thermofisher Scientific, Waltham, MA, USA). Reads shorter than 15 nucleotides were removed from downstream analysis in the small RNA dataset. The remaining reads were aligned against a miRBase reference genome using an in-house developed script[26]. Read per million mapped reads (RPM) was applied to quantify the expression of each miRNAs. Differential expression and fold changes of miRNAs between each of the patients sets was determined using the statistical package DEseq, with the cut-off fold discovery rate (FDR) < 0.05 (v.1.32.0)[27.] The miRNAs at low expression levels were removed by requiring an average of at least 250 RPM. Short Time-Series Expression Miner[28], under the K-mean clustering method, was used to perform the miRNA expression clustering analysis. The long sequencing reads (>25 bp) were aligned to the human reference genome (hg19) with TopHat2[29]. Genes at low expression level were removed by the requiring an average of at least 10 RPM. Differentially expressed genes were identified using DEseq[30] with the cut-off FDR < 0.05. Genes were considered to be differentially expressed if they had at least a log2FC of 1.5. The selected resulting genes were used as input for Ingenuity Pathway Analysis (IPA) (Qiagen) for the canonical pathway analysis. All analyses were performed using R statistical environment version 3.5.1.

miRNA Target Gene Prediction and Validation

To obtain functional information from the differentially expressed miRNAs we integrated mRNA expression data with the miRNA expression data by cluster analysis. A list of putative target genes from the differentially expressed miRNAs was composed using miRwalk 3.0[31], Targetscan 7.2[32], Diana micro-T 5.0[33], and miRDB 6.0[34]. Genes were considered to be target genes if they were reported by at least two different prediction algorithms.

Acquisition of TCGA Data

miRNA expression data of 80 UM samples[35] were retrieved from the publicly accessible data repository at the Genomic Data Commons Data Portal (https://portal.gdc.cancer.gov/)

Results

Sample Collection and Analysis

Twenty-six UM patients were enrolled in this study and grouped into three subtypes based on risk of developing metastasis (i.e. disease-free survival (DFS) and mutation sta-

tus). Clinical, molecular, and histopathological characteristics of all patients are listed in Figure 1A. All patients had a choroidal or ciliary body UM, iris UM were excluded. Seven patients showed a mean DFS of 145 months and had an UM harboring an *EIF1AX* mutation. These patients were included in the low-risk group and did not show disease progression. Twelve patients with a mean DFS of 103 months and an *SF3B1* mutated UM were included in the intermediate-risk group. The high-risk group consisted of seven patients with a mean DFS of 28 months, a *BAP1*-mutated tumor, and a negative BAP1 immunohistochemistry (IHC). Within the high-risk UM, all patients died due to metastasis, whereas in the intermediate group three patient were still metastasis-free and died because of other causes. From all 26 samples, mRNA and miRNA sequencing was performed and differentially expressed (DE) miRNA and mRNA were identified (Figure 1B). DE-miRNAs were verified in The Cancer Genome Atlas (TCGA) dataset. The target genes identified by the prediction algorithm analysis that also showed a significant negative correlation with the corresponding miRNA were considered to be a potential miRNA target gene and were used subsequently in the expression network.

A

	Low risk group (n=7)	Intermediate risk group (n=12)	High risk group (n=7)
Age			
Mean ± SD	58 ± 9	50 ± 15	69 ± 14
Gender, N (%)			
Male	5 (71)	5 (42)	1 (14)
Female	2 (29)	7 (58)	6 (86)
Disease free survival			
Mean ± SD	145.1 ± 45.1	103.3 ± 50.6	28.2 ± 9.26
Mutation status, N (%)			
GNAQ	4 (57)	7 (58)	4 (57)
GNA11	3 (43)	5 (42)	3 (43)
EIF1AX	7 (100)	0 (0)	0 (0)
SF3B1	0 (0)	12 (100)	0 (0)
BAP1	0 (0)	0 (0)	7 (100)
Monosomy 3, N (%)			
Present	0 (0)	0 (0)	7 (100)
Absent	7 (100)	11 (92)	0 (0)
NE	0 (0)	1 (8)	0 (0)
BAP1 IHC, N (%)			
Positive	7 (100)	12 (100)	0 (0)
Negative	0 (0)	0 (0)	7 (100)
Metastasis			
Present	0 (0)	9 (75)	7 (100)
Absent	7 (0)	3 (25)	0 (0)

B

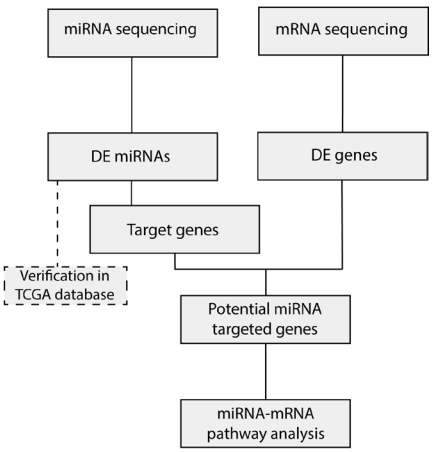

Figure 1. A) The clinical, histological and molecular characteristics of all 26 UM patients **B)** Flowchart indicating the downstream analysis of the miRNA and mRNA sequencing data. Differentially expressed (DE) miRNAs between the high-risk samples and low/intermediate-risk samples were integrated with the DE genes extracted from the mRNA data. Subsequently, pathway analysis was performed in order to identify which canonical pathways were affected by differential miRNA expression.

Identification of Differentially Expressed miRNAs

To investigate which miRNAs might be involved in the metastatic progression of UM, differential count analyses were performed among the three risk groups. We found 423 mature miRNAs to be expressed in UM. To identify samples with a similar miRNA expression, we generated a principal component analysis (PCA) plot based on total miRNA expression. Unsupervised clustering revealed different clusters; one containing the high-risk UM and the other cluster containing low-risk UM (Figure 2A). The intermediate-risk UM were found in a larger cluster that partially overlapped with the other two clusters. Seventeen miRNAs were differentially expressed between high- vs. low-risk UM, 20 DE-miRNAs were identified between high- vs. intermediate-risk UM, and two DE-miRNAs were found between low- vs. intermediate-risk UM (Figure 2B,C and Figure S1). Since we aimed to identify miRNAs involved in the early metastasis of UM, we continued with thirteen miRNAs that were differentially expressed in the high-risk group, compared to the other two groups (Figure 2D). Of these thirteen, five miRNAs were upregulated significantly in high-risk UM and eight miRNAs were downregulated significantly in high-risk UM. Specifically, miRNA 132-5p, 151a-3p, 17-5p, 16-5p, and 21-5p all had a higher

expression in high-risk tumors, whereas miRNA 181b-5p, 101-3p, 378d, 181a-2-3p, 99a-5p, let-7c-5p, 1537-3p, and 99a-3p showed downregulation in the high-risk UM (Figure 2E). The DE-miRNAs were also analyzed in TCGA dataset (Figure S2).

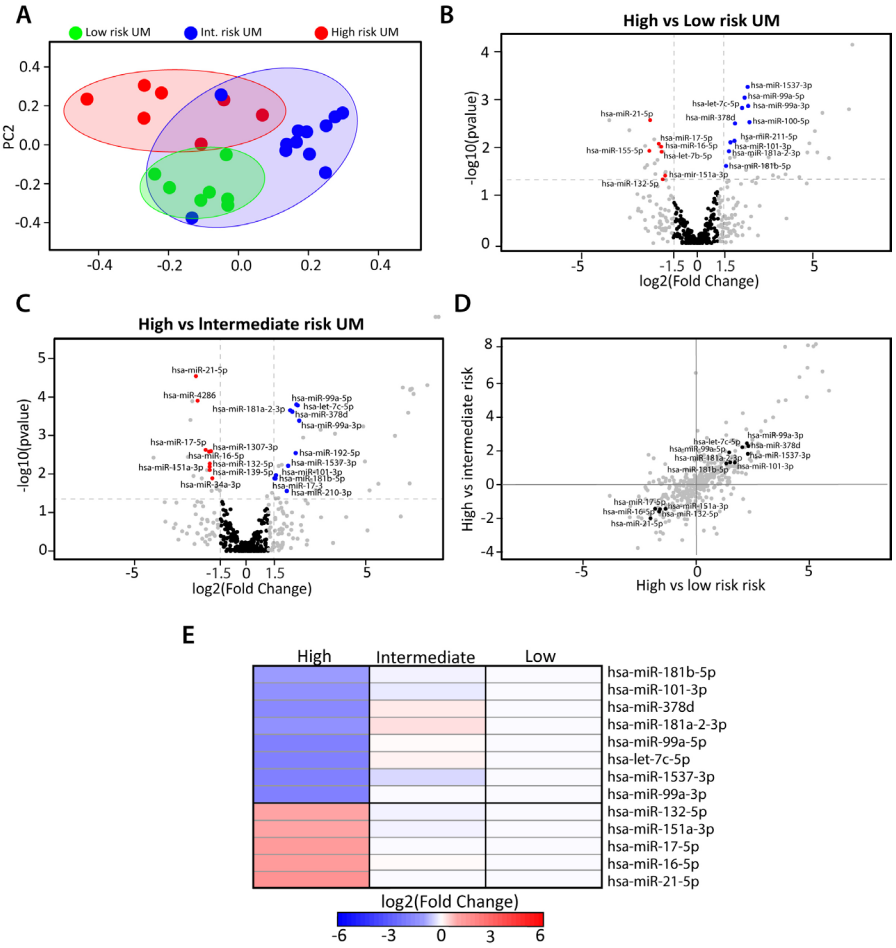

Figure 2. Differential miRNA expression within UM subtypes. **(A)** Principal Component Analysis (PCA) plot showing the unsupervised clustering based on total miRNA expression of all samples. **(B)** Volcano plot indicating which miRNAs are differentially expressed between high- vs. low-risk UM. **(C)** High- vs. intermediate-risk UM. Blue dots indicate downregulation and red dots indicate upregulation of the miRNA **(D)** The correlation between high- vs. low-risk and high- vs. intermediate-risk UM **(E)** Heatmap showing the set of 13 miRNAs identified to be potentially involved in the high-metastatic-risk UM.

Integration of miRNA and mRNA Expression Data Identifies Target Genes

To explore the biological relevance of the differentially expressed miRNAs involved in the metastatic progression of UM, such as their interaction with cancer-related genes, miRNA expression data were integrated with mRNA expression data. We performed mRNA sequencing on all 26 tumors and unsupervised clustering based on total mRNA expression showed a similar clustering as seen with the miRNA data (Figure 3A). The high-risk UM clustered in a separate group, whereas the low and intermediate-risk UM showed a partial overlap. All DE genes (log2FC > 1.5) with a p-value of less than 0.05 were separated into two clusters; one cluster contained all genes that showed downregulation in the high-risk UM and the other group contained the upregulated genes (Figure 3B). From this list, we

subsequently generated a target gene list for each miRNA by using four different prediction algorithms (Figure S3). If a gene was predicted to be a target gene by at least two prediction algorithms and showed anti-correlation with its predicted miRNA, the gene was included into our analysis (n = 106) (Figure 3C).

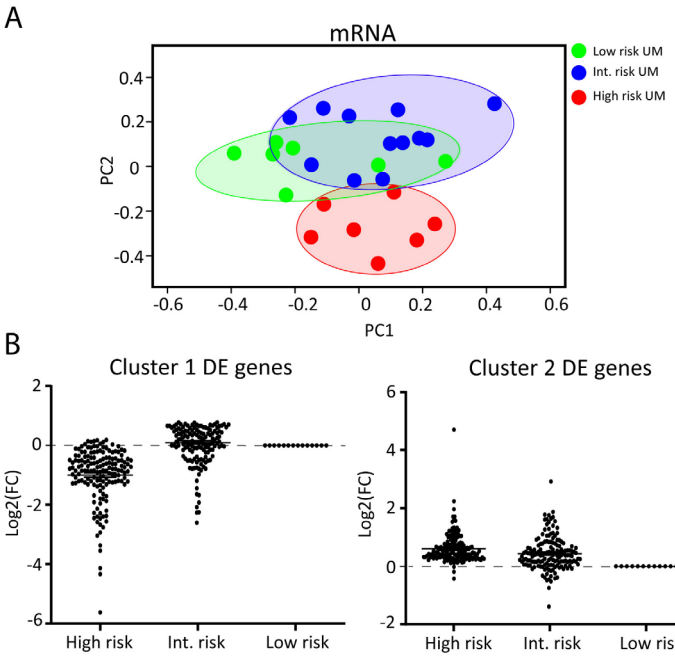

C

miRNA	Target gene
let-7c-5p	CCND2*², CDV3¹, CPEB1¹*, CUX1², DVL3¹, ESPL1², FRMD4B¹, LINGO1², MTDH², PALD1², PARP8², PLEKHA8¹, PPP1R15B², RGS16¹*, RORC¹, SNX6¹, STARD13¹, TMOD2¹
miR-16-5p	CNTN3¹, DIXDC1¹, EXTL3¹, ITPR1¹, KIF1B², MBNL2¹, OTUD4¹, PDK4¹, PHACTR2¹, RNF43², SLC7A2¹, SNRK¹, STOX2¹, TNIK¹, VEGFA², ZMAT3¹*
miR-17-5p	ARAP2¹*, CDC5L², ETV1¹, NR4A3¹*, NTNG1¹, PCDHA6¹, PKD2², TLE4¹, TUSC2¹, SESN3¹
miR-21-5p	AMER1¹*, ARHGAP24², CSRNP3¹, LIFR¹*, MEF2C¹, NKIRAS1¹, PAIP2B¹, PCSK6¹, PDZD2¹, PLAG1¹, SATB1¹, SCN8A¹*, SLC22A15¹, SPRY1¹, ST6GAL1¹, TIMP3¹
miR-99a-5p	FGFR3², TRIB2¹*, ZNF197¹
miR-99a-3p	HLF¹, SFMBT1¹
miR-101-3p	ASAP1², ATAD2B², ATP11B¹, C6orf62¹, C8orf44-SGK3², CDK6², DCBLD2¹, DMD¹, IMPA1², MAGI2¹*, MAP3K13¹, MED20¹, MITF¹*, NR6A1¹, PALM2¹, PCDH20¹, PRPF4B²*, RANBP6²*, SGK3², SH3PXD2A², SORL1², SSBP2¹, *, TRIB1², ZNF532¹
miR-132-5p	ANO10¹, DUSP7¹, PIK3R5¹, PLEKHG5¹
miR-151a-3p	RANBP17², SEC22C¹, ZNF704²
miR-181a-2-3p	ATP8A1¹, BBX¹*, HDAC4²*,OSBPL11¹, PAG1²*, PRICKLE2¹, SALL1²*, ZBTB34¹*, ZFP62², ZYG11B¹
miR-181b-5p	DERL1², FBXL17², KLHL5¹, LMO3¹, MBOAT2², NCALD¹, SRGAP2*, YTHDF3²*
miR-378d	PPP1R12B¹
miR-1537-3p	NSMAF², POU3F1¹, SNX8², SOBP¹, TOP2B¹

Figure 3. Integration of miRNA and mRNA data. **(A)** PCA plot showing the unsupervised clustering of all samples based on total mRNA expression. **(B)** DE genes were clustered according to gene expression pattern. One group contained all genes that showed downregulation in the high-risk group, compared to the low-risk group. The other group contained genes that were upregulated in the high-risk group. **(C)** The predicted target genes that show anti-correlation with a specific DE miRNA. An asterisk indicates that more than one miRNA regulates the gene.

miRNA Target Genes From Several Cancer-Related Pathways

The 106 identified target genes were analyzed by Ingenuity Pathway Analysis (IPA) software, to elucidate which canonical pathways were mainly affected by aberrant miRNA expression (Table S1). One of the most significantly enriched pathways was the cell cycle: G1/S-checkpoint regulation pathway. Moreover, 13 other pathways from

IPA also showed a highly significant enrichment, including fibroblast growth factor signaling, Apelin endothelial signaling, and Leukocyte extravasation signaling (Figure 4A). Four target genes were found to be involved in cell cycle regulation (Figure 4B and Figure S4). MiRNA-101-3p inhibits the cyclin-dependent kinase 6 (CDK6) which regulates the G1/S phase transition by inhibiting RB1. It also targets E2F transcription factor 8 (E2F8), which inhibits the G1/S phase transition. The miRNA let-7c-5p inhibits cyclin D2 (CCND2) which binds to CDK6, in order to activate the protein kinase complex. Histone deacetylase 4 (HDAC4) is being targeted by two different miRNAs; miRNA-1537-5p and microRNA-181a-2-3p. Whereas all other genes are involved in the G1/S phase transition, HDAC is mainly active in the G2/M phase transition.

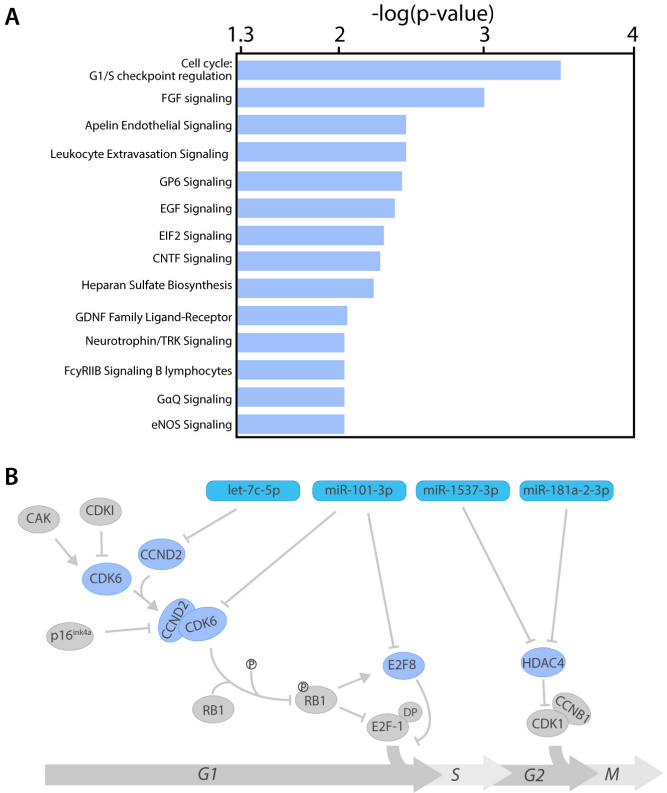

Figure 4. Ingenuity Pathway Analysis. **(A)** Ingenuity pathways with at least three target genes and a log (p-value) above 2. **(B)** A cluster analysis visualizing the involvement of DE-miRNAs in the cell cycle. The light blue nodes indicate genes targeted by DE-miRNAs (darker blue nodes), whereas the grey genes are not.

Discussion

In this study we identified a set of miRNAs that are likely to be involved in the metastatic progression of UM by comparing miRNA expression in high-metastatic-risk UM and low/intermediate-metastatic-risk UM. Hierarchical clustering of total miRNA expression showed three different clusters, which corresponded to metastatic risk. In the UM samples, 423 mature miRNAs were shown to be present, of which 13 miRNAs were differentially expressed between low-, intermediate- or, high-risk UM. MiRNAs that are highly expressed in high-risk UM include several known oncomirs such as miRNA-17-5p[36-38] miRNA-151a-3p[39], and miRNA-21-5p[40-43]. MiRNA-17-5p has been described to promote cell proliferation, invasion, and metastasis through several mechanisms, such as PTEN repression, downregulation of EGFR2, and TGFBR2 targeting. Whereas, miRNA-21-5p and

miR-151a-3p have been shown to be involved in the epithelial-mesenchymal transition necessary for metastasis. However, we also identified two new potential oncomirs; miRNA-16-5p and miRNA-132-5p. Interestingly, miRNA-16-5p has been described to be stably expressed in breast cancer and normal breast tissue[44], indicating that aberrant miRNA expression differs per tumor type. We observed a downregulation of eight miRNAs, of which most are known to function as tumor suppressors. MiRNA-99a-5p has been shown to inhibit cell proliferation in bladder and breast cancer[45,46]. Whereas miRNA-101-3p is involved in suppressing epithelial-to-mesenchymal transition, necessary for metastasis[47-49].

Several studies have investigated miRNA expression in UM, of which most are done in cell lines or very small sample sizes. These studies already identified miRNAs that were shown to be differentially expressed in high-risk UM, such as miRNA-21, miRNA-146b, miRNA-143, miRNA-199a, and miRNA-134[17,23,43]. However, not all of these previously identified miRNAs showed differential expression in our dataset. The lack of overlap between these studies and our results can be explained by the employment of different techniques and different tissues (cell lines versus tumor tissue). The majority of the articles describing the miRNA expression in UM analyze the miRNA expression by microarrays, which is known to produce data that does not fully overlap with RNA sequencing data. Comparing our dataset to The Cancer Genome Atlas (TCGA) dataset, which is the only study that performed miRNA analysis in UM by using next-generation sequencing, we did observe an overlap (e.g., miRNA-21-5p, miR-101-3p, miR-181a-2-3p, miR-181b-5p, let-7c-5p, and miRNA-17-5p)[35]. As shown in Figure S2, the observed fold changes of each miRNA have the same directionality in both studies, but the observed fold changes and corresponding p-values do show some differences. This could be explained by a platform bias, but also by the fact that we could not differentiate in our own analysis of the TCGA dataset between the 3p- and 5p-miRNAs.

In order to determine the downstream effect of the DE-miRNAs, we integrated miRNA data with matching mRNA data containing expression data of target genes by at least two different prediction algorithms. Since miRNAs are known to downregulate or degrade mRNA of their target genes, we only selected genes that were negatively correlated with miRNA expression. Four of these identified target genes (*HDAC4*, *CDK6*, *E2F8*, and *CCND2*) play a crucial role in the regulation of the cell cycle. The development of cancer is tightly linked to changes in the activity of the cell cycle[50]. In normal cells there is a checkpoint between the G1 phase and S phase, in order to regulate proliferation. This checkpoint is controlled by several regulators, such as CDK6[51]. Cancer cells; however, require increased cell division in order to proliferate and invade other tissues and one way to achieve this is by aberrant miRNA expression. Previous research has shown that high metastatic risk UM vastly express Ki-67, a protein that is only present in actively dividing cells, indicating that high-metastatic-risk UM has a greater proliferative activity than low-metastatic-risk UM[52]. Since no UM-specific mutations have been identified in cell cycle-related genes, this indicates that miRNAs probably play a crucial role in cell cycle deregulation in UM. We also observed several target genes to be deregulated in the EIF2 signaling pathway. Protein synthesis is a regulated process in the cell and initiation of translation requires several eukaryotic initiation factors (eIFs), such as eIF2. In cancer cells the function of these eIFs is hampered, inhibiting translation and, thereby, promoting translation of mRNA by alternative mechanisms[43]. Incorrect translation of oncogenes and tumor suppressor genes can promote abnormal proliferation in cancer cells. Restoring these eIFs in UM cells could reduce the oncogenic potential of UM and might; therefore, be an interesting therapeutic target[53].

Another pathway that could affect the metastatic potential of UM cells is epidermal

growth factor (EGF) signaling. Several studies show involvement of aberrant EGF signaling in the development of several cancer types[54]. The EGF pathway plays a crucial role in several cellular processes, such as proliferation, migration, and survival. In addition, the fibroblast growth factor (FGF) pathway contributes to the same cellular processes[56]. All of these processes could make uveal melanocytes more malignant and promote metastasis. However, functional assays in which a specific miRNA is overexpressed or knocked-down in an UM cell line are still needed to investigate to what extent these DE-miRNAs contribute to metastasis. Since one miRNA can target a large number of genes and most studies use target genes identified by online prediction algorithms, it is important to perform these additional experiments. For several miRNAs this has already been done in UM cell lines or other cancer cell lines; overexpressing miRNA-21 in UM cell lines resulted in increased migration and invasion[43]. Whereas inhibition of miRNA-17 suppresses the epithelial-mesenchymal transition in gastric cancer cell lines[57].

Because of their stable nature in tissues and body fluids, it is often suggested that miRNAs are excellent biomarkers for clinical applications. They could serve as early prognosis indicators and as a marker for therapy efficiency[58,59]. In our study we have observed a large number of differentially expressed miRNAs between low/intermediate-risk UM and high-risk UM, indicating that these miRNAs could be used to distinguish between these UM subtypes. However, differentiating between low- and intermediate-risk UM based on miRNAs expression will be challenging, since we only identified two miRNAs to be differentially expressed. The miRNA signature specific for high-risk UM might also be detectable in the plasma of UM patients and could; therefore, be a promising non-invasive biomarker to identify high-risk UM patients. This has already been shown in several cancer types, such as germ-cell tumor[60]. Non-invasive biomarkers will allow us to provide all UM patients, including the patients treated with radiotherapy or proton therapy, with a prognosis and good clinical counselling.

This study shows that miRNAs play an important role in the deregulation of several oncogenic pathways in UM and can, thereby, promote metastatic spreading to distant organs, such as the liver. Differentially expressed miRNAs could be an interesting biomarker for metastatic risk in diagnostics, furthermore it also offers us a promising therapeutic target. Until now, no successful treatment has been developed for metastatic UM. miRNA mimics and molecules targeted at miRNAs (anti-miRs) have shown promising results in preclinical development and could compensate for the upregulation of oncogenic pathways, and thereby aid in UM management and treatment[61-63] .

Conclusion

In this study we elucidated the potential role of miRNAs in the early metastasis of UM by integrating miRNA and mRNA sequencing data derived from 26 UM samples. We showed that differentially expressed miRNAs could play an important role in several oncogenic pathways, such as cell cycle regulation and EGF signaling, which could contribute to the early metastasis of UM. These results do not only bring us one step closer to unraveling the mechanisms that drive UM metastasis, but it also provides us with a promising potential target for future treatment. Targeting these differentially expressed miRNAs could compensate for the deregulation of oncogenic pathways and, thereby, aid in UM treatment.

References

1. Damato, B.; Eleuteri, A.; Taktak, A.F.; Coupland, S.E. Estimating prognosis for survival after treatment of choroidal melanoma. Prog. Retin. Eye Res. 2011, 30, 285–295.
2. Van Raamsdonk, C.D.; Griewank, K.G.; Crosby, M.B.; Garrido, M.C.; Vemula, S.; Wiesner, T.; Obenauf, A.C.; Wackernagel, W.; Green, G.; Bouvier, N., et al. Mutations in gna11 in uveal melanoma. N. Engl. J. Med. 2010, 363, 2191–2199.
3. Van Raamsdonk, C.D.; Bezrookove, V.; Green, G.; Bauer, J.; Gaugler, L.; O'Brien, J.M.; Simpson, E.M.; Barsh, G.S.; Bastian, B.C. Frequent somatic mutations of gnaq in uveal melanoma and blue naevi. Nature 2009, 457, 599–602.
4. Koopmans, A.E.; Vaarwater, J.; Paridaens, D.; Naus, N.C.; Kilic, E.; de Klein, A.; Rotter dam Ocular Melanoma Study, g. Patient survival in uveal melanoma is not affected by oncogenic mutations in gnaq and gna11. Br. J. Cancer 2013, 109, 493–496.
5. Yavuzyigitoglu, S.; Koopmans, A.E.; Verdijk, R.M.; Vaarwater, J.; Eussen, B.; van Bodegom, A.; Paridaens, D.; Kilic, E.; de Klein, A.; Rotterdam Ocular Melanoma Study, G. Uveal melanomas with sf3b1 mutations: A distinct subclass associated with late-onset metastases. Ophthalmology 2016, 123, 1118–1128.
6. Harbour, J.W.; Onken, M.D.; Roberson, E.D.; Duan, S.; Cao, L.; Worley, L.A.; Council, M.L.; Matatall, K.A.; Helms, C.; Bowcock, A.M. Frequent mutation of bap1 in metastasiz ing uveal melanomas. Science 2010, 330, 1410–1413.
7. Farquhar, N.; Thornton, S.; Coupland, S.E.; Coulson, J.M.; Sacco, J.J.; Krishna, Y.; Hei mann, H.; Taktak, A.; Cebulla, C.M.; Abdel-Rahman, M.H., et al. Patterns of bap1 protein expression provide insights into prognostic significance and the biology of uveal mela noma. J. Pathol. Clin. Res. 2018, 4, 26–38.
8. Yu, H.; Mashtalir, N.; Daou, S.; Hammond-Martel, I.; Ross, J.; Sui, G.; Hart, G.W.; Rauscher, F.J., 3rd; Drobetsky, E.; Milot, E., et al. The ubiquitin carboxyl hydrolase bap1 forms a ternary complex with yy1 and hcf-1 and is a critical regulator of gene expression. Mol. Cell Biol. 2010, 30, 5071–5085.
9. Yu, H.; Pak, H.; Hammond-Martel, I.; Ghram, M.; Rodrigue, A.; Daou, S.; Barbour, H.; Corbeil, L.; Hebert, J.; Drobetsky, E., et al. Tumor suppressor and deubiquitinase bap1 promotes DNA double-strand break repair. Proc. Natl. Acad. Sci. USA 2014, 111, 285–290.
10. Martin, M.; Masshofer, L.; Temming, P.; Rahmann, S.; Metz, C.; Bornfeld, N.; van de Nes, J.; Klein-Hitpass, L.; Hinnebusch, A.G.; Horsthemke, B., et al. Exome sequencing identi fies recurrent somatic mutations in eif1ax and sf3b1 in uveal melanoma with disomy 3. Nat. Genet. 2013, 45, 933–936.
11. Harbour, J.W.; Roberson, E.D.; Anbunathan, H.; Onken, M.D.; Worley, L.A.; Bowcock, A.M. Recurrent mutations at codon 625 of the splicing factor sf3b1 in uveal melanoma. Nat. Genet. 2013, 45, 133–135.
12. Onken, M.D.; Worley, L.A.; Ehlers, J.P.; Harbour, J.W. Gene expression profiling in uveal melanoma reveals two molecular classes and predicts metastatic death. Cancer Res. 2004, 64, 7205–7209.
13. Ambros, V. The functions of animal micrornas. Nature 2004, 431, 350–355.
14. Bartel, D.P. Microrna: Target recognition and regulatory functions. Cell 2009, 136, 215–233.
15. Chen, X.; Wang, J.; Shen, H.; Lu, J.; Li, C.; Hu, D.N.; Dong, X.D.; Yan, D.; Tu, L. Epi genetics, microrna, and carcinogenesis: Functional role of microrna-137 in uveal mela noma. Investig. Ophthalmol Vis. Sci. 2011, 52, 1193–1199.
16. Dong, F.; Lou, D. Microrna-34b/c suppresses uveal melanoma cell proliferation and mi gration through multiple targets. Mol. Vis. 2012, 18, 537–546.
17. Larsen, A.C.; Holst, L.; Kaczkowski, B.; Andersen, M.T.; Manfe, V.; Siersma, V.D.; Kolko, M.; Kiilgaard, J.F.; Winther, O.; Prause, J.U., et al. Microrna expression analysis and multi plex ligation-dependent probe amplification in metastatic and non-metastatic uveal mela noma. Acta Ophthalmol 2014, 92, 541–549.
18. Li, Z.; Yu, X.; Shen, J.; Jiang, Y. Microrna dysregulation in uveal melanoma: A new player enters the game. Oncotarget 2015, 6, 4562–4568.
19. Liu, J.; Ma, L.; Li, C.; Zhang, Z.; Yang, G.; Zhang, W. Tumor-targeting trail expression mediated by mirna response elements suppressed growth of uveal melanoma cells. Mol. Oncol. 2013, 7, 1043–1055.
20. Ma, Y.B.; Song, D.W.; Nie, R.H.; Mu, G.Y. Microrna-32 functions as a tumor suppressor and directly targets ezh2 in uveal melanoma. Genet. Mol. Res. 2016, 15, 7935.

21. Ragusa, M.; Barbagallo, C.; Statello, L.; Caltabiano, R.; Russo, A.; Puzzo, L.; Avitabile, T.; Longo, A.; Toro, M.D.; Barbagallo, D., et al. Mirna profiling in vitreous humor, vitreal exosomes and serum from uveal melanoma patients: Pathological and diagnostic implica tions. Cancer Biol. Ther. 2015, 16, 1387–1396.
22. Yan, D.; Zhou, X.; Chen, X.; Hu, D.N.; Dong, X.D.; Wang, J.; Lu, F.; Tu, L.; Qu, J. Microrna-34a inhibits uveal melanoma cell proliferation and migration through downregulation of c-met. Investig. Ophthalmol Vis. Sci. 2009, 50, 1559–1565.
23. Worley, L.A.; Long, M.D.; Onken, M.D.; Harbour, J.W. Micro-rnas associated with metas tasis in uveal melanoma identified by multiplexed microarray profiling. Melanoma Res. 2008, 18, 184–190.
24. Yang, C.; Wei, W. The mirna expression profile of the uveal melanoma. Sci. China Life Sci. 2011, 54, 351–358.
25. Koopmans, A.E.; Verdijk, R.M.; Brouwer, R.W.; van den Bosch, T.P.; van den Berg, M.M.; Vaarwater, J.; Kockx, C.E.; Paridaens, D.; Naus, N.C.; Nellist, M., et al. Clinical signifi cance of immunohistochemistry for detection of bap1 mutations in uveal melanoma. Mod. Pathol. 2014, 27, 1321–1330.
26. Derks, K.W.; Misovic, B.; van den Hout, M.C.; Kockx, C.E.; Gomez, C.P.; Brouwer, R.W.; Vrieling, H.; Hoeijmakers, J.H.; van, I.W.F.; Pothof, J. Deciphering the rna landscape by rnaome sequencing. RNA Biol. 2015, 12, 30–42.
27. Anders, S.; Huber, W. Differential expression analysis for sequence count data. Genome Biol. 2010, 11, R106.
28. Ernst, J.; Bar-Joseph, Z. Stem: A tool for the analysis of short time series gene expression data. BMC Bioinformatics 2006, 7, e191.
29. Kim, D.; Pertea, G.; Trapnell, C.; Pimentel, H.; Kelley, R.; Salzberg, S.L. Tophat2: Accurate alignment of transcriptomes in the presence of insertions, deletions and gene fusions. Genome Biol. 2013, 14, R36.
30. Robinson, M.D.; McCarthy, D.J.; Smyth, G.K. Edger: A bioconductor package for differen tial expression analysis of digital gene expression data. Bioinformatics 2010, 26, 139–140.
31. Sticht, C.; De La Torre, C.; Parveen, A.; Gretz, N. Mirwalk: An online resource for predic tion of microrna binding sites. PLoS. ONE 2018, 13, e0206239.
32. Agarwal, V.; Bell, G.W.; Nam, J.W.; Bartel, D.P. Predicting effective microrna target sites in mammalian mrnas. Elife. 2015, 4, e05005.
33. Maragkakis, M.; Reczko, M.; Simossis, V.A.; Alexiou, P.; Papadopoulos, G.L.; Dalamagas, T.; Giannopoulos, G.; Goumas, G.; Koukis, E.; Kourtis, K., et al. Diana-microt web server: Elucidating microrna functions through target prediction. Nucleic. Acids Res. 2009, 37, 273–276.
34. Wong, N.; Wang, X. Mirdb: An online resource for microrna target prediction and func tional annotations. Nucleic. Acids Res. 2015, 43, 146–152.
35. Robertson, A.G.; Shih, J.; Yau, C.; Gibb, E.A.; Oba, J.; Mungall, K.L.; Hess, J.M.; Uzunan gelov, V.; Walter, V.; Danilova, L., et al. Integrative analysis identifies four molecular and clinical subsets in uveal melanoma. Cancer Cell 2017, 32, 204–220.
36. Qu, Y.; Zhang, H.; Duan, J.; Liu, R.; Deng, T.; Bai, M.; Huang, D.; Li, H.; Ning, T.; Zhang, L., et al. Mir-17-5p regulates cell proliferation and migration by targeting transforming growth factor-beta receptor 2 in gastric cancer. Oncotarget 2016, 7, 33286–33296.
37. Fang, L.; Li, H.; Wang, L.; Hu, J.; Jin, T.; Wang, J.; Yang, B.B. Microrna-17-5p promotes chemotherapeutic drug resistance and tumour metastasis of colorectal cancer by repress ing pten expression. Oncotarget 2014, 5, 2974–2987.
38. Chen, P.; Zhao, H.; Huang, J.; Yan, X.; Zhang, Y.; Gao, Y. Microrna-17-5p promotes gastric cancer proliferation, migration and invasion by directly targeting early growth response 2. Am. J. Cancer Res. 2016, 6, 2010–2020.
39. Daugaard, I.; Sanders, K.J.; Idica, A.; Vittayarukskul, K.; Hamdorf, M.; Krog, J.D.; Chow, R.; Jury, D.; Hansen, L.L.; Hager, H., et al. Mir-151a induces partial emt by regulating e-cadherin in nsclc cells. Oncogenesis 2017, 6, e366.
40. Jiang, Y.; Zhang, M.; Guo, T.; Yang, C.; Zhang, C.; Hao, J. Microrna-21-5p promotes prolif eration of gastric cancer cells through targeting smad7. Onco. Targets Ther. 2018, 11, 4901–4911.
41. Han, M.; Wang, Y.; Liu, M.; Bi, X.; Bao, J.; Zeng, N.; Zhu, Z.; Mo, Z.; Wu, C.; Chen, X. Mir-21 regulates epithelial-mesenchymal transition phenotype and hypoxia-inducible factor-1alpha expression in third-sphere forming breast cancer stem cell-like cells. Cancer Sci.

2012, 103, 1058–1064.
42. Cai, L.; Wang, W.; Li, X.; Dong, T.; Zhang, Q.; Zhu, B.; Zhao, H.; Wu, S. Microrna-21-5p induces the metastatic phenotype of human cervical carcinoma cells in vitro by targeting the von hippel-lindau tumor suppressor. Oncol. Lett. 2018, 15, 5213–5219.
43. Wang, Y.C.; Yang, X.; Wei, W.B.; Xu, X.L. Role of microrna-21 in uveal melanoma cell invasion and metastasis by regulating p53 and its downstream protein. Int. J. Ophthalmol 2018, 11, 1258–1268.
44. Rinnerthaler, G.; Hackl, H.; Gampenrieder, S.P.; Hamacher, F.; Hufnagl, C.; Hauser-Kron berger, C.; Zehentmayr, F.; Fastner, G.; Sedlmayer, F.; Mlineritsch, B., et al. Mir-16-5p is a stably-expressed housekeeping microrna in breast cancer tissues from primary tumors and from metastatic sites. Int. J. Mol. Sci. 2016, 17, 156.
45. Qin, H.; Liu, W. Microrna-99a-5p suppresses breast cancer progression and cell-cycle pathway through downregulating cdc25a. J. Cell Physiol. 2019, 234, 3526–3537.
46. Liu, Y.; Li, B.; Yang, X.; Zhang, C. Mir-99a-5p inhibits bladder cancer cell proliferation by directly targeting mammalian target of rapamycin and predicts patient survival. J. Cell Biochem. 2018.
47. Li, L.; Shao, M.Y.; Zou, S.C.; Xiao, Z.F.; Chen, Z.C. Mir-101-3p inhibits emt to attenuate proliferation and metastasis in glioblastoma by targeting trim44. J. Neurooncol 2019, 141, 19–30.
48. Zheng, F.; Liao, Y.J.; Cai, M.Y.; Liu, T.H.; Chen, S.P.; Wu, P.H.; Wu, L.; Bian, X.W.; Guan, X.Y.; Zeng, Y.X., et al. Systemic delivery of microrna-101 potently inhibits hepatocellular carcinoma in vivo by repressing multiple targets. PLoS. Genet. 2015, 11, e1004873.
49. Zhao, S.; Zhang, Y.; Zheng, X.; Tu, X.; Li, H.; Chen, J.; Zang, Y.; Zhang, J. Loss of mi crorna-101 promotes epithelial to mesenchymal transition in hepatocytes. J. Cell Physiol. 2015, 230, 2706–2717.
50. Hartwell, L.H.; Kastan, M.B. Cell cycle control and cancer. Science 1994, 266, 1821–1828.
51. Tadesse, S.; Yu, M.; Kumarasiri, M.; Le, B.T.; Wang, S. Targeting cdk6 in cancer: State of the art and new insights. Cell Cycle. 2015, 14, 3220–3230.
52. Onken, M.D.; Worley, L.A.; Harbour, J.W. Association between gene expression profile, proliferation and metastasis in uveal melanoma. Curr. Eye Res. 2010, 35, 857–863.
53. Martinez-Salas, E.; Pineiro, D.; Fernandez, N. Alternative mechanisms to initiate transla tion in eukaryotic mrnas. Comp. Funct. Genomics 2012, 2012, 391546.
54. Sharma, D.K.; Bressler, K.; Patel, H.; Balasingam, N.; Thakor, N. Role of eukaryotic initia-tion factors during cellular stress and cancer progression. J. Nucleic. Acids 2016, 2016, 8235121.
55. Normanno, N.; De Luca, A.; Bianco, C.; Strizzi, L.; Mancino, M.; Maiello, M.R.; Carotenu to, A.; De Feo, G.; Caponigro, F.; Salomon, D.S. Epidermal growth factor receptor (egfr) signaling in cancer. Gene 2006, 366, 2–16.
56. Korc, M.; Friesel, R.E. The role of fibroblast growth factors in tumor growth. Curr. Cancer Drug Targets 2009, 9, 639–651.
57. Wu, D.M.; Hong, X.W.; Wang, L.L.; Cui, X.F.; Lu, J.; Chen, G.Q.; Zheng, Y.L. Microrna-17 inhibition overcomes chemoresistance and suppresses epithelial-mesenchymal transition through a dedd-dependent mechanism in gastric cancer. Int. J. Biochem. Cell Biol. 2018, 102, 59–70.
58. Chen, X.; Ba, Y.; Ma, L.; Cai, X.; Yin, Y.; Wang, K.; Guo, J.; Zhang, Y.; Chen, J.; Guo, X., et al. Characterization of micrornas in serum: A novel class of biomarkers for diagnosis of cancer and other diseases. Cell Res. 2008, 18, 997–1006.
59. Mitchell, P.S.; Parkin, R.K.; Kroh, E.M.; Fritz, B.R.; Wyman, S.K.; Pogosova-Agadjanyan, E.L.; Peterson, A.; Noteboom, J.; O'Briant, K.C.; Allen, A., et al. Circulating micrornas as stable blood-based markers for cancer detection. Proc. Natl. Acad Sci. USA 2008, 105, 10513–10518.
60. van Agthoven, T.; Looijenga, L.H.J. Accurate primary germ cell cancer diagnosis using serum based microrna detection (amptsmir test). Oncotarget 2017, 8, 58037–58049.
61. Rupaimoole, R.; Slack, F.J. Microrna therapeutics: Towards a new era for the management of cancer and other diseases. Nat. Rev. Drug Discov. 2017, 16, 203–222.
62. Stenvang, J.; Petri, A.; Lindow, M.; Obad, S.; Kauppinen, S. Inhibition of microrna func tion by antimir oligonucleotides. Silence 2012, 3, e1.
63. Cheng, C.J.; Saltzman, W.M.; Slack, F.J. Canonical and non-canonical barriers facing anti mir cancer therapeutics. Curr. Med. Chem. 2013, 20, 3582–3593.

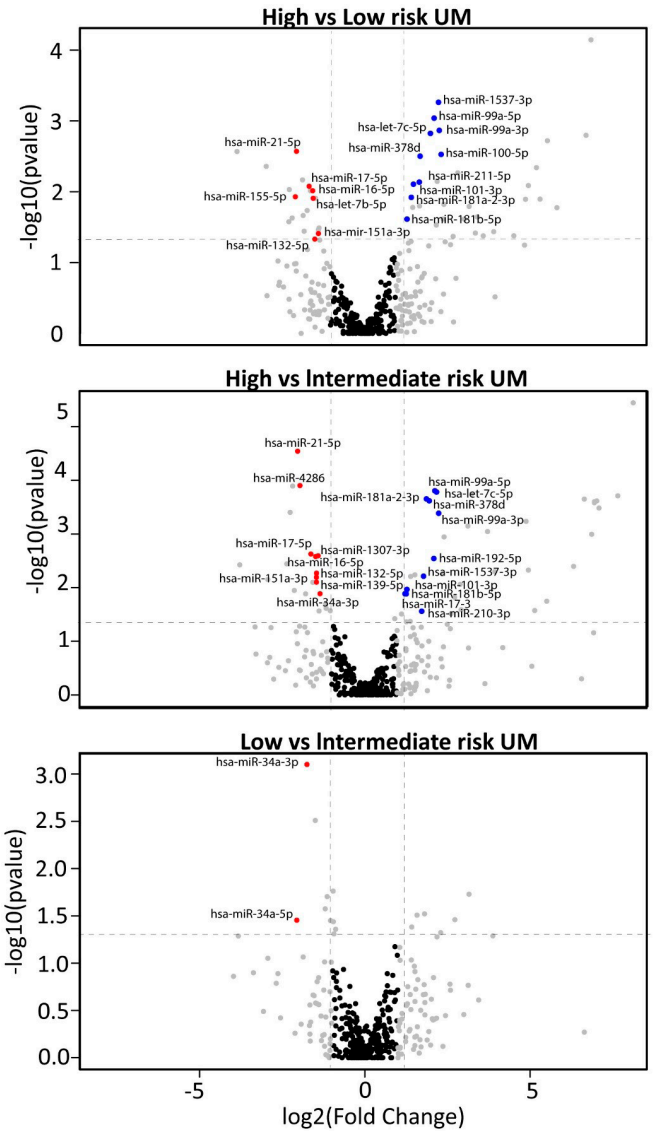

Supplementary Figure 1. Volcano plots indicating the differentially expressed miRNAs between high vs low-risk UM, high vs intermediate-risk UM and low vs intermediate-risk UM upplementary Figure 1. Volcano plots indicating the differentially expressed miRNAs between high vs low-risk UM, high vs intermediate-risk UM and low vs intermediate-risk UM

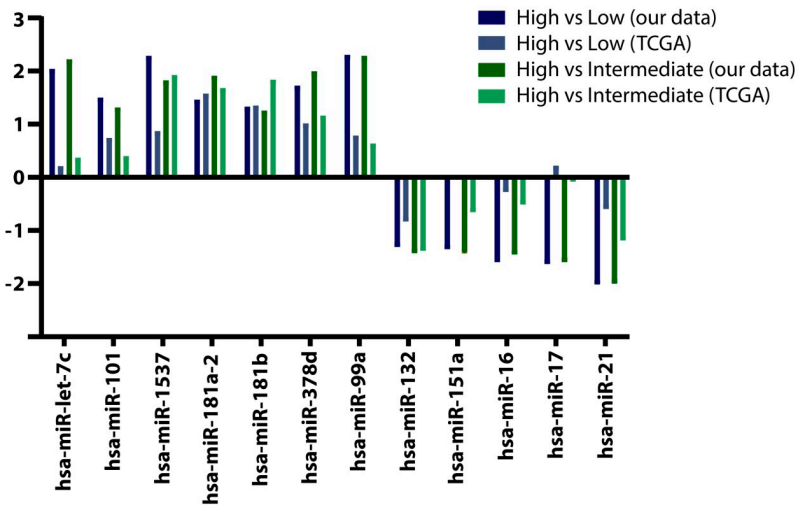

Supplementary Figure 2. miRNA expression analysis of TCGA cohort

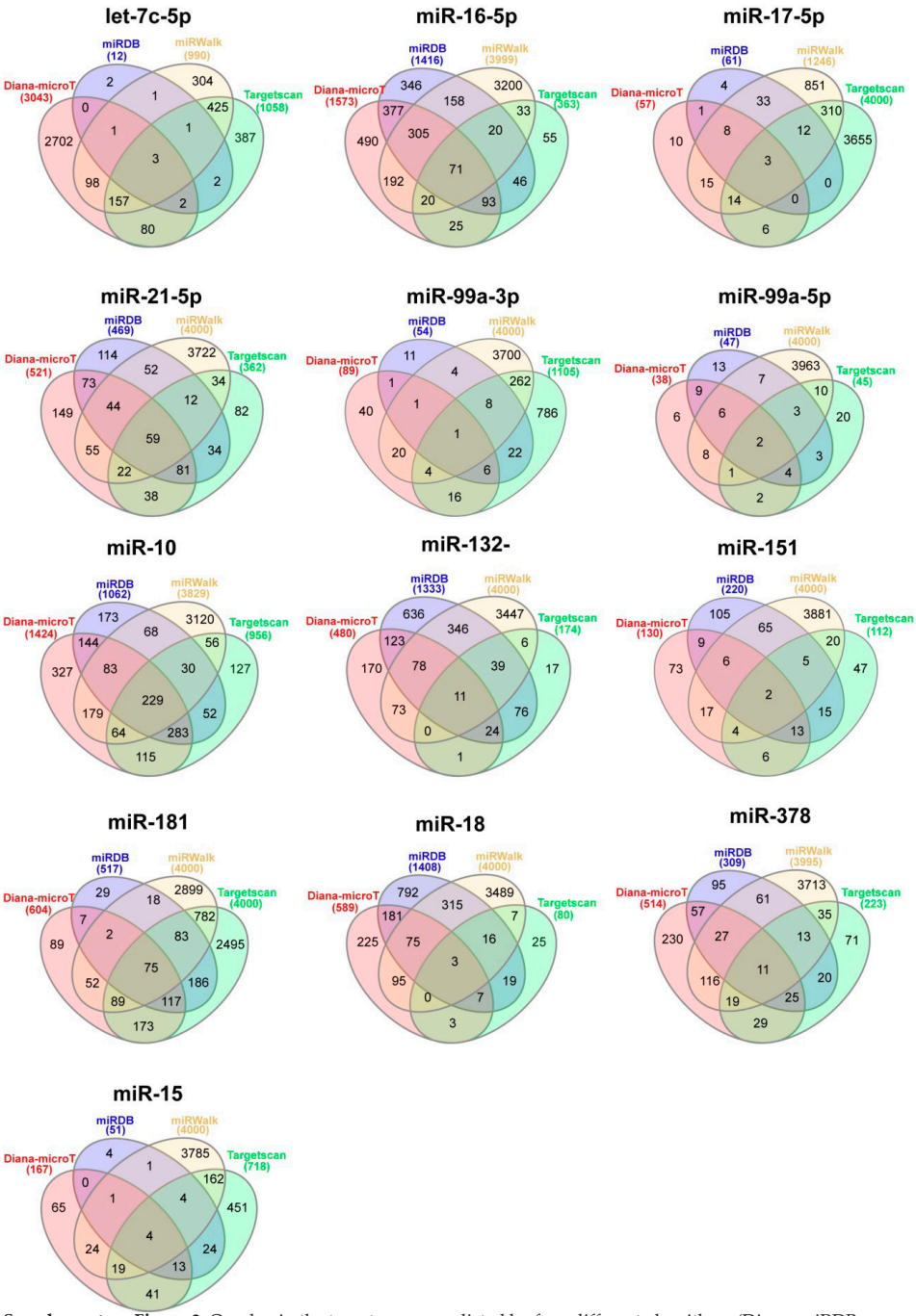

Supplementary Figure 3. Overlap in the target genes predicted by four different algorithms (Diana, miRDB, miRWalk and Targetscan).

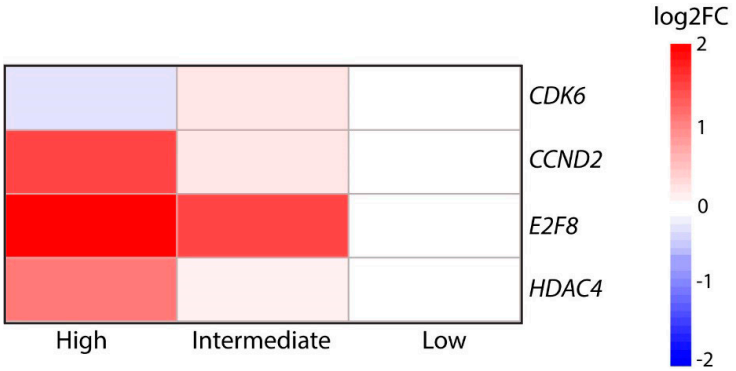

Supplementary Figure 4. Heatmap showing the differential expression of the four cell-cycle related genes; *CDK6*, *CCND2*, *E2F8* and *HDAC4*

Supplementary Table 1. IPA target analysis

Ingenuity Canonical Pathways	-log (pvalue)	Molecules
Chronic Myeloid Leukemia Signaling	3,63E00	FGFR3,HDAC4,PTPN11,CDK6,E2F8
Cell Cycle: G1/S Checkpoint Regulation	3,53E00	HDAC4,CCND2,CDK6,E2F8
Osteoarthritis Pathway	3,27E00	FGFR3,VEGFA,TIMP3,HDAC4,FGF2,MEF2C
Cyclins and Cell Cycle Regulation	3,22E00	HDAC4,CCND2,CDK6,E2F8
Role of NFAT in Cardiac Hypertrophy	3,1E00	FGFR3,HDAC4,PTPN11,CACNB4,MEF2C,ITPR1
Non-Small Cell Lung Cancer Signaling	3,08E00	FGFR3,PTPN11,CDK6,ITPR1
Type II Diabetes Mellitus Signaling	3,06E00	FGFR3,PTPN11,CACNB4,ACSL6,NSMAF
FGF Signaling	3,01E00	FGFR3,PTPN11,FGF2,ITPR1
Endocannabinoid Cancer Inhibition Pathway	3,01E00	FGFR3,VEGFA,CCND2,PTPN11,NSMAF
Glioblastoma Multiforme Signaling	2,77E00	FGFR3,PTPN11,CDK6,ITPR1,E2F8
Nitric Oxide Signaling in the Cardiovascular System	2,65E00	FGFR3,VEGFA,PTPN11,ITPR1
Pancreatic Adenocarcinoma Signaling	2,53E00	FGFR3,VEGFA,PTPN11,E2F8
Glioma Signaling	2,52E00	FGFR3,PTPN11,CDK6,E2F8
Apelin Endothelial Signaling Pathway	2,46E00	FGFR3,HDAC4,PTPN11,MEF2C
Leukocyte Extravasation Signaling	2,45E00	FGFR3,TIMP3,CLDN11,PTPN11,RDX
GP6 Signaling Pathway	2,4E00	FGFR3,PTPN11,COL24A1,ITPR1
EGF Signaling	2,34E00	FGFR3,PTPN11,ITPR1
Corticotropin Releasing Hormone Signaling	2,31E00	VEGFA,CACNB4,MEF2C,ITPR1
EIF2 Signaling	2,3E00	FGFR3,VEGFA,MYCN,PTPN11,AGO4
CNTF Signaling	2,28E00	FGFR3,LIFR,PTPN11
Heparan Sulfate Biosynthesis (Late Stages)	2,24E00	HS3ST3B1,EXTL3,HS3ST5
Hereditary Breast Cancer Signaling	2,19E00	FGFR3,HDAC4,PTPN11,CDK6
Heparan Sulfate Biosynthesis	2,14E00	HS3ST3B1,EXTL3,HS3ST5
Small Cell Lung Cancer Signaling	2,08E00	FGFR3,PTPN11,CDK6
GDNF Family Ligand-Receptor Interactions	2,08E00	FGFR3,PTPN11,ITPR1
Neurotrophin/TRK Signaling	2,07E00	FGFR3,PTPN11,SPRY1
FcγRIIB Signaling in B Lymphocytes	2,04E00	FGFR3,PTPN11,CACNB4
Glioma Invasiveness Signaling	2,04E00	FGFR3,TIMP3,PTPN11
Gαq Signaling	2,03E00	FGFR3,PTPN11,RGS16,ITPR1
eNOS Signaling	2,02E00	FGFR3,VEGFA,PTPN11,ITPR1
Cardiac Hypertrophy Signaling (Enhanced)	2,01E00	FGFR3,HDAC4,PTPN11,FGF2,TNFSF15,MEF2C,ITPR1
Renal Cell Carcinoma Signaling	2	FGFR3,VEGFA,PTPN11
Bladder Cancer Signaling	1,95E00	FGFR3,VEGFA,FGF2
HER-2 Signaling in Breast Cancer	1,93E00	FGFR3,PTPN11,CDK6
VEGF Family Ligand-Receptor Interactions	1,93E00	FGFR3,VEGFA,PTPN11
Ceramide Signaling	1,87E00	FGFR3,PTPN11,NSMAF
Role of NFAT in Regulation of the Immune Response	1,84E00	FGFR3,PTPN11,MEF2C,ITPR1
B Cell Receptor Signaling	1,84E00	FGFR3,PTPN11,PAG1,MEF2C
Xenobiotic Metabolism Signaling	1,83E00	FGFR3,HS3ST3B1,HDAC4,PTPN11,HS3ST5
FAK Signaling	1,81E00	FGFR3,PTPN11,ASAP1
Amyotrophic Lateral Sclerosis Signaling	1,78E00	FGFR3,VEGFA,PTPN11
p53 Signaling	1,78E00	FGFR3,CCND2,PTPN11
Calcium Signaling	1,77E00	HDAC4,CACNB4,MEF2C,ITPR1
UVA-Induced MAPK Signaling	1,77E00	FGFR3,PTPN11,PARP8
VEGF Signaling	1,77E00	FGFR3,VEGFA,PTPN11
Clathrin-mediated Endocytosis Signaling	1,76E00	FGFR3,VEGFA,PTPN11,FGF2
Apelin Cardiomyocyte Signaling Pathway	1,76E00	FGFR3,PTPN11,ITPR1
Neuropathic Pain Signaling In Dorsal Horn Neurons	1,74E00	FGFR3,PTPN11,ITPR1
Mouse Embryonic Stem Cell Pluripotency	1,74E00	FGFR3,LIFR,PTPN11
IL-8 Signaling	1,71E00	FGFR3,VEGFA,CCND2,PTPN11
Breast Cancer Regulation by Stathmin1	1,71E00	FGFR3,PTPN11,ITPR1,E2F8
Role of p14/p19ARF in Tumor Suppression	1,71E00	FGFR3,PTPN11
T Cell Receptor Signaling	1,71E00	FGFR3,PTPN11,PAG1
Synaptogenesis Signaling Pathway	1,7E00	FGFR3,PTPN11,SYT3,CACNB4,ITPR1
Dermatan Sulfate Biosynthesis (Late Stages)	1,69E00	HS3ST3B1,HS3ST5
Telomerase Signaling	1,69E00	FGFR3,HDAC4,PTPN11
IL-9 Signaling	1,68E00	FGFR3,PTPN11
Paxillin Signaling	1,67E00	FGFR3,PTPN11,ITGA8
CREB Signaling in Neurons	1,67E00	FGFR3,PTPN11,CACNB4,ITPR1
iCOS-iCOSL Signaling in T Helper Cells	1,66E00	FGFR3,PTPN11,ITPR1
Chondroitin Sulfate Biosynthesis (Late Stages)	1,64E00	HS3ST3B1,HS3ST5
Myo-inositol Biosynthesis	1,63E00	IMPA1
HIF1α Signaling	1,63E00	FGFR3,VEGFA,PTPN11
Integrin Signaling	1,62E00	FGFR3,PTPN11,ASAP1,ITGA8
fMLP Signaling in Neutrophils	1,6E00	FGFR3,PTPN11,ITPR1
Actin Cytoskeleton Signaling	1,59E00	FGFR3,PTPN11,FGF2,RDX
Renin-Angiotensin Signaling	1,59E00	FGFR3,PTPN11,ITPR1

Role of NANOG in Mammalian Embryonic Stem Cell Pluripotency	1,59E00	FGFR3,LIFR,PTPN11
CD28 Signaling in T Helper Cells	1,58E00	FGFR3,PTPN11,ITPR1
Adipogenesis pathway	1,58E00	FGFR3,HDAC4,FGF2
Role of Tissue Factor in Cancer	1,58E00	FGFR3,VEGFA,PTPN11
STAT3 Pathway	1,58E00	FGFR3,VEGFA,FGF2
Docosahexaenoic Acid (DHA) Signaling	1,56E00	FGFR3,PTPN11
IL-6 Signaling	1,54E00	FGFR3,VEGFA,PTPN11
CCR3 Signaling in Eosinophils	1,53E00	FGFR3,PTPN11,ITPR1
Chondroitin Sulfate Biosynthesis	1,52E00	HS3ST3B1,HS3ST5
Dermatan Sulfate Biosynthesis	1,49E00	HS3ST3B1,HS3ST5
Apelin Pancreas Signaling Pathway	1,49E00	FGFR3,PTPN11
Huntington's Disease Signaling	1,49E00	FGFR3,HDAC4,PTPN11,ITPR1
Axonal Guidance Signaling	1,49E00	FGFR3,VEGFA,NTNG1,PTPN11,SRGAP1,LINGO1
Gα12/13 Signaling	1,49E00	FGFR3,PTPN11,MEF2C
Human Embryonic Stem Cell Pluripotency	1,48E00	FGFR3,PTPN11,FGF2
IL-23 Signaling Pathway	1,48E00	FGFR3,PTPN11
Ephrin A Signaling	1,45E00	FGFR3,PTPN11
Ovarian Cancer Signaling	1,42E00	FGFR3,VEGFA,PTPN11
Pyridoxal 5'-phosphate Salvage Pathway	1,42E00	PRPF4B,CDK6
Melanoma Signaling	1,4E00	FGFR3,PTPN11
UVB-Induced MAPK Signaling	1,38E00	FGFR3,PTPN11
Lymphotoxin β Receptor Signaling	1,37E00	FGFR3,PTPN11
Relaxin Signaling	1,37E00	FGFR3,VEGFA,PTPN11
Molecular Mechanisms of Cancer	1,37E00	FGFR3,CCND2,PTPN11,CDK6,E2F8
Role of IL-17A in Arthritis	1,36E00	FGFR3,PTPN11
ERK5 Signaling	1,34E00	PTPN11,MEF2C
Regulation of eIF4 and p70S6K Signaling	1,34E00	FGFR3,PTPN11,AGO4
Role of Pattern Recognition Receptors in Recognition of Bacteria and Viruses	1,33E00	FGFR3,PTPN11,TNFSF15
PKCθ Signaling in T Lymphocytes	1,32E00	FGFR3,PTPN11,CACNB4
MSP-RON Signaling Pathway	1,32E00	FGFR3,PTPN11
Thrombopoietin Signaling	1,3E00	FGFR3,PTPN11
Endometrial Cancer Signaling	1,3E00	FGFR3,PTPN11
IL-2 Signaling	1,3E00	FGFR3,PTPN11
Aldosterone Signaling in Epithelial Cells	1,3E00	FGFR3,PTPN11,ITPR1

Chapter 3.2

Novel DNA-methylation silenced tumor suppressor genes identified for BAP1-mediated uveal melanoma metastasis

Kyra N Smit, Ruben Boers, Jolanda Vaarwater, Joachim Boers, Tom Brands, Hanneke Mensink, Robert M Verdijk, Wilfred FJ van IJcken, Joost Gribnau, Annelies de Klein and Emine Kiliç

Submitted

Abstract

Purpose: Uveal melanoma (UM) is an aggressive intra-ocular cancer with a strong tendency to metastasize. Metastatic UM is associated with mutations in *BAP1* and *SF3B1*. It is well established that both genetic and epigenetic modifications of the genome, such as methylation, contribute to the development of metastatic traits in tumors. In this study we aim to unravel epigenetic changes that contribute to UM metastasis.

Methods: Using a new genome-wide methylation analysis technique that covers over 50% of all CpG's, we identified aberrant methylation contributing to BAP1 and SF3B1-mediated UM metastasis.

Results: Differentially methylated regions (DMRs) were observed in all chromosomes, however a large number of DMRs was found on chromosomes 1, 8, 12 and 16. To investigate biological relevance of these differentially methylated genes, methylation data was integrated with gene expression data. Between 8-16% of the differentially methylated genes resulted in concurrent altered expression. The aberrantly methylated regions identified in this study include both previously identified DNA-methylation sensitive genes, as well as three novel DNA-methylation silenced tumor suppressor genes; *GSTP1*, *KLF10* and *MEGF10*. Furthermore, we confirmed differential methylation of these tumor suppressor genes in UM metastases from the liver, skin and bone.

Conclusion: Our findings reveal epigenetic modifications and thus aberrant repression of the genes KLF10, GSTP1 and MEGF10 which have previously not been linked to UM metastases. These observations strongly point towards additional layers of complexity at the level of gene expression and its regulation, which may explain the low mutational burden of UM.

Introduction

Uveal melanoma (UM) is an aggressive malignancy that arises from melanocytes located in the uveal tract of the eye. At the time of diagnosis, only a few patients show metastases, however up to half of the UM will eventually metastasize to other organs. Although the primary tumor can be successfully controlled by surgery or radiation therapy and metastatic risk can be reliably predicted in most patients, there are no effective therapies for metastatic UM[1, 2]. Once metastases have been detected disease-related death usually occurs within one year[3]. Metastatic spreading is a complex multi-step process driven by multiple independent (epi)genetic mechanisms. Understanding the specific pathways that initiate and facilitate UM metastasis is essential for the development of a successful treatment.

Metastatic UM is associated with several genetic features, such as loss of chromosome 3 and mutations in BRCA-associated protein 1 (*BAP1*) and splicing factor 3b (*SF3B1*)[4]. UM that harbor a loss of function mutation in *BAP1* often show concurrent loss of chromosome 3, thereby resulting in total loss of the BAP1 protein. BAP1-mediated metastasis typically occurs within 5 years after diagnosis, whereas SF3B1-mediated metastasis can occur up to 15 years after diagnosis[5, 6]. UM that harbor a mutation in eukaryotic transcription initiation factor 1A (*EIF1AX*) rarely metastasize[7]. The genetic alterations that contribute to metastatic spread have been extensively described, however the epigenetic alterations contributing to UM metastasis have been investigated to a lesser extent.

Epigenetic mechanisms, such as DNA methylation, assure the proper regulation of gene expression by altering chromatin accessibility. The human genome exhibits mainly methylation of cytosines in the context of a CpG dinucleotide[8]. Most cancer types show a global reduction of methylated cytosine's, compared to normal tissues[9]. This hypomethylation can contribute to the tumor phenotype by activating oncogenes that are normally silenced by methylation. However, hypomethylation of the gene body can reduce gene expression [10-12]. More striking is the large number of tumor suppressor genes that are inactivated by DNA methylation in their promoter region[13]. Since UM is a disease with relatively few genetic abnormalities[14], epigenetic regulation might play a pivotal role in BAP1 and SF3B1-mediated metastatic spreading of UM .

In recent years, several studies have focused on identifying aberrant methylation in high metastatic risk, *BAP1*-mutated UM. These studies were performed by using bisulphite conversion of the DNA and subsequently analyzed methylation by Sanger sequencing of one specific gene or using an Illumina methylation array chip[14-18]. One shortcoming of the methylation-array is that the design is based on the co-methylation assumption[19]. Probes detect methylation in one CpG and assume that adjacent CpG sites are similarly methylated, which might result in identifying false positives and negatives. Additionally, it has been shown that methylation arrays are not entirely hypothesis-neutral, since the probes are designed to cover CpGs that have been identified as differentially methylated in other studies. Therefore, we analyzed the genome-wide methylome of 26 primary UM and 15 UM metastases in an unbiased manner by making use of a recently developed method; MeD-seq[20]. This assay allows sequencing of only methylated DNA by digesting DNA with the DNA-methylation dependent restriction enzyme LpnPI. More than 50% of the CpG's in the human genome are covered, whereas most commonly used techniques will detect less than 2% of the CpG's.

In this study we aim to identify potential epigenetic mechanisms contributing to BAP1 and SF3B1-mediated metastasis. By performing an integrated genome-wide methylomic and transcriptomic approach (Supplementary Figure 1) we identified novel regions of differential

methylation in metastatic UM, including regions in tumor suppressor genes and confirmed the presence of these DMRs in *BAP1* and *SF3B1*-mutated UM metastases samples as well.

Methods

Sample collection

Twenty-six primary UM samples and 15 UM metastases samples, consisting of three matching sets, were selected from our Rotterdam Ocular Melanoma Study Group (ROMS) database (Supplementary Table 1). All primary tumors were diagnosed as UM and as a primary therapy the eyes were enucleated between 1990 and 2010 at the Department of Ophthalmology, Erasmus MC and the Rotterdam Eye Hospital. Fifteen metastases were obtained from 10 UM patients and were resected from liver, lung or bone at the Department of Ophthalmology, Erasmus MC and the Rotterdam Eye Hospital. All primary tumors were collected as fresh specimens, whereas the UM metastases samples included formalin-fixed, paraffin-embedded (FFPE) and fresh specimens. BAP1 immunohistochemistry, copy number profiling and mutation detection was performed as described previously[21, 22]. This study was approved by the local ethics committee, all patients signed an informed consent and the study was performed according to the guidelines of the Declaration of Helsinki.

DNA isolation and processing

After enucleation, a part of the primary tumor was extracted and DNA was isolated from fresh or fresh-frozen tumor by using the QIAmp DNA mini kit (Qiagen, Hilden, Germany) according to the manufacturer's protocol. All FFPE samples were de-paraffinized and hematoxylin-stained prior to DNA isolation. FFPE-sections were micro-dissected by manually scraping the metastatic UM cells from the sections and sodiumthiocyanate was used to remove the crosslinks formed after fixation. Subsequently, DNA was isolated by using the QIAmp DNA mini kit (Qiagen). DNA concentrations were measured using the Quant-iT Picogreen assay kit (Thermo Fisher Scientific, Grand Island, NY, USA) as described by the manufacturer.

MeD-seq sample preparation

LpnPI (New England Biolabs, Ipswhich, MA, USA) digestions were carried out on DNA samples according to the manufacturer's protocol. Reactions contained 50 ng in 10 µl volume and digestion took place overnight in the absence of enzyme activators. Digests of genomic DNA with LpnPI resulted in snippets of 32 bp around the fully-methylated recognition site that contains CpG. These short fragments were either purified on TBE gel before preparation or purified by Pippin system gel after preparation. Gel purification was performed with 10% TBE gels using the Xcell SureLock system. Sixty microliters of each sample was loaded on the gel, leaving at least one empty well between samples. After running, gels were colored by ethidiumbromide and scanned on a Typhoon Trio. DNA was cut out based on ladder sizes at 30-40 bp and extracted from gel using gelbreaker tubes and centrifugation. DNA was washed with 70% EtOH and dissolved in 10 mM Tris-HCl (pH 8.5). The DNA concentration was determined by the Quant-iT™ High-Sensitivity assay (Life technologies; Q33120) and 50 ng ds DNA was prepared using the ThruPlex DNA-seq 96D kit (Takara Bio Inc, Kusatasu, Japan). For Pippin gel purification, twenty microliters of amplified end product was purified om a Pippin HT system with 3% agarose gel cassettes (Sage Science). Stem-loop adapters were blunt end ligated to repaired input DNA and amplified (4+10 cycles) to include dual indexed barcodes using a high fidelity polymerase to yield an indexed Illumina NGS library. Multiplexed samples were sequenced on Illumina HiSeq2500 systems for single read of 50 base pairs according to the manufacturer's instructions. Dual indexed samples were demultiplexed using bcl2fastq software (Illumina).

MeD-seq data processing

Data processing was carried out as described before[20] using specifically created scripts in Python 2.7.5. In short, raw FASTQ files were subjected to Illumina adaptor trimming and reads were filtered based on LpnPI restriction site occurrence between 13-17 bp from either 5′ of 3′ end of the read. Reads that passed the filter were mapped to hg38 using bowtie 2.1.0. Multiple and unique mapped reads were used to assign read count scores to each individual LpnPI site in the hg38 genome. BAM files were generated using SAMtools for visualization. Gene and CpG island annotations were downloaded from UCSC (hg38). Genome wide individual LpnPI site scores were used to generate read count scores for the following annotated regions: transcription start site (TSS) (1kb before and 1kb after), CpG island and gene body (1kb after TSS until TES).

Med-Seq data analysis

Data analysis was carried out in Python 2.7.5. DMR detected was performed between two datasets containing the regions of interest (TSS, gene body or CpG islands) using the Chi-Squared test on read counts. Significance was called by either Bonferroni or FDR using the Benjamini-Hochberg procedure. Differentially methylated regions were used for unsupervised hierarchical clustering, the Z-score of the read counts was used for normalization and is also shown in the heatmaps. In addition, a genome wide sliding window was used to detect sequentially differentially methylated LpnPI sites. Statistical significance was called between LpnPI sites in predetermined groups using the Chi-squared test and Bonferroni correction. Neighboring significantly called LpnPI sites were binned and reported, DMR threshold was set at a minimum of ten LpnPI sites, a minimum size of 100 bp and either twofold or fivefold change in read counts. Overlap of genome wide detected DMRs was reported for TSS, CpGisland or gene body regions. Annotation overlap for DMRs detected were called on any overlap (partial or total) based on previous described TSS and Genebody region boundaries and CpG Island annotations.

mRNA sequencing

Total RNA was extracted from snap-frozen tumor samples using the Qiagen miRNeasy isolation kit (Qiagen) according to the manufacturer's instructions. The RNA concentration and purity of the RNA was determined using a Bioanalyzer (Agilent Genomics, Santa Clara, CA, USA). Two μg RNA with a minimal RIN-value of 7 was used for the preparation of the RNA library using the Ion Total RNA-sequencing kit (Thermo Fisher Scientific), following the manufacturer's instructions and subsequently sequenced with the Ion Proton sequencer (Thermo Fisher). Sequencing reads larger than 25 bp were aligned to the transcriptome (Homo_sapiens.GRCh37.75.cdna.all.fa) using TopHat2. Normalization of the read counts was performed by using sequencing depths. Genes were considered to be differentially expressed if they had at least a log-2FC of 1.5. All analyses were performed using R statistical environment version 3.3.3

Results

Global methylation profiles within UM

To identify DMRs in metastatic UM, we performed whole-genome sequencing on LpnP1-digested DNA from 26 UM samples. Of these 26 samples; 7 were UM harboring an *EIF1AX* mutation, 12 *SF3B1*-mutated UM, and 7 UM with a *BAP1* mutation (Table 1). Unique DMRs were identified by comparing the total amount of reads generated per group at every LpnpI-site. Examples of these DMRs are the CTF1 promoter-region and the MNX1 gene body in the BAP1 group (Supplementary Figure 2). 757 unique DMRs (FC>2) were identified, of which 169 were specific for the *EIF1AX*-mutated UM, 188 for the *SF3B1*-mutated UM and 400 for the *BAP1*-mutated UM (Figure 1A). The majority of

the DMRs identified in these three groups were located in genes, whereas only 11-19% of the DMRs were intergenic (Figure 1B). Most DMRs showed hypermethylation, as observed in other cancer types, however in the *SF3B1*-mutated group hypomethylation was observed more frequently (36%) than in the other two groups (16% and 6%, respectively).

Table 1. Clinical and molecular characteristics of 26 UM samples

	EIF1AX group	SF3B1 group	BAP1 group
Number			
n=	7	12	7
Metastasis			
yes	-	12	7
no	7	-	-
Disease-free survival (months)			
Mean +/- SD	145.1 +/- 45.1	103.3 +/- 50.6	28.2 +/- 9.26
Chromosome 1			
1p loss	-	6	4
Chromosome 3			
3 loss	-	-	7
Chromosome 6			
6q loss	-	7	-
6p loss	1	-	-
6q gain	3	11	-
6p gain	-	-	-
Chromosome 8			
8q gain	1	7	6
8p loss	1	1	3

Next, we investigated whether certain chromosomes showed enrichment of DMRs. Chromosome 1, 8, 12 and 16 showed a relative high number of DMRs, however these chromosomes did not contain the most significant DMRs (Figure 1A, 1C). Fifty-two DMRs with a FC>5 were selected to perform hierarchical clustering on all UM samples (Supplementary Figure 3), which resulted in one cluster containing all BAP1-mutated samples, whereas the *SF3B1* and *EIF1AX*-mutated samples clustered together in several branches with one outlier harboring an *EIF1AX*-mutation.

Functional implications of DNA methylation changes

Alterations in the accessibility of DNA by methylation can affect gene expression. In order to determine which genes might be affected by differential methylation in a specific region, each DMR location was matched to the corresponding gene promoter, gene body or CpG island according to the UCSC annotations (Hg38). Since approximately 15% of the DMRs were located outside genes, these could not be matched with expression data. To identify methylation changes associated with significant differential gene expression, we performed an integrative analysis with gene expression data from all 26 UM samples. All DMRs located in the promoter or gene body of a gene were used in this analysis.

A

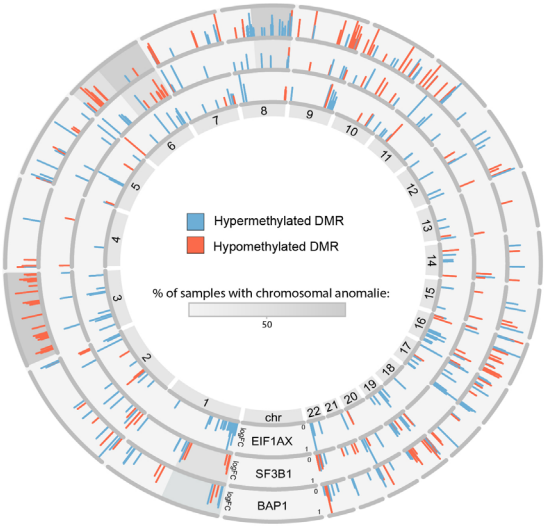

B

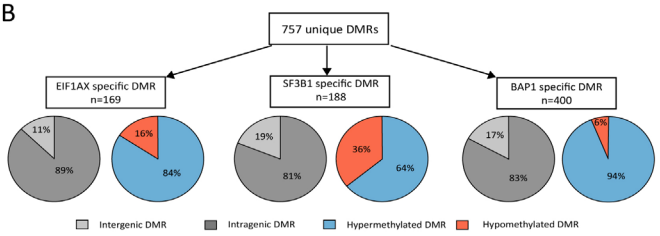

C

Chromosome	1	2	3	4	5	6	7	8	9	10	11	12	13	14	15	16	17	18	19	20	21	22
EIF1AX	17	8	8	1	4	5	5	3	8	3	5	2	2	3	2	10	4	1	4	1	1	3
SF3B1	14	9	2	1	3	12	5	5	3	6	2	3	1	2	1	4	9	0	9	3	2	4
BAP1	3	4	8	2	4	4	5	17	7	5	4	2	1	1	2	12	4	1	7	3	1	3

Figure 1 A) All differentially methylated regions (DMR) visualized per chromosome in a donut plot. The height of the bar indicates the log Fold Change (0-1). Chromosomal anomalies are indicated by the grey scale. The outer ring shows the BAP1 unique DMRs, the middle ring the SF3B1 unique DMRs and the inner ring the EIF1AX unique DMRs. **B)** Quantification of all unique DMRs per group. The genomic location of each DMR is indicated by the grey pie chart, where light grey indicates an intergenic location and dark grey indicates a intragenic location. The amount of methylation of each DMR is shown by the red (hypomethylation) or blue (hypermethylation) pie chart. **C)** The percentage of DMRs per chromosome is shown for each individual group.

Hypomethylated promoter and hypermethylated gene body DMRs were integrated with genes that were shown to be significantly upregulated on mRNA level, whereas hypermethylated promoter and hypomethylated gene body DMRs were matched to downregulated genes[23] (Figure 2A). Larger DMRs that were located in the promoter and at the start of the gene body, were analyzed as promoter-DMRs. Between 8-16% of the DMRs resulted in a gene expression change (Figure 2B). All BAP1 and SF3B1-specific DMRs that show association with mRNA expression are listed in Supplementary Table 2 and 3. The most significant DMRs, that are also associated with gene expression changes, include several cancer-related genes such as *KLF10*, *GSTP1*, *MEGF10*, *SOX8* and *IRX1* (Figure 2C).

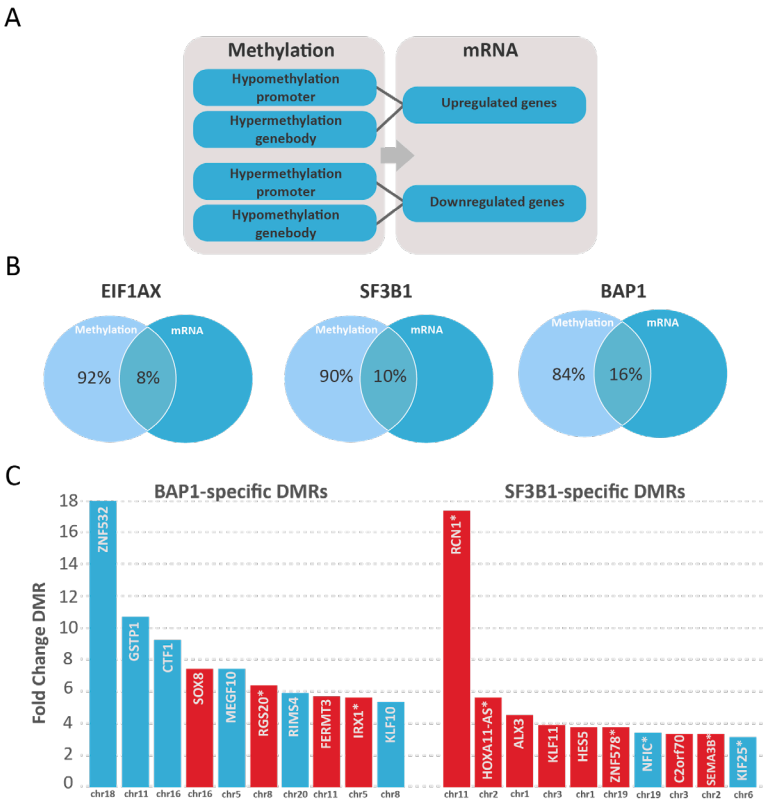

Figure 2 A) Integration of mRNA and methylation data. Upregulated genes were overlapped with DMRs that show promoter hypomethylation or gene body hypermethylation, whereas downregulated genes were overlapped with genes that show promoter hypermethylation or gene body hypomethylation. **B)** The overlap of differential methylation with differential gene expression in the EIF1AX, SF3B1 and BAP1 group. **C)** The top ten most significantly methylated regions specific for the *BAP1*-mutated, early metastasizing UM and the *SF3B1*-mutated, late metastasizing UM. Blue bars indicate downregulated expression, whereas red indicates upregulation of expression. Bars without an asterisk indicate differential methylation in promoters, whereas bars with an asterisk indicate differential methylation in the gene body.

Differential methylation in SF3B1 and BAP1-mutated UM metastases

The methylome of 15 UM metastases was investigated to validate if the identified DMRs were present in UM metastases from liver, skin or bone as well. Tumor cell percentages were determined on HE stained tissue sections by an experienced ocular pathologist and ranged from 30-98% (Supplementary Table 1). Despite this varying tumor cell content and different tissues, unsupervised clustering showed that UM metastases clustered together with either *BAP1* or *SF3B1*-mutated UM implicating that they showed the same secondary driver mutation (Figure 3). Three matched primary tumor and metastases sets were included and clustered in proximity of each other. All identified DMRs that showed correlation with gene expression were validated in the UM metastases. Not all DMRs showed differential methylation in the metastases samples. However, differential methylation of the tumor suppressor genes *KLF10*, *GSTP1* and *MEGF10* and several other genes was observed in the metastases samples as well (Figure 4A and supplementary figure 4). High methylation levels of these genes were associated with a significant worse survival as shown in figure 4B. Whereas *BAP1*-mutated UM mainly showed downregulation of transcription factors, *SF3B1*-mutated UM showed upregulation of the two transcription factors KLF11 and ZNF578 by promoter hypomethylation and gene body hypermethylation,

respectively (Figure 4C).

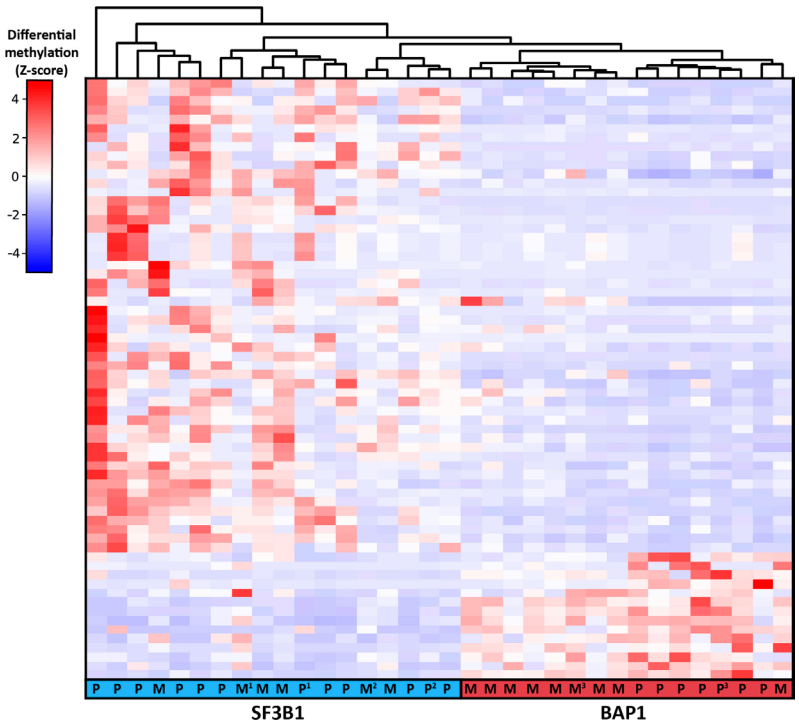

Figure 3. Heatmap visualizing the clustering of primary UM (P) and UM metastases (M). *SF3B1*-mutated primary UM show a similar methylome as *SF3B1*-mutated metastases and the same is observed for the *BAP1*-mutated primary UM and *BAP1*-mutated metastases. Red indicates hypermethylation, whereas blue indicated hypomethylation of the DMR. Matched primary UM and metastases samples are marked by the numbers 1, 2 or 3.

Discussion

Developing a successful treatment for metastatic UM remains one of the most significant challenges in UM research. While current UM research has primarily focused on the genetic factors contributing to UM metastasis, here we aim to elucidate the epigenetic landscape of metastatic UM. We performed MeD-seq, a novel genome-wide sequencing technique with higher coverage and improved distribution compared to most other techniques, to explore associations between aberrant methylation and BAP1 and SF3B1-mutated mediated metastasis[20]. We identified 757 genes affected by differential methylation, of which 188 were found in *SF3B1*-mutated UM and 400 in the BAP1-mutated UM. This shows DNA methylation is most disrupted in *BAP1*-mutated UM, however *SF3B1*-mutated UM also showed significant levels of aberrant methylation and both might therefore profit from treatments regulating methylation activity. We do not exclude the possibility of a fourth group; tumors with non-recurrent mutations might exhibit different methylation patterns, than UM with a mutation in *EIF1AX*, *SF3B1* or *BAP1*.

Interestingly, *SF3B1*-mutated UM contain a larger percentage of hypomethylation, than other UM. It has been shown that *SF3B1* mutations initiate aberrant splicing in a cell, resulting in the formation of aberrantly spliced transcripts[24]. Since aberrant transcripts are often degraded by nonsense-mediated RNA decay and thereby cause downregulation of expression[25]. Changes in methylation in *SF3B1*-mutated UM can be directly caused by downregulation of genes involved in the maintenance of the cells' methylome[26, 27]. One

EIF1AX-mutated sample clustered together with *SF3B1*-mutated samples. We could not detect any mutations in *SF3B1*, however it could be that another spliceosome gene such as *U2AF1* or *SRSF2* is mutated in this sample.

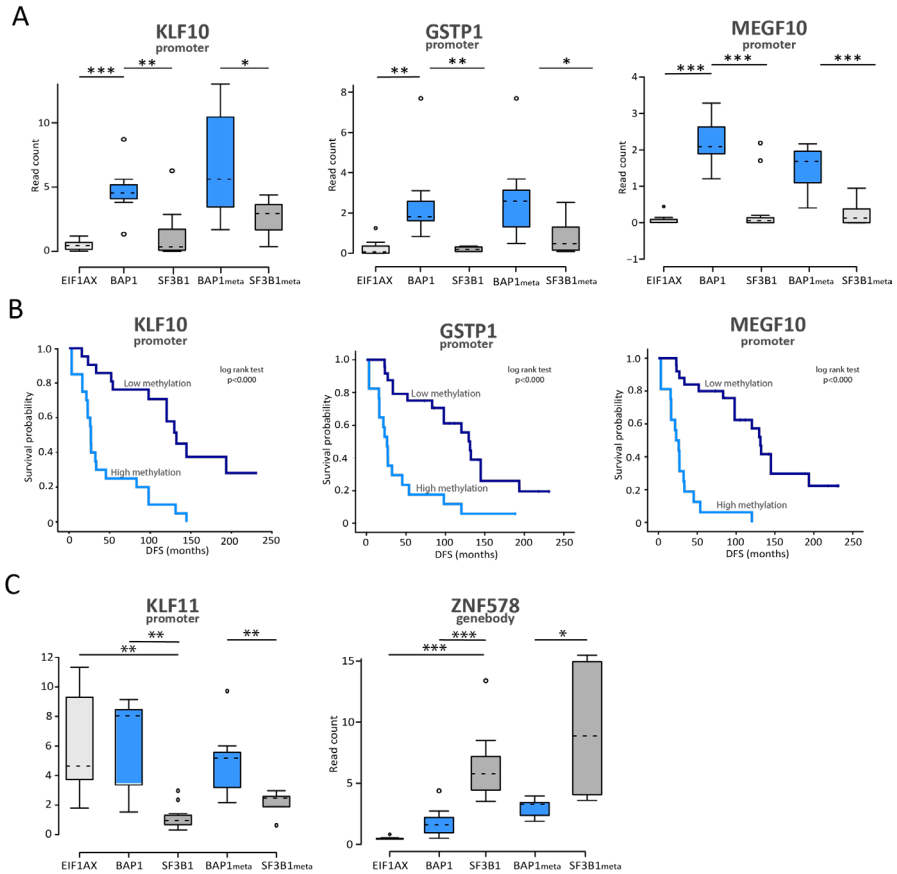

Figure 4. Boxplots showing the normalized read count level, which indicates the level of methylation, for **A)** differentially methylated genes in BAP1-mediated metastasis. **B)** Kaplan-Meier plots showing survival curves for all UM patients stratified based on methylation levels of *KLF10*, *GSTP1*, *MEGF10* **C)** Differentially methylated genes in SF3B1-mediated metastasis. Significance differences between the groups are indicated on the top. *P<0.05, **P<0.01, ***P<0.001.

Integrating methylation data with expression data showed that 8-16% of the DMRs is associated with aberrant gene expression. Approximately 15% of the identified DMRs are located outside genes and could therefore not be matched with expression data. Since our goal was to identify DMRs with functional implications, we only included genes that showed significant differential expression (FC>2). Our obtained results correspond to what is found in other studies; where it was shown that DNA methylation is not limited to active genes, but is often targeting silent genes. DNA methylation ensures that decisions made by transcription factors are stabilized and transcription is precise and robust but limited to the sub-set of genes required[28].

UM is known to harbor several chromosomal alterations, such as loss of chromosome 3 and gain of chromosome 6p and 8q. Chromosome alterations can affect the MeD-seq read counts and these counts could therefore be used to detect chromosomal abnormalities. However, they can also result in the detection of false-positive DMRs. However, by inte-

grating the methylation data with gene expression we excluded the majority of the false positive DMRs from our analysis. A study by Field et al described the methylation pattern in *BAP1*-mutated UM and found a dense cluster of hypermethylated genes on chromosome 3[15]. We also detected a number of DMRs on chromosome 3, however the most significant DMRs that resulted in expression changes were found on other chromosomes.

In metastatic *BAP1*-mutated tumors, we observed increased promoter methylation in the tumor suppressor genes *MEGF10*, *GSTP1* and *KLF10*. These genes showed significant differential methylation in the metastases samples as well. Interestingly, we also observed an association between methylation levels of these genes and DFS. Although these genes are not directly involved in the BAP1-related pathways, an indirect effect of BAP1 on MEGF10, GSTP1 and KLF10 might explain this association. Multiple EGF like domains 10 (*MEGF10*) encodes for a transmembrane protein that is highly expressed in the neural tube during early development. It regulates cell migration and adhesion, such as during patterning of retinal neurons[29]. Recently it has been shown that MEGF10 functions as an important tumor suppressor gene and is often epigenetically repressed in several other cancer types, including high-risk neuroblastoma[30, 31]. Glutathione S-transferase Pi 1 (*GSTP1*) is a gene that regulates lipid and glycolytic metabolism in a cell[32]. It can regulate oncogenic signaling pathways by activating glyceraldehyde-3-phosphate dehydrogenase and it has been reported that the *GSTP1* promoter is often hypermethylated in tumors[33, 34]. Kruppel-like factor 10 (*KLF10*) is a DNA-transcription regulator that binds GC-rich sequences in gene promoters to inhibit growth and initiate apoptosis through TGFβ-signaling. The TGFβ-signaling pathway is known to play an important role in the maintenance of tissue homeostasis by regulating proliferation and apoptosis. Several studies have described a putative tumor suppressor role for *KLF10*[35-37]. Epigenetic repression of KLF10 has been observed to correlate with poor progression in pancreatic cancer[38]. Surprisingly, *SF3B1*-mutated UM showed upregulation of several transcription factors, such as KLF11 and ZNF578. As mentioned previously, upregulation of certain genes through differential methylation might be a direct or indirect consequence of aberrant splicing. Additionally, it has been shown that despite the fact that KLF10 and KLF11 are family members showing a high similarity in their DNA-domains, they have different effects on transcription regulation. KLF10 and KLF11 were originally introduced as transcriptional repressors, however several studies have shown that they can also function as transcriptional activators depending on the cellular context[39]. It has been described for example that KLF11 promotes invasion and migration in gastric cancer through activation of Twist1[40].

Not every DMR that resulted in differential expression could be confirmed in the UM metastases samples. However, this does not mean that they do not contribute to UM metastasis. Firstly, our metastases samples did not consist of a pure population of tumor cells. The non-tumor cells present in UM metastases samples could interfere in the methylation analysis, therefore causing only detection of the highly significant DMRs. Secondly, metastasized UM cells lose a part of their phenotype once they are fully integrated in the hosting organ. Thirdly, UM metastases represent a single cell clone that disseminated early in the development of UM and therefore evolved differently than the primary tumor. The most significant DMR in *BAP1*-mutated primary UM was observed for the zinc-finger transcription factor ZNF532 (Supplementary Table 2); unfortunately, no specific description is available in literature about the function of this gene. Given the strong significance, this might be an interesting gene for future UM research. Other genes that showed demethylation in the *BAP1*-mutated primary UM are *SOX8*, *RGS20*, *IRX1*, *RCN1*. SRY-box 8 (SOX8) and Iroquois homeobox protein 1 (IRX1) are both transcription factors that are involved during embryonal development. Field et al also observed a similar stem-cell like phenotype when investigating the methylome of *BAP1*-mutated UM[15]. Overexpression of

these genes can contribute to cancer by activating genes that induce a more stem cell-like properties in UM cells, which eventually can result in metastasis. Interestingly, metastasizing hepatocellular carcinomas and squamous cell carcinomas show higher expression of SOX8 too[41, 42]. *IRX1* is upregulated in metastasized osteosarcoma[43] and in leukemia, where it predicts worse outcome[44].

Several differentially methylated regions in UM were identified in previous studies, such as *p16ink4a*[45], *TIMP3*[46], *RASSF1A*[16, 18], *TERT*[17], *LZTS1*[47], *EFS*[48] and *PRAME*[49]. Of these previously identified genes *p16ink*, *TERT*, *LZTS1*, *EFS* and *PRAME* were found to be differentially methylated in our analysis as well (data available upon request). However, none showed differential gene expression. A recent whole genome methylation study from Robertson and colleagues[14], identified several genes as differentially methylated, such as *PVT1*, *ENPP2*, *C2orf70*, *DGKB* and *PACSIN3*. In our analysis we only identified *ENPP2* and *C2orf70* to be differentially methylated. These differences can be explained by the techniques used to detect DMRs. In our study, DMR calling is based on a large number of CpGs per gene, whereas HM450 arrays identify differential methylation based on few CpGs per gene. DNA methylation rarely takes place in isolated CpGs and is more likely to affect continuous gene regions containing many CpGs as interrogated by MeD-seq.

The identified differentially methylated regions might be an interesting target for liquid biopsies in UM. Detecting methylated cell-free DNA in the circulation of UM patients could be an indicator for high risk UM, but another important advantage is that it might provide us with an interesting therapeutic target[50, 51]. Unlike mutations in the DNA, methylation on the DNA can be easily reversed by (de)methylating agents. By removing excessive methylation, tumor suppressor genes can be reactivated in tumors which reduces proliferation and migration of tumor cells. Our findings can be interpreted in two ways. It is possible that the mutations in *EIF1AX*, *SF3B1* and *BAP1* initiate de novo methylation and demethylation and thereby promote a series of gene expression changes. Alternatively, the aberrant methylation may arise early in the oncogenic transformation of uveal melanocytes, in which case targeting the methylation might strike the Achilles heel of UM.

Conclusion

We show aberrant DNA methylation in three novel genes, *KLF10*, *GSTP1* and *MEGF10*, that correlate with altered gene expression in UM metastases. We propose a potential epigenetic mechanism in BAP1 and SF3B1-mediated metastasis using a novel approach integrating MeD-seq derived methylation data and gene expression data. Confirming our results in a larger cohort and subsequent biological analysis of the proteins encoded by these aberrantly methylated genes may lead to a better understanding of UM metastasis.

Funding

This study was supported by a grant of the Combined Ophthalmic Research Rotterdam, The Netherlands (CORR 4.2.0). The funding source had no involvement in decisions with regard to study design; data collection, analysis and interpretation.

Conflict of interest statement

The authors declare no conflict of interest of financial interests except for R.B, J.B., W.V.I. and J.G. who report being shareholder in Methylomics B.V., a commercial company that applies MeD-seq to develop methylation markers for cancer staging.

References

1. Damato B: Ocular treatment of choroidal melanoma in relation to the prevention of metastatic death - A personal view. Prog Retin Eye Res 2018, 66:187-199.
2. Virgili G, Gatta G, Ciccolallo L, Capocaccia R, Biggeri A, Crocetti E, Lutz JM, Paci E, Group EW: Incidence of uveal melanoma in Europe. Ophthalmology 2007, 114(12):2309-2315.
3. Augsburger JJ, Correa ZM, Shaikh AH: Effectiveness of treatments for metastatic uveal melanoma. Am J Ophthalmol 2009, 148(1):119-127.
4. Smit KN, Jager MJ, de Klein A, Kili E: Uveal melanoma: Towards a molecular understanding. Prog Retin Eye Res 2019:100800.
5. Yavuzyigitoglu S, Koopmans AE, Verdijk RM, Vaarwater J, Eussen B, van Bodegom A, Paridaens D, Kilic E, de Klein A, Rotterdam Ocular Melanoma Study G: Uveal Melanomas with SF3B1 Mutations: A Distinct Subclass Associated with Late-Onset Metastases. Ophthalmology 2016, 123(5):1118-1128.
6. Harbour JW, Onken MD, Roberson ED, Duan S, Cao L, Worley LA, Council ML, Matatall KA, Helms C, Bowcock AM: Frequent mutation of BAP1 in metastasizing uveal melanomas. Science 2010, 330(6009):1410-1413.
7. Martin M, Masshofer L, Temming P, Rahmann S, Metz C, Bornfeld N, van de Nes J, Klein-Hitpass L, Hinnebusch AG, Horsthemke B et al: Exome sequencing identifies recurrent somatic mutations in EIF1AX and SF3B1 in uveal melanoma with disomy 3. Nat Genet 2013, 45(8):933-936.
8. Bird AP: CpG-rich islands and the function of DNA methylation. Nature 1986, 321(6067):209-213.
9. Gama-Sosa MA, Slagel VA, Trewyn RW, Oxenhandler R, Kuo KC, Gehrke CW, Ehrlich M: The 5-methylcytosine content of DNA from human tumors. Nucleic Acids Res 1983, 11(19):6883-6894.
10. Feng S, Cokus SJ, Zhang X, Chen PY, Bostick M, Goll MG, Hetzel J, Jain J, Strauss SH, Halpern ME et al: Conservation and divergence of methylation patterning in plants and animals. Proc Natl Acad Sci U S A 2010, 107(19):8689-8694.
11. Hellman A, Chess A: Gene body-specific methylation on the active X chromosome. Science 2007, 315(5815):1141-1143.
12. Lister R, Pelizzola M, Dowen RH, Hawkins RD, Hon G, Tonti-Filippini J, Nery JR, Lee L, Ye Z, Ngo QM et al: Human DNA methylomes at base resolution show widespread epigenomic differences. Nature 2009, 462(7271):315-322.
13. Jones PA, Baylin SB: The epigenomics of cancer. Cell 2007, 128(4):683-692.
14. Robertson AG, Shih J, Yau C, Gibb EA, Oba J, Mungall KL, Hess JM, Uzunangelov V, Walter V, Danilova L et al: Integrative Analysis Identifies Four Molecular and Clinical Subsets in Uveal Melanoma. Cancer Cell 2018, 33(1):151.
15. Field MG, Kuznetsov JN, Bussies PL, Cai LZ, Alawa KA, Decatur CL, Kurtenbach S, Harbour JW: BAP1 Loss Is Associated with DNA Methylomic Repatterning in Highly Aggressive Class 2 Uveal Melanomas. Clin Cancer Res 2019.
16. Calipel A, Abonnet V, Nicole O, Mascarelli F, Coupland SE, Damato B, Mouriaux F: Status of RASSF1A in uveal melanocytes and melanoma cells. Mol Cancer Res 2011, 9(9):1187-1198.
17. Moulin AP, Clement G, Bosman FT, Zografos L, Benhattar J: Methylation of CpG island promoters in uveal melanoma. Br J Ophthalmol 2008, 92(2):281-285.
18. Maat W, van der Velden PA, Out-Luiting C, Plug M, Dirks-Mulder A, Jager MJ, Gruis NA: Epigenetic inactivation of RASSF1a in uveal melanoma. Invest Ophthalmol Vis Sci 2007, 48(2):486-490.
19. Stirzaker C, Taberlay PC, Statham AL, Clark SJ: Mining cancer methylomes: prospects and challenges. Trends Genet 2014, 30(2):75-84.
20. Boers R, Boers J, de Hoon B, Kockx C, Ozgur Z, Molijn A, van IW, Laven J, Gribnau J: Genome-wide DNA methylation profiling using the methylation-dependent restriction enzyme LpnPI. Genome Res 2018, 28(1):88-99.
21. Smit KN, van Poppelen NM, Vaarwater J, Verdijk R, van Marion R, Kalirai H, Coupland SE, Thornton S, Farquhar N, Dubbink HJ et al: Combined mutation and copy-number variation detection by targeted next-generation sequencing in uveal melanoma. Mod Pathol 2018, 31(5):763-771.
22. Koopmans AE, Verdijk RM, Brouwer RW, van den Bosch TP, van den Berg MM, Vaarwa-

ter J, Kockx CE, Paridaens D, Naus NC, Nellist M et al: Clinical significance of immunohistochemistry for detection of BAP1 mutations in uveal melanoma. Mod Pathol 2014, 27 (10):1321-1330.
23. Arechederra M, Daian F, Yim A, Bazai SK, Richelme S, Dono R, Saurin AJ, Habermann BH, Maina F: Hypermethylation of gene body CpG islands predicts high dosage of functional oncogenes in liver cancer. Nat Commun 2018, 9(1):3164.
24. Furney SJ, Pedersen M, Gentien D, Dumont AG, Rapinat A, Desjardins L, Turajlic S, Piperno-Neumann S, de la Grange P, Roman-Roman S et al: SF3B1 mutations are associated with alternative splicing in uveal melanoma. Cancer Discov 2013, 3(10):1122-1129.
25. Darman RB, Seiler M, Agrawal AA, Lim KH, Peng S, Aird D, Bailey SL, Bhavsar EB, Chan B, Colla S et al: Cancer-Associated SF3B1 Hotspot Mutations Induce Cryptic 3′ Splice Site Selection through Use of a Different Branch Point. Cell Rep 2015, 13(5):1033-1045.
26. Ostler KR, Davis EM, Payne SL, Gosalia BB, Exposito-Cespedes J, Le Beau MM, Godley LA: Cancer cells express aberrant DNMT3B transcripts encoding truncated proteins. Oncogene 2007, 26(38):5553-5563.
27. Saito Y, Kanai Y, Sakamoto M, Saito H, Ishii H, Hirohashi S: Overexpression of a splice variant of DNA methyltransferase 3b, DNMT3b4, associated with DNA hypomethylation on pericentromeric satellite regions during human hepatocarcinogenesis. Proc Natl Acad Sci U S A 2002, 99(15):10060-10065.
28. Easwaran H, Johnstone SE, Van Neste L, Ohm J, Mosbruger T, Wang Q, Aryee MJ, Joyce P, Ahuja N, Weisenberger D et al: A DNA hypermethylation module for the stem/progenitor cell signature of cancer. Genome Res 2012, 22(5):837-849.
29. Kay JN, Chu MW, Sanes JR: MEGF10 and MEGF11 mediate homotypic interactions required for mosaic spacing of retinal neurons. Nature 2012, 483(7390):465-469.
30. Charlet J, Tomari A, Dallosso AR, Szemes M, Kaselova M, Curry TJ, Almutairi B, Etchevers HC, McConville C, Malik KT et al: Genome-wide DNA methylation analysis identifies MEGF10 as a novel epigenetically repressed candidate tumor suppressor gene in neuroblastoma. Mol Carcinog 2017, 56(4):1290-1301.
31. Huang M, Weiss WA: Neuroblastoma and MYCN. Cold Spring Harb Perspect Med 2013, 3(10):a014415.
32. Louie SM, Grossman EA, Crawford LA, Ding L, Camarda R, Huffman TR, Miyamoto DK, Goga A, Weerapana E, Nomura DK: GSTP1 Is a Driver of Triple-Negative Breast Cancer Cell Metabolism and Pathogenicity. Cell Chem Biol 2016, 23(5):567-578.
33. Fang C, Wei XM, Zeng XT, Wang FB, Weng H, Long X: Aberrant GSTP1 promoter methylation is associated with increased risk and advanced stage of breast cancer: a meta-analysis of 19 case-control studies. BMC Cancer 2015, 15:920.
34. Martignano F, Gurioli G, Salvi S, Calistri D, Costantini M, Gunelli R, De Giorgi U, Foca F, Casadio V: GSTP1 Methylation and Protein Expression in Prostate Cancer: Diagnostic Implications. Dis Markers 2016, 2016:4358292.
35. Mishra VK, Subramaniam M, Kari V, Pitel KS, Baumgart SJ, Naylor RM, Nagarajan S, Wegwitz F, Ellenrieder V, Hawse JR et al: Kruppel-like Transcription Factor KLF10 Suppresses TGFbeta-Induced Epithelial-to-Mesenchymal Transition via a Negative Feedback Mechanism. Cancer Res 2017, 77(9):2387-2400.
36. Weng CC, Hawse JR, Subramaniam M, Chang VHS, Yu WCY, Hung WC, Chen LT, Cheng KH: KLF10 loss in the pancreas provokes activation of SDF-1 and induces distant metastases of pancreatic ductal adenocarcinoma in the Kras(G12D) p53(flox/flox) model. Oncogene 2017, 36(39):5532-5543.
37. Memon A, Lee WK: KLF10 as a Tumor Suppressor Gene and Its TGF-beta Signaling. Cancers (Basel) 2018, 10(6).
38. Chang VH, Chu PY, Peng SL, Mao TL, Shan YS, Hsu CF, Lin CY, Tsai KK, Yu WC, Chang HJ: Kruppel-like factor 10 expression as a prognostic indicator for pancreatic adenocarci noma. Am J Pathol 2012, 181(2):423-430.
39. Spittau B, Krieglstein K: Klf10 and Klf11 as mediators of TGF-beta superfamily signaling. Cell Tissue Res 2012, 347(1):65-72.
40. Ji Q, Li Y, Zhao Q, Fan LQ, Tan BB, Zhang ZD, Zhao XF, Liu Y, Wang D, Jia N: KLF11 promotes gastric cancer invasion and migration by increasing Twist1 expression. Neoplasma 2019, 66(1):92-100.
41. Zhang S, Zhu C, Zhu L, Liu H, Liu S, Zhao N, Wu J, Huang X, Zhang Y, Jin J et al: Oncogenicity of the transcription factor SOX8 in hepatocellular carcinoma. Med Oncol 2014,

31(4):918.
42. Xie SL, Fan S, Zhang SY, Chen WX, Li QX, Pan GK, Zhang HQ, Wang WW, Weng B, Zhang Z et al: SOX8 regulates cancer stem-like properties and cisplatin-induced EMT in tongue squamous cell carcinoma by acting on the Wnt/beta-catenin pathway. Int J Cancer 2018, 142(6):1252-1265.
43. Kuhn A, Loscher D, Marschalek R: The IRX1/HOXA connection: insights into a novel t(4;11)- specific cancer mechanism. Oncotarget 2016, 7(23):35341-35352.
44. Lu J, Song G, Tang Q, Zou C, Han F, Zhao Z, Yong B, Yin J, Xu H, Xie X et al: IRX1 hypomethylation promotes osteosarcoma metastasis via induction of CXCL14/NF-kappaB signaling. J Clin Invest 2015, 125(5):1839-1856.
45. van der Velden PA, Metzelaar-Blok JA, Bergman W, Monique H, Hurks H, Frants RR, Gruis NA, Jager MJ: Promoter hypermethylation: a common cause of reduced p16(INK4a) expression in uveal melanoma. Cancer Res 2001, 61(13):5303-5306.
46. van der Velden PA, Zuidervaart W, Hurks MH, Pavey S, Ksander BR, Krijgsman E, Frants RR, Tensen CP, Willemze R, Jager MJ et al: Expression profiling reveals that methylation of TIMP3 is involved in uveal melanoma development. Int J Cancer 2003, 106(4):472-479.
47. Onken MD, Worley LA, Harbour JW: A metastasis modifier locus on human chromosome 8p in uveal melanoma identified by integrative genomic analysis. Clin Cancer Res 2008, 14(12):3737-3745.
48. Neumann LC, Weinhausel A, Thomas S, Horsthemke B, Lohmann DR, Zeschnigk M: EFS shows biallelic methylation in uveal melanoma with poor prognosis as well as tissue-specific methylation. BMC Cancer 2011, 11:380.
49. Field MG, Durante MA, Decatur CL, Tarlan B, Oelschlager KM, Stone JF, Kuznetsov J, Bowcock AM, Kurtenbach S, Harbour JW: Epigenetic reprogramming and aberrant expression of PRAME are associated with increased metastatic risk in Class 1 and Class 2 uveal melanomas. Oncotarget 2016, 7(37):59209-59219.
50. Esteller M: DNA methylation and cancer therapy: new developments and expectations. Curr Opin Oncol 2005, 17(1):55-60.
51. Cheng JC, Weisenberger DJ, Gonzales FA, Liang G, Xu GL, Hu YG, Marquez VE, Jones PA: Continuous zebularine treatment effectively sustains demethylation in human bladder cancer cells. Mol Cell Biol 2004, 24(3):1270-1278.

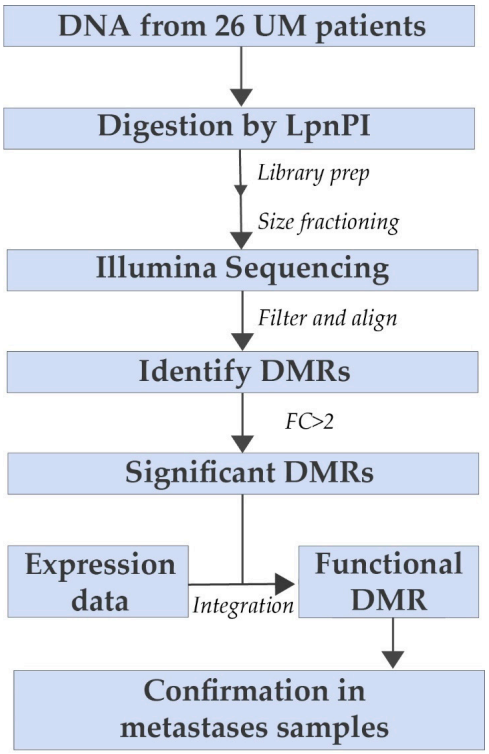

Supplementary Figure 1. Flowchart showing the different steps taken to identify methylation associated with SF3B1 and BAP1-mediated metastases

Supplementary Table 1. Clinical and molecular characteristics of the 26 primary UM and 15 metastases

	Primary or meta	Mutation	DFS (months)	Metastasized	BAP1 IHC	Chr 1	Chr 3	Chr 6	Chr 8	Tumor cell percentage	Location	Material
UM1	Primary	*EIF1AX*	188,4	N	Positive			+p		~ 100%	Eye	Fresh
UM2	Primary	*EIF1AX*	230,7	N	Positive				+	~ 100%	Eye	Fresh
UM3	Primary	*EIF1AX*	218,1	N	Positive					~ 100%	Eye	Fresh
UM4	Primary	*EIF1AX*	231,7	N	Positive					~ 100%	Eye	Fresh
UM5	Primary	*EIF1AX*	111,9	N	Positive			+		~ 100%	Eye	Fresh
UM6	Primary	*EIF1AX*	141,7	N	Positive			+p		~ 100%	Eye	Fresh
UM7	Primary	*EIF1AX*	73,2	N	Positive			+		~ 100%	Eye	Fresh
UM8	Primary	*SF3B1*	23.2	Y	Positive	+q		+p/-q	-p	~ 100%	Eye	Fresh
UM9	Primary	*SF3B1*	33.4	Y	Positive			+p/-q	+q	~ 100%	Eye	Fresh
	Meta	SF3B1			Negative	?	?	?	?	72%	Bone	FFPE
UM10	Primary	*SF3B1*	51,9	Y	Positive	-p	-	+p		~ 100%	Eye	Fresh
UM11	Primary	*SF3B1*	102,6	Y	Positive	-p		+p	+q	~ 100%	Eye	Fresh
UM12	Primary	*SF3B1*	129,6	Y	Positive				+q	~ 100%	Eye	Fresh
UM13	Primary	*SF3B1*	120,3	Y	Positive	-p		+p/-q	+	~ 100%	Eye	Fresh
	Meta	SF3B1		Y	Positive	-p				30%	Liver	Fresh
UM14	Primary	*SF3B1*	144,7	Y	Positive	-p		+p/-q		~ 100%	Eye	Fresh
UM15	Primary	*SF3B1*	83,2	Y	Positive	-p		+p/-q		~ 100%	Eye	Fresh
UM16	Primary	*SF3B1*	105,1	Y	Positive	+q	-q	+p	+q	~ 100%	Eye	Fresh
UM17	Primary	*SF3B1*	132,2	Y	Positive		-q	+p/-q		~ 100%	Eye	Fresh
UM18	Primary	*SF3B1*	193,6	Y	Positive			+p	+q	~ 100%	Eye	Fresh
UM19	Primary	*SF3B1*	131,2	Y	Positive	-p		+p/-q	+	~ 100%	Eye	Fresh
UM20	Primary	*BAP1*	54,4	Y	Negative		-			~ 100%	Eye	Fresh
UM21	Primary	*BAP1*	32,4	Y	Negative	-p	-		+q	~ 100%	Eye	Fresh
UM22	Primary	*BAP1*	15,9	Y	Negative		-		-p/+q	~ 100%	Eye	Fresh
UM23	Primary	*BAP1*	26,9	Y	Negative		-		-p/+q	~ 100%	Eye	Fresh
	Meta	NE			Negative		-		-p/+q	70%	Liver	Fresh
UM24	Primary	*BAP1*	26,1	Y	Negative		-		-p/+q	~ 100%	Eye	Fresh
UM25	Primary	*BAP1*	21,4	Y	Negative	-p	-		+q	~ 100%	Eye	Fresh
UM26	Primary	*BAP1*	27,1	Y	Negative	-p	-		+q	~ 100%	Eye	Fresh
UM27	Meta	SF3B1	98	Y	Positive	-p/+q	+p/-q	-q	-p	96%	Liver	Fresh
	Meta	SF3B1			Positive	-p/+q	+p/-q	-q	-p	NE	Liver	Fresh
	Meta	SF3B1			Positive	-p/+q	-q	-q	-p	NE	Pancreas	Fresh
UM28	Meta	SF3B1	144,7	Y	Positive	-p	+p/-q			94%	Liver	FFPE
UM29	Meta	BAP1	22,9	Y	Negative		-	+p/-q	-p/+q	70%	Liver	Fresh
UM30	Meta	BAP1	23	Y	Negative		-		-p/+q	50%	Liver	Fresh
UM31	Meta	BAP1	53,9	Y	Negative		-			52%	Liver	Fresh
UM32	Meta	BAP1	16,3	Y	Negative	-p	-		+q	70%	Liver	Fresh
	Meta	BAP1			Negative		-		+q	70%	Skin	Fresh
UM33	Meta	BAP1	3,2	Y	Negative	-p	-	-q	-p/+q	76%	Liver	Fresh
	Meta	BAP1			NE	-p	-	-q	-p/+q	62%	Skin	Fresh
	Meta	BAP1			NE	-p	-	-q	-p/+q	80%	Skin	Fresh

NE; not evaluated

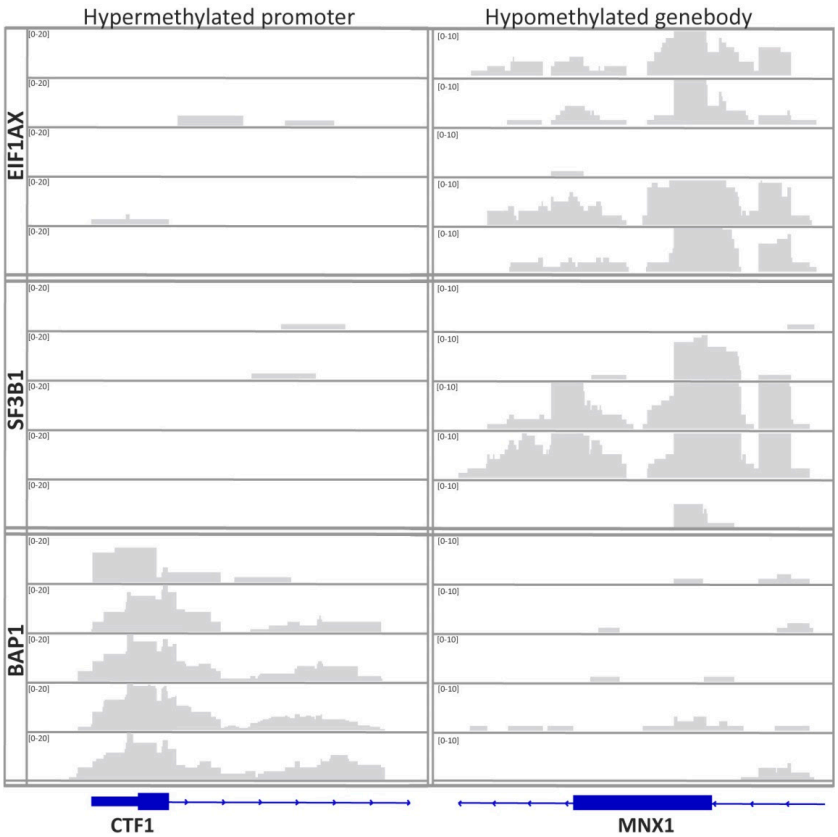

Supplementary Figure 2. *CTF1* promoter hypermethylation and *MNX1* genebody hypomethylation in *BAP1*-mutated UM compared to *SF3B1* and *EIF1AX*-mutated UM. From top to bottom the following samples are shown: UM1 – UM5, UM8 – UM12 and UM21 – UM25.

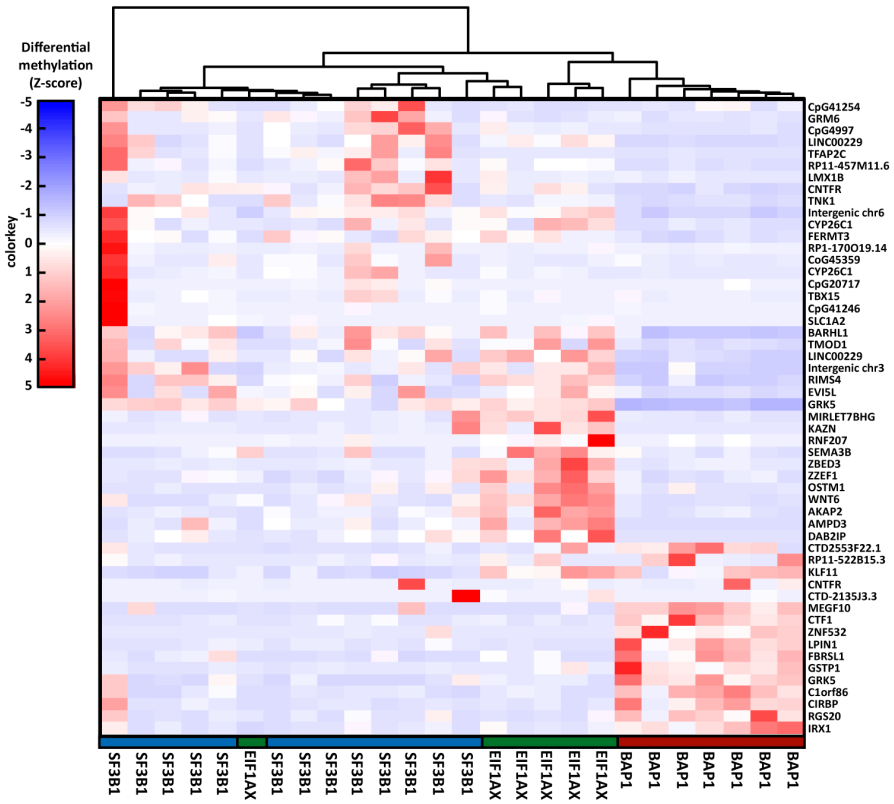

Supplementary Figure 3. Heatmap showing the most significant DMRs (FC>5) in *BAP1*-mutated, *SF3B1*-mutated and *EIF1AX*-mutated primary UM. Red indicates hypermethylation, whereas blue indicated hypomethylation of the DMR.

Supplementary Table 2. BAP1-specific DMRs that cause a significant gene expression change

Gene	Chromosome	Location DMR	Type of methylation	FC DMR	Expression
ZNF532	18	Promoter	Hypermethylation	17.6	Downregulated
GSTP1	11	Promoter	Hypermethylation	10.3	Downregulated
CTF1	16	Promoter	Hypermethylation	8.8	Downregulated
SOX8	16	Promoter	Hypomethylation	7	Upregulated
MEGF10	5	Promoter	Hypermethylation	7	Downregulated
RGS20	8	Genebody	Hypermethylation	6	Upregulated
RIMS4	20	Promoter	Hypomethylation	5.5	Downregulated
FERMT3	11	Promoter	Hypomethylation	5.3	Upregulated
IRX1	5	Genebody	Hypermethylation	5.2	Downregulated
KLF10	8	Promoter	Hypermethylation	4.9	Downregulated
CMSS1	3	Genebody	Hypomethylation	4.7	Upregulated
ZNF517	8	Genebody	Hypermethylation	4.6	Downregulated
SHC4	15	Promoter	Hypermethylation	4.6	Downregulated
RCOR2	11	Promoter	Hypomethylation	4.4	Upregulated
NECAB2	16	Promoter	Hypomethylation	4	Upregulated
FZD6	8	Promoter	Hypermethylation	4	Downregulated
DMRT2	9	Genebody	Hypomethylation	4	Downregulated
ZFP57	6	Promoter	Hypomethylation	3.8	Upregulated
PITX2	4	Genebody	Hypermethylation	3.7	Downregulated
ENPP2	8	Promoter	Hypermethylation	3.6	Downregulated
FAM195A	16	Genebody	Hypermethylation	3.5	Upregulated
ELFN1-AS	7	Promoter	Hypomethylation	3.4	Upregulated
TMC6	17	Genebody	Hypermethylation	3.2	Upregulated
RUSC2	9	Genebody	Hypermethylation	2.9	Upregulated
LINC01234	12	Genebody	Hypomethylation	2.9	Downregulated
ZC3H3	8	Genebody	Hypermethylation	2.8	Upregulated
FLYWCH	16	Genebody	Hypermethylation	2.8	Upregulated
COL9A3	20	Genebody	Hypermethylation	2.8	Upregulated
EIF2B5	3	Genebody	Hypomethylation	2.8	Downregulated
ARHGAP21	10	Promoter	Hypermethylation	2.7	Downregulated
TNFRSF1B	1	Promoter	Hypomethylation	2.6	Upregulated
SLC9A3	5	Genebody	Hypomethylation	2.6	Downregulated
EFS	14	Promoter	Hypermethylation	2.5	Downregulated
SGK1	6	Promoter	Hypomethylation	2.3	Upregulated
MROH6	8	Genebody	Hypermethylation	2.3	Upregulated
NAT14	19	Genebody	Hypermethylation	2.3	Upregulated
MAP4	3	Genebody	Hypomethylation	2.3	Downregulated
SLC22A20	11	Genebody	Hypomethylation	2.2	Downregulated
RAB40C	16	Genebody	Hypermethylation	2.2	Upregulated
IFT140	16	Genebody	Hypermethylation	2.2	Upregulated
CACNA1H	16	Genebody	Hypermethylation	2.2	Upregulated
IGSEQ1	3	Genebody	Hypomethylation	2.2	Downregulated
ZNF296	19	Promoter	Hypomethylation	2.1	Upregulated
KIFC2	8	Genebody	Hypermethylation	2.1	Upregulated
PARP10	8	Genebody	Hypermethylation	2.1	Upregulated
CHD7	8	Genebody	Hypermethylation	2.1	Upregulated
EFEMP2	11	Promoter	Hypermethylation	2.1	Downregulated
RBM15B	3	Genebody	Hypomethylation	2.1	Downregulated
AC024560.2	3	Genebody	Hypomethylation	2.1	Downregulated
WNK2	9	Promoter	Hypomethylation	2	Upregulated
BAIAP2	17	Genebody	Hypermethylation	2	Upregulated
PCDHA1-13	5	Genebody	Hypomethylation	2	Downregulated
ZBTB47	3	Genebody	Hypomethylation	2	Downregulated

Supplementary Table 2. SF3B1-specific DMRs that cause a significant gene expression change

Gene	Chromosome	Location DMR	Type of methylation	FC DMR	Expression
RCN1	11	Genebody	Hypermethylation	17	Upregulated
HOXA11-AS	2	Genebody	Hypermethylation	5.2	Upregulated
ALX3	1	Promoter	Hypomethylation	4.1	Upregulated
KLF11	3	Promoter	Hypomethylation	3.5	Upregulated
HES5	1	Promoter	Hypomethylation	3.3	Upregulated
ZNF578	19	Genebody	Hypermethylation	3.3	Upregulated
NFIC	19	Genebody	Hypomethylation	3	Downregulated
C2orf70	2	Promoter	Hypomethylation	2.9	Upregulated
SEMA3B	3	Genebody	Hypermethylation	2.9	Upregulated
KIF25	6	Genebody	Hypomethylation	2.7	Downregulated
ITGA5	12	Promoter	Hypermethylation	2.6	Downregulated
SLC9A3R2	16	Genebody	Hypomethylation	2.5	Downregulated
PCAT7	9	Promoter	Hypomethylation	2.4	Upregulated
TMEM151B	6	Genebody	Hypermethylation	2.1	Upregulated
AGPAT4	6	Genebody	Hypomethylation	2	Downregulated

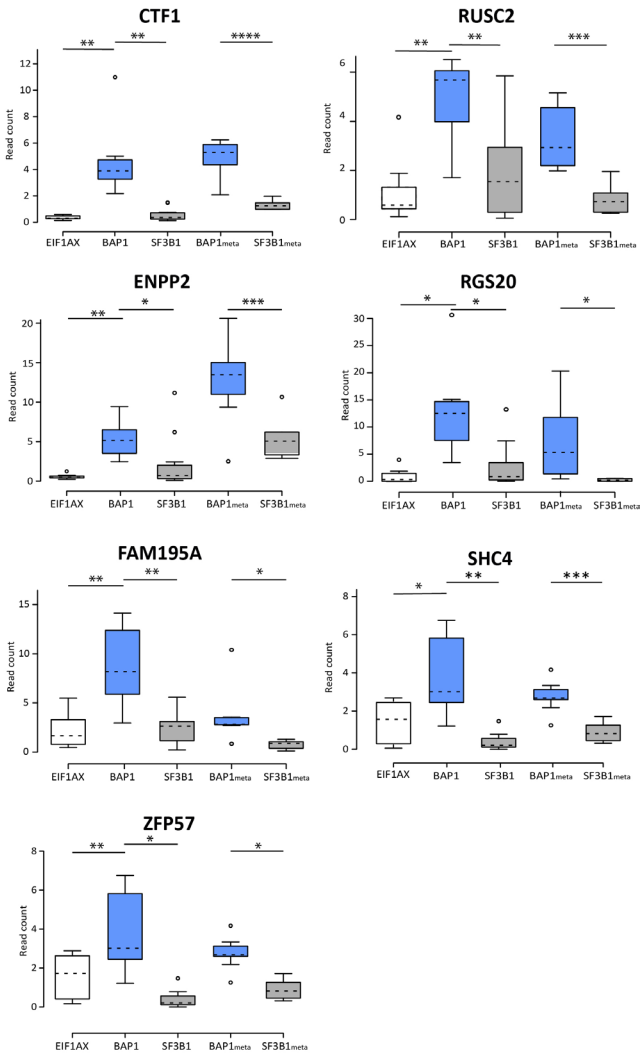

Supplementary Figure 4. Boxplots showing the read count level, which indicates the level of methylation in all primary UM and all UM metastases.

Chapter 4

Potential biomarkers and therapeutics

Chapter 4.1

Exosome-encapsulated microRNAs as a potential non-invasive biomarker for metastatic uveal melanoma

K.N. Smit, T. Lunavat, S.C. Jang, T. Brands, C. Lässer, R.M. Verdijk, R. Willemsen, H. Mensink, W. F.J. van IJcken, J. Lotvall, A. de Klein, E. Kiliç

In progress

Abstract

Uveal melanoma is an intra-ocular malignancy that causes metastasis-related death in approximately half of the patients. Histopathological and genetic analyses can prognostically categorize patients, however this can only be done in uveal melanoma patients that underwent enucleation or, in case of eye-preserving treatments, a biopsy. Since biopsies are not entirely without risk there is an urgent and unmet need for a non-invasive biomarker that can predict the metastatic risk in uveal melanoma patients. In this study we characterize extracellular vesicles secreted by three uveal melanoma cell lines harboring an *EIF1AX*, *SF3B1* or *BAP1*-mutation. Respectively, mass spectrometry was performed to characterize the membrane-proteins present in uveal melanoma exosomes. Forty-two percent of the membrane proteins were shared between the three exosome samples. Amongst these shared proteins were classical UM proteins, such as CD81, Flotillin-1 and CD63, but also proteins that are generally only present in melanocytes, like GP100 and TYRP1. Subsequently, exosomal and cellular small-RNA was sequenced and we observed a unique miRNA signature in each subset of exosomes. Exosomes secreted by the *BAP1*-mutated cell line showed an increased expression of the oncomiRs miRNA-21, miRNA-365 and miRNA-10B. Exosomes with a unique, metastatic uveal melanoma signature are a promising, non-invasive biomarker for metastatic UM. The presence of melanocyte-specific proteins on UM exosomes can be used to enrich for melanocyte exosomes and thereby achieve a higher diagnostic and prognostic efficiency. However, further research is needed to validate whether exosome-encapsulated miRNAs can be interesting novel targets for future UM prognosis.

Introduction

Uveal melanoma (UM) is an aggressive type of cancer arising from the uveal melanocytes located in the eye. The primary tumor can be treated by enucleation or by eye-conserving treatments, such as proton therapy, radiotherapy or brachytherapy[1]. Approximately half of all UM patients will develop metastatic disease; some metastasize a few years after diagnosis, whereas others metastasize several decades after diagnosis[2]. Several histopathologic and genetic biomarkers can discriminate between low, intermediate metastatic risk UM and high metastatic risk UM. However, an increasing amount of UM patients is treated with eye-conserving treatments and these patients cannot be classified into a prognostic group, unless a biopsy is taken. Since biopsies are not entirely without risk[3, 4], there is an urgent and unmet need for a non-invasive biomarker that can predict metastatic risk in UM patients without the necessity of tumor material.

While efforts have been made to develop a non-invasive biomarker for metastatic risk in UM, results have been limited so far which could be caused by the relatively small tumor size. Recently, extracellular vesicles (EVs) have been acknowledged to be advantageous over the circulating tumor cells and cell-free DNA, as they are increased in the blood of cancer patients[5]. EVs are lipid-bilayer particles that are released by all eukaryotic cells into various body fluids, such as blood. They are packed with nucleic acids, proteins and lipids which they can transfer from one cell to another. The ability of EVs to transfer their cellular cargo and effectively deliver it to recipient cells has been primarily demonstrated for the transfer of functional RNA and proteins[6]. EVs are known to be intricately involved in cancer progression, metastasis and angiogenesis by shuttling their cargo from cancer cells to other cells[7-9].

The size of EVs differs; exosomes are vesicles with a size of approximately 100 nm and are generated by the fusion of multivesicular endosomes with the plasma membrane, whereas the larger microvesicles (~500 nm) are shed by outward vesiculation of the plasma membrane[10, 11]. It was shown that exosomes are enriched for miRNAs, suggesting a selective loading mechanism, while the larger microvesicles contained less RNA[12, 13]. In addition, exosomal miRNA patterns differ between cancer patients and healthy individuals, suggesting that pathophysiological changes can influence this mechanism[14]. Exosomes from mesenchymal stem cells could promote tumor progression in adjacent cells by delivering specific miRNAs[15].

In this study we explore the use of exosomes as a non-invasive biomarker for metastatic UM. Firstly, we perform mass spectrometry on exosomal membrane-proteins to characterize the proteome of UM exosomes. The exosomes are obtained from three different UM cell lines; 92.1, MEL202 and MP38. The latter shows loss of BAP1, an important indicator for high metastatic risk, whereas 92.1 and MEL202 contain a *EIF1AX* and *SF3B1* mutation indicating a low or intermediate metastatic risk, respectively. Moreover, exosomal and cellular small RNA was sequenced from each cell line, in order to investigate the miRNA pattern in UM exosomes. Taken together, the knowledge gained in this study bring us one step closer to the development of a highly-specific, non-invasive biomarker for UM.

Material and methods

Cell culture

Three established UM cell lines, 92.1, MEL202 and MP38, were used for this study (kindly gifted by Prof. M. Jager, Leiden University, The Netherlands). 92.1 and MEL202 cells were cultured in RPMI 1640 medium (Gibco, Thermo Fisher Scientific, Waltham, MA, USA), containing 10% FBS, 100 units/ml penicillin, 100 μg/ml streptomycin and 2 mM L-Gluta-

mine. MP38 cells were cultured using IMDM-Glutamax medium (Gibco) containing 20% FBS, 100 units/ml penicillin and 100 ug/ml streptomycin. Prior to use, FBS was EV-depleted by ultracentrifugation at 120.000 x g for 18h at 4°C and subsequently filtered through a 0.22 um filter[16]. For the RNA profiling experiments, commercially available depleted FCS (Gibco) was used. All cells were grown at 37°C in a 5% CO2 humidified incubator. Cells were passaged every 2-3 days at 70-80% confluency.

Exosome isolation

Conditioned cell culture medium (150-200 ml) was obtained from 80% confluent cells grown in T175 cell culture flasks. Cells were first removed from the medium by centrifugation of the medium at 300 x g for 10min at 4°C and cell debris and larger vesicles were removed by subsequent centrifugation at 2,000 x gavg for 20min at 4°C. Microvesicles were purified from the conditioned medium by ultracentrifugation at 16,500 x gavg for 20min at 4°C using polypropene Quick-seal tubes (Beckman Coulter, Brea, CA, USA) in a Type 45 Ti fixed-angle rotor in the Optima XE-90 Ultracentrifuge (Beckman Coulter). Subsequently, exosomes were pelleted by centrifugation at 118,000 x gavg for 3h at 4°C. EV pellets were resuspended in 200 µl PBS (Sigma-Aldrich, St Louis, MO, USA) and were freshly processed or stored at -80°C.

Western blot

Purified exosomes were treated with RIPA-buffer (Sigma-Aldrich) and subjected to several sonication steps, to extract proteins. For protein extraction from cells, cells were collected and washed twice in ice-cold PBS before lysing them in RIPA-buffer (Sigma-Aldrich) supplemented with cOmplete Protease Inhibitor-cocktail (Roche, Basel, Switzerland) immediately before use. The lysed samples were incubated on ice for 15min, followed by several vortex steps. The protein concentration was determined using the BCA protein assay kit (Thermo Fisher Scientific) according to the manufacturer's protocol. Twenty µg of protein was separated by SDS-page and transferred to a Trans-Blot mini PVDF membrane using the Trans-Blot Turbo Transfer system (Bio-Rad, Hercules, CA, USA). The membranes were blocked in 5% non-fat dry milk in TBS containing 0.05% Tween-20 and subsequently incubated with primary antibodies overnight at 4°C and HRP-conjugated secondary antibodies for 1h at RT. The antibodies used were as followed: anti-CD81 (1:1000 dilution, sc-9158, Santa Cruz, Dallas, TX, USA); anti-Flotillin-1(1:1000 dilution, sc-74566); anti-Calnexin (1:1000 dilution, sc-11397); donkey anti-rabbit IgG HRP-linked (1:10.000 dilution, NA9340, GE Healthcare, Chicago, IL, USA) and sheep anti-mouse IgG HRP-linked (1:10.000, NA9310). The protein staining was visualized with ECL Prime Western Blotting Detection (GE Healthcare) according to the manufacturer's recommendations using the VersaDoc 4000 MP imaging system (Bio-Rad).

Flow Cytometry

Exosomes were coupled to magnetic anti-CD81 and CD9 beads (Invitrogen, Carlsbad, CA, USA) by incubating them together in assay buffer (0.1% BSA in PBS; 0.22 µm filtered) for 16h at 4°C under constant agitation. Bead-exosome complexes were purified by using a magnetic rack and subsequently incubated for 1h at RT under constant agitation with the following fluorochrome-conjugated antibodies; PB anti-CD81 (clone 5A6, Biolegend, San Diego, CA, USA), PE anti-CD63 (clone H5C6, Biolegend) and PerCP-Cy5.5 anti-CD9 (clone H19a, Biolegend). The samples were analyzed using the LSR Fortessa (BD Biosciences, Franklin lakes, NJ, USA) and the FACSdiva software (BD Biosciences). The data was analyzed using FlowJo software (BD Biosciences).

Particle measurement

EVs (5 µg/ml total protein) were dispersed in equal volumes of PBS and NTS and DLS

(Malvern Nano ZS, Malvern, UK) were used to determine the size of the EV samples.

Transmission Electron Microscopy

Carbon-coated formvar 200-mesh grids (Ted Pealla Inc, Redding, CA, USA) were UV-treated for 5 minutes. 10 μg exosomes was loaded, incubated for 15 minutes, fixed for 10 minutes in 2% paraformaldehyde (Sigma-Aldrich) and 1% glutaraldehyde (Sigma-Aldrich) and contrasted using 2% uranyl acetate (Sigma-Aldrich). Immunostaining of the exosomes was performed with the anti-CD63 antibody (BD Bioscience), isotype control (Sigma-Aldrich) and anti-GP100 (sc-393094, Santa Cruz) followed by staining with 10 nm gold-labelled secondary antibody (Sigma-Aldrich) and subsequent fixation with 2,5% glutaraldehyde (Sigma-Aldrich), washed and contrasted in 2% uranyl acetate. Samples were examined using an LEO 912AB Omega electron microscope operated at 120 kV (Carl Zeiss NTS, Jena, Germany).

RNA isolation and RNA sequencing

Total RNA was extracted from exosomes and cells using the miRCURY RNA isolation kit (Exiqon, Vedbaek, Denmark) according to the manufacturer's protocol. The RNA concentration and size distribution was analyzed using capillary electrophoresis (Agilent 2100 Bioanalyzer, Agilent Technologies, Santa Clara, CA, USA) with a total RNA 6000 Nano chip. Cellular and exosomal RNA was sequenced using an updated version of a previously published RNAome protocol[17]. Briefly, total RNA was rRNA depleted using the Illumina Ribo-Zero magnetic gold kit (Illumina, San Diego, CA, USA) and sheared using a Covaris instrument (Covaris, Brighton, UK). Subsequently, the cDNA libraries were prepared using the NEXTflex Small RNA-seq Kit (v3; PerkinElmer, Waltham, MA, USA) and sequenced on an Illumina HiSeq2500 sequencer (Illumina). After removing the adapter sequences, the fragments were aligned to the human GRCh38 reference genome using HISAT2.

Purification of exosomal membrane-proteins by Iodixanol density cushion

To open the exosome membrane-structure, exosome samples were incubated with 200mM sodium carbonate solution (Na_2CO_3 ; pH 12) for 1h at RT with rotation. 1 M potassium chloride solution (KCl) was added and further incubated for 1h to remove non-covalently bound to the membrane. Subsequently, the samples were subjected to a Iodixanol (Sigma-Aldrich) density gradient to purify the EV-membranes. In brief, a 60% Iodixanol layer was mixed with the sample and overlaid with a 30% and 10% Iodixanol layer respectively forming a discontinuous gradient. The samples were centrifuged at 178,000 x gavg (SW41 TI Rotor, Beckman Coulter) for 2h at 4°C. The exosomal membranes were collected from the interphase between the 30% and 10% Iodixanol and analyzed using liquid chromatography-tandem mass-spectometry (LC-MS/MS).

Proteomic analysis by LC-MS/MS

Mass spectrometry was performed at the Proteomics Core Facility at the Sahlgrenska Academy, University of Gothenburg as described before[18]. In short, samples contained 30 μg protein and were digested using the previously described filter-aided sample preparation (FASP) method[19]. The samples were reduced by incubating with 100 mM dithiotrheitol for 30 minutes at 60°C, transferred to a 30 kDa MWCO Pall Nanosep centrifugation filter (Sigma-Aldrich) and washed with 8 M urea and once with digestion buffer prior to alkylation with 10 mM methyl methanethiosulfanote in digestion buffer for 3 minutes. Subsequently, the sample was digested by adding 300 ng trypsin (Pierce MS-grade; Thermo Fisher Scientific) in 50 mM triethylammonium bicarbonate (TEAB) and 1% sodium deoxycholate (SDC) buffer for 3 hours, followed by the addition of another 300 ng trypsin (Thermo Fisher Scientific) which was incubated overnight at 37°C. The digested samples were desalted using PepClean C18 spin columns (Thermo Fisher Scientific) according to the manufac-

turer's protocol. Peptide samples were resolved in 3% acetonitrile, 0.1% formic acid solution and analysed on a Q Exactive mass spectrometer (Thermo Fisher Scientific) interfaced with an Easy-nLC 1200 nanoflow liquid chromatography system. The peptides were separated using a C18 analytical column (200x0.075mm I.D., 3uM) using a gradient from 5% to 25% acetonitrile in 0.1% formic acid for 75 minutes and finally from 25% to 80% acetronile in 0.1% formic acid for 5 minutes at a flow rate of 200 nl/minute. The obtained results were analysed using the Proteome Discover software (version 1.4; Thermo Fisher Scientific) and the human Swissprot database 2017 (Swiss Institute of Bioinformatics, Switzerland).

Bioinformatics

To identify the proteins enriched in the vesicle proteome the Database for Annotation, Visualization and Integrated Discovery (DAVID; http://david.abcc.ncifcrf.gov/) was used. To compare protein content between samples Venny was used (http://bioinfogp.cnb.csic.es/tools/venny/index.html)

Results

Characterization of extracellular vesicles

Extracellular vesicles were isolated from conditioned cell culture medium according to a serial centrifugation protocol (Supplementary Figure 1). By western blot we analyzed the protein content in cell lines, exosomes and microvesicles (Figure 1A). All samples showed presence of the cell membrane marker flottilin-1, whereas the vesicle marker CD81 was only present in exosomes and microvesicles. Calnexin, an endoplasmic reticulum marker only present in cells, was absent in exosomes and microvesicles. Flow cytometry confirmed the presence of CD81 and CD63 in all samples, whereas only the exosomes derived from MP38 were positive for CD9 (Supplementary Figure 2). We characterized the exosomes based on their size and morphology using electron microscopy and nanoparticle tracking analysis. Particle analysis showed that the isolated exosome samples contained particles with a size of approximately 100 nm, which corresponds with the size described in literature (Figure 1B). Electron microscopy revealed vesicles with a typical spherical shape with a size of approximately 100 nm (Figure 1C).

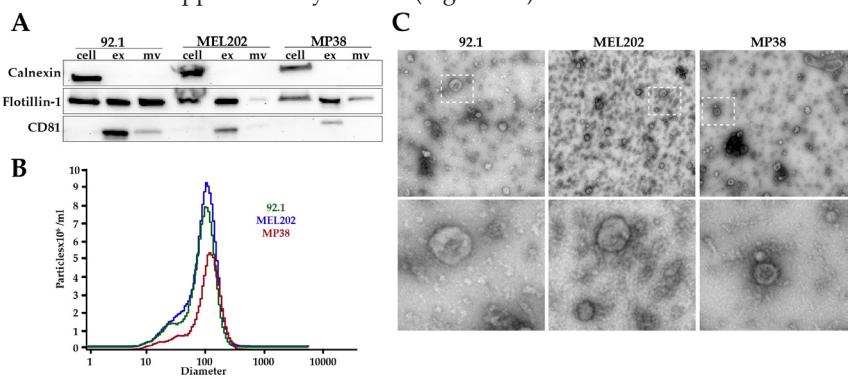

Figure 1. Characterization of extracellular vesicles. **A)** Immunoblotting of the exosomal protein CD81, the endoplasmic reticulum protein calnexin and the exosomal and cellular protein flotilin-1 in isolates from cellular extract, exosomes and microvesicles **B)** Particle analysis shows that the exosome-fraction mainly contain vesicles of a 100 nm size **C)** A representative electron microscopy image of an exosomes derived from the 92.1; MEL202 and MP38 cell line. The dotted white box indicates which region is enlarged in the bottom row.

Proteomic analysis of exosomes reveals the presence of melanocyte-specific membrane proteins

To analyze the membrane-protein repertoire on exosomes isolated from all three UM cell lines we treated exosomes with a high pH-solution, causing the exosomal membrane to open. Proteins that were ionically bound to the exosomal membrane were removed and membrane proteins were isolated by applying the sample on a density gradient. Subsequently the samples were analyzed by mass spectrometry. We detected 1714 different proteins, of which 727 were found in exosomes from all three cell lines (Figure 2A). In total, 1052, 1311 and 1244 were identified from MEL202, 92.1 and MP38 exosomes, respectively. Among these 727 common proteins, were the classic exosome proteins CD81, CD63 and flotillin-1, suggesting that the exosomes are indeed exosomes rather than artefacts of the isolation procedure or necrotic particles. The exosomal protein CD9 was only detected in the MP38 exosomes, as also observed in previous flow cytometry experiments. Interestingly, we also found a set of melanocyte-specific proteins to be present in the exosomal membrane (Figure 2B). This was confirmed by performing electron microscope using anti-GP100 antibodies conjugated to a gold particle. Both for CD63 and GP-100, we observed antibody-binding at the surface of MEL202 exosomes (Figure 2C). This implies that besides the tetraspanin proteins CD81, CD63 and CD9 and the lipid raft flottilin-1, UM exosomes also harbor melanocyte-specific proteins in their membrane (Figure 2D). Among the highly abundant proteins we detected six proteins that were increased in the MP38 exosomes, such as MYOF and EPHX1, and 10 proteins decreased in the MP38 exosomes, including PCDH7 (Supplementary Figure 3).

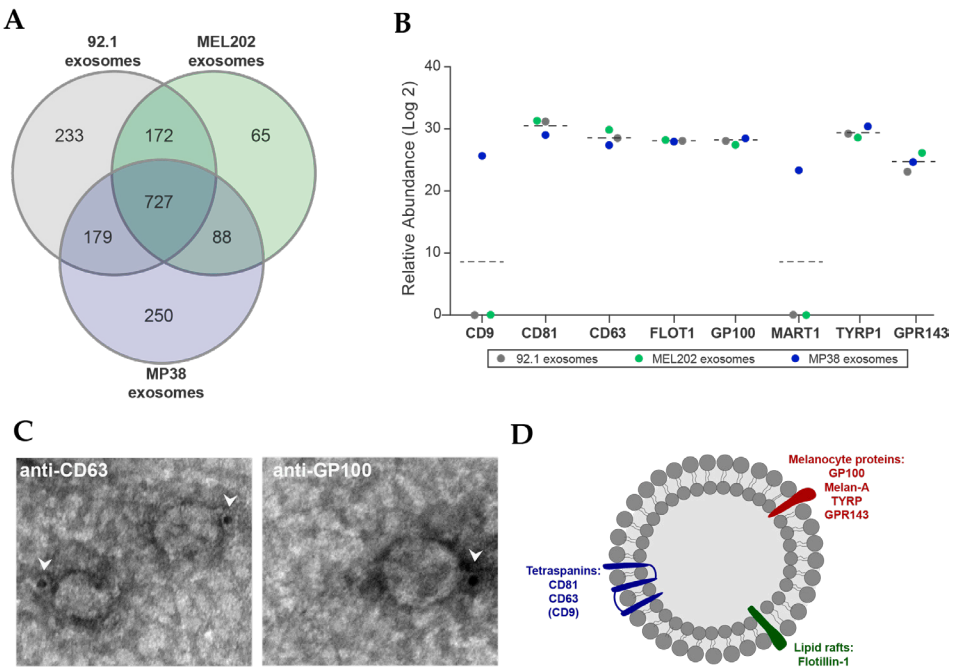

Figure 2. A) Membrane proteins present in 92.1; MEL202 and MP38 derived exosomes were compared amongst each other **B)** Several membrane proteins were plotted with their relative abundance derived from mass spectrometry analysis. Blue indicate the MP38-derived exosomes, green indicates the MEL202-derived exosomes and grey indicate the 92.1-derived exosomes. **C)** Presence of CD63 and GP100 was validated by EM analysis **D)** Visualization of some of the membrane-proteins present in UM exosomes.

Exosomal RNA analysis

The RNA profile in cells, microvesicles and exosomes from all three UM cell lines was analyzed by capillary electrophoresis. Since microvesicles contained far less RNA than exosomes, we performed RNA sequencing on exosomal RNA. RNA extracted from exosomes showed a typical exosomal RNA profile, lacking the 18S and 28S ribosomal subunit (Supplementary Figure 4). The electrophoresis profile included RNA in the size of miRNA and to analyze the exosomal miRNA content we performed RNA sequencing. The majority of the miRNAs that were detected in the cell, were observed in the exosomes as well (Figure 3A). However there were slight differences between the miRNA patterns of the three UM cell lines. The ten most common miRNAs observed in exosomes were miRNA-3142HG, miRNA-146A, miRNA-92A, miRNA-17HG, miRNA-30D, miRNA-92A , miRNA-423, miRNA-211, miRNA-let-7b and miRNA-21 (Figure 3B). Most miRNAs correlated well between exosome samples, however we did observe miRNA expression patterns specific for the exosomes from each cell line (Figure 3C). Reassuringly, one of the miRNAs that showed a higher read count in the *BAP1*-mutated MP38 cell line, indicative for higher expression, was the oncomiR miRNA-21.

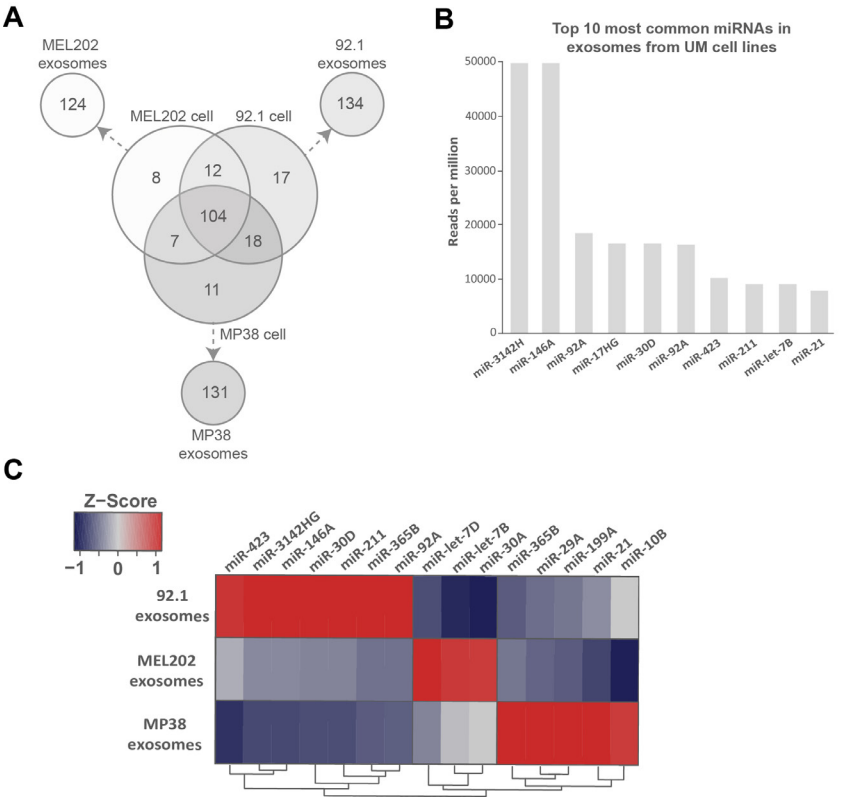

Figure 3 A) The amount of miRNAs detected in the three UM cell lines and exosomes **B)** The top 10 highest expressed miRNAs in the exosome samples. The read counts per million is shown for every miRNA **C)** Exosomes from the three different UM cell lines show differential expression of several microRNAs. Red indicated upregulation, whereas blue indicates downregulation.

Discussion

The aim of this study was to explore the possibility of using exosome-encapsulated miRNAs as a liquid biomarker. Using western blot, flow cytometry and EM we could detect significant amounts of extracellular vesicles secreted from UM cell lines. Since exosomes are known to be enriched for miRNAs, we analyzed the miRNA pattern in exosomes from all three UM cell lines. Most of the miRNAs that were identified in the cells, were present in the exosomes as well, indicating that the exosome content partially reflects the donor cells content, however we did observe differences in miRNA-levels. Interestingly, miRNA profiling suggested that exosomes from the *BAP1*-mutated cell line have a different miRNA profile compared to the two other UM cell lines. We observed an increased normalized read count for miRNA-365, miRNA-21, miRNA-10B, miRNA-199a and miRNA-29A in the *BAP1*-mutated UM cell line, implying that these miRNAs are more abundant in exosomes secreted by high risk UM. MiRNAs-21, 365 and 10B have already been described in literature as oncomiRs. A study by Duan et al revealed that miRNA-365 binds PKHD1, thereby suppressing cell-cell adhesion[20]. Both miRNA-21 and miRNA-10B were found to be upregulated in hepatocellular cancer and promoted metastasis[21, 22]. miRNA-21 is a well-known oncomiR that promotes carcinogenesis by inhibiting the expression of the tumor-suppressor gene *PDCD4*[23]. Exosomes secreted by colon cancer cells and esophageal squamous cancer cells have been shown to contain an increased number of miRNA-21 as well[24, 25]. These significant amounts of miRNAs can induce several functional effects in recipient cells. Uptake of exosomal oncomiRs could stimulate the oncogenic features of recipient cells present in the same tissue, in addition they could be taken up by distant future metastatic sites given their stabile structure.

A previous study by Eldh et al investigated the RNA content from exosomes extracted from the liver perfusate of 12 patients with metastatic UM[5]. They observed a higher concentration of exosomes in the blood of metastatic UM patients compared to healthy controls. However, this study could not identify exosomal miRNAs that are differentially expressed high metastatic risk UM and low metastatic risk UM, since they only analyzed exosomal miRNA from metastatic UM and non-UM cell lines.

Exosome-encapsulated miRNAs could be an attractive candidate for metastatic liquid biomarkers. In particular by using a fluorescent detection system. Quantitative detection of exosomal miRNAs has already been validated in a study by Lee et al[26]. A recently developed method using FAM-labelled hairpin-probes and gold nanoparticles could very sensitively quantify miRNA-21 down to 50 pM by combining fluorescent and colorimetric signaling[27]. In addition to utilizing exosomal miRNAs as biomarkers, they could also provide us with interesting possibility for future therapies. Since exosomes show good bioavailability and little toxicity, they could be promising drug delivery vehicles[28, 29]. By modulating the cargo of exosomes, genetically engineered exosomes can mediate multiple biological effects in recipient cells. Additionally, it has been shown that exosomes contain a specific repertoire of integrines on their surfaces which can dictate a preference for specific recipient cells[30]. Certain integrines, such as ITβ5, on UM exosomes might dictate a specific preference for liver cells, the most common metastatic site in UM. Interestingly, our preliminary data show presence of ITβ5 on MEL202 and MP38 exosomes, while most other integrines were present on exosomes from all three cell lines. In future studies, UM exosomes could be produced in large quantities and be engineered to provide liver cells with therapeutic molecules. A study by Monfared et al described the use of engineered exosomes packed with a miRNA-21 sponge construct. In a rat model of glioblastoma these engineered exosomes could reduce the level miRNA-21 and consequently upregulate the miRNA-21 target gene *PDCD4* and *RECK*, resulting in less proliferation and more apoptosis[31].

Mass spectrometry protein analysis allowed us to study the membrane proteome of UM exosomes in an unbiased manner. We detected four melanocyte-specific proteins to be present in the membrane of UM exosomes; GP100, MART1, TYRP1 and GPR143. The presence of these proteins might offer us to the possibility to capture exosomes with a melanocytic origin, by making use of antibody-coated magnetic beads. Immuno-isolation of exosomes by magnetic beads is a simple and rapid method that has been shown to obtain a higher recovery and purity, than ultracentrifugation[32]. Immuno-isolation of exosomes has already been successfully done for a number of cancer cells, including lung and colon cancer[33, 34]. As UM are known to be relatively small tumors, isolating non-specific biomarkers will obtain an incredibly low amount of tumor material. By incubating plasma of UM patients with magnetic beads conjugated to antibodies against GP100, MART1, TYRP1 and GPR143 only exosomes that were secreted by melanocytes will be extracted from the plasma (Figure 4).

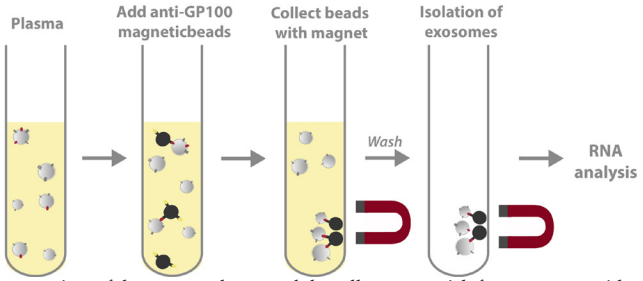

Figure 4 Schematic overview of the proposed protocol that allows to enrich for exosomes with a melanocyte-origin in plasma samples.

Additionally, we identified highly abundant surface proteins that were specifically upregulated or downregulated in the exosomes from *BAP1*-mutated UM cell line. The diagnostic potential of exosomal membrane proteins definitely deserves additional studies in which the presence of these proteins is validated and quantified in an antibody-based assay. Exosomal membrane proteins are of biological interest as well, since they can act as a ligand for certain receptors and thereby activate downstream signaling pathways. One of the proteins that showed strong upregulation in exosomes from *BAP1*-mutated UM cell line was myoferlin (MYOF). This membrane protein regulates tyrosine kinase receptor functioning and has been shown to be overexpressed in cancers where it stimulates migration and invasion[35].

However multiple critical issues should be considered when interpreting our study. Firstly, since our results are based on cultured UM cells, they may not entirely reflect the true situation in vivo. Therefore, further validation is required in exosomes secreted by dissected primary UM before continuing with plasma samples. Second, enrichment for melanocyte-exosomes will result in only a low number of exosomes, therefore it will require a highly specific and highly sensitive downstream technique to analyze the nucleic acid content. Third, it should be investigated whether non-malignant skin or uveal melanocytes secrete exosomes with these markers as well, since this might mean our method will extract non tumorigenic exosomes as well.

Taken together, given that exosomes from UM cells with different secondary driver mutations show a unique miRNA signature and they are widely distributed in body fluids, exosomes might be a promising non-invasive biomarker for metastatic UM. The presence of melanocyte-specific membrane proteins could allow the selective extraction of melanocyte-exosomes from a plasma sample, thereby providing us with a highly specific non-invasive biomarker for metastatic UM. In the future, a simple, cost-effective and efficient lab-on-a-chip device can facilitate prognostication in all UM patients.

References

1. Damato B. Ocular treatment of choroidal melanoma in relation to the prevention of metastatic death - A personal view. Prog Retin Eye Res. 2018;66:187-99.
2. Singh AD, Turell ME, Topham AK. Uveal melanoma: trends in incidence, treatment, and survival. Ophthalmology. 2011;118(9):1881-5.
3. Singh AD, Medina CA, Singh N, Aronow ME, Biscotti CV, Triozzi PL. Fine-needle aspiration biopsy of uveal melanoma: outcomes and complications. Br J Ophthalmol. 2016;100 (4):456-62.
4. Sellam A, Desjardins L, Barnhill R, Plancher C, Asselain B, Savignoni A, et al. Fine Needle Aspiration Biopsy in Uveal Melanoma: Technique, Complications, and Outcomes. Am J Ophthalmol. 2016;162:28-34 e1.
5. Eldh M, Olofsson Bagge R, Lasser C, Svanvik J, Sjostrand M, Mattsson J, et al. MicroRNA in exosomes isolated directly from the liver circulation in patients with metastatic uveal melanoma. BMC Cancer. 2014;14:962.
6. Valadi H, Ekstrom K, Bossios A, Sjostrand M, Lee JJ, Lotvall JO. Exosome-mediated transfer of mRNAs and microRNAs is a novel mechanism of genetic exchange between cells. Nat Cell Biol. 2007;9(6):654-9.
7. Peinado H, Aleckovic M, Lavotshkin S, Matei I, Costa-Silva B, Moreno-Bueno G, et al. Melanoma exosomes educate bone marrow progenitor cells toward a pro-metastatic phenotype through MET. Nat Med. 2012;18(6):883-91.
8. Costa-Silva B, Aiello NM, Ocean AJ, Singh S, Zhang H, Thakur BK, et al. Pancreatic cancer exosomes initiate pre-metastatic niche formation in the liver. Nat Cell Biol. 2015;17(6):816-26.
9. Greening DW, Gopal SK, Mathias RA, Liu L, Sheng J, Zhu HJ, et al. Emerging roles of exosomes during epithelial-mesenchymal transition and cancer progression. Semin Cell Dev Biol. 2015;40:60-71.
10. Abels ER, Breakefield XO. Introduction to Extracellular Vesicles: Biogenesis, RNA Cargo Selection, Content, Release, and Uptake. Cell Mol Neurobiol. 2016;36(3):301-12.
11. Colombo M, Raposo G, Thery C. Biogenesis, secretion, and intercellular interactions of exosomes and other extracellular vesicles. Annu Rev Cell Dev Biol. 2014;30:255-89.
12. Guduric-Fuchs J, O'Connor A, Camp B, O'Neill CL, Medina RJ, Simpson DA. Selective extracellular vesicle-mediated export of an overlapping set of microRNAs from multiple cell types. BMC Genomics. 2012;13:357.
13. Crescitelli R, Lasser C, Szabo TG, Kittel A, Eldh M, Dianzani I, et al. Distinct RNA profiles in subpopulations of extracellular vesicles: apoptotic bodies, microvesicles and exosomes. J Extracell Vesicles. 2013;2.
14. Skog J, Wurdinger T, van Rijn S, Meijer DH, Gainche L, Sena-Esteves M, et al. Glioblastoma microvesicles transport RNA and proteins that promote tumour growth and provide diagnostic biomarkers. Nat Cell Biol. 2008;10(12):1470-6.
15. Sharma A. Role of stem cell derived exosomes in tumor biology. Int J Cancer. 2018;142(6): 1086-92.
16. Shelke GV, Lasser C, Gho YS, Lotvall J. Importance of exosome depletion protocols to eliminate functional and RNA-containing extracellular vesicles from fetal bovine serum. J Extracell Vesicles. 2014;3.
17. Derks KW, Misovic B, van den Hout MC, Kockx CE, Gomez CP, Brouwer RW, et al. Deciphering the RNA landscape by RNAome sequencing. RNA Biol. 2015;12(1):30-42.
18. Jang SC, Crescitelli R, Cvjetkovic A, Belgrano V, Olofsson Bagge R, Sundfeldt K, et al. Mitochondrial protein enriched extracellular vesicles discovered in human melanoma tissues can be detected in patient plasma. J Extracell Vesicles. 2019;8(1):1635420.
19. Wisniewski JR, Zougman A, Nagaraj N, Mann M. Universal sample preparation method for proteome analysis. Nat Methods. 2009;6(5):359-62.
20. Duan J, Huang H, Lv X, Wang H, Tang Z, Sun H, et al. PKHD1 post-transcriptionally modulated by miR-365-1 inhibits cell-cell adhesion. Cell Biochem Funct. 2012;30(5):382-9.
21. Tian XP, Wang CY, Jin XH, Li M, Wang FW, Huang WJ, et al. Acidic Microenvironment Up-Regulates Exosomal miR-21 and miR-10b in Early-Stage Hepatocellular Carcinoma to Promote Cancer Cell Proliferation and Metastasis. Theranostics. 2019;9(7):1965-79.
22. Sheedy P, Medarova Z. The fundamental role of miR-10b in metastatic cancer. Am J Cancer Res. 2018;8(9):1674-88.
23. Asangani IA, Rasheed SA, Nikolova DA, Leupold JH, Colburn NH, Post S, et al. Micro-

RNA-21 (miR-21) post-transcriptionally downregulates tumor suppressor Pdcd4 and stimulates invasion, intravasation and metastasis in colorectal cancer. Oncogene. 2008; 27(15):2128-36.
24. Ogata-Kawata H, Izumiya M, Kurioka D, Honma Y, Yamada Y, Furuta K, et al. Circulating exosomal microRNAs as biomarkers of colon cancer. PLoS One. 2014;9(4):e92921.
25. Tanaka Y, Kamohara H, Kinoshita K, Kurashige J, Ishimoto T, Iwatsuki M, et al. Clinical impact of serum exosomal microRNA-21 as a clinical biomarker in human esophageal squamous cell carcinoma. Cancer. 2013;119(6):1159-67.
26. Lee JH, Kim JA, Kwon MH, Kang JY, Rhee WJ. In situ single step detection of exosome microRNA using molecular beacon. Biomaterials. 2015;54:116-25.
27. Huang J, Shangguan J, Guo Q, Ma W, Wang H, Jia R, et al. Colorimetric and fluorescent dual-mode detection of microRNA based on duplex-specific nuclease assisted gold nanoparticle amplification. Analyst. 2019;144(16):4917-24.
28. Batrakova EV, Kim MS. Using exosomes, naturally-equipped nanocarriers, for drug delivery. J Control Release. 2015;219:396-405.
29. Wahlgren J, Statello L, Skogberg G, Telemo E, Valadi H. Delivery of Small Interfering RNAs to Cells via Exosomes. Methods Mol Biol. 2016;1364:105-25.
30. Hoshino A, Costa-Silva B, Shen TL, Rodrigues G, Hashimoto A, Tesic Mark M, et al. Tumour exosome integrins determine organotropic metastasis. Nature. 2015;527(7578): 329-35.
31. Monfared H, Jahangard Y, Nikkhah M, Mirnajafi-Zadeh J, Mowla SJ. Potential Therapeutic Effects of Exosomes Packed With a miR-21-Sponge Construct in a Rat Model of Glioblastoma. Front Oncol. 2019;9:782.
32. Tauro BJ, Greening DW, Mathias RA, Ji H, Mathivanan S, Scott AM, et al. Comparison of ultracentrifugation, density gradient separation, and immunoaffinity capture methods for isolating human colon cancer cell line LIM1863-derived exosomes. Methods. 2012;56(2): 293-304.
33. Rabinowits G, Gercel-Taylor C, Day JM, Taylor DD, Kloecker GH. Exosomal microRNA: a diagnostic marker for lung cancer. Clin Lung Cancer. 2009;10(1):42-6.
34. Mathivanan S, Lim JW, Tauro BJ, Ji H, Moritz RL, Simpson RJ. Proteomics analysis of A33 immunoaffinity-purified exosomes released from the human colon tumor cell line LIM1215 reveals a tissue-specific protein signature. Mol Cell Proteomics. 2010;9(2):197-208.
35. Blomme A, Costanza B, de Tullio P, Thiry M, Van Simaeys G, Boutry S, et al. Myoferlin regulates cellular lipid metabolism and promotes metastases in triple-negative breast cancer. Oncogene. 2017;36(15):2116-30.

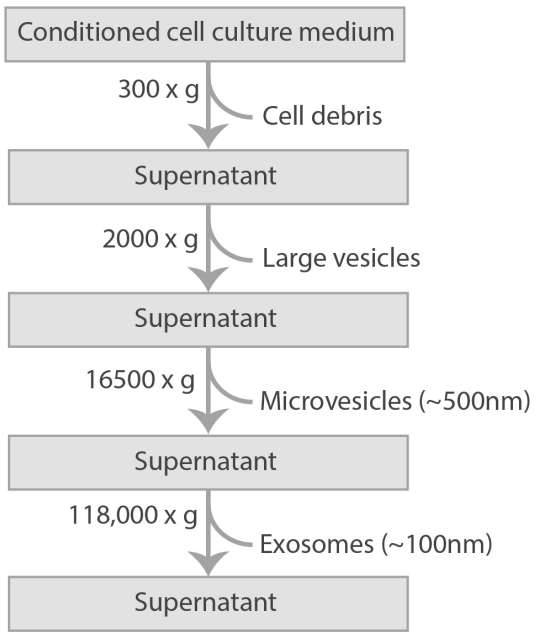

Supplementary Figure 1. Flowchart showing the serial centrifugation protocol for vesicle isolation from conditioned cell culture medium

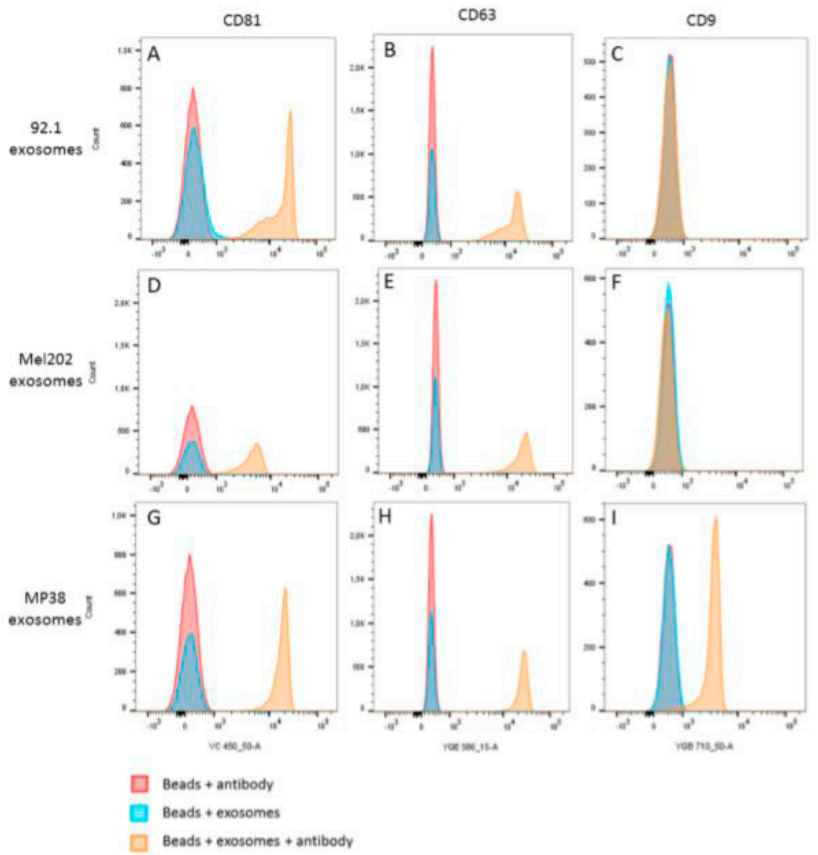

Supplementary Figure 2. Detection of CD81, CD9 and CD63 by flow cytometry in exosome isolates from the cell lines 92.1, MEL202 and MP38. The orange peaks show the exosomes samples, whereas the blue curve indicates the autofluorescence with only beads and exosomes and the red curve shows the negative control with only beads and antibody.

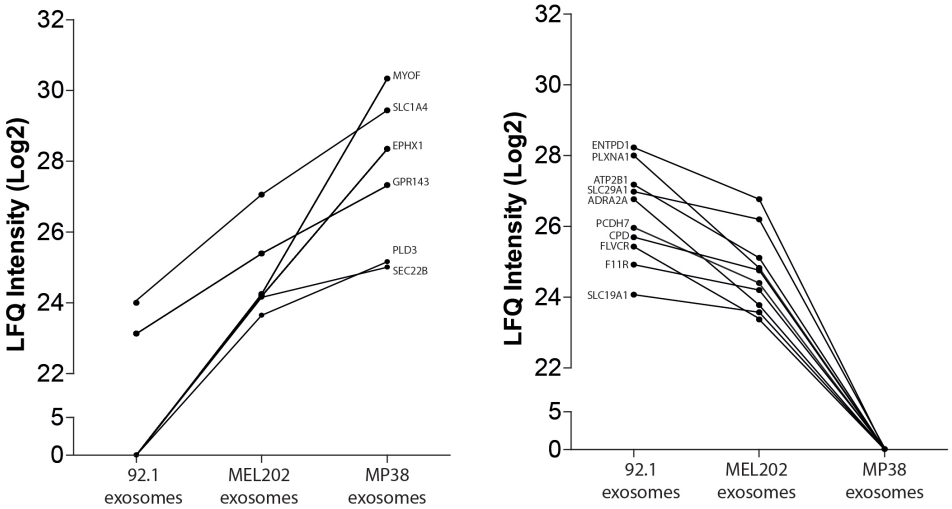

Supplementary figure 3. Highly abundant proteins that were shown to be increased (left) or decreased (right) in the MP38 exosomes. The line indicates the expression-trend of the membrane proteins.

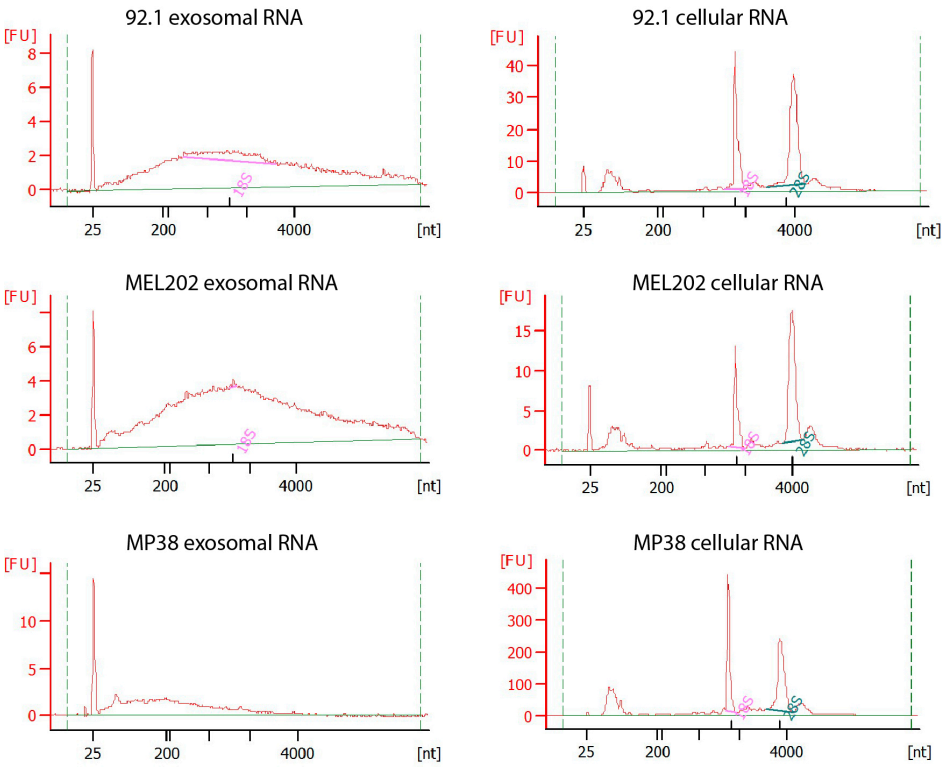

Supplementary Figure 4. The Bioanalyzer RNA profiles obtained from exosomal and cellular RNA from the UM cell lines; 92.1; MEL202 and MP38

Chapter 4.2

Uveal melanoma: towards a molecular understanding

Kyra N Smit, Martine J Jager, Annelies de Klein and Emine Kiliç

Progress in Retinal and Eye Research. 2019 Accepted for publication

Abstract

Uveal melanoma is an aggressive malignancy that originates from melanocytes in the eye. Even if the primary tumor has been successfully treated with radiation or surgery, up to half of all UM patients will eventually develop metastatic disease. Despite the common origin from neural crest-derived cells, uveal and cutaneous melanoma have few overlapping genetic signatures and uveal melanoma has been shown to have a lower mutational burden. As a consequence, many therapies that have proven effective in cutaneous melanoma -such as immunotherapy- have little or no success in uveal melanoma. Several independent studies have recently identified the underlying genetic aberrancies in uveal melanoma, which allow improved tumor classification and prognostication of metastatic disease. In most cases, activating mutations in the Gα11/Q pathway drive uveal melanoma oncogenesis, whereas mutations in the *BAP1*, *SF3B1* or *EIF1AX* genes predict progression towards metastasis. Intriguingly, the composition of chromosomal anomalies of chromosome 3, 6 and 8, shown to correlate with an adverse outcome, are distinctive in the *BAP1*mut, *SF3B1*mut and *EIF1AX*mut uveal melanoma subtypes. Expression profiling and epigenetic studies underline this subdivision in high-, intermediate-, or low-metastatic risk subgroups and suggest a different approach in the future towards prevention and/or treatment based on the specific mutation present in the tumor of the patients. In this review we discuss the current knowledge of the underlying genetic events that lead to uveal melanoma, their implication for the disease course and prognosis, as well as the therapeutic possibilities that arise from targeting these different aberrant pathways.

Introduction

Uveal melanoma (UM) is the second most common form of melanoma, arising from melanocytes located in the uveal tract of the eye. It is a highly aggressive disease, with a strong tendency to metastasize from the eye to other organs, such as the liver. The primary tumor can be treated successfully using several options, such as enucleation, stereotactic radiotherapy, brachytherapy and proton therapy[1, 2]. At the time of diagnosis of the primary tumor, only 4% of patients show detectable metastases; however, up to half of all UM patients will eventually develop metastatic disease despite earlier successful local treatment of the primary tumor. This implies that UM already develops micro-metastases early during tumorigenesis and that these micro-metastases may remain dormant for several months or even years[3]. Once these micro-metastases become overt, the prognosis is poor and disease-related death usually occurs within one year[4]. Metastases are often detected within a few years after diagnosis, but they can also be observed several decades after the initial diagnosis[5-7]. In general, UM can be subdivided into three metastatic risk groups: high, intermediate and low risk.

Several clinical and histological features can predict high metastatic risk, such as large tumor size, extraocular extension, high mitotic activity and an epithelioid cell type, whereas the spindle cell type is associated with low metastatic risk (Figure 1)[8-10]. Genetic features associated with metastatic disease include loss of chromosome 3 and mutations in the *BAP1* and *SF3B1* gene. BRCA-associated protein 1 (*BAP1*) mutations are observed in approximately half of all UM and usually result in metastasis within 5 years[11]. Our group has shown that tumors with an *SF3B1* mutation also frequently metastasize, but this can take up to 15 years and these tumors are therefore considered to have an intermediate metastatic risk[12]. UM that harbor a mutation in the *EIF1AX* gene seldom metastasize[13]. None of the 45 UM patients in our cohort with only an *EIF1AX* mutation developed metastasis.

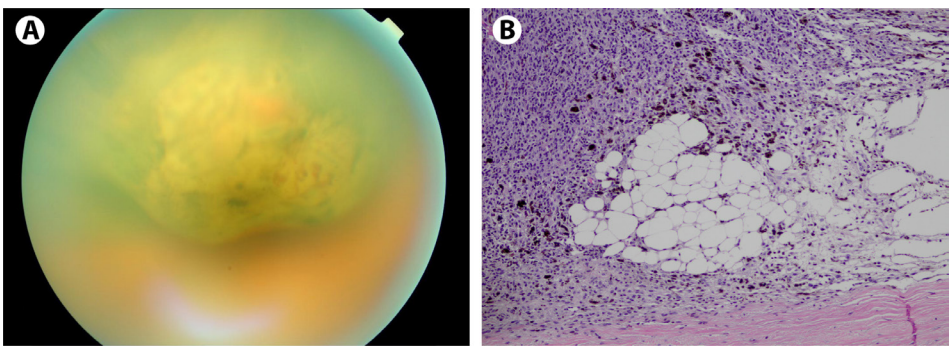

Figure 1. The fundoscopic and histologic appearance of UM. A) A dome-shaped pigmented mass in the posterior pole. **B)** Hematoxylin-eosin (HE) staining shows that the tumor consists of spindle-type UM cells and several adipocytic appearing cells (100x). Reproduced with permission from Yavuzyigitoglu et al, 2016a, via Copyright Clearance Center.

Recurrent chromosomal alterations are frequently observed in UM and the majority occur in the context of a specific mutation. Most of the *BAP1*-mutated UM show loss of chromosome 3, as well as gain of 8q. Tumors with a mutation in the *EIF1AX* or *SF3B1* gene often show gain of chromosome 6p[14]. Since there is little heterogeneity in UM, it is likely that although these mutational and chromosomal events can occur sequentially, both are mandatory in the development of UM to result in tumor growth[15]. Downstream mRNA expression can also be determined to predict metastatic risk. As previously described by Onken et al, UM patients can be classified into a low or high metastatic risk group based on the expression profile of 15 genes[16]. These two groups are known as class 1 and class 2, with class 2 having the worst prognosis; class 1 can be divided into 1a and 1b. A more

recent subdivision which is based on chromosomal data from The Cancer Genome Atlas[17], separates the tumors into categories A-D[18].

Despite extensive research, the survival of metastasized UM patients did not improve over the last three decades[1]. Whereas treatments such as immunotherapy and BRAF-inhibitors show promising results in patients with cutaneous melanoma (CM), UM seem to be unresponsive despite their shared origin as neural-crest derived melanocytes. This indicates that different mechanisms play a role in tumorigenesis. Oncogenic mutations in *BRAF* and *NRAS* are the main drivers in CM, but these mutations have only been found in iris melanoma and do not occur in posterior UM[19, 20]. Most CM (80%) exhibit a mutational signature specific to DNA damage caused by ultraviolet radiation, characterized by C>T transitions at the 3' end of pyrimidine dinucleotides. Even though population studies suggest a geographic predisposition, there is no molecular evidence for this signature in UM[17]. UM has a remarkably low mutational burden; with a rate of <1 single nucleotide variations (SNVs) per Mb, this mutation burden is much lower than observed in most cancer types. Only 35% of the observed SNVs in UM are C>T transitions and there is no enrichment of these lesions at the 3' position of pyrimidine dinucleotides, further showing that CM and UM have a different etiology[21].

So far, UM clinical trials have focused on treatment modalities copied from CM. However, despite these therapeutic options, the prognosis of patients with metastatic UM has not improved, which emphasizes the need to explore and develop UM-specific therapies. In this review, we highlight several scientific findings and studies that provide us with insight into the mechanisms of oncogenesis of *GNAQ*, *GNA11*, *BAP1*, *SF3B1* and *EIF1AX* mutations. Elucidating the development of UM and obtaining a better understanding of the complex interaction between genetic factors, molecular signaling and potential targets will aid in developing new therapies specific for UM.

2. Genes involved in the development of UM

An updated mutational overview of our previously published ROMS cohort containing over 900 UM patients, shows initiating hotspot mutations in *GNAQ* in 57% of the UM tumors and in *GNA11* in 41% (Figure 2A)[12]. Samples that do not contain a *GNAQ* or *GNA11* mutation are usually found to harbor a mutation in another gene linked to the Gα11/Q pathway: *PLCB4* and *CYSTLR2*. *GNAQ* and *GNA11* mutations are already observed in most nevi[22]. In addition, in UM, one can often discern a mutation in one of the three secondary driver genes (*BAP1*, *SF3B1*, *EIF1AX*): forty-four percent of our 175 UM samples showed a *BAP1* mutation, 26% a mutation in *SF3B1* and 21% a mutation in *EIF1AX*. We and others have noticed that even with next generation sequencing (NGS) technology mutations in *BAP1*, especially deletions encompassing whole exons, can be missed and more sophisticated calling algorithms, in combination with RNA sequencing have to be applied to detect these *BAP1* mutations[15]. We are using a combined BAP1-immunohistochemistry (IHC) and targeted NGS approach which is also suitable for small biopsies and formalin-fixed, paraffin-embedded (FFPE) tissue samples[23]. The *BAP1* gene acts as a classic tumor-suppressor gene and in combination with loss of chromosome 3, no active nuclear BAP1 protein is present in the tumor cells[24]. Missense mutations in *SF3B1* or indels in *EIF1AX* mutations are in-frame and create a small change in the respective proteins, albeit with a large effect on many cellular RNAs and proteins[13]. Missense mutations in *SF3B1* usually arise at amino acid R625, a UM hotspot; however, some samples also show mutations outside this hotspot region, such as at amino acids K666 or H662 or in related spliceosome complex genes as *SRSF2* and *U2AF1*[17]. Although not actually a hotspot, *EIF1AX* in-frame mutations are located in the first 10-15 AA of this gene which limits the region to be analyzed. A complicating factor in NGS analysis is the closely-related pseudogene *EIF1AXP1*

on chromosome 1. When possible, we use a SNP array to detect chromosomal aberrations to confirm the UM subclass. Our results and the observed percentages do not deviate substantially from previously observed mutation rates (Figure 2B)[11-13, 25-29]. The secondary mutations are in general mutually exclusive, although 1-2% of the tumors did harbor (hotspot) mutations in two of these metastasis-associated genes. In these latter cases it would be interesting to see whether these mutations arise in the same cells.

A

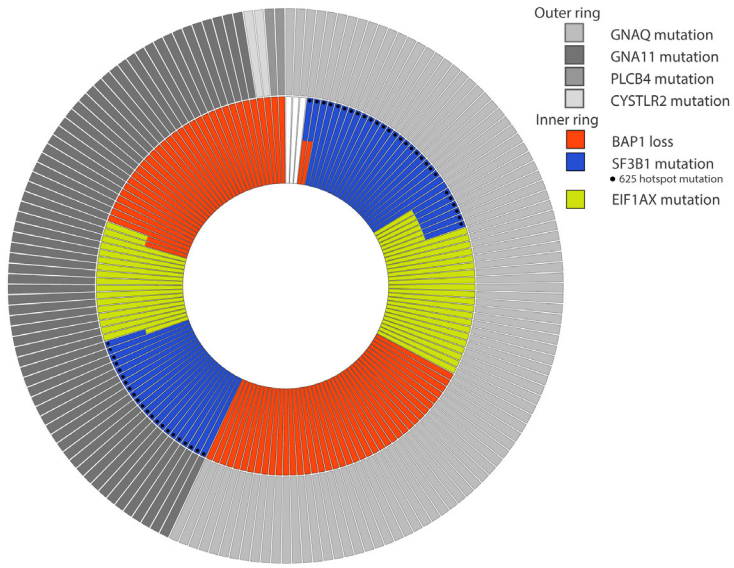

B

Gene	Mutation rates		References
	Our study	Other studies	
GNAQ	56%	42 - 46%	*Raamsdonk 2010; Dono 2014; Ewens 2014; Robertson 2017*
GNA11	40%	32 - 35%	*Raamsdonk 2010; Dono 2014; Ewens 2014; Robertson 2017*
BAP1	43%	31 - 50%	*Harbour 2010; Dono 2014; Ewens 2014; Robertson 2017*
SF3B1	26%	10 - 23%	*Martin 2013; Harbour 2013; Ewens 2014; Robertson 2017*
EIF1AX	21%	13 - 21%	*Martin 2013; Dono 2014; Robertson 2017*

Figure 2. Driver mutations in UM. **A)** Donut chart showing the mutation status of 165 UM patients of the ROMS cohort. The outer ring shows initiating mutations in *GNAQ*, *GNA11*, *PLCB4* and *CYSTLR*. The inner ring indicates co-mutations in *BAP1*, *SF3B1* or *EIF1AX*. The black dots indicate *SF3B1* Q625 hotspot mutations **B)** The mutation rate of each gene observed in our study and other studies. Adapted from (Yavuzyigitoglu et al, 2016b)

2.1 Activation of the Gα11/Q pathway drives neoplastic growth of uveal melanocytes

The first gene reported to be mutated in UM was the guanine nucleotide-binding protein alpha Q (*GNAQ*) gene[26]. Most of the UM samples that do not harbor a mutation in *GNAQ* carry a mutation in its paralogue *GNA11*[25]. Both proteins are involved in the Gα11/Q pathway, which regulates several cellular processes such as proliferation and cell growth. In this pathway, leukotrienes activate the G protein-coupled receptor CYSTLR2 located at the cell surface. Guanine nucleotide-binding proteins (G-proteins) consist of three subunits: alpha, beta and gamma. GNAQ and GNA11 are alpha subunits (Gα) bound to a guanosine diphosphate (GDP). Upon binding of the ligand to CYSTLR2, G proteins are activated by exchanging GDP for guanosine triphosphate (GTP)[30]. GTP binding initiates a conformation change in the G-protein, which allows the G protein to be released from the CYSTLR2 receptor and to activate a large number of downstream effectors, such as PLCB4 and ARF6[31, 32](Figure 3).

Activation of ADP-ribosylation factor 6 (ARF6) by GNAQ or GNA11 initiates several processes, such as β-catenin release from the cytoplasm to the nucleus and activation of the

growth-inducing gene *YAP1*[33]. YAP1 is critical for growth and is therefore often found in the nucleus of proliferating cells. Inhibiting YAP1 strongly limits the proliferation of UM cells[33, 34]. Activated PLCB4 causes a rise in cytoplasmic Ca2+, thereby activating several calcium-regulated pathways[35]. PLCB4 also indirectly activates the mitogen-activated protein kinase (MAPK) and AKT/mTOR pathway through the downstream effector RasGRP3[32, 36]. MAPK and AKT/mTOR promote cell growth and proliferation and are often upregulated in cancer.

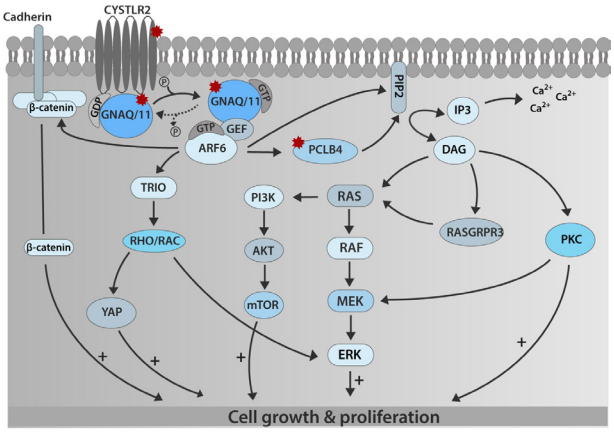

Figure 3. Schematic overview of the Gα11/Q pathway and their downstream effectors. Activated GNAQ binds to a guanine nucleotide exchange factor (GEF), which in turn activates ARF6. ARF6 initiates β-catenin release, which promotes gene transcription. GNAQ and GNA11 can also activate the protein TRIO and the TRIO dependent RHO-GTPases; RHOA and RAC1. Once activated, RHO and RAC1 trigger the release of YAP and stimulate YAP-dependent transcription . ARF6 also activates PLCB4 which initiates hydrolysis of phosphatidylinositol 4,5-biphosphate (PIP2) and produces two second messengers; inositol 1,4,5-triphosphate (IP3) and diacylglycerol (DAG). The production of IP3 causes a rise in cytoplasmic Ca^{2+}, which stimulates several calcium-regulated pathways. With the help of DAG, protein kinase C (PKC) is activated and subsequently stimulates several processes, such as cell proliferation. DAG and PKC together also activate RAS guanyl-releasing protein 3 (RASGRP3), by binding and phosphorylation. RASGRPR3 is a GEF, that integrates GNAQ and GNA11 to the MAPK- and PI3K/AKT pathway by activating RAS. GEFs stimulate the release of GDP and the subsequent binding of GTP, thereby yielding active RAS(RAS-GTP)[31, 33,34,36, 38].

Over 95% of the UM contain a mutually exclusive mutation in *GNAQ* or *GNA11*. Mutations in *GNAQ* and *GNA11* affect residues Q209 and R183, which are required for the GTPase activity[25, 26]. In non-malignant cells, this activation is intrinsically terminated by a guanosine triphosphate (GTPase); oncogenic GNAQ or GNA11 on the other hand are constitutively activated and therefore result in over-activation of the aforementioned signaling pathways. UM that do not harbor a mutation in *GNAQ* or *GNA11* usually have a somatic mutation in *CYSTLR2* (3%) or *PLCB4* (2%)[37, 38]. Wildtype CYSTLR receptors become active after binding of the ligand and transition to the inactivated state is initiated upon release of the ligand. However, mutated receptors stay active even after ligand dissociation and thereby constitutively activate GNAQ and GNA11[38]. This confirms the requirement of aberrant Gα11/Q signaling in the development of UM.

Introducing *GNAQ* and *GNA11* mutations (Q209L) in zebrafish results in increased proliferation, signaling and migration[39]. However, most UM carry a *GNAQ* and *GNA11* mutation regardless of their tumor stage. This suggests that *GNAQ* and *GNA11* mutations are necessary to initiate tumorigenesis, but are insufficient to induce full malignant transformation, as is also shown by our finding that these mutations are also present in nevi[22]. The aggressiveness of UM is determined by secondary driver mutations but treatments targeting oncogenic GNAQ and GNA11 signaling or one of their many downstream targets might reduce the proliferative potential of UM and can therefore be promising for future therapy modalities as will be discussed later in this review.

2.2 Loss of BAP1 is linked to metastatic UM

The majority of the metastasizing UM harbor -in addition to a *GNAQ* or *GNA11* mutation- a mutation in the *BAP1* gene located on chromosome 3[11]. We and others observed, using immunohistochemical analysis, (partial) loss of the BAP1 protein in *BAP1*-mutated UM (Figure 4)[40-44]. Other studies show that loss of BAP1 staining is strongly correlated to GEP class 2 and chromosome 3 loss and that loss of BAP1 protein expression is often associated with lower BAP1 mRNA expression[45]. This implies that these mutations are loss-of-function mutations, requiring the loss of the other allelic copy harboring the wildtype gene (monosomy 3). Surprisingly, some *BAP1*-mutated/immunohistochemically BAP1-negative tumors still show expression of BAP1 mRNA, suggesting that negative nuclear staining for BAP1 protein is not solely caused by nonsense-mediated RNA decay but rather by an as yet unexplained different mechanism (unpublished data). Mutations in *BAP1* are found throughout the entire gene and are not restricted to a specific domain, although we did observe a skewed distribution towards the N-terminal region (Figure 5)[40]. In the ROMS cohort, we observed a large variety of mutations, such as large out-of-frame deletions, but also missense mutations. In a preliminary analysis we did not find a significant association between mutation-type or location with disease-free survival.

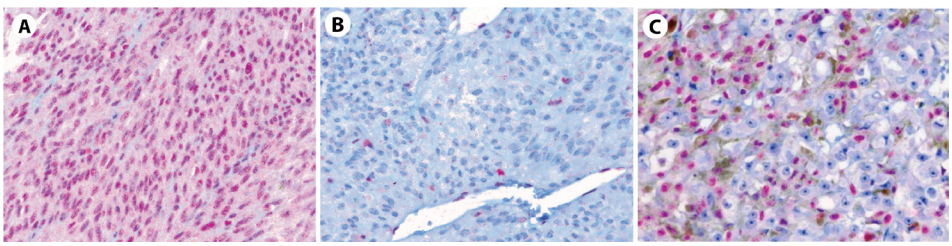

Figure 4. **BAP1-stained sections from three UM**. Immunohistochemistry (IHC) staining of BAP1 protein (red) in **A)** A UM with positive BAP1 expression **B)** A UM with negative BAP1 expression and **C)** A UM showing a heterogeneous distribution of BAP1 throughout the tumor (400x). Reproduced with permission from: Koopmans et al, 2014.

Despite extensive research exploring the function of the BAP1 protein, it is as yet unclear how BAP1 loss in UM promotes the development of UM metastasis. BAP1 belongs to a specific group of proteases, called deubiquitinating enzymes (DUB), which function as a critical regulator of ubiquitin signaling by removing ubiquitin from proteins. Initially, BAP1 was identified because of its interaction with breast cancer 1 (BRCA1), a tumor suppressor gene involved in homology directed DNA-repair. The absence of BAP1 inhibits homology directed DNA-repair and thereby forces cells to rely on the more error-prone non-homologous end joining (NHEJ)[46]. Surprisingly, the mutational load in UM is significantly lower than in other cancer types, suggesting that BAP1 loss in UM does not heavily impair DNA-damage repair mechanisms. Other proteins that interact more frequently with BAP1 could therefore be a more interesting target.

Some new proteins identified in these studies as interactors with BAP1 are the forkhead transcription factors FOXK1 and FOXK2, the histone acetyltransferase HAT1, the histone lysine demethylase KDMB1B, the polycomb group proteins ASXL1 and ASXL2, host cell factor C1 HCF1, and the ubiquitin-conjugated enzyme UBE20[47-52]. Most of these proteins are involved in the regulation of chromatin-associated processes such as transcription. This large number of interacting proteins implicates that absence of BAP1 can have a plethora of downstream effects. One protein that predominantly interacts with BAP1 is HCF1, a protein involved in regulating the cellular localization of BAP1 through the formation of multiprotein complexes with transcription factors such as Yin Yang1 (YY1) and FOXK1/2[48, 53]. HCF1 plays an important role in stem cell maintenance by regulating genes involved in RNA processing and the cell cycle[49]. RNAi-mediated depletion of BAP1 ex-

pression triggered a primitive, stem-like phenotype in UM cells. Genes involved in the maintenance of stem cells and developmental processes were upregulated and melanocyte-specific genes, such as *MITF*, were downregulated[54]. Thus, loss of BAP1 dysregulates transcriptional programs which are essential in the maintenance of the differentiated melanocytic phenotype. The acquisition of a stem cell like-phenotype is a common event in cells undergoing the epithelial-to-mesenchymal (EMT) transition required for metastasis. EMT programming may contribute to the highly metastasizing potential of *BAP1*-mutated UM cells by enabling cells to physically disseminate from the primary tumor. It also provides cells with the self-renewal capability that is crucial for clonal expansion at the site of dissemination [55].

The interaction of BAP1 with ASXL1 and ASXL2, important catalytic subunits of the polycomb repressive deubiquitinase (PR-DUB) complex, could influence the regulation of homeobox genes by deubiquitinating histone H2A[56, 57]. Histone H2A plays a role in several cellular processes, such as stem cell maintenance and cell proliferation[58]. The ubiquitination of histones alters the chromatin structure and thereby regulates the accessibility of the DNA for the transcriptional machinery[59]. Knock down of *BAP1* by RNA interference induced an increase in H2A ubiquitination in UM cells, implying that H2A ubiquitination might be an interesting therapeutic target in high-risk UM.

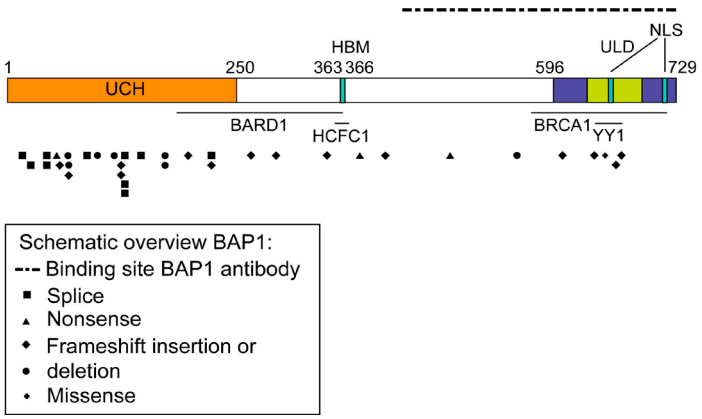

Figure 5. **Overview of the BAP1 protein and its functional and interacting domains.** The *BAP1* mutations we observe in our ROMS cohort are depicted below the protein and classified according to their mutation type and location. The N-terminal UCH domain ranges from amino acid 1-250, the HCF1-binding domain (HMB)-like motif from amino acid 363-366, the UCH37-like domain (ULD) from 634-396 and the two nuclear-localization signaling (NLS) from amino acid 656-661 and 717-722. BAP1 also shows binding domains for BARD1, HCFC1, BRCA1 and YY1. The binding site of the BAP1 IHC antibody is indicated with the dashed line. Reproduced with permission from: Koopmans et al, 2014.

Besides the aforementioned nuclear roles of BAP1, it also plays a role outside the nucleus. BAP1 can be localized in the endoplasmic reticulum (ER), where it stabilizes the type 3 inositol-1,4,5-triphosphate receptor (IP3R3). IP3R3 is involved in promoting apoptosis by tightly regulating the release of Ca2+ from the ER into the cytosol. Loss of BAP1 reduces the amount of stable IP3R3, resulting in reduction of Ca2+ influx and thereby preventing cell apoptosis[60]. However, recent work from Farquhar et al questioned the role of cytoplasmic BAP1 in the metastasis of UM, since they did not find a correlation between disease-free survival of UM patients and the cytoplasmic expression of BAP1[24, 44].

This large number of potentially relevant proteins makes it difficult to determine the exact function of BAP1 due to the complex interaction networks. BAP1 assembles into a multiprotein complex, which contains several transcription- and co-factors. It is not clear

yet which of these many transcription factors plays the crucial role in the metastasis of UM, showing that additional research regarding BAP1 in UM is necessary. For this, it is interesting to study the outliers in the *BAP1*-mutated group. For example, in our cohort we observed seven patients with *BAP1*-mutated tumors who remained metastasis-free for over 10 years. It has also been described that patients who carry a germline *BAP1* mutation do not have a substantially earlier age-of-onset of UM than other UM patients [61]. Additionally, these UM patients with germline mutations in *BAP1* have a better prognosis than patients with somatic mutations in *BAP1*. This suggests that in these patients, mechanism(s) have developed that could temporarily counteract the metastasis-promoting effect of BAP1 loss. Elucidating which mechanisms would be capable of doing that will contribute significantly to the development of a therapy targeted against BAP1 loss in UM.

2.3 *SF3B1* mutations result in aberrantly spliced mRNA

Metastasizing UM that do not show a *BAP1* mutation often harbor a mutation in the gene *SF3B1*[12, 13, 21, 27]. *SF3B1* encodes subunit 1 of the splicing factor 3b, which is responsible for proper branchpoint recognition during splicing of pre-mRNA. Correct RNA splicing is crucial for cell survival and allows cells to produce multiple proteins from one single gene. Somatic mutations in components of the spliceosome have been observed in several malignancies, such as breast, pancreatic and hematologic cancers[62-64]. The prevalence of cancer-associated mutations in spliceosome genes suggests that dysregulation of splicing can efficiently lead to the development of cancer.

SF3B1 mutations can result in aberrant splicing and it has been shown that these mutations in UM result in alternative splicing at the 3′ end of exon borders[65]. These aberrantly spliced transcripts can be degraded by nonsense-mediated RNA decay, resulting in a loss of expression, but they can also be translated into unique, aberrant proteins[66] (Figure 6). Several genes have been shown to be affected in UM, such as ubiquinol-cytochrome C reductase complex chaperone (*UQCC*) and the multidrug resistance-associated protein *ABCC5*[21].

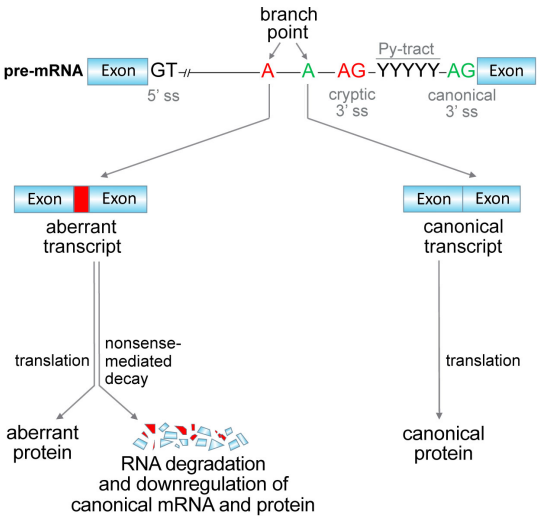

Figure 6. Splicing of pre-mRNA into mature mRNA. Wildtype SF3B1 binds to the branchpoint (BP) of the pre-mRNA, which is usually an adenosine located ~25 nt upstream of the 3′ splice site (3′ ss). This allows a correct assembly of the spliceosome on the pre-mRNA, resulting in mature mRNA and a canonical protein. Whereas mutant SF3B1 recognizes an alternative BP (BP′), resulting in mis-spliced mRNA. This mis-spliced mRNA can be translated into an aberrant protein or degraded by nonsense-mediated RNA decay, resulting in downregulation of the RNA and protein. Reproduced with permission from Darman et al, 2015, via Copyright Clearance Center.

The SF3B1 protein consists of an N-terminal hydrophilic region and a C-terminal region consisting of 22 non-identical HEAT (Huntington, elongation factor 3, protein phosphatase 2A, targets of rapamycin) repeats. UM-associated mutations in *SF3B1* are found almost exclusively in the fifth HEAT-repeat at codon position arginine (R) 625. In other cancer types, such as breast cancer and leukemia, mutations in *SF3B1* are more prevalent in the sixth and seventh HEAT-repeat at lysine residues K666 and K700, respectively. These lineage-specific mutations can be explained by several factors, such as tissue-specific interaction partners, the mutation rate of the gene and the activity of several pathways in a specific tissue that might confer survival advantage[67]. However, since these residues are predicted to be spatially close to one another, it is not surprising that these mutations have a similar functional impact on transcription. RNA-sequencing data from *SF3B1*-mutated UM and breast cancer samples show some unique aberrant transcripts but the majority of the aberrant transcripts is observed in both malignancies (unpublished data). Samples harboring a mutation outside the HEAT-domains do not show aberrant splicing, implying a different effector on splicing or no effect at all[68].

SF3B1 is the most frequently mutated spliceosome gene in UM, but mutations in *U2AF1* and *SRSF2* have also been described[17]. U2AF1 and SRSF2 are both involved in the assembly of the spliceosome and it has been shown that mutations in these genes produce alternative transcripts in hematological malignancies. Similar to the *SF3B1* gene, particular *SRSF2* mutations are more prevalent: we observed that 4 of the 5 in-frame deletions involve the same protein residues (AA 92-99), indicating that this particular activity of SRSF2 creates a specific effect on splicing, required in UM etiology[69]. Whether the downstream effects of these mutations are similar is unclear but these observations are intriguing and are the subject of further research by us and others.

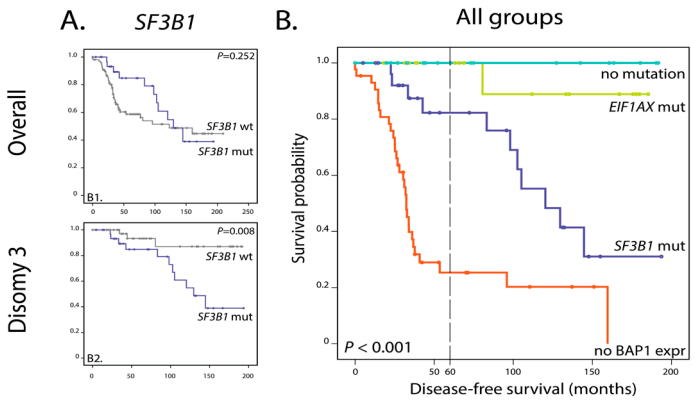

Figure 7. Disease-free survival of UM patients. A) Kaplan-Meier curve showing the disease-free survival of the *SF3B1*mut UM in the overall or disomy 3 group. **B)** In the overall survival curve containing all UM; it can be observed that every mutation status corresponds with a distinct survival pattern. Reproduced with permission from Yavuzyigitoglu et al, 2016, via Copyright Clearance Center.

Most patients in our cohort with *SF3B1*-mutated UM eventually developed metastasis, but have a longer disease-free survival than *BAP1*-mutated UM, implying that *SF3B1*-mutated micro-metastases remain longer in their dormant state than *BAP1*-mutated micro-metastases. In our own patient cohort, the effect of SF3B1 is probably masked by the bulk of UM patients with *BAP1* mutations, as we did not observe a significant difference in prognosis for patients with or without a *SF3B1*-mutated UM (Figure 7A). However, in the disomy 3 group, *SF3B1* mutations do show an association with a worse prognosis. The overall survival curve of all UM, stratified by mutation subtype, confirms that *SF3B1*-mutated UM are a distinct subclass associated with late metastasis. It can also be observed that the

overall survival can vary greatly between *SF3B1*-mutated cases, as some develop metastases within 5 years whereas others after a decade (Figure 7B)[12]. What causes this difference in metastatic potential is not clear and we did not find a specific segregation with the other well-known clinical-pathological or genetic prognostic markers using principle component analysis. However the number of patients in the early metastasizing subgroups was small which could have prohibited a proper analysis. We are in the process of collecting data of more patients with *SF3B1*-mutated tumors to survey RNA expression and epigenetic differences between these early and late metastasizing tumors, which might help us understand these different effects of aberrant splicing on metastatic risk.

2.4 EIF1AX plays an important role in the initiation of translation

The *EIF1AX* gene is mutated in approximately 20% of UM and is involved in the initiation of gene translation in eukaryotic cells[13]. Ribosomes bind the 5′ end of the mRNA in a relatively unstable state, which allows scanning of the mRNA for the start codon. Several eukaryotic initiation factors (EIFs) support the ribosome in this process and subsequently stabilize the ribosome once it reaches a start codon. EIF1A consists of a globular domain and two unstructured tails, the N- and C-terminal tail, which are involved in the scanning of the mRNA and the accurate recognition of the start codon.

UM patients harboring only an *EIF1AX* mutation (in addition to a *GNAQ* or *GNA11* mutation) hardly metastasize; in our cohort, none of the patients with a pure *EIF1AX* mutation developed metastases: the only *EIF1AX*-mutated patient who developed metastases had a concurrent *BAP1* mutation (Figure 7B). Remarkably, UM-associated mutations in *EIF1AX*-indicated in figure 8 by the red dots- occur exclusively in the N-terminal tail of the protein, a highly conserved region in eukaryotes. Mutations in the N-terminal tail inhibit the scanning process by stabilizing the ribosome. This promotes the utilization of less optimal start codons and thereby alters gene expression in UM[70]. Experiments in yeast show that *EIF1A* mutations alter the relative use of start codons in mRNA encoded by tumor suppressor genes or oncogenes. Immunohistochemical staining of EIF1AX in samples harboring a mutation showed a positive staining throughout the cytoplasm of the cell, showing that mutations in the *EIF1AX* gene do not cause loss of the protein[13]. *EIF1AX* mutations have also been observed in other cancer types, such as breast cancer, prostate cancer, adenocarcinoma and glioma (indicated in figure 8 by the grey dots)[71]. Surprisingly, these mutations are found throughout the entire protein-coding DNA, as opposed to UM, where mutations are only observed in the N-terminal tail. This raises the question if the N-terminal region of EIF1AX executes specific functions or engages with specific binding partners in UM. Change of function mutations in the *EIF1AX* gene might make melanocytes more malignant and stimulate their division, but not enough to initiate metastasis. Whether UM cells do not spread at all or whether micro-metastases are present in distant organs but remain dormant, is unknown.

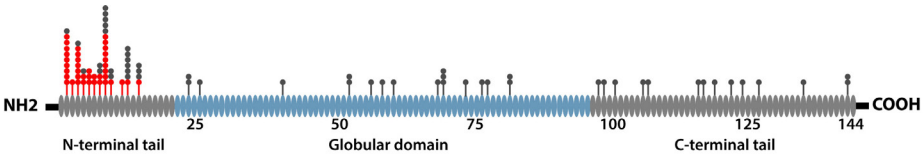

Figure 8. *EIF1AX* mutations. Malignant mutations in the EIF1AX protein observed in UM (red) and other cancer types (grey). All observed mutations are in-frame mutations[71]

3. Chromosomal abnormalities and RNA expression in UM

UM progression involves several chromosomal gains and losses. Chromosome 8q gain and complete loss of chromosome 3 frequently occur in high-risk UM, whereas low metastatic risk UM carry two copies of chromosome 3 and often show gains of chromosome 6q (UM type A) and distal 8q (UM category B)[18, 72-74]. Thirty percent of UM patients also have a deletion of chromosome 1p, which is associated with a higher metastatic risk [75]. Aberrations on other chromosomes have been observed, but are less frequent and show no correlation to metastatic risk. Cytogenetic analyses are useful but very time and labor consuming. Culturing UM tumor cells is hampered by overgrowth of fibroblasts and only short time cultures can be used to obtain an accurate karyotype. Nowadays, a Single Nucleotide Polymorphism (SNP) array technology is used to determine copy number variations (CNV) in tumor specimens. Apart from the observation that CNV analysis as such is an independent prognostic test and does contribute to prognostication models[76, 77], we have observed earlier intriguing differences between these CNVs in metastasizing UM which did urge us to go back to the results obtained with karyotype analysis. We noticed that whereas *BAP1*-mutated tumors did harbor in general a few whole chromosome anomalies resulting in isochromosome formation (e.g. (i)8q or (i)6p), in *SF3B1*-mutated tumors smaller gain or losses of the terminal parts of chromosome 6p and 8q are more prevalent[14]. Whether this is a consequence of the underlying *BAP1* or *SF3B1* mutation causing a different route to generate these chromosomal aberrations or that the resulting genetic changes sort out the most optimal effect in combination with the specific mutated gene, is not clear. Most, if not all UM, present with both the mutation and the matching set of CNVs, but we occasionally observe these mutations without the corresponding CNV patterns or vice versa. A scrutinized genetic survey of these rare cases, preferably with –when available- also the subsequent metastatic tissues may shed more light on this causality dilemma. Alternatively, site-directed mutagenesis of these genes using CRISPR/Cas9 in melanocytic cells could help us to answer the chicken and egg story and analyze other intriguing differences regarding the altered pathways and route towards metastasis between *BAP1* or *SF3B1*-mutated tumors.

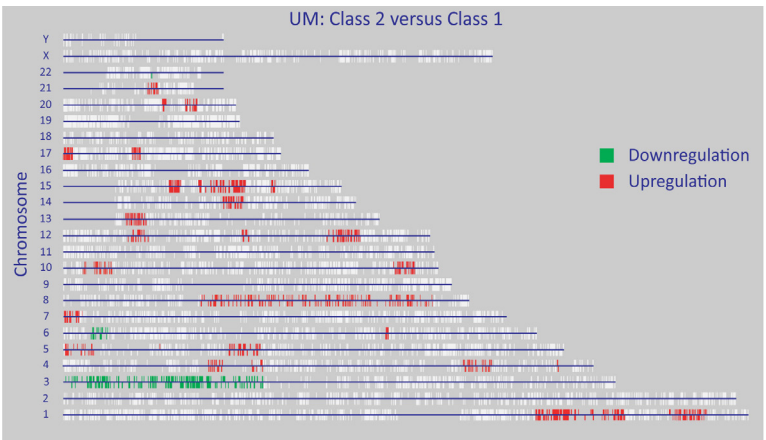

Figure 9. Differential gene expression between class 1 and class 2 UM. Several chromosomal regions contain differentially expressed genes identified by a locally adaptive statistical procedure (LAP)-analysis. White bars indicate locations of the microarray-probes, whereas red (upregulation) or green (downregulation) indicate a differentially expressed gene. Adapted from van Gils et al, 2008.

Nevertheless, these chromosomal abnormalities contribute to the development of UM by altering gene expression. Specific gene expression profiles (GEP) are associated with low metastatic risk (class 1a), intermediate metastatic risk (class 1b) or high metastatic risk

(class 2)[16, 78-80]. Interestingly, we described in a previous publication that differential expression only partially correlated with chromosomal abnormalities (Figure 9). For example, a large part of the genes located on chromosome 3p were significantly downregulated in class 2 UM, whereas genes located on chromosome 3q were not[81]. In addition, parts of chromosome 8q and 6q showed upregulation. This indicates that other mechanisms, such as methylation, might compensate for chromosomal abnormalities.

The oncogene MYC is located in the frequently amplified chromosome 8q24 region. Several analyses show that the presence of extra copies of chromosome 8 is associated with a worse prognosis[74, 82-84]. Although MYC signaling has been shown to be involved in UM development, no direct association has been observed between MYC expression and metastatic death[17]. Expression of the adjacently-located long non-coding RNA *PVT1* (plasmacytoma variant translocation gene) does show a direct association with metastasis. This indicates that gene expression regulation is complex and that other processes, in addition to copy number status, are involved in regulating expression levels. PVT1 is often amplified in several cancer types and acts as an oncogene by regulating transcriptional activity and acting as a miRNA sponge by binding to complementary miRNAs, thereby preventing the miRNAs from exerting their role in gene expression. Another oncogene located on the amplified 8q region is development and differentiation enhancing factor 1 (DDEF). High-risk UM show higher DDEF expression than low-risk UM. DDEF regulates the remodeling of the cytoskeleton, which is necessary for cell motility. Overexpression of DDEF in low-risk UM cells increases their motility, suggesting that upregulation of DDEF contributes to the invasive phenotype of high-risk UM. However, most of these studies do not discriminate between *SF3B1* and *BAP1*-mutated tumors, so these observations might not be valid for the often small 8q amplified regions of *SF3B1*-mutated tumors. Hence, repeating these analyses in well-defined UM subgroups based on genetic changes in the secondary driver genes might result in a different set of classifier genes. Furthermore, amplification of an isochromosome 8q (8q gain in combination with 8p loss), as seen frequently in *BAP1*-mutated tumors is also present in other tumor types. In a recent study on hepatocellular carcinoma performed by The Cancer Genome Atlas (TCGA) network, 14 of 23 *BAP1*-mutated samples did show signs of isochromosome 8q, suggesting a similar common and perhaps more universal underlying genetic mechanism[85]. It would be interesting to determine whether other *SF3B1*-mutated tumors harbor similar *SF3B1*-CNV patterns in addition to the observed overlap in altered expressed RNAs.

Gene expression can also be used to predict disease-free survival of UM patients. Unsupervised clustering of primary UM based on mRNA expression shows two distinct classes as shown by Onken et al[16]. Class 1 consists of *EIF1AX* and *SF3B1*-mutated UM that show the transcriptome of a differentiated melanocyte, whereas class 2 contains monosomy 3/*BAP1*-mutated tumors characterized by a stem cell-like expression profile. Functional annotation of these differentially-expressed genes revealed involvement in development, cell communication, cell growth, cell motility and apoptosis. Interestingly, most of the identified developmental genes are known to be implicated in neural crest development[16].

TCGA contains the expression data of 80 primary UM. Monosomy 3 TCGA samples showed increased transcription of MAPK, AKT and the transcription factors FOXA1 and FOXM1, indicating increased proliferation in this group[17]. Several long non-coding RNAs were found to be higher expressed in monosomy 3 samples, such as the aforementioned *PVT1* gene, as well as the oncogenes *CYTOR* and *BANCR*. The expression of multiple immunological genes was also significantly elevated in the poor prognosis clusters. This indicates an activation of the immune system, which is in contrast to what has been observed in other cancer types, where an activated immune system is typically seen in tu-

mors with low metastatic risk. An association between monosomy 3 and an inflammatory phenotype has been described previously[86]. An important difference may be that UM metastasizes hematogeneously, and that the presence of infiltrating macrophages contributes to intratumoral vessel growth[87-90].

Within the monosomy 3 TCGA samples, two separate clusters were observed, categories C and D[17, 18]. Surprisingly, one cluster showed an activation of the DNA damage response (DDR) pathway, which, however is not reflected in the mutational load of UM. MYC signaling and HIF1a were also upregulated in this cluster, which is consistent with aberrant BAP1 expression. The other cluster is characterized by elevated levels of MAPK and AKT, two effectors of the Gα11/Q pathway. This implies that BAP1 loss may enhance the effect of oncogenic GNAQ and GNA11.

4. UM metastases

Most UM research focuses on primary UM, although the metastases cause death in UM patients and not the primary tumor. Metastatic outgrowth of a tumor is a complicated, multi-step process that is often difficult to unravel. Only a few UM patients with metastases undergo liver resection, and diagnostic biopsies usually do not provide sufficient material for additional research. Moreover, metastases samples can contain a mixture of UM cells, admixed reactive cells as well as hepatocytes, making a proper description of the genomic profile of UM metastases challenging.

4.1 Metastatic spread of UM.

The metastatic capacity of cancer cells is mainly determined by the interaction with the microenvironment. In order to allow UM cells to grow in distant organs, several steps have to be taken; they must lose contact with neighboring cells, home and survive in the host organ, become established and finally also be able to grow into macro-metastases[91]. Therefore, it could be hypothesized that UM cells need to acquire several additional genetic aberrancies in order to successfully grow in distant organs.

In 1882, the ophthalmologist Ernst Fuchs described the predisposition of uveal melanoma to metastasize to the liver and postulated an organ-specific predisposition for metastases[92]. Seven years later, Paget formulated the famous Seed and Soil hypothesis[93] which suggests that metastasis is not random and cancer cells (the seeds) show a preference when metastasizing to distant organs (the soil). Since the large majority of UM metastasize to the liver, it could be implied that there is a favorable microenvironment in the liver for UM cells. Whether the primary tumor stimulates this microenvironment by promoting the development of pre-metastatic niches remains unclear. Unraveling which factors in the liver contribute to this favorable microenvironment might provide us with possible therapeutic targets. One factor that is thought to play an important role in creating a pre-metastatic niche in specific organs are exosomes. These small (~100 nm) lipid bilayer-delimited vesicles are released from cells and carry several functional biomolecules that can be transferred to recipient cells. A specific repertoire of integrines on the exosome-surface dictates the adhesion of exosomes to specific cell types; Hoshino et al. have shown that tumor-derived exosomes preferentially interact with cells at the future metastatic site[94]. After these exosomes are taken up by the target cells, several signaling pathways and inflammatory responses are initiated which are necessary to complete the development of the pre-metastatic niche[95]. Since a study by Angi et al. has shown that primary cultured UM cells secrete almost half of their secreted proteins via exosomes, one may speculate that exosomes play a role in metastasis formation in UM[96].

UM patients who have undergone successful treatment of the primary tumor still develop

metastases. This implies that UM cells have already spread into the circulation before the primary tumor was diagnosed and treated. A study by Eskelin et al calculated tumor doubling times for UM and showed that primary UM metastasize already several years before treatment[3]. With this in mind, one would expect that circulating tumor cells (CTCs) could be detected at time of diagnosis. However, CTCs are mainly detected in blood of patients with metastatic UM, whereas patients with primary UM often show no CTCs[97]. Whether this is due to the low number of CTCs in blood at the time of diagnosis or the seeding of CTCs by metastatic lesions is unknown. Isolating these rare CTCs both at diagnosis and during the metastatic phase could aid our understanding of the metastatic process in UM. Another promising biomarker that could identify dissemination of UM is cell-free DNA (cfDNA). CfDNA are small fragments of DNA that are released in the circulation by (tumor) cells and are present in increased amount in cancer patients. Several studies have showed that *GNAQ* and *GNA11*-mutations could be detected in cfDNA from metastatic UM patients and that their presence showed an association with metastases-volume and overall survival[97-99].

4.2 Chromosomal alterations in UM metastases.

A wide spectrum of chromosomal alterations can be identified in UM metastases, such as gain of 8q, 6q, 1q and alterations in chromosome 3. These chromosomal alterations are also commonly found in primary UM, however, the frequencies are different[100]. UM metastases showed more copies of 8q than the corresponding primary UM[101]. Given this high prevalence of 8q amplifications in UM metastases, it could be hypothesized that the 8q region contains gene(s) that potentially promote metastasis. However, further investigation is necessary in order to determine whether upregulation of oncogenes such as *MYC* and *PTP4A3* have a direct effect on metastasis, or that this is just a consequence of extra copies of chromosomal region 8q. As expected, the majority of UM metastases contained alterations in chromosome 3. Whereas primary UM mainly show monosomy 3, UM metastases frequently showed isodisomy 3 and large regions of homozygosity[100, 102]. Monosomy 3 at first stimulates tumor progression through BAP1 inactivation; however, haploinsufficiency of some chromosome 3 genes could result in a reduced expression of genes such as *MITF*, *MBD4* and *CTNNB1* and thereby limit UM progression[16, 81]. In response to this limitation, duplication of chromosome 3 could be a compensating mechanism in metastasizing UM cells.

4.3 Mutational analysis in UM metastases

As described in the introduction, UM shows a remarkable low mutational burden compared to other malignancies. Rodrigues et al sequenced 15 UM trio's (germline, primary UM and UM metastases) and did not observe a significant increase in SNVs between primary UM and its metastases (median 13 SNVs vs 16 SNVs)[102]. All UM metastases contained a mutually exclusive *GNAQ* or *GNA11* mutation that matched with the primary UM, confirming that these mutations arise early in the development of the disease. Interestingly, Shain et al also observed LOH of mutant GNAQ in multiple metastases samples, suggesting that *GNAQ*-mutated UM require a second hit later in UM progression. LOH of mutant GNAQ shifts the allelic balance towards mutant GNAQ, which activates the GαQ signaling even further, thus allowing cells to become fully malignant[101]. This corresponds with previous studies suggesting that *GNA11*-mutations are more potent oncogenes, since an over-representation of mutations in *GNA11* was observed in UM metastases[103]. Secondary driver mutations in *BAP1* and *SF3B1* were observed in high frequencies in UM metastases as well, indicating early occurrence. Surprisingly, additional mutations in new oncogenes were also observed in UM metastases, which however, occurred in much lower frequencies than the secondary driver mutations. This indicates that these tertiary driver mutations occur later in UM progression, after mutational activation of *BAP1* and

SF3B1. Tertiary driver mutations were found in oncogenes, such as *PTEN*, *EZH2*, *CDKN2A*, *TP53*[101, 102]. These newly-identified mutations might offer new opportunities in UM therapeutics. However, it is still early for the field to develop therapies targeting these genes. Firstly, it remains unclear to what extent each of these mutations contributes to the malignant phenotype. Secondly, novel targeted treatment may possibly only have an effect on metastatic UM subclones harboring particular actionable mutations.

5. Therapeutic options

We have gained considerable insight into the genetic background of UM, but this has not yet resulted in successful treatments of metastatic UM. Treatment of metastatic UM with classic chemotherapy has been disappointing, with low response rates[104, 105]. Over the past 35 years, survival of patients with metastatic UM has not improved[106]. However, now that we know the genes and the pathways they might be involved in, we can start developing new therapeutic modalities for UM.

5.1 Targeting the Gα11/Q pathway

Since the majority of UM contain mutations that deregulate the Gα11/q pathway, drugs targeting this pathway might be effective in the majority of UM, regardless of their further mutational background. Inhibiting GNAQ and GNA11 themselves might be difficult, because of high GTP levels in the cytoplasm. Several studies have therefore focused on interfering with the critical downstream effectors, such as MAPK, PKC, PI3K and AKT signaling. Clinical trials with the MEK1/2 inhibitor selumetinib resulted in promising preliminary results[107]. UM patients treated with selumetinib had an improved progression-free survival of up to 15 weeks, compared to patients treated with chemotherapy. Unfortunately, selumetinib did not improve overall survival in UM patients. This indicates that selumetinib can inhibit metastatic growth only for a limited time: once the tumor acquires resistance to MEK inhibition, it grows even more aggressively than non-treated metastatic tumors. A combination of the chemotherapeutic drug dacarbazine and selumetinib did not give improvement in survival[108]. Similar results were obtained with the MEK inhibitor trametinib and the Akt inhibitor GSK795: no improved survival rate was observed in 40 metastatic UM patients[109].

These disappointing results could be explained by acquired resistance, which also causes CM patients to become resistant to the BRAF inhibitor vemurafenib[110]. Another reason for this limited response could be that these inhibitors act far downstream of oncogenic GNAQ and GNA11. As shown by Mouti et al, progression of UM in zebrafish is dependent on YAP activation, rather than activated extracellular signal-regulated kinases (ERK). Only a subset of the malignant uveal melanocytes showed activation of ERK, while knockdown of *GNAQ* or PLCB4 did not affect the levels of activated ERK, suggesting that MAPK signaling only partially contributes to the development and maintenance of UM[111]. Inhibiting only one arm of an oncogenic network is likely less efficient than interfering with nodes that act closer to GNAQ and GNA11, such as ARF6.

ARF6 regulates multiple downstream signaling pathways and might therefore be a more suitable target for treatment of UM. Knockdown of ARF6 induces the re-localization of GNAQ and GNA11 from the cytoplasm to the plasma membrane, resulting in a decrease of all Gα11/q -mediated pathways. Yoo et al showed that inhibition of ARF6 in the *GNAQ*- and *SF3B1*-mutated UM cell line, Mel202, resulted in a lower tumor incidence and size when injected into immune-compromised mice[31]. A significant reduction in the levels of downstream activated ERK, RAC/RHO, p38, JNK and C-JUN was observed as well. Treating cells and xenograft mouse models with NAV-2729, a direct inhibitor of ARF6, resulted in similar results as the knockdown experiments. Until now, the results have been promis-

ing and no toxicity was observed; however, this treatment is not yet FDA-approved and additional studies have to be performed to investigate whether pharmacological inhibition of ARF6 is an effective treatment for UM.

Other targets for UM treatment could be PLCB4 and YAP. YAP can be successfully inhibited by the well-tolerated compound verteporfin. Treatment of xenograft mouse models with this drug showed a reduction in UM growth[112]. However, these compounds too only target one arm of the oncogenic Gα11/q network and it is therefore likely that they will only show a limited effect unless they are used in combination with another drug.

5.2 HDAC inhibitors to reverse the effect of BAP1 loss

Several studies have described histone deacetylase inhibitors (HDACI) as promising anti-cancer drugs. HDACIs interfere with HDACs, which are frequently upregulated in cancer[113-115]. These HDACs remove acetyl groups from histones, which changes the structure and accessibility of chromatin and thereby affects gene expression[116]. UM cell lines or xenograft models treated with HDACI show a reduced proliferation and an induced cell cycle arrest. A study by Landreville[117] et al described that BAP1-deficient cells have an increased sensitivity for HDACI. HDACIs initiated morphologic and transcriptomic changes consistent with melanocyte differentiation and reduced proliferation through G1 cell cycle arrest. BAP1-deficient cells might be more sensitive to HDAC inhibition because of their increased H2A ubiquitination. It has been shown that distinct histone modifications act together to regulate chromatin structure and gene expression: for example, the deubiqituitinase enzyme H2A-DUB not only regulates deubiquitination of histones, but also acetylation[118]. Interfering with the acetylation of histones in BAP1-deficient UM might reverse the biochemical deficit caused by BAP1 loss by shifting the cell to a less aggressive, more differentiated state. HDACIs could therefore prolong survival of UM patients by keeping micro-metastases in a quiescent, differentiated state.

5.3 Spliceosome inhibitors

SF3B1-mutated UM require a different approach. As mentioned before, tumors with an *SF3B1* mutation show aberrant splicing of pre-mRNA resulting in an increased rate of transcripts containing premature termination codons. Mutations in splicing factors always occur in a heterozygous state and have never been observed to coincide with another splicing-factor mutation. The spliceosome is essential for survival and cancer cells require wildtype splicing to survive. Inhibiting the spliceosome in cancer cells with spliceosome inhibitors has shown exciting results in several different malignancies and might therefore also be a promising treatment for UM.

Several components have been identified that are able to successfully inhibit the spliceosome assembly at an early stage, such as sudemycin[119], E7107[120] and spliceostatin A[121]. E7107 and spliceostatin A bind non-covalently to SF3B1 and thereby prevent exposure of the branchpoint-binding region of U2 snRNP. This results in defective formation of the spliceosome early in the splicing process. Mutations in the *SF3B1* gene result in resistance to E7107, as shown by long term treatment of human colorectal cancer cell lines with E7107[122], indicating that only wildtype (WT) SF3B1 is affected. Since *SF3B1*-mutated UM require wildtype splicing in order to survive, interference of WT SF3B1 by E7107 will result in cell death.

In vivo treatment of isogenic murine myeloid leukemias that harbor an *SRSF2* mutation with E7107, reduced the leukemic burden by inducing preferential cell death of cells bearing an *SRSF2* mutation[123]. Inhibition with this compound showed the same effects as RNAi-mediated silencing of SF3B1, such as an accumulation of unspliced mRNA in the

nucleus. A subset of this unspliced mRNA leaked into the cytoplasm, which resulted in the production of aberrant proteins, including an unusually stable form of the cell cycle inhibitor p27[120]. Unfortunately, clinical trials with E7107 in patients with metastatic solid cancer had to be suspended due to an unexpected side effect in bilateral optic neuritis, resulting in loss of vision. However, in most patients the drug was well tolerated and inhibition of splicing was observed[124, 125]. Additional compound screens will be necessary to identify spliceosome inhibitors that act on the spliceosome assembly at a later stage. Recently, a phase 1 trial was started with the new spliceosome inhibitor H3B-8800[126].

While targeting the spliceosome will probably have most potential in *SF3B1*-mutated UM, it might also be beneficial to treat *BAP1*-mutated UM with these compounds, as it has been shown that cancer cells with an increased MYC activity might also be more vulnerable to spliceosome inhibition[127]. Since a subset of the *BAP1*-mutated tumors show an upregulation of MYC, treatment of these tumors with spliceosome inhibitors might be a promising option. A possible problem with spliceosome-inhibitors might be their lack of specificity. Another method to alter splicing in cells is through oligonucleotides. Oligonucleotides bind to RNA in a sequence-specific manner and prevent interaction between the spliceosome and pre-mRNA by steric hindrance. Aberrantly-spliced genes, that contribute significantly to the malignant phenotype of UM, can thereby be specifically targeted and inhibited. Oligonucleotides have been shown to regulate the presence of aberrant splice variants and restore the production of essential proteins[128]. Unfortunately, no oligonucleotide-based treatment has yet been approved for the treatment of cancer patients.

5.4 Immunotherapy in UM

Metastasis can arise several years after successful removal of the primary tumor. This long latency period can be explained by the presence of dormant UM cells, and dormancy may be due to immunological inhibition. Once a cancer cell is able to overcome the immune response, micro-metastases can start to proliferate, which will result in a fatal outcome.

A new, exciting area of cancer drug development is immunotherapy. One example of immunotherapy is the use of monoclonal antibodies against CTLA-4, PD-1 and PD-L1. CTLA-4 and PD-L1 act as natural immune checkpoints in T cells, to tune down and thereby avoid exaggerated immune responses. It has been shown that cancer cells suppress immune responses by upregulating the ligand PD-L1. The monoclonal antibodies used in immunotherapy block the checkpoints and subsequently unblock and thus activate T cells, which results in the removal of cancer cells. Many of these monoclonal antibodies have already been approved for clinical use, such as nivolumab targeting PD-1. Immunotherapy treatment of advanced melanoma, lung cancer and renal cancer patients showed remission and in some cases even eradicated metastatic disease. Unfortunately, these antibodies show only limited activity in UM patients[129-131]. Dual immune-checkpoint blocking resulted in a response rate of 38% in CM, but no response was observed in UM patients[132]. These disappointing results cannot solely be explained by the fact that UM do not express PD-L1, since two studies show heterogeneous expression of PD-L1 (>5% positivity) in approximately 50% of the UM (Figure 10)[131, 133].

However, a potentially more promising strategy would be to inhibit checkpoints that have been shown to be consistently highly upregulated in metastatic UM, such as indoleamine-pyrrole 2,3-dioxygenase (IDO) and T cell immunoreceptor with Ig and ITIM domains (TIGIT)[17, 134]. Interestingly, Rodrigues et al describe an unexpected high sensitivity to the PD-1 inhibitor pembrolizumab in one UM patient[135]. DNA sequencing identified a germline mutation in *MBD4*, a gene located on chromosome 3 and involved in base excision repair. Mutations in this gene result in an unusual high mutational load, thereby sensitizing

the tumor to PD-1 inhibition. A similar UM patient was recently described [136], while within the TCGA-dataset, two other UM patients with *MBD4* mutations were identified, indicating that a small fraction of the UM patients could directly profit from PD1-inhibition.

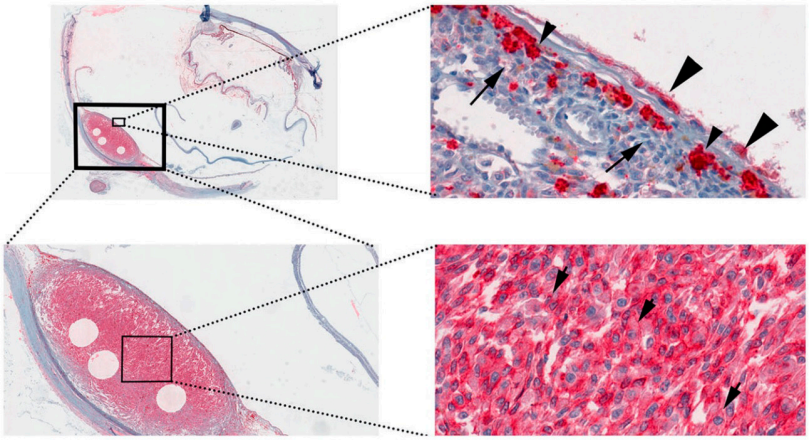

Figure 10. Heterogenous PD-L1 expression in primary UM. The lowest magnification (0.3x) shows the flat choroidal tumor, whereas the medium magnification (1.4x) shows diffuse membranous expression of PD-L1. This is confirmed at higher magnifications; the top right and lower right picture (20x and 40x respectively) show positive membranous PD-L1 expression in UM cells (small arrowheads), positively-stained retinal pigmented epithelium cells (large arrowheads) and tumor-infiltrating macrophages (small arrows). Reproduced with permission from Zoroquiain et al, 2018 via Copyright Clearance Center.

A more classic approach to immunotherapy is inducing an immune response by making use of activated dendritic cells (DCs). A collaborative study in The Netherlands by Bol et al treated UM patients with autologous DCs loaded with antigens derived from gp100 or tyrosinase, two melanocyte-specific proteins[137]. No severe toxicities were observed after the vaccinations and 74% (n=17) of the patients showed the presence of tumor-specific T cells after DC vaccination, indicating an activation of the immune system. These patients showed a significantly longer disease-free and overall survival than patients that did not show an immune response (58 months vs 45 months respectively) (Figure 11). However, no significant difference in the overall survival rate was observed compared to the control group[137]. A new approach uses a novel molecule, tebentafusp, to initiate an immune response in UM patients. Tebentafusp acts as a bridge between UM and cytotoxic T cells and thereby ultimately results in T-cell activation and subsequent killing of UM cells [138, 139]. Preliminary results indicate that biopsies, which were taken after the injection, confirmed the influx of lymphocytes and an increase in PD-L1 expression.

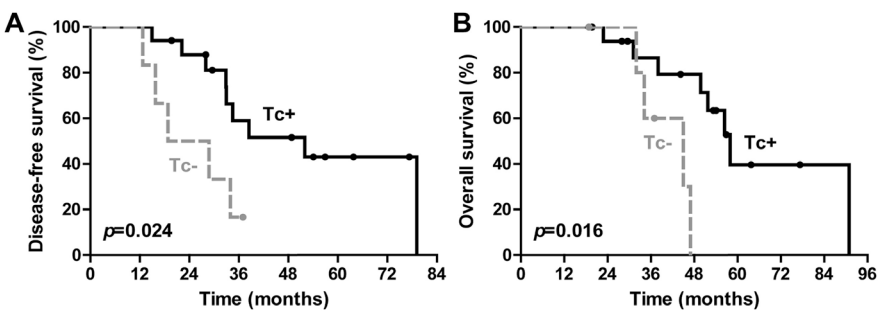

Figure 11. Survival of high risk UM patients after dendritic cell treatment. Kaplan-Meier curve showing the disease-free survival **(A)** and overall survival **(B)** in correlation with the presence of tumor antigen-specific T cells after receiving dendritic cell vaccination. Reproduced with permission from Bol et al, 2016, via Copyright Clearance Center.

Still, the results obtained from widely used immunotherapy unfortunately present less promising results in UM patients than in CM patients. As the eye is an immune-privileged site, immune responses may not develop as easily as in other locations, and may even be inhibited actively[140]. In most cancer types, immune infiltration is associated with good prognosis and sensitivity to immunotherapy. However, especially the prognostically infaust monosomy 3 UM show a dense immune infiltrate and increased HLA Class I expression[89, 141, 142]. This different response rates could be explained by the presence of immunosuppressive cells, such as regulatory T cells and macrophages, which dampen the immune response. A study of low risk and high risk tumors indicated that extra copies of chromosome 8q were associated with influx of macrophages, while loss of BAP1 was linked to higher numbers of T cells[142, 143]. These data show that genetic changes are related to the development of the inflammatory phenotype in UM, but they do not explain why the immune system is so unresponsive in most patients. However, all these results imply that future immunotherapy agents should mainly focus on overcoming the immune suppression in UM. By determining the precise immune landscape in every tumor, we might be able to predict which UM would be sensitive to immunotherapy. Another factor that could explain the disappointing response rate to immunotherapy is the low mutational load of UM cells. As previously described, CM show a high mutational burden which correlates with a plethora of neo-antigens and thus renders them particularly suitable for immunotherapy. However, *SF3B1*-mutated UM could very well be more sensitive to immunotherapy if this is directed against the proteins produced by aberrant splicing. Mass spectrometry analysis of the proteome secreted by *SF3B1*-mutated UM could identify and characterize these aberrant proteins.

These aforementioned treatments can be given systemically in order to remove any metastases in distant organs; however they can also be given locally to UM patients with liver metastases by isolated hepatic perfusion (IHP). In case metastatic disease is confined to the liver, the liver can be isolated from the systemic circulation, which allows a much higher concentration of therapeutics to be used. Fifty to seventy-five percent of metastatic UM patients responded to IHP with the chemotherapeutic agent melphalan. The most common adverse effects were hematological events – such as thrombocytopenia, anemia, and neutropenia – which were clinically manageable, indicating that IHP with melphalan could be a promising treatment for UM patients with liver metastasis [144-146]. Currently IHP is performed for established metastatic disease, but future drugs with less side-effects might allow targeted adjuvant treatment in high-risk UM patients[147].

6. Future directions and conclusions

Even though our understanding of UM has advanced in the last decade, UM remains one of the very few malignancies for which there is no treatment available for metastatic disease. In recent years, there has been a tendency to transpose treatments shown to be effective in CM to UM, such as immunotherapy and MEK-inhibitors. However, as described in multiple studies, the biological behavior of these two malignancies is completely different and therefore they require a different approach. A better understanding of the complex genetic and immunologic background of UM will allow a more personalized approach which is necessary for effective treatment. Treatments targeting oncogenic GNAQ and GNA11 signaling could be applied to all UM patients, although it remains unclear if this will be sufficient for effective UM treatment. GNAQ and GNA11 are relatively weak oncoproteins and can only become truly malignant when combined with co-mutations in secondary driver genes. Therefore, additional research into agents targeting these deregulated processes, such as spliceosome inhibitors and HDAC inhibitors, is necessary.

The genetic background could also play a role in the treatment outcome. *SF3B1*-mutated tu-

mors could benefit from different therapeutic agents than *BAP1*-mutated tumors. This might require a more personalized approach, where the genetic background of each UM patient is investigated in the diagnostic setting and determines the best treatment option (Figure 12).

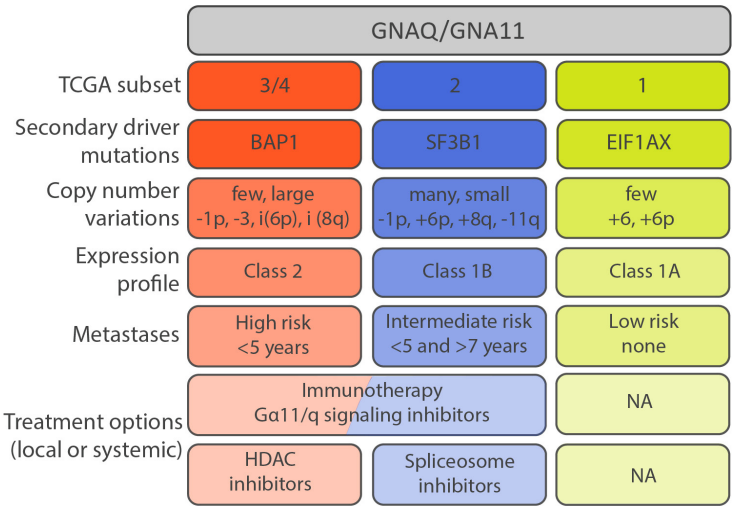

Figure 12. Schematic overview of the different UM subtypes. Each UM subtype is characterized by a TCGA subset, a specific mutation in one of the secondary driver-genes, several copy number variations and a different expression profile. Both intermediate and high risk UM could profit from immunotherapy or therapies that interfere with oncogenic GαQ signaling. Additionally, high risk, *BAP1*mut UM could profit from treatment with HDAC inhibitors, whereas intermediate risk, *SF3B1*mut UM could be more sensitive to spliceosome inhibitors. These treatments can be administered systemically, but also locally by isolated hepatic perfusion.

In the case of an *EIF1AX*-mutated UM, local treatment of the primary tumor could already be sufficient. However, *SF3B1* and *BAP1*-mutated UM will require a more rigorous treatment protocol. For these patients it is known that in many cases micro-metastases are already present at the time of diagnosis, meaning that besides treatment of the primary tumor, the dormant micro-metastases have to be targeted as well to improve overall patient survival. We therefore hypothesize that a combinatorial treatment approach in which local treatment of the primary tumor is combined with systemic treatment targeting the micro-metastases in high-risk cases would have the most potential in UM therapeutics. However, it remains controversial which specific characteristics are necessary to define high-risk UM patients, since different research groups use different prognostic parameters. In order to synchronize UM prognostication and treatment, an universal prognostication model using a combination of clinical, histological and genetic parameters should be considered to reliably identify high-risk UM patients[76, 77, 148]. A number of important questions still remain open and research into these questions will dramatically aid the development of treatments for metastatic UM: does the entire GNAQ and GNA11-signaling network contribute to the development and progression of UM or is it only one arm of the network? Which gene on chromosome 8q plays a role in the development of metastases? Which functions of the BAP1 protein contribute mostly to the aggressive phenotype observed in UM? What is the role of macrophages versus infiltrating T lymphocytes in high risk tumors, or are both only bystanders? And what stimulates dormant UM micrometastases in the liver to suddenly proliferate and give rise to fatal metastatic foci? The complexity and rarity of this type of cancer has made research into this malignancy difficult, but the recent progress in our understanding of UM will bring us step-by-step closer to effective treatments.

Declaration of interests
None.

Acknowledgements
This work was made possible by a grant of the Combined Ophthalmic Research Rotterdam. We would like to thank Tom Brands for his help with the figures.

References

1. Singh, A.D., M.E. Turell, and A.K. Topham, Uveal melanoma: trends in incidence, treat ment, and survival. Ophthalmology, 2011. 118(9): p. 1881-5.
2. Damato, B., Ocular treatment of choroidal melanoma in relation to the prevention of metastatic death - A personal view. Prog Retin Eye Res, 2018. 66: p. 187-199.
3. Eskelin, S., et al., Tumor doubling times in metastatic malignant melanoma of the uvea: tumor progression before and after treatment. Ophthalmology, 2000. 107(8): p. 1443-9.
4. Augsburger, J.J., Z.M. Correa, and A.H. Shaikh, Effectiveness of treatments for metastatic uveal melanoma. Am J Ophthalmol, 2009. 148(1): p. 119-27.
5. Coupland, S.E., et al., Metastatic choroidal melanoma to the contralateral orbit 40 years after enucleation. Arch Ophthalmol, 1996. 114(6): p. 751-6.
6. Singh, A.D., et al., The Zimmerman-McLean-Foster hypothesis: 25 years later. Br J Oph thalmol, 2004. 88(7): p. 962-7.
7. Zimmerman, L.E., I.W. McLean, and W.D. Foster, Does enucleation of the eye containing a malignant melanoma prevent or accelerate the dissemination of tumour cells. Br J Oph thalmol, 1978. 62(6): p. 420-5.
8. Shields, C.L., et al., Metastasis of uveal melanoma millimeter-by-millimeter in 8033 con secutive eyes. Arch Ophthalmol, 2009. 127(8): p. 989-98.
9. McLean, I.W., W.D. Foster, and L.E. Zimmerman, Uveal melanoma: location, size, cell type, and enucleation as risk factors in metastasis. Hum Pathol, 1982. 13(2): p. 123-32.
10. Yavuzyigitoglu, S., et al., Lipomatous Change in Uveal Melanoma: Histopathological, Im munohistochemical and Cytogenetic Analysis. Ocul Oncol Pathol, 2016. 2(3): p. 133-5.
11. Harbour, J.W., et al., Frequent mutation of BAP1 in metastasizing uveal melanomas. Sci ence, 2010. 330(6009): p. 1410-3.
12. Yavuzyigitoglu, S., et al., Uveal Melanomas with SF3B1 Mutations: A Distinct Subclass Associated with Late-Onset Metastases. Ophthalmology, 2016. 123(5): p. 1118-28.
13. Martin, M., et al., Exome sequencing identifies recurrent somatic mutations in EIF1AX and SF3B1 in uveal melanoma with disomy 3. Nat Genet, 2013. 45(8): p. 933-6.
14. Yavuzyigitoglu, S., et al., Correlation of Gene Mutation Status with Copy Number Profile in Uveal Melanoma. Ophthalmology, 2017. 124(4): p. 573-575.
15. Field, M.G., et al., Punctuated evolution of canonical genomic aberrations in uveal mela noma. Nat Commun, 2018. 9(1): p. 116.
16. Onken, M.D., et al., Gene expression profiling in uveal melanoma reveals two molecular classes and predicts metastatic death. Cancer Res, 2004. 64(20): p. 7205-9.
17. Robertson, A.G., et al., Integrative Analysis Identifies Four Molecular and Clinical Subsets in Uveal Melanoma. Cancer Cell, 2017. 32(2): p. 204-220 e15.
18. Jager, M.J., N.J. Brouwer, and B. Esmaeli, The Cancer Genome Atlas Project: An Integrated Molecular View of Uveal Melanoma. Ophthalmology, 2018. 125(8): p. 1139-1142.
19. Rimoldi, D., et al., Lack of BRAF mutations in uveal melanoma. Cancer Res, 2003. 63(18): p. 5712-5.
20. van Poppelen, N.M., et al., Genetic Background of Iris Melanomas and Iris Melanocytic Tumors of Uncertain Malignant Potential. Ophthalmology, 2018. 125(6): p. 904-912.
21. Furney, S.J., et al., SF3B1 mutations are associated with alternative splicing in uveal mela noma. Cancer Discov, 2013. 3(10): p. 1122-1129.
22. Vader, M.J.C., et al., GNAQ and GNA11 mutations and downstream YAP activation in choroidal nevi. Br J Cancer, 2017. 117(6): p. 884-887.
23. Smit, K.N., et al., Combined mutation and copy-number variation detection by targeted next-generation sequencing in uveal melanoma. Mod Pathol, 2018. 31(5): p. 763-771.
24. Farquhar, N., et al., Patterns of BAP1 protein expression provide insights into prognostic significance and the biology of uveal melanoma. J Pathol Clin Res, 2018. 4(1): p. 26-38.

25. Van Raamsdonk, C.D., et al., Mutations in GNA11 in uveal melanoma. N Engl J Med, 2010. 363(23): p. 2191-9.
26. Van Raamsdonk, C.D., et al., Frequent somatic mutations of GNAQ in uveal melanoma and blue naevi. Nature, 2009. 457(7229): p. 599-602.
27. Harbour, J.W., et al., Recurrent mutations at codon 625 of the splicing factor SF3B1 in uveal melanoma. Nat Genet, 2013. 45(2): p. 133-5.
28. Dono, M., et al., Mutation frequencies of GNAQ, GNA11, BAP1, SF3B1, EIF1AX and TERT in uveal melanoma: detection of an activating mutation in the TERT gene promoter in a single case of uveal melanoma. Br J Cancer, 2014. 110(4): p. 1058-65.
29. Ewens, K.G., et al., Chromosome 3 status combined with BAP1 and EIF1AX mutation profiles are associated with metastasis in uveal melanoma. Invest Ophthalmol Vis Sci, 2014. 55(8): p. 5160-7.
30. O'Hayre, M., et al., The emerging mutational landscape of G proteins and G-protein-coupled receptors in cancer. Nat Rev Cancer, 2013. 13(6): p. 412-24.
31. Yoo, J.H., et al., ARF6 Is an Actionable Node that Orchestrates Oncogenic GNAQ Signal ing in Uveal Melanoma. Cancer Cell, 2016. 29(6): p. 889-904.
32. Moore, A.R., et al., GNA11 Q209L Mouse Model Reveals RasGRP3 as an Essential Signal ing Node in Uveal Melanoma. Cell Rep, 2018. 22(9): p. 2455-2468.
33. Feng, X., et al., Hippo-independent activation of YAP by the GNAQ uveal melanoma on cogene through a trio-regulated rho GTPase signaling circuitry. Cancer Cell, 2014. 25(6): p. 831-45.
34. Yu, F.X., et al., Mutant Gq/11 promote uveal melanoma tumorigenesis by activating YAP. Cancer Cell, 2014. 25(6): p. 822-30.
35. Griner, E.M. and M.G. Kazanietz, Protein kinase C and other diacylglycerol effectors in cancer. Nat Rev Cancer, 2007. 7(4): p. 281-94.
36. Chen, X., et al., RasGRP3 Mediates MAPK Pathway Activation in GNAQ Mutant Uveal Melanoma. Cancer Cell, 2017. 31(5): p. 685-696 e6.
37. Johansson, P., et al., Deep sequencing of uveal melanoma identifies a recurrent mutation in PLCB4. Oncotarget, 2016. 7(4): p. 4624-31.
38. Moore, A.R., et al., Recurrent activating mutations of G-protein-coupled receptor CYSL TR2 in uveal melanoma. Nat Genet, 2016. 48(6): p. 675-80.
39. Perez, D.E., et al., Uveal melanoma driver mutations in GNAQ/11 yield numerous changes in melanocyte biology. Pigment Cell Melanoma Res, 2018.
40. Koopmans, A.E., et al., Clinical significance of immunohistochemistry for detection of BAP1 mutations in uveal melanoma. Mod Pathol, 2014. 27(10): p. 1321-30.
41. Kalirai, H., et al., Lack of BAP1 protein expression in uveal melanoma is associated with increased metastatic risk and has utility in routine prognostic testing. Br J Cancer, 2014. 111(7): p. 1373-80.
42. Shah, A.A., T.D. Bourne, and R. Murali, BAP1 protein loss by immunohistochemistry: a potentially useful tool for prognostic prediction in patients with uveal melanoma. Pathol ogy, 2013. 45(7): p. 651-6.
43. Stalhammar, G., et al., Digital Image Analysis of BAP-1 Accurately Predicts Uveal Mela noma Metastasis. Transl Vis Sci Technol, 2019. 8(3): p. 11.
44. Szalai, E., et al., Uveal Melanoma Nuclear BRCA1-Associated Protein-1 Immunoreactivity Is an Indicator of Metastasis. Ophthalmology, 2018. 125(2): p. 203-209.
45. van Essen, T.H., et al., Prognostic parameters in uveal melanoma and their association with BAP1 expression. Br J Ophthalmol, 2014. 98(12): p. 1738-43.
46. Yu, H., et al., Tumor suppressor and deubiquitinase BAP1 promotes DNA double-strand break repair. Proc Natl Acad Sci U S A, 2014. 111(1): p. 285-90.
47. Peng, H., et al., Familial and Somatic BAP1 Mutations Inactivate ASXL1/2-Mediated Allo steric Regulation of BAP1 Deubiquitinase by Targeting Multiple Independent Domains. Cancer Res, 2018. 78(5): p. 1200-1213.
48. Yu, H., et al., The ubiquitin carboxyl hydrolase BAP1 forms a ternary complex with YY1 and HCF-1 and is a critical regulator of gene expression. Mol Cell Biol, 2010. 30(21): p. 5071-85.
49. Machida, Y.J., et al., The deubiquitinating enzyme BAP1 regulates cell growth via interac tion with HCF-1. J Biol Chem, 2009. 284(49): p. 34179-88.
50. Ji, Z., et al., The forkhead transcription factor FOXK2 acts as a chromatin targeting factor for the BAP1-containing histone deubiquitinase complex. Nucleic Acids Res, 2014. 42(10):

p. 6232-42.
51. Mashtalir, N., et al., Autodeubiquitination protects the tumor suppressor BAP1 from cytoplasmic sequestration mediated by the atypical ubiquitin ligase UBE2O. Mol Cell, 2014. 54(3): p. 392-406.
52. Sowa, M.E., et al., Defining the human deubiquitinating enzyme interaction landscape. Cell, 2009. 138(2): p. 389-403.
53. Dey, A., et al., Loss of the tumor suppressor BAP1 causes myeloid transformation. Sci ence, 2012. 337(6101): p. 1541-6.
54. Matatall, K.A., et al., BAP1 deficiency causes loss of melanocytic cell identity in uveal melanoma. BMC Cancer, 2013. 13: p. 371.
55. Mani, S.A., et al., The epithelial-mesenchymal transition generates cells with properties of stem cells. Cell, 2008. 133(4): p. 704-15.
56. Scheuermann, J.C., et al., Histone H2A deubiquitinase activity of the Polycomb repressive complex PR-DUB. Nature, 2010. 465(7295): p. 243-7.
57. Chittock, E.C., et al., Molecular architecture of polycomb repressive complexes. Biochem Soc Trans, 2017. 45(1): p. 193-205.
58. Bommi, P.V., et al., The polycomb group protein BMI1 is a transcriptional target of HDAC inhibitors. Cell Cycle, 2010. 9(13): p. 2663-73.
59. van Leeuwen, F. and B. van Steensel, Histone modifications: from genome-wide maps to functional insights. Genome Biol, 2005. 6(6): p. 113.
60. Bononi, A., et al., BAP1 regulates IP3R3-mediated Ca(2+) flux to mitochondria suppress ing cell transformation. Nature, 2017. 546(7659): p. 549-553.
61. Walpole, S., et al., Comprehensive Study of the Clinical Phenotype of Germline BAP1 Variant-Carrying Families Worldwide. J Natl Cancer Inst, 2018. 110(12): p. 1328-1341.
62. Wang, L., et al., SF3B1 and other novel cancer genes in chronic lymphocytic leukemia. N Engl J Med, 2011. 365(26): p. 2497-506.
63. Ciriello, G., et al., Comprehensive Molecular Portraits of Invasive Lobular Breast Cancer. Cell, 2015. 163(2): p. 506-19.
64. Bailey, P., et al., Genomic analyses identify molecular subtypes of pancreatic cancer. Nature, 2016. 531(7592): p. 47-52.
65. Alsafadi, S., et al., Cancer-associated SF3B1 mutations affect alternative splicing by pro moting alternative branchpoint usage. Nat Commun, 2016. 7: p. 10615.
66. Paolella, B.R., et al., Copy-number and gene dependency analysis reveals partial copy loss of wild-type SF3B1 as a novel cancer vulnerability. Elife, 2017. 6.
67. Seiler, M., et al., Somatic Mutational Landscape of Splicing Factor Genes and Their Func tional Consequences across 33 Cancer Types. Cell Rep, 2018. 23(1): p. 282-296 e4.
68. Darman, R.B., et al., Cancer-Associated SF3B1 Hotspot Mutations Induce Cryptic 3′ Splice Site Selection through Use of a Different Branch Point. Cell Rep, 2015. 13(5): p. 1033-45.
69. van Poppelen, N.M., et al., SRSF2 Mutations in Uveal Melanoma: A Preference for In-Frame Deletions? Cancers (Basel), 2019. 11(8).
70. Martin-Marcos, P., et al., eIF1A residues implicated in cancer stabilize translation preini tiation complexes and favor suboptimal initiation sites in yeast. Elife, 2017. 6.
71. Tate, J.G., et al., COSMIC: the Catalogue Of Somatic Mutations In Cancer. Nucleic Acids Res, 2019. 47(D1): p. D941-D947.
72. Prescher, G., et al., Prognostic implications of monosomy 3 in uveal melanoma. Lancet, 1996. 347(9010): p. 1222-5.
73. van den Bosch, T., et al., Higher percentage of FISH-determined monosomy 3 and 8q amplification in uveal melanoma cells relate to poor patient prognosis. Invest Ophthalmol Vis Sci, 2012. 53(6): p. 2668-74.
74. Damato, B., et al., Estimating prognosis for survival after treatment of choroidal mela noma. Prog Retin Eye Res, 2011. 30(5): p. 285-95.
75. Kilic, E., et al., Concurrent loss of chromosome arm 1p and chromosome 3 predicts a decreased disease-free survival in uveal melanoma patients. Invest Ophthalmol Vis Sci, 2005. 46(7): p. 2253-7.
76. Drabarek, W., et al., Multi-Modality Analysis Improves Survival Prediction in Enucleated Uveal Melanoma Patients. Invest Ophthalmol Vis Sci, 2019. 60(10): p. 3595-3605.
77. Eleuteri, A., et al., Enhancing survival prognostication in patients with choroidal mela noma by integrating pathologic clinical and genetic predictors of metastases. Int J Biomed Eng Technol., 2012(8): p. 18-35.

78. Field, M.G., et al., Epigenetic reprogramming and aberrant expression of PRAME are associated with increased metastatic risk in Class 1 and Class 2 uveal melanomas. Onco target, 2016. 7(37): p. 59209-59219.
79. Zuidervaart, W., et al., Gene expression profiling identifies tumour markers potentially playing a role in uveal melanoma development. Br J Cancer, 2003. 89(10): p. 1914-9.
80. Tschentscher, F., et al., Tumor classification based on gene expression profiling shows that uveal melanomas with and without monosomy 3 represent two distinct entities. Cancer Res, 2003. 63(10): p. 2578-84.
81. van Gils, W., et al., Gene expression profiling in uveal melanoma: two regions on 3p related to prognosis. Invest Ophthalmol Vis Sci, 2008. 49(10): p. 4254-62.
82. Dogrusoz, M., et al., The Prognostic Value of AJCC Staging in Uveal Melanoma Is En hanced by Adding Chromosome 3 and 8q Status. Invest Ophthalmol Vis Sci, 2017. 58(2):p. 833-842.
83. Versluis, M., et al., Digital PCR validates 8q dosage as prognostic tool in uveal melanoma. PLoS One, 2015. 10(3): p. e0116371.
84. Cassoux, N., et al., Genome-wide profiling is a clinically relevant and affordable prognos tic test in posterior uveal melanoma. Br J Ophthalmol, 2014. 98(6): p. 769-74.
85. Cancer Genome Atlas Research Network. Electronic address, w.b.e. and N. Cancer Ge nome Atlas Research, Comprehensive and Integrative Genomic Characterization of Hepa tocellular Carcinoma. Cell, 2017. 169(7): p. 1327-1341 e23.
86. Maat, W., et al., Monosomy of chromosome 3 and an inflammatory phenotype occur together in uveal melanoma. Invest Ophthalmol Vis Sci, 2008. 49(2): p. 505-10.
87. Bronkhorst, I.H., et al., Detection of M2-macrophages in uveal melanoma and relation with survival. Invest Ophthalmol Vis Sci, 2011. 52(2): p. 643-50.
88. Ly, L.V., et al., In aged mice, outgrowth of intraocular melanoma depends on proangiog enic M2-type macrophages. J Immunol, 2010. 185(6): p. 3481-8.
89. Jager, M.J., et al., Macrophages in uveal melanoma and in experimental ocular tumor models: Friends or foes? Prog Retin Eye Res, 2011. 30(2): p. 129-46.
90. Brouwer, N.J., et al., Tumour Angiogenesis in Uveal Melanoma Is Related to Genetic Evolution. Cancers (Basel), 2019. 11(7).
91. Lambert, A.W., D.R. Pattabiraman, and R.A. Weinberg, Emerging Biological Principles of Metastasis. Cell, 2017. 168(4): p. 670-691.
92. Fuchs, E., Das Sarkom des Uvealtractus. Graefe's Archiv für Ophthalmologie, 1882(XII): p. 233.
93. Paget, S., The distribution of secondary growths in cancer of the breast. The Lancet, 1889. 133(3421): p. 571-573.
94. Hoshino, A., et al., Tumour exosome integrins determine organotropic metastasis. Nature, 2015. 527(7578): p. 329-35.
95. Liu, Y. and X. Cao, Organotropic metastasis: role of tumor exosomes. Cell Res, 2016. 26(2): p. 149-50.
96. Angi, M., et al., In-depth proteomic profiling of the uveal melanoma secretome. Oncotar get, 2016. 7(31): p. 49623-49635.
97. Beasley, A., et al., Clinical Application of Circulating Tumor Cells and Circulating Tumor DNA in Uveal Melanoma. JCO Precision Oncology, 2018(2): p. 1-12.
98. Bidard, F.C., et al., Detection rate and prognostic value of circulating tumor cells and circulating tumor DNA in metastatic uveal melanoma. Int J Cancer, 2014. 134(5): p. 1207-13.
99. Metz, C.H.D., et al., Ultradeep sequencing detects GNAQ and GNA11 mutations in cell-free DNA from plasma of patients with uveal melanoma. Cancer medicine, 2013. 2(2): p. 208-215.
100. McCarthy, C., et al., Insights into genetic alterations of liver metastases from uveal mela noma. Pigment Cell Melanoma Res, 2016. 29(1): p. 60-7.
101. Shain, A.H., et al., The genetic evolution of metastatic uveal melanoma. Nat Genet, 2019. 51(7): p. 1123-1130.
102. Rodrigues, M., et al., Evolutionary routes in metastatic uveal melanomas depend on MBD4 alterations. Clin Cancer Res, 2019.
103. Griewank, K.G., et al., Genetic and clinico-pathologic analysis of metastatic uveal mela noma. Mod Pathol, 2014. 27(2): p. 175-83.
104. Chattopadhyay, C., et al., Uveal melanoma: From diagnosis to treatment and the science

in between. Cancer, 2016. 122(15): p. 2299-312.
105. Carvajal, R.D., et al., A phase 2 randomised study of ramucirumab (IMC-1121B) with or without dacarbazine in patients with metastatic melanoma. Eur J Cancer, 2014. 50(12): p. 2099-107.
106. Rantala, E.S., M. Hernberg, and T.T. Kivela, Overall survival after treatment for metastatic uveal melanoma: a systematic review and meta-analysis. Melanoma Res, 2019.
107. Carvajal, R.D., et al., Effect of selumetinib vs chemotherapy on progression-free survival in uveal melanoma: a randomized clinical trial. JAMA, 2014. 311(23): p. 2397-405.
108. Carvajal, R.D., et al., Selumetinib in Combination With Dacarbazine in Patients With Metastatic Uveal Melanoma: A Phase III, Multicenter, Randomized Trial (SUMIT). J Clin Oncol, 2018. 36(12): p. 1232-1239.
109. Alexander Noor, S., et al., A randomized phase 2 study of trametinib with or without GSK2141795 in patients with advanced uveal melanoma. Journal of Clinical Oncology, 2016. 34(15_suppl): p. 9511-9511.
110. Nazarian, R., et al., Melanomas acquire resistance to B-RAF(V600E) inhibition by RTK or N-RAS upregulation. Nature, 2010. 468(7326): p. 973-7.
111. Mouti, M.A., et al., Minimal contribution of ERK1/2-MAPK signalling towards the main tenance of oncogenic GNAQQ209P-driven uveal melanomas in zebrafish. Oncotarget, 2016. 7(26): p. 39654-39670.
112. Yu, F.X., K. Zhang, and K.L. Guan, YAP as oncotarget in uveal melanoma. Oncoscience, 2014. 1(7): p. 480-1.
113. Song, J., et al., Increased expression of histone deacetylase 2 is found in human gastric cancer. APMIS, 2005. 113(4): p. 264-8.
114. Zhang, Z., et al., Quantitation of HDAC1 mRNA expression in invasive carcinoma of the breast. Breast Cancer Res Treat, 2005. 94(1): p. 11-6.
115. Halkidou, K., et al., Upregulation and nuclear recruitment of HDAC1 in hormone refrac tory prostate cancer. Prostate, 2004. 59(2): p. 177-89.
116. Li, G., et al., Highly compacted chromatin formed in vitro reflects the dynamics of tran scription activation in vivo. Mol Cell, 2010. 38(1): p. 41-53.
117. Landreville, S., et al., Histone deacetylase inhibitors induce growth arrest and differen tiation in uveal melanoma. Clin Cancer Res, 2012. 18(2): p. 408-16.
118. Zhu, P., et al., A histone H2A deubiquitinase complex coordinating histone acetylation and H1 dissociation in transcriptional regulation. Mol Cell, 2007. 27(4): p. 609-21.
119. Fan, L., et al., Sudemycins, novel small molecule analogues of FR901464, induce alternative gene splicing. ACS Chem Biol, 2011. 6(6): p. 582-9.
120. Kotake, Y., et al., Splicing factor SF3b as a target of the antitumor natural product pladienolide. Nat Chem Biol, 2007. 3(9): p. 570-5.
121. Kaida, D., et al., Spliceostatin A targets SF3b and inhibits both splicing and nuclear reten tion of pre-mRNA. Nat Chem Biol, 2007. 3(9): p. 576-83.
122. Yokoi, A., et al., Biological validation that SF3b is a target of the antitumor macrolide pladienolide. FEBS J, 2011. 278(24): p. 4870-80.
123. Lee, S.C., et al., Modulation of splicing catalysis for therapeutic targeting of leukemia with mutations in genes encoding spliceosomal proteins. Nat Med, 2016. 22(6): p. 672-8.
124. Eskens, F.A., et al., Phase I pharmacokinetic and pharmacodynamic study of the first-in-class spliceosome inhibitor E7107 in patients with advanced solid tumors. Clin Cancer Res, 2013. 19(22): p. 6296-304.
125. Hong, D.S., et al., A phase I, open-label, single-arm, dose-escalation study of E7107, a precursor messenger ribonucleic acid (pre-mRNA) splicesome inhibitor administered intravenously on days 1 and 8 every 21 days to patients with solid tumors. Invest New Drugs, 2014. 32(3): p. 436-44.
126. Seiler, M., et al., H3B-8800, an orally available small-molecule splicing modulator, induces lethality in spliceosome-mutant cancers. Nat Med, 2018. 24(4): p. 497-504.
127. Hsu, T.Y., et al., The spliceosome is a therapeutic vulnerability in MYC-driven cancer. Nature, 2015. 525(7569): p. 384-8.
128. McClorey, G. and M.J. Wood, An overview of the clinical application of antisense oligo nucleotides for RNA-targeting therapies. Curr Opin Pharmacol, 2015. 24: p. 52-8.
129. van der Kooij, M.K., et al., Anti-PD1 treatment in metastatic uveal melanoma in the Netherlands. Acta Oncol, 2017. 56(1): p. 101-103.

130. Zimmer, L., et al., Phase II DeCOG-study of ipilimumab in pretreated and treatment-naive patients with metastatic uveal melanoma. PLoS One, 2015. 10(3): p. e0118564.
131. Wierenga, A.P.A., et al., Immune Checkpoint Inhibitors in Uveal and Conjuncti val Melanoma. Int Ophthalmol Clin, 2019. 59(2): p. 53-63.
132. Kirchberger, M.C., et al., Real world experience in low-dose ipilimumab in com bination with PD-1 blockade in advanced melanoma patients. Oncotarget, 2018. 9(48): p. 28903-28909.
133. Zoroquiain, P., et al., Programmed cell death ligand-1 expression in tumor and immune cells is associated with better patient outcome and decreased tumor-infiltrating lymphocytes in uveal melanoma. Mod Pathol, 2018. 31(8): p. 1201-1210.
134. Stalhammar, G., S. Seregard, and H.E. Grossniklaus, Expression of immune checkpoint receptors Indoleamine 2,3-dioxygenase and T cell Ig and ITIM do main in metastatic versus nonmetastatic choroidal melanoma. Cancer Med, 2019. 8(6): p. 2784-2792.
135. Rodrigues, M., et al., Outlier response to anti-PD1 in uveal melanoma reveals germline MBD4 mutations in hypermutated tumors. Nat Commun, 2018. 9(1): p. 1866.
136. Johansson, P.A., et al., Prolonged stable disease in a uveal melanoma patient with germline MBD4 nonsense mutation treated with pembrolizumab and ipilimumab. Immunogenetics, 2019.
137. Bol, K.F., et al., Adjuvant Dendritic Cell Vaccination in High-Risk Uveal Melanoma. Ophthalmology, 2016. 123(10): p. 2265-7.
138. Komatsubara, K.M. and R.D. Carvajal, Immunotherapy for the Treatment of Uveal Melanoma: Current Status and Emerging Therapies. Curr Oncol Rep, 2017. 19(7): p. 45.
139. Damato, B.E., et al., Tebentafusp: T Cell Redirection for the Treatment of Metastatic Uveal Melanoma. Cancers (Basel), 2019. 11(7).
140. Niederkorn, J.Y., Immune escape mechanisms of intraocular tumors. Prog Retin Eye Res, 2009. 28(5): p. 329-47.
141. de Lange, M.J., et al., Heterogeneity revealed by integrated genomic analysis uncovers a molecular switch in malignant uveal melanoma. Oncotarget, 2015. 6(35): p. 37824-35.
142. Bronkhorst, I.H., et al., Different subsets of tumor-infiltrating lymphocytes correlate with macrophage influx and monosomy 3 in uveal melanoma. Invest Ophthalmol Vis Sci, 2012. 53(9): p. 5370-8.
143. Gezgin, G., et al., Genetic evolution of uveal melanoma guides the development of an inflammatory microenvironment. Cancer Immunol Immunother, 2017. 66(7): p. 903-912.
144. Meijer, T.S., et al., Safety of Percutaneous Hepatic Perfusion with Melphalan in Patients with Unresectable Liver Metastases from Ocular Melanoma Using the Delcath Systems' Second-Generation Hemofiltration System: A Prospective Non-randomized Phase II Trial. Cardiovasc Intervent Radiol, 2019. 42(6): p. 841-852.
145. Artzner, C., et al., Chemosaturation with percutaneous hepatic perfusion of melphalan for liver-dominant metastatic uveal melanoma: a single center experience. Cancer Imaging, 2019. 19(1): p. 31.
146. Vogel, A., et al., Chemosaturation Percutaneous Hepatic Perfusion: A Systematic Review. Adv Ther, 2017. 33(12): p. 2122-2138.
147. Olofsson, R., et al., Isolated hepatic perfusion as a treatment for uveal melanoma liver metastases (the SCANDIUM trial): study protocol for a randomized controlled trial. Trials, 2014. 15: p. 317.
148. Vaquero-Garcia, J., et al., PRiMeUM: A Model for Predicting Risk of Metastasis in Uveal Melanoma. Invest Ophthalmol Vis Sci, 2017. 58(10): p. 4096-4105.

Chapter 5

General discussion & summary

Chapter 5.1
General discussion

General Discussion

The first observations about uveal melanoma metastasis were made over a century ago by the Austrian ophthalmologist Ernst Fuchs. In 1882 he described the concept of metastatic tropism of the 'sarcom des uveal tractus' to the liver and stated that enucleation was the best treatment[1]. In 1970 Zimmerman, McLean and Foster casted their doubts on the benefit of enucleation and described that other treatment modalities, such as radiotherapy, were also effective[2]. The first metastatic risk predictors were histological features, such as the presence of epithelioid cells and high mitotic count[3]. In 1996 the first genetic predictor of metastasis, loss of chromosome 3, was described by Prescher et al [4]. With the rise of next-generation sequencing techniques, loss of function of the tumor suppressor gene *BAP1* was identified[5] and later on mutations in *SF3B1* were detected in late metastasizing UM[6].

Improving risk stratification in UM patients

Determining metastatic risk by performing BAP1 immunohistochemistry (IHC) is nowadays part of routine UM diagnostics[7, 8]. However, we recently implemented targeted next-generation sequencing in UM diagnostics as well. With this technique, we can stratify patients that have underwent enucleation, endoresection or a prognostic biopsy, in either a low, intermediate or high metastatic risk group by combining mutation and copy number data[9]. Routine UM diagnostics allows us to investigate *BAP1* expression, mutation status and copy number status, thereby providing us with the complete genetic make-up of the tumor. Diagnostic techniques, such as FISH, MLPA and IHC, only look at one feature. These techniques are still useful in UM diagnostics, however the percentage of sensitivity will likely be lower. Since it remains controversial which specific features should be present in UM in order to stratify a patient in the high risk group, it is important that we strive for an universal risk stratification method. The methods used for UM prognostication differ largely between different countries[10, 11]. If future treatment strategies are partially dependent on the risk stratification, a united prognostication model using clinical, histological and genetic parameters should be considered to reliably identify UM patients with high metastatic risk.

A drawback of all of these aforementioned methods is that patients that underwent eye-conserving therapies cannot be prognostically categorized since in general there is no tumor tissue available to perform genetic testing on. Moreover, treatment of the primary tumor by eye-preserving therapies has become increasingly common for small and medium-sized UM. In some cases, patients undergo a biopsy, such as a fine-needle aspiration biopsy or a small incisional biopsy of the tumor. It has been shown that biopsies do not increase the risk of metastasis, however the procedure can have other complications such as retinal detachment, endophalmitis and vitreous bleeding[12-14]. Hence, there is a need for a non-invasive biomarker in blood that allows risk stratification of patients.

Many advances have been made in the field of liquid biomarkers. The employment of circulating fetal DNA in maternal blood to detect chromosomal aberrations of the fetus, set the example for cancer diagnostics[15]. For some cancer types, circulating tumor DNA (ctDNA) harboring a specific mutation is being detected to allow monitoring of the tumor growth and treatment[16-18]. Several groups have investigated ctDNA presence in the blood of UM patients[19-21]. So far, results have been disappointing since ctDNA could not be detected in all metastatic UM patients. Additionally, all of these studies focused on mutations in *GNAQ* and *GNA11*, which hold little prognostic value. It has been shown that tumors need to be a certain size in order to allow ctDNA detection in blood[22]. The amount of ctDNA in blood depends on the tumor size and when the amount of ctDNA is low compared to the total amount of cell-free DNA, it will be hard to distinguish between true mutations and false positives. When there is only one copy of ctDNA mixed with

10.000 copies of normal DNA (0.01%), detection of ctDNA with current technologies is impossible. Most studies that describe detection of ctDNA, show a ctDNA percentage of 0.1% or higher, which corresponds to a tumor with a diameter larger than 27 mm[23]. Since only 2% of the enucleated patients from our cohort had a UM with a basal diameter larger than 20 mm, we hypothesize that with current methods, ctDNA cannot be used to reliably predict prognosis for UM patients.

A more promising approach might be to enrich for tumor DNA or RNA by capturing melanocyte-specific exosomes or circulating tumor cells from blood. If tumor DNA or RNA is specifically extracted from either melanocyte-specific exosomes or circulating tumor cells (CTCs), the percentage of tumor-derived material will be higher and once subjected to ultra-deep sequencing the sensitivity will be much higher. Subsequent detection of an aberrant, BAP1-specific microRNA expression pattern in exosomes or identification of aberrantly methylated DNA in CTCs, will allow risk stratification. Since CTCs originate from the tumor, hypermethylation of the tumor suppressor genes *KLF10*, *GSTP1* and *MEGF10* can be detected in BAP1-negative CTCs. As it has been shown that ctDNA still bears the methylation patterns of its originating cell, aberrant methylation might also be detectable in ctDNA[24]. In the future it may be possible to combine several molecular markers to increase sensitivity. A combination of proteins, aberrant miRNA patterns, aberrant DNA methylation or DNA mutations can be analyzed in order to stratify every UM patient into a certain metastatic-risk group.

Unravelling UM tumorigenesis

Although chromosome 3 loss was shown to be strongly associated with high metastatic risk, it took almost 15 years to identify the responsible tumor-suppressor gene. Identifying particular key genes in the development and progression towards metastasis of UM is an important step, however, this does not mean that the mechanisms that drive UM have been unraveled. Many other processes in the cell contribute to this malignant phenotype, such as epigenetic alterations. The discovery of hundreds of miRNAs which aberrant expression is implicated in tumor phenotypes, has already led to profound changes in our understanding. Yet, these only scratch the surface of the real complexity as microRNAs possess the capacity to target between tens and hundreds of genes simultaneously. We identified a set of microRNAs that show aberrant expression in *BAP1*-mutated UM. Several of these microRNAs have already been identified previously as oncomiRs, however other microRNAs might be more instrumental for UM development. To translate these results into a clinical application, we need to validate our results in larger cohorts before we continue with determining the prognostic and therapeutic value of miRNAs. At this moment, there are no FDA-approved miRNA-based therapeutics being used in the clinic, but several miRNA therapeutics are currently being tested in phase 1/phase 2 clinical trials[25] . These therapies involve small RNA molecules that act as miRNA mimics or inhibitors of miRNAs (antimiRs). One challenge for miRNA-based therapeutics is the delivery of the small RNA molecules. However, with the discovery of several miRNA-delivery vehicles, small RNA molecules can be delivered to specific tissues, which avoids potential toxicities[26]. Once we elucidated which aberrantly expressed miRNAs are essential for the development of metastatic properties in UM, we could either block or stimulate their function by making using of antimiRs or mimics, respectively. Since we identified several known oncomiRs, such as miRNA-17-5p, miRNA-151a-3p, miRNA-21-5p, we can benefit from studies that already investigated the therapeutic potential of these miRNAs[27-29].

Additionally, we identified several functionally significant epigenetic alterations in UM. There are several well-established DNA methylation biomarkers in oncology, such as MGMT for glioblastoma, GSTP1 in prostate cancer[30] and VIM methylation for colorectal

cancer. We identified several aberrantly methylated tumor-suppressor genes specific for high-risk UM; *GSTP1*, *MEGF10* and *KLF10*. This knowledge will not only be useful in the clinic, as it might provide us with a biomarker for high-metastatic risk, but it also leads to new insights into the mechanisms that drive UM carcinogenesis. Our current challenge is to move from demonstrating an association with metastatic disease, to elucidating the etiological role of aberrant DNA methylation in UM. It is currently unclear whether these epigenetic alterations directly provide the tumor cell with oncogenic capabilities or that they simply add to the regulatory circuitry that are already known to be deregulated by gene mutations. The interesting aspect of methylation in cancer is the reversibility of the process. Whereas DNA mutations are set in stone, epigenetic processes have the immense advantage that they can be reversed. Treatment protocols using the two DNA-methylation inhibitors, 5-azacytidine and 5-aza-2'deoxycytidine force cells to return to their normal cell phenotype and have been approved by the FDA for myelodysplastic syndromes and chronic myelomonocytic leukemia treatment[31-33].

Towards reducing UM-metastasis related deaths

Research into the mechanisms that drive carcinogenesis has resulted into a large number of mechanism-based targeted therapies that have shown to be successful in specific cancer types. The efficiency of these targeted therapy depends on the importance of the capability it is targeting[34]. Hanahan and Weinberg described the hallmarks of cancer; six biological capabilities acquired by cells during the development to human tumors. These capabilities enable tumor growth and metastatic outgrowth and include sustained proliferation, induce replicative immortality, avoid growth suppression, resisting cell death, induce angiogenesis, activate invasion and metastasis[35]. If a capability is truly important in a tumor cell, inhibition of this feature should impair tumor growth and progression. Developing a mechanism-based targeted therapy for UM is vital, as metastatic UM is in general incurable. An additional advantage is that most of the targeted therapeutics have in principle, less off-target effects and thus less nonspecific toxicity. In order to develop these therapies, significant advances in our understanding of invasion and metastases need to be made.

Several studies have focused on characterizing the genome of metastatic UM cells. Just like primary UM, metastatic UM show a remarkable low mutational load[36]. Initiating mutations in *GNAQ* or *GNA11* are present throughout the entire tumor, as well as secondary driver mutations in *SF3B1* or *BAP1*. The chromosomal aberrations are similar as well, however the frequencies do change in some cases. One paper described a low percentage of tertiary mutations in oncogenes, such as, *PTEN*, *EZH2* and *TP53*[37]. Since the driver mutations are conserved in metastases and there is no significant increase in genetic instability, it is likely that the metastatic potential of UM is already determined early in the development. It has been shown by Eskelin et al that the tumor metastasizes several years before diagnosis, treatment of the primary tumor will therefore not be enough to prevent metastatic spreading. Thus, future therapies have to focus on removing or delaying the growth of micrometastases while treating the primary tumor simultaneously[38].

It is not entirely known which exact events initiate the malignant potential in UM and this hampers the development of an efficient therapy for metastatic UM. Since primary UM without secondary driver mutations are rare, *GNAQ* and *GNA11* mutations alone are probably insufficient for malignant transformation. Additionally, a study by Shain et al showed that mutations in *GNAQ* and *GNA11* were found in all samples from a given patient, which further confirms that these mutations are an early event[37]. Inhibiting this pathway might therefore reduce the proliferative potential of UM cells, whether they are needed for the malignant properties caused by the secondary driver mutations is unclear.

Since a large majority of the metastatic UM show loss of the tumor suppressor BAP1, the most direct therapy would be to reinitiate the expression of BAP1. Unfortunately, reactivating proteins remains a great challenge in cancer therapeutics. Instead, it might be more promising to use agents that modulate the downstream effect of BAP1. Interestingly, our ROMS cohort contains several patients with a UM that show loss of BAP1, but that remained metastasis-free for over 10 years. Remarkably, patients with a germline BAP1-mutation have a longer DFS than patients with somatic mutations in *BAP1*[39]. This confirms that the metastasis-promoting effect of BAP1 can be modulated by mechanism(s) that temporarily counteract this effect. Whether this is the presence of mutation in *GNAQ* or *GNA11*, upregulation of other pathways, change in methylation or something completely else, is unknown. We have shown for example that *BAP1*-mutated UM displayed a distinct epigenetic profile. Reverting this malignant phenotype by making use of HDAC inhibitors, could be applied to prevent metastatic UM cells from proliferating[40, 41]. Elucidating the mechanisms that contribute to the malignant potential in UM could aid significantly to the development of a therapy for *BAP1*-mutated UM.

Metastatic UM that still show BAP1 expression generally harbor a mutation in a spliceosome gene, such as *SF3B1*, *SRSF2* or *U2AF1*[6, 42] Mutations in these genes do not result in loss of function, but rather a change of function and might therefore require a different approach. Shifting the splicing balance with splicing modulators, such as E7107, has been shown to selectively kill tumor cells with mutations in their splicing machinery. However, this small molecule inhibits both aberrant as canonical splicing and therefore caused considerate side-effects such as loss of vision, due to optic-nerve dysfunction[43]. Interestingly, the new spliceosome modulator H3B-8800 shows increased selectivity for spliceosome-mutant tumor cells, compared to E7107[44] and might therefore be a promising drug for future clinical tests. Another method would be to investigate which genes are mainly affected by aberrant splicing. *SF3B1* is the most commonly mutated spliceosome-gene in cancer and it has been shown that mutant SF3B1 induces aberrant splicing of the tumor-suppressor gene *BRD9*, thereby triggering subsequent degradation of BRD9 mRNA by nonsense-mediated decay[45]. BRD9 is a core component of the BAF nucleosome-remodeling complex, which regulates chromatin remodeling and transcription. Disruption of this tumor-suppressor promotes tumor maintenance and metastatic progression. As preliminary data show different splicing patterns between early and late metastasizing *SF3B1*-mutated UM, we hypothesize that certain mechanisms can reduce the oncogenic effect of mutant SF3B1. If we determine which other affected genes contribute to the development and metastatic spreading of UM and shift the balance towards the canonical mRNA, we potentially could dampen the oncogenic effect of aberrant splicing in tumor cells.

Another approach to target metastatic UM would be to prolong UM latency. Research into the mechanisms that stimulate or prevent metastatic UM cells from expanding might provide us with new targets for future therapies. Borthwick et al performed autopsies on liver specimens of UM patients[46]. Even though these patients had no symptoms of metastatic disease, single cells or small cell clumps were observed in the liver of all patients. Furthermore, it was shown that bone marrow samples contained melanoma cells in some cases, while bone marrow is not a frequent metastatic site for UM. This further supports the concept of early metastatic spreading to several organs, however these metastatic cells are unable to immediately develop metastatic lesions because several mechanisms in these distant organs prevent them from growing. A recent study by Babchia et al showed bidirectional crosstalk between UM cells and hepatic stellate cells influences homing of UM cells to the liver[47]. Co-culturing UM cells with liver cells allows us to study the signals exchanged by different cell types that exist symbiotically within the tumor mass. Describing the intercommunication between these various cell types might help us to understand

which mechanism can suppress or facilitate colonization and growth of metastatic UM cells.

An important mediator of communication between cells are extracellular vesicles, such as exosomes. Exosomes perform intercellular transfer of bioactive molecules, such as RNA, proteins and lipid, both locally as systemically. Recent research has shown that exosomes are considered to be major drivers in the development of a pre-metastatic niche. Tumor cells release vesicles that can help prepare specific recipient organs for metastatic spreading[48, 49]. Exosomes can upregulate pro-inflammatory S100 molecules in distant tissues, thereby creating a local inflammatory microenvironment, one of the basic requirements for the formation of a pre-metastatic niche[50]. In order for circulating tumor cells to colonize, the extracellular matrix needs to be remodeled in pre-metastatic niches. It has been shown that exosomes co-localize with laminin and fibronectin, two factors that increase the adhesion of the extracellular matrix[51]. Another important prerequisite in the pre-metastatic niche is the formation of new blood vessels and increase in vascular permeability, which is also promoted by exosomes[52-54]. Thus, exosomes can contribute to several aspects of the pre-metastatic niche development. Further exploration of the exact function of UM exosomes might allow us to identify mechanisms that could inhibit, prevent or maybe even alter the formation of a pre-metastatic niche and thereby avoid metastatic outgrowth.

Future prospects

In general, most published studies are describing features associated with metastatic UM. Fundamental research is relatively rare in the field of ocular oncology. However, in order to design an effective treatment, a more fundamental understanding of the multiple molecular aberrations in UM is a prerequisite. Elucidating the processes that drive UM development and metastasis will depend increasingly on refined culturing models, such as organoids, and eventually on animal models[55]. Such models will help us to develop comprehensive maps of aberrant signaling networks in UM. Since the UM field is small compared to other cancer types, it is essential that research groups all around the world join forces. An example of such an initiative is the ocular oncology group (OOG), which consists of international research groups that meet and initiate multicenter collaborations. Ideally, there should be collaborations with groups that work on malignancies with a similar genetic background as well, such as *SF3B1*-mutated leukemia and *BAP1*-mutated mesothelioma, since they could provide us with useful knowledge.

In order to develop a more effective and durable therapy for UM, it is important to selectively co-target multiple capabilities because therapeutic treatments can shift the dependence of UM cells to other capabilities. We envision a combination of drugs that target the primary tumor and adjuvant drugs that will prevent distant micrometastases from developing further and thereby improve the survival of patients. This has already proofed its efficacy in breast cancer, where adjuvant therapy is commonly given to every patient, and colon cancer[56-58]. A study by Bol et al, applied dendritic-cell therapy as an adjuvant treatment in patients with *BAP1*-mutated UM[59]. Immunotherapy has been shown to be extremely efficient in cutaneous melanoma, however the results were less exciting in UM, which could be explained by the low mutational load. Therefore, we emphasize that adjuvant treatments should be targeting UM-specific deregulated processed, such as the aberrant miRNA expression or aberrant DNA methylation identified in this thesis (Figure 1).

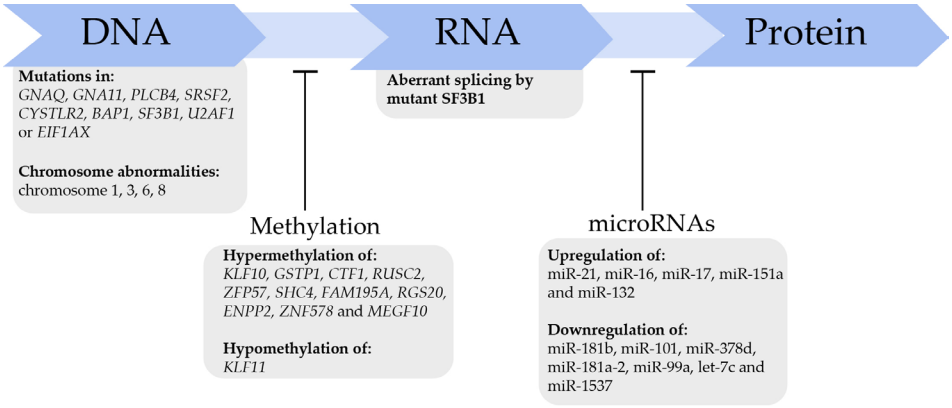

Figure 1. Deregulated processes that contribute to the development and metastasis of UM are found in every level of the central dogma

At present, description of the tumor cell genome of a recently dissected UM is routine procedure and allows UM patients to be prognostically categorized. Nonetheless, the treatment strategies do not differ based on this data. When we look 10 or 20 years ahead of time, the (epi)genetic features present in the UM cells will determine the treatment strategy. We foresee a far deeper insight into the roles played by the mutated genes. By then, the Achilles heel of every UM subtype has been identified and successful treatment have been developed accordingly.

References

1. Fuchs, E., Das Sarkom des Uvealtractus. Graefe's Archiv für Ophthalmologie, 1882(XII): p. 233.
2. Zimmerman, L.E., I.W. McLean, and W.D. Foster, Does enucleation of the eye containing a malignant melanoma prevent or accelerate the dissemination of tumour cells. Br J Ophthalmol, 1978. 62(6): p. 420-5.
3. Seddon, J.M., et al., Death from uveal melanoma. Number of epithelioid cells and inverse SD of nucleolar area as prognostic factors. Arch Ophthalmol, 1987. 105(6): p. 801-6.
4. Prescher, G., et al., Prognostic implications of monosomy 3 in uveal melanoma. Lancet, 1996. 347(9010): p. 1222-5.
5. Harbour, J.W., et al., Frequent mutation of BAP1 in metastasizing uveal melanomas. Science, 2010. 330(6009): p. 1410-3.
6. Yavuzyigitoglu, S., et al., Uveal Melanomas with SF3B1 Mutations: A Distinct Subclass Associated with Late-Onset Metastases. Ophthalmology, 2016. 123(5): p. 1118-28.
7. Koopmans, A.E., et al., Clinical significance of immunohistochemistry for detection of BAP1 mutations in uveal melanoma. Mod Pathol, 2014. 27(10): p.1321-30.
8. Kalirai, H., et al., Lack of BAP1 protein expression in uveal melanoma is associated with increased metastatic risk and has utility in routine prognostic testing. Br J Cancer, 2014. 111(7): p. 1373-80.
9. Smit, K.N., et al., Combined mutation and copy-number variation detection by targeted next-generation sequencing in uveal melanoma. Mod Pathol, 2018. 31 (5): p. 763-771.
10. Damato, B., et al., Estimating prognosis for survival after treatment of choroidal melanoma. Prog Retin Eye Res, 2011. 30(5): p. 285-95.
11. Drabarek, W., et al., Multi-Modality Analysis Improves Survival Prediction in Enucleated Uveal Melanoma Patients. Invest Ophthalmol Vis Sci, 2019. 60(10): p. 3595-3605.
12. Karcioglu, Z.A., R.A. Gordon, and G.L. Karcioglu, Tumor seeding in ocular fine needle aspiration biopsy. Ophthalmology, 1985. 92(12): p. 1763-7.
13. Glasgow, B.J., et al., Quantitation of tumor seeding from fine needle aspiration of ocular melanomas. Am J Ophthalmol, 1988. 105(5): p. 538-46.
14. Bagger, M.M., Intraocular biopsy of uveal melanoma Risk assessment and identification of genetic prognostic markers. Acta Ophthalmol, 2018. 96 Suppl A112: p. 1-28.
15. Chiu, R.W., et al., Noninvasive prenatal diagnosis of fetal chromosomal aneuploidy by massively parallel genomic sequencing of DNA in maternal plasma. Proc Natl Acad Sci U S A, 2008. 105(51): p. 20458-63.
16. Anker, P., et al., K-ras mutations are found in DNA extracted from the plasma of patients with colorectal cancer. Gastroenterology, 1997. 112(4): p. 1114-20.
17. Dawson, S.J., et al., Analysis of circulating tumor DNA to monitor metastatic breast cancer. N Engl J Med, 2013. 368(13): p. 1199-209.
18. Lee, R.J., et al., Circulating tumor DNA predicts survival in patients with resected high-risk stage II/III melanoma. Ann Oncol, 2018. 29(2): p. 490-496.
19. Metz, C.H., et al., Ultradeep sequencing detects GNAQ and GNA11 mutations in cell-free DNA from plasma of patients with uveal melanoma. Cancer Med, 2013. 2(2): p. 208-15.
20. Beasley, A., et al., Clinical Application of Circulating Tumor Cells and Circulating Tumor DNA in Uveal Melanoma. JCO Precision Oncology, 2018(2): p. 1-12.
21. Bidard, F.C., et al., Detection rate and prognostic value of circulating tumor cells and circulating tumor DNA in metastatic uveal melanoma. Int J Cancer, 2014. 134(5): p. 1207-13.
22. Fiala, C. and E.P. Diamandis, Cell-free DNA Analysis in Cancer. N Engl J Med, 2019. 380 (5): p. 501.
23. Fiala, C. and E.P. Diamandis, Utility of circulating tumor DNA in cancer diagnostics with emphasis on early detection. BMC Med, 2018. 16(1): p. 166.
24. Board, R.E., et al., DNA methylation in circulating tumour DNA as a biomarker for cancer. Biomark Insights, 2008. 2: p. 307-19.
25. Hanna, J., G.S. Hossain, and J. Kocerha, The Potential for microRNA Therapeutics and Clinical Research. Front Genet, 2019. 10: p. 478.
26. Rupaimoole, R. and F.J. Slack, MicroRNA therapeutics: towards a new era for the management of cancer and other diseases. Nat Rev Drug Discov, 2017. 16 (3): p. 203-222.
27. Morelli, E., et al., Therapeutic vulnerability of multiple myeloma to MIR17PTi, a first-in-class inhibitor of pri-miR-17-92. Blood, 2018. 132(10): p. 1050-1063.

28. Dhanasekaran, R., et al., Anti-miR-17 therapy delays tumorigenesis in MYC-driven hepatocellular carcinoma (HCC). Oncotarget, 2018. 9(5): p. 5517-5528.
29. Monfared, H., et al., Potential Therapeutic Effects of Exosomes Packed With a miR-21-Sponge Construct in a Rat Model of Glioblastoma. Front Oncol, 2019. 9: p. 782.
30. Cairns, P., et al., Molecular detection of prostate cancer in urine by GSTP1 hypermethylation. Clin Cancer Res, 2001. 7(9): p. 2727-30.
31. Daskalakis, M., et al., Demethylation of a hypermethylated P15/INK4B gene in patients with myelodysplastic syndrome by 5-Aza-2′-deoxycytidine (decitabine) treatment. Blood, 2002. 100(8): p. 2957-64.
32. Fenaux, P., et al., Efficacy of azacitidine compared with that of conventional care regimens in the treatment of higher-risk myelodysplastic syndromes: a randomised, open-label, phase III study. Lancet Oncol, 2009. 10(3): p. 223-32.
33. Garcia-Manero, G., et al., Phase I study of oral azacitidine in myelodysplastic syndromes, chronic myelomonocytic leukemia, and acute myeloid leukemia. J Clin Oncol, 2011. 29(18) :p. 2521-7.
34. Hanahan, D. and R.A. Weinberg, The hallmarks of cancer. Cell, 2000. 100(1): p. 57-70.
35. Hanahan, D. and R.A. Weinberg, Hallmarks of cancer: the next generation. Cell, 2011. 144 (5): p. 646-74.
36. Rodrigues, M., et al., Evolutionary routes in metastatic uveal melanomas depend on MBD4 alterations. Clin Cancer Res, 2019.
37. Shain, A.H., et al., The genetic evolution of metastatic uveal melanoma. Nat Genet, 2019. 51(7): p. 1123-1130.
38. Eskelin, S., et al., Tumor doubling times in metastatic malignant melanoma of the uvea: tumor progression before and after treatment. Ophthalmology, 2000. 107(8): p. 1443-9.
39. Walpole, S., et al., Comprehensive Study of the Clinical Phenotype of Germline BAP1 Variant-Carrying Families Worldwide. J Natl Cancer Inst, 2018. 110(12): p. 1328-1341.
40. Suraweera, A., K.J. O'Byrne, and D.J. Richard, Combination Therapy With Histone Deacetylase Inhibitors (HDACi) for the Treatment of Cancer: Achieving the Full Therapeutic Potential of HDACi. Front Oncol, 2018. 8: p. 92.
41. Landreville, S., et al., Histone deacetylase inhibitors induce growth arrest and differentiation in uveal melanoma. Clin Cancer Res, 2012. 18(2): p. 408-16.
42. Martin, M., et al., Exome sequencing identifies recurrent somatic mutations in EIF1AX and SF3B1 in uveal melanoma with disomy 3. Nat Genet, 2013. 45(8): p. 933-6.
43. Hong, D.S., et al., A phase I, open-label, single-arm, dose-escalation study of E7107, a pre cursor messenger ribonucleic acid (pre-mRNA) splicesome inhibitor administered intravenously on days 1 and 8 every 21 days to patients with solid tumors. Invest New Drugs, 2014. 32(3): p. 436-44.
44. Seiler, M., et al., H3B-8800, an orally available small-molecule splicing modulator, induces lethality in spliceosome-mutant cancers. Nat Med, 2018. 24(4): p. 497-504.
45. Inoue, D., et al., Spliceosomal disruption of the non-canonical BAF complex in cancer. Nature, 2019. 574(7778): p. 432-436.
46. Borthwick, N.J., et al., The biology of micrometastases from uveal melanoma. J Clin Pathol, 2011. 64(8): p. 666-71.
47. Babchia, N., et al., The bidirectional crosstalk between metastatic uveal melanoma cells and hepatic stellate cells engenders an inflammatory microenvironment. Exp Eye Res, 2019. 181: p. 213-222.
48. Grange, C., et al., Microvesicles released from human renal cancer stem cells stimulate angiogenesis and formation of lung premetastatic niche. Cancer Res, 2011. 71(15): p. 5346-56.
49. Costa-Silva, B., et al., Pancreatic cancer exosomes initiate pre-metastatic niche formation in the liver. Nat Cell Biol, 2015. 17(6): p. 816-26.
50. Hiratsuka, S., et al., The S100A8-serum amyloid A3-TLR4 paracrine cascade establishes a pre-metastatic phase. Nat Cell Biol, 2008. 10(11): p. 1349-55.
51. Hoshino, A., et al., Tumour exosome integrins determine organotropic metastasis. Nature, 2015. 527(7578): p. 329-35.
52. Zeng, Z., et al., Cancer-derived exosomal miR-25-3p promotes pre-metastatic niche formation by inducing vascular permeability and angiogenesis. Nat Commun, 2018. 9(1): p. 5395.
53. Pasquier, J., et al., Microparticles mediated cross-talk between tumoral and endothelial

cells promote the constitution of a pro-metastatic vascular niche through Arf6 up regulation. Cancer Microenviron, 2014. 7(1-2): p. 41-59.
54. Kucharzewska, P., et al., Exosomes reflect the hypoxic status of glioma cells and mediate hypoxia-dependent activation of vascular cells during tumor development. Proc Natl Acad Sci U S A, 2013. 110(18): p. 7312-7.
55. Burnier, J.V., et al., Animal models in Uveal Melanoma. Clinical Ophthalmic Oncology, 2019(Springer, Cham): p. 135-154.
56. Romond, E.H., et al., Trastuzumab plus adjuvant chemotherapy for operable HER2-positive breast cancer. N Engl J Med, 2005. 353(16): p. 1673-84.
57. Moertel, C.G., et al., Levamisole and fluorouracil for adjuvant therapy of resected colon carcinoma. N Engl J Med, 1990. 322(6): p. 352-8.
58. Ragaz, J., et al., Adjuvant radiotherapy and chemotherapy in node-positive premenopausal women with breast cancer. N Engl J Med, 1997. 337(14): p. 956-62.
59. Bol, K.F., et al., Adjuvant Dendritic Cell Vaccination in High-Risk Uveal Melanoma. Ophthalmology, 2016. 123(10): p. 2265-7.

Chapter 5.2
Summary

Summary

Uveal melanoma (UM) is an aggressive malignancy arising from the melanocytes present in the uveal tract of the eye. Although it is a relatively rare disease, UM is the most common primary intra-ocular tumor in adults. It is characterized by the frequent development of metastases, which in most cases results in a poor outcome. The metastatic risk varies greatly and depends on primary tumor characteristics. Several cytogenetic and genetic features have been demonstrated to have a strong association with metastatic risk, such as monosomy 3 and mutations in the *BAP1* gene. The majority of the UM show a mutation in *GNAQ* or *GNA11* and these are considered to arise early in the development of UM. In addition, UM often harbor a mutation in *EIF1AX*, *SF3B1* or *BAP1*. Mutations in these so-called secondary driver genes determine the metastatic potential of the tumor. In this thesis we describe new advances in the research into prognostic markers. Furthermore, we investigate the role of epigenetic players, miRNAs and DNA methylation, in UM metastasis. Finally, we discuss future treatments and biomarkers for metastatic UM.

In **chapter 1** the clinical, histological and genetic features of UM is introduced and we highlight the current challenges in the field. In **chapter 2** we focus on predicting the metastatic risk in UM. In **chapter 2.1** a novel, custom-designed sequencing method is described that can simultaneously detect mutations and copy number variations, thereby allowing rapid stratification of UM patients. It shows a good overlap with BAP1 immunohistochemistry, a commonly used technique in UM diagnostics, and has the additional advantage that it can identify late-metastasizing UM patients harboring a *SF3B1*-mutation. Since only a small amount of DNA (~10ng) is necessary, it can also be used for patients that underwent a tumor biopsy. With the development of this new, inexpensive method, we can rapidly identify patients with high metastatic risk and subsequently predict the patients' outcome and in the future potentially asses and stratify eligibility for new treatments. In **chapter 2.2** we describe an association between secondary driver mutations and chromosomal patterns. Copy number analysis by Single Nucleotide Polymorphism-array showed four distinct groups, which corresponded to specific gene mutations. The first group contained the BAP1-negative UM and showed frequent loss of chromosome 3, gain of the chromosome-arms 8q, 6q and loss of the chromosome-arms 1p, 8p and 16q. The second group contained the *SF3B1*-mutated UM and harbored frequent loss of parts of the chromosome-arms 1p, 6q, 8p and 11q and gain of chromosome-arm 8q. The third group consisted of the *EIF1AX*-mutated UM and in this group we observed very little chromosomal abnormalities, apart from gain of chromosome-arm 6p. The fourth group consisted of UM that showed no recurrent mutations (NRM) in *EIF1AX*, *SF3B1* or *BAP1*. These results show that UM with different secondary driver mutations have a distinct biological mechanism contributing to UM pathogenesis. Whether the secondary driver genes mutations cause the chromosomal aberrations or whether it is the other way around is unknown.

The genetic features associated with the development and metastatic spreading of UM are well described and both genetic and epigenetic mechanisms play a role in the development, progression and metastatic spreading of a tumor. In **chapter 3** we aim to elucidate how epigenetic mechanisms, such as altered miRNA expression or methylation changes, contribute to metastatic spreading of UM. **Chapter 3.1** focuses on the potential role of microRNAs in the metastatic spreading of UM. Next-generation RNA sequencing in 26 primary UM revealed differential expression of 13 microRNAs, including the known oncomiR's miRNA-17-5p, miRNA-21-5p and miRNA-151a-3p. The differentially expressed microRNAs corresponded to 106 differentially expressed target genes. These genes were shown to be involved in several cancer-related pathways, such as cell cycle regulation, EGF signaling and EIF2 signaling. By deregulating these pathways

aberrant microRNA expression might thereby promote metastatic spreading to distant organs. The identification of these aberrantly expressed microRNAs might offer an interesting biomarker for UM diagnostics and putative, interesting therapeutic target.

In **chapter 3.2** we look at another important epigenetic feature that is often deregulated in cancer; DNA methylation. The genome-wide methylome of 26 primary UM was analyzed making use of the recently developed method MeD-seq. Regions with differential methylation were observed in all chromosomes, however a large number of differentially methylated regions was found on chromosomes 1, 8, 12 and 16. We found 757 genes to be differentially methylated in UM, of which the majority was found in *BAP1*-mutated UM. *SF3B1*-mutated UM were characterized by a large percentage of hypomethylation, whereas the *EIF1AX* and *BAP1*-mutated UM showed mostly hypermethylation. Interestingly, we observed increased promoter methylation in BAP1-mutated primary UM and UM metastases specimens in the tumor-suppressor genes *MEGF10*, *KLF11* and *GSTP1*. The results obtained in this study could be exploited for therapeutic purposes. Unlike DNA mutations, methylation can be easily reversed by demethylating agents. Removing excessive methylation in UM cells can reactivate tumor-suppressor genes and might thereby reduce proliferation and migration in UM. Whether aberrant methylation arises as a result of mutations in *EIF1AX*, *SF3B1* and *BAP1* or as an independent event early in the oncogenic transformation of melanocytes is unknown. In case of the latter, demethylating agents might strike the Achilles heel of UM.

Although significant advances have been made in UM research, the disease-free survival has remained unchanged the last 35 years. The development of a successful treatment for metastatic UM is vital, as metastatic UM is currently incurable. In addition, it is crucial to develop a biomarker that can predict the metastatic risk in all UM patients, including the ones treated with an eye-preserving therapy. In **chapter 4.1** we describe a potential new non-invasive technique that could improve UM diagnostics. Extracellular vesicles from cultured UM cells are characterized by electron microscopy, western blot and flow cytometry. Our preliminary results indicate that the exosomes secreted by *BAP1*-mutated, high metastatic risk cells showed a higher amount of several miRNAs, including the oncomiRs miRNA-21, miRNA-10B and miRNA-365. To characterize the proteins present on UM exosomes, we performed mass spectrometry on exosomal, membrane proteins. Here we identified several proteins to be present in all exosome samples, such as the classical exosome markers CD81, CD63 and flotillin-1, as well as proteins that are only present in melanocytes. The presence of melanocyte-specific proteins on UM exosomes might allow us to develop a method that can selectively enrich for melanocyte exosomes in plasma. Detecting exosomes with a unique, metastatic uveal melanoma signature could potentially offer us a non-invasive biomarker for metastatic UM.

In order to develop an effective, targeted treatment against metastatic UM, we need to have a more comprehensive understanding of the multiple molecular mechanism that contribute to UM carcinogenesis. In **chapter 4.2** we review the molecular mechanisms behind the known DNA mutations and the therapeutic possibilities that arise from targeting these different aberrant pathways. Several treatments that have shown to be effective in other cancer types, such as immunotherapy and MEK-inhibitors, have been applied on UM as well. So far, the results have been disappointing. We hypothesize that this lack of success can be explained by differences in biological behavior between different cancer types. UM treatment might profit from a more personalized approach in which the genetic background of each UM is investigated and determines the best treatment option.

In **chapter 5** the main results compiled in this thesis are summarized, discussed and where

possible, conclusions are drawn. Finally, challenges for the field and future perspectives are discussed. In conclusion, this thesis provides new insights into the multifaceted epigenetic regulation of uveal melanoma cells. The gained knowledge provides us with a better understanding of the biological processes behind UM which will bring us step-by-step closer to effective treatments.

Chapter 5.3
Samenvatting

Samenvatting

Oogmelanomen zijn tumoren, die ontstaan uit melanocyten die zich in het oog bevinden. Ondanks dat het een zeldzame ziekte is (~7 op 1.000.000), is het de meest voorkomende intra-oculaire maligniteit bij volwassenen. Bij ongeveer de helft van de patiënten metastaseert het oogmelanoom naar andere organen in het lichaam. Aangezien er tot op heden geen succesvolle therapie beschikbaar is voor gemetastaseerde oogmelanomen, leiden metastases vaak binnen een jaar tot de dood. Het risico op metastases wordt bepaald door de afwijkingen, die aanwezig zijn in de primaire tumor. De afgelopen jaren zijn er een aantal (cyto)genetische afwijkingen geïdentificeerd, die sterk geassocieerd zijn met metastasering, zoals verlies van chromosoom 3 en mutaties in het *BAP1* gen. Het merendeel van de oogmelanomen bevat een mutatie in *GNAQ* of *GNA11*, waarvan gedacht wordt, dat deze vroeg in de ontwikkeling van de tumor ontstaat. Daarnaast bevatten oogmelanomen vaak een mutatie in *BAP1*, *SF3B1* of *EIF1AX*. Mutaties in deze zogenoemde secundaire driver genen bepalen of een tumor kan metastaseren. In het eerste deel van dit proefschrift bespreken we de nieuwe ontwikkelingen die bijdragen aan het voorspellen van het risico op metastasen. Vervolgens onderzoeken wij, welke epigenetische afwijkingen aanwezig zijn in metastaserende oogmelanomen. Daarnaast beschrijven we de ontwikkeling van toekomstige niet-invasieve biomarkers en bespreken we welke behandelingsstrategieën het beste zijn voor gemetastaseerde oogmelanomen.

In **hoofdstuk 1** wordt een korte introductie gegeven over de klinische, histologische en genetische eigenschappen van oogmelanomen. Daarnaast benoemen wij de grootste uitdagingen in het veld. Vervolgens gaan wij in **hoofdstuk 2** door met het beschrijven van verschillende ontwikkelingen, die ons kunnen helpen bij het identificeren van patiënten met een hoog risico op metastasen. In **hoofdstuk 2.1** wordt een nieuwe methode beschreven, die gelijktijdig mutaties en chromosoomafwijkingen kan oppikken, waardoor het risico op metastasering bepaald kan worden. Aangezien er maar een kleine hoeveelheid DNA nodig is (~10 ng), kan deze methode ook gebruikt worden voor biopten. Deze techniek is inmiddels al in de routine oogmelanoom-diagnostiek geïmplementeerd en maakt het mogelijk om bij een groot deel van de oogmelanoompatiënten snel en betrouwbaar de prognose te bepalen. In **hoofdstuk 2.2** focussen wij ons op de verschillende chromosoomafwijkingen die voorkomen in oogmelanomen met verschillende mutaties. Eventuele chromosoomafwijkingen worden opgepikt door DNA te analyseren met behulp van een Single Nucleotide Polymorphism (SNP)-array. Op basis van chromosoomafwijkingen kunnen er vier verschillende groepen gemaakt worden, die elk geassocieerd zijn met een specifieke mutatie. De eerste groep omvat oogmelanomen zonder BAP1 expressie met frequent verlies van heel chromosoom 3 en de chromosoom-regio's 1p, 8p 16q en winst van de chromosoom-regio's 8q en 6q. De *SF3B1*-gemuteerde oogmelanomen bevinden zich in groep 2 en laten frequent verlies van de chromosoom-regio's 1p, 6q, 8q en 11q zien. De derde groep bevat de *EIF1AX*-gemuteerde oogmelanomen en deze tumoren laten weinig tot geen chromosoomafwijkingen zien. In de vierde groep zitten oogmelanomen, die geen mutaties hebben in *SF3B1*, *BAP1* of *EIF1AX*. Deze resultaten bevestigen, dat oogmelanomen met verschillende secundaire driver mutaties ook daadwerkelijk een andere biologische achtergrond hebben. Of de secundaire driver mutaties leiden tot deze specifieke chromosoomafwijkingen of dat de chromosoomafwijkingen onafhankelijke gebeurtenissen zijn, die plaatsvinden vroeg in de ontwikkeling van de tumor, is nog niet bekend.

In **hoofdstuk 3** onderzoeken wij epigenetische veranderingen, die plaatsvinden in metastaserende oogmelanomen. Een groot deel van het oogmelanoom-onderzoek focust zich op veranderingen in het DNA zelf, terwijl epigenetische aspecten (d.w.z. veranderingen op of om het DNA, waarbij de DNA-sequentie niet verandert) ook een grote

rol spelen in de ontwikkeling en metastasering van tumoren. **Hoofdstuk 3.1** beschrijft afwijkende expressie van microRNAs in metastaserende oogmelanomen. Met behulp van next-generation RNA sequencing hebben wij 13 microRNAs geïdentificeerd, die afwijkend tot expressie komen in metastaserende oogmelanomen, waaronder een aantal microRNAs waarvan al bewezen is dat ze een rol spelen bij de tumorgenese (bijv. microRNA-17, microRNA-21 en microRNA-151a). Aangezien microRNAs de expressie van bepaalde genen kunnen veranderen door specifieke, complementaire binding aan mRNA, hebben wij de microRNA data gecombineerd met mRNA data. Hierdoor hebben wij 106 genen geïdentificeerd, die afwijkende expressie vertonen. Deze genen zijn betrokken bij verschillende processen, zoals regulatie van de celcyclus, EGF-signalering en EIF2-signalering, waarvan bekend is dat ze vaak gedereguleerd zijn in tumoren. Afwijkende expressie van bepaalde microRNAs kan metastasering van een tumor stimuleren door dit soort essentiële processen te verstoren. In de toekomst kunnen wij wellicht deze afwijkende microRNA-niveaus gebruiken als biomarker. Daarnaast kunnen wij met toekomstige therapieën proberen, deze afwijkende microRNAs weer naar normale niveaus te brengen door ze te remmen of te stimuleren, waardoor gedereguleerde processen in een tumorcel afnemen.

Hoofdstuk 3.2 focust zich op een ander epigenetisch aspect, namelijk DNA methylatie. DNA methylatie kan de transcriptie van genen beïnvloeden doordat de aan het DNA gekoppelde methylgroepen (CH_3) de structuur van het DNA veranderen. Om de DNA methylatie binnen oogmelanomen te analyseren hebben wij gebruik gemaakt van een nieuwe techniek; MeD-seq. Vergeleken met andere technieken, bekijkt MeD-seq een veel groter deel van het genoom. In deze studie hebben wij afwijkende DNA-methylatie gevonden in alle chromosomen, maar vooral in de chromosomen 1, 8, 12 en 16. De *BAP1*-gemuteerde oogmelanomen lieten het hoogste aantal afwijkingen in DNA-methylatie zien. Waar in de *SF3B1*-gemuteerde oogmelanomen vooral hypomethylatie (afname van methylatie in DNA) te zien was, vertoonden de *BAP1*- en *EIF1AX*-gemuteerde oogmelanomen vooral hypermethylatie (toename van methylatie in DNA). Een interessante bevinding was de hypermethylatie in promoteren van de tumor-suppressie genen *MEGF10*, *KLF11* en *GSTP1* in de *BAP1*-gemuteerde oogmelanomen. Aangezien oogmelanomen relatief weinig DNA-mutaties bevatten, kan afwijkende DNA methylatie van genen die de deling, groei en ontwikkeling van een cel beïnvloeden, sterk bijdragen aan de maligne eigenschappen van een tumor. Waar mutaties in het DNA bijna onmogelijk zijn om te corrigeren met therapieën, kan afwijkende DNA methylatie worden teruggedraaid door middel van bepaalde chemische stoffen. Hierdoor kunnen gemethyleerde tumor-suppressie genen weer gereactiveerd worden om zo de celdeling en migratie van tumorcellen te beperken. Het is nog onduidelijk of afwijkende DNA methylatie geïnitieerd wordt door de DNA-mutaties, of dat het een onafhankelijke gebeurtenis is vroeg in de ontwikkeling van de tumor. In het laatste geval zal het corrigeren van DNA methylatie wellicht een effectieve behandelingsstrategie zijn.

De laatste jaren is er veel onderzoek gedaan naar oogmelanomen, wat ertoe geleid heeft, dat onze kennis in dit veld flink gegroeid is. Helaas is de overleving van oogmelanoompatiënten de laatste 35 jaar niet veranderd. Het ontwikkelen van een succesvolle therapie voor gemetastaseerde oogmelanomen is essentieel, aangezien het op dit moment ongeneeslijk is. Daarnaast is het belangrijk om in de toekomst een biomarker in het bloed te identificeren, aangezien we hiermee voor alle patiënten – dus ook de patiënten die behandeld zijn met oog-sparende behandelingen- het risico op metastasen kunnen voorspellen. In **hoofdstuk 4.1** beschrijven wij een potentiële niet-invasieve biomarkers, namelijk exosomen. Oogmelanoom-exosomen werden geanalyseerd met electronen microscopie, western blot en flow cytometry. Vervolgens hebben we ook RNA se-

quencing en mass spectometry uitgevoerd, om de RNA-inhoud en membraan-eiwitten respectievelijk te analyseren. In onze eerste resultaten zien we, dat de exosomen van de *BAP1*-gemuteerde oogmelanoomcellen een specifiek microRNA patroon laten zien. In deze exosomen zien we een verhoogde expressie van bepaalde microRNAs, zoals microRNA-21, microRNA-10B en microRNA-365. Daarnaast hebben wij ontdekt, dat er eiwitten in het membraan van de oogmelanoom-exosomen zitten, die specifiek zijn voor melanocytaire-cellen. Daarom gaan wij uit van de hypothese dat oogmelanoom-exosomen uit het bloed kunnen worden geïsoleerd met behulp van magnetische kralen, die specifiek binden aan de melanoom-eiwitten, waardoor er verrijkt kan worden voor genetisch materiaal, dat afkomstig is van de tumor. Vervolgens kan het RNA-patroon geanalyseerd worden in deze exosomen en kunnen we bepalen of een patiënt een hoog risico *BAP1*-gemuteerde oogmelanoom heeft.

Zodra patiënten met een verhoogd risico geïdentificeerd worden, moet er een efficiënte behandeling kunnen worden aangeboden Voor de ontwikkeling van nieuwe succesvolle therapieën voor de behandeling van metastaserende oogmelanomen, is het belangrijk om een beter begrip te hebben van de verschillende moleculaire mechanismen, die bijdragen aan de metastasering van oogmelanomen. In **hoofdstuk 4.2** beschrijven wij verschillende studies, die onderzoeken welke moleculaire processen er in een cel worden verstoord door mutaties in *GNAQ*, *GNA11*, *SF3B1*, *EIF1AX* of *BAP1*. We bespreken hoe de deregulatie van deze processen kan bijdragen aan de tumorgenese en we benoemen therapeutische strategieën, die eventueel kunnen ingrijpen in deze gedereguleerde processen. Behandelingen die goede resultaten laten zien in andere vormen van kanker hebben geen tot weinig resultaat bij de behandeling van oogmelanoom-patiënten. Deze teleurstellende resultaten kunnen verklaard worden door het feit, dat oogmelanomen een andere biologische achtergrond hebben en daarom dus niet of nauwelijks reageren op deze behandelingen. Daarom benadrukken wij in deze review, dat het essentieel is om een op maat gemaakte behandeling te ontwikkelen bij de behandeling van oogmelanoom-patiënten.

In **hoofdstuk 5** worden de belangrijkste bevindingen van dit proefschrift samengevat en besproken. We benoemen de grootste uitdagingen in het veld en adviseren over de na te streven toekomstige doelen. Kortom, dit proefschrift beschrijft de epigenetische veranderingen, die optreden in metastaserende oogmelanomen en geeft nieuwe inzichten in potentiële niet-invasieve biomarkers en behandelingen voor gemetastaseerde oogmelanomen.

Chapter 6
Epilogue

Chapter 6.1
List of abbreviations

List of abbreviations

AA	amino acid
ABs	apoptotic bodies
ABCC5	multidrug resistance-associated protein 5
ARF6	ADP-ribosylation factor 6
BAP1	BRCA1-associated protein 1
BARD1	BRCA1-associated RING domain protein 1
bp	base pair
BRAF	v-raf murine sarcoma viral oncogene homolog B1
BRCA1	breast cancer 1, early obset
BRD9	bromodomain containing 9
CD	cluster of differentiation
cDNA	copy deoxyribonucleic acid
cfDNA	cell-free DNA
CDK6	cyclin-dependent kinase 6
CM	cutaneous melanoma
CN	copy number
CNV	copy number variation
CpG	cytosine-phosphate-guanine
CTC	circulating tumor cells
ctDNA	circulating tumor DNA
CYSTLR2	cysteinyl leukotriene receptor 2
DC	dendritic cell
DDR	DNA-damage response
DE	differentially expressed
DFS	disease-free survival
DNA	deoxyribonucleic acid
DUB	deubiquitinating enzyme
EIF1AX	eukaryotic translation initiation factor 1A,X-linked
EIF2	eukaryotic initiation factor 2
EGF	epidermal growth factor
EMT	epithelial-mesenchymal transition
ER	endoplasmic reticulum
EV	extracellular vesicle
EZH2	enhancer of zeste homolog 2
FC	fold change
FCS	fetal calf serum
FDA	food and drug administration
FDR	fold discovery rate
FFPE	formalin-fixed, paraffin-embedded
FGF	fibroblast growth factor
FNAB	fine-needle aspiration biopsy
FLOT1	flotillin-1
FISH	fluorescence in situ hybridization
GDP	guanosine diphosphate
GEF	guanine nucleotide exchange factor
GEP	gene expression profile
GNAQ	guanine nucleotide-binding protein G subunit alpha Q
GNA11	guanine nucleotide-binding protein G subunit alpha 11
GP-100	glycoprotein 100
GPCR	G-protein coupled receptor
GPR143	G-protein coupled receptor 143

GSTP1	glutathione S-transferase P 1
GTP	guanine triphosphate
HDAC	histone deacetylase
HLA	human leukocyte antigen
HE	haematoxylin-eosin
IDO	indoleamine-pyrrole 2,3-dioxygenase
IHC	immunohistochemistry
IHP	isolated hepatic perfusion
IP3R3	inositol 1,4,5-triphosphate receptor type 3
IPA	ingenuity pathway analysis
KLF11	krueppel-like factor 11
LC-MS/MS	liquid chromatography-tandem mass-spectrometry
LOH	loss of heterozygosity
MAPK	mitogen-activated kinase
MART-1	melanoma antigen recognized by T cells
mb	megabase
MEGF10	multiple EGF-like domains
MEK	mitogen-activated protein kinase kinase
METC	medical ethical testing committee
miRNA	micro ribonucleic acid
MITF	melanocyte inducing transcription factor
MLPA	multiplex ligation-dependent probe amplification
mRNA	messenger ribonucleic acid
MVs	microvesicles
NGS	next-generation sequencing
NHEJ	non-homologous end joining
NLS	nuclear localisation signal
NMD	nonsense-mediated decay
NRM	no recurrent mutations
N/A	not available
OOG	Ocular Oncology group
PCA	principal component analysis
PCR	polymerase chain reaction
PCLB4	phospholipase C beta 4
PD-1	programmed cell death protein 1
PRAME	preferentially expressed antigen in melanoma
PR-DUB	polycomb respressive deubiquitinase
PTEN	phosphatase and tensin homolog
PVT1	plasmacytoma variant translocation 1
qPCR	quantitative polymerase chain reaction
RIN	RNA integrity number
RISC	RNA-induced silencing complex
RNA	ribonucleic acid
rRNA	ribosomal ribonucleic acid
ROMS	rotterdam ocular melanoma studygroup
RPM	reads per million
RT	room temperature
RT-PCR	real-time polymerase chain reaction
SF3B1	splicing factor 3B subunit1
SNP	single nucleotide polymorphism
SNV	single nucleotide variations
SRSF2	splicing factor, arginine/serine-rich 2

TCGA	The Cancer Genome Atlas
TP53	tumor protein P53
tRNA	transfer ribonucleic acid
TYRP1	tyrosinase-related protein 1
U2AF1	U2 small nuclear RNA auxiliary factor 1
UCH	ubiquitin carboxy-terminal hydrolase
ULD	ubiqituin-like domain
UM	uveal melanoma
WT	wildtype
YAP1	yes-associated protein
YY1	yin yang 1

Chapter 6.2
About the author

About the author

Kyra Noëlle Smit was born on the 8th of May 1990 in Capelle aan den IJssel, The Netherlands. She graduated from secondary school at the Emmauscollege in 2008. After studying one year Liberal Arts and Sciences, she continued to study Biology at the University of Utrecht. During her bachelor, she specialized in molecular biology. In August 2012, she obtained her bachelor degree in biology and then transferred to the Erasmus University in Rotterdam to continue with her master in Molecular Medicine. During her first research internship, she investigated the role of *FOXD1* in chemoresistant melanoma cells under the supervision of Dr. de Keizer at the Department of Molecular Genetics. She performed her second internship at the Department of Immunology where she studied the effect of gut microbiota on the development and reactivity of the adaptive immune system. In September 2014, she started as a PhD candidate at the Departments of Clinical Genetics and Ophthalmology under the supervision of Dr. A de Klein and Dr. E Kiliç. During her PhD, she initiated and executed several projects on uveal melanoma. In 2016, she spent 4 months of her PhD project at the Gothenburg University in Sweden under the supervision of Prof.J. Lötvall to obtain more experience on exosome-isolation techniques. The results of her PhD study are described in this thesis ' Looking beyond genetic alterations in metastatic uveal melanoma'. In April 2020 she started a four-year training at the St. Antonius Hospital (Nieuwegein) to become a Clinical Biochemist.

Chapter 6.3
PhD portfolio

PhD Portfolio

Name PhD candidate:	Kyra Noëlle Smit
PhD period:	2014-2019
Erasmus MC Department:	Clinical Genetics & Ophthalmology
Research school:	Medical Genetics Centre (MGC)
Supervisors:	Dr. A. de Klein & Dr. E Kiliç

PhD Training		**ECTS**
2014	Biochemistry and Biophysics	3
2015	Genetics	3
2015	Safely working in the laboratory	0.3
2015	Basic course on R	2
2015	Ingenuity Pathway Analysis	0.3
2015	Gene expression data analysis using R	2
2016	SNP course	2
2015	Integrity in Science	0.3
2017	CRISPR/Cas9 course	3
2017	Basic course on Statistics	2
2017	NGS course	0.3
2018	Biomedical English Writing and Communication	3
2019	Workshop on InDesign CC	0.3
Seminars and meetings		
2014-2019	Weekly Clinical Genetics research meetings	1
2014-2019	Seminars at the Department of Clinical Genetics	1
2017-2019	Journal club at the Department of Clinical Genetics	1
(Inter)national conferences		
2014	MGC annual meeting	0.3
2015	Cancer Genomics Congress	0.3
2015	Annual Meeting Ophthalmic Oncology Group (Moscow)**	1
2015	DOPPS*	1
2015	Genetics Retreat (Rolduc)**	1
2015	miRNA Keystone Conference*	3
2016	Annual Meeting Ophthalmic Oncology Group (Athens)**	1
2016	Meeting International Society for Extracellular Vesicles	2
2017	Annual Meeting Ophthalmic Oncology Group (Rotterdam)**	1
2017	Genetics Retreat (Rolduc)**	1
2017	MGC PhD workshop (Dortmund) *	2
2018	Annual Meeting Ophthalmic Oncology Group (Siena)**	1
2018	MGC PhD workshop (Leuven) **	2
2018	Extracellular Vesicles Keystone Conference*	3
2018	MGC annual meeting**	0.3
2019	Meeting Ophthalmic Oncology Group (London)**	1
2019	Welcome Genome Course; CRISPR and Beyond (Cambridge)	1

** Poster presentation; ** Oral presentation*

Teaching activities		
2015	Supervision Junior Med School students	1
2015-2016	Supervision HLO student Stanley van Herk	2
2017-2018	Supervision MSc student Emma Schmeitz	2

2018-2019	Supervision MSc student Begüm Kayhan	2

Awards and Funds

2016	Best Talk at the Annual Meeting of the OOG
2016	Nelly Reef Travel Fund (€2000)
2016	Donders Fund (€2000)
2017	Best Talk at the MGC PhD workshop
2017	Co-applicant Bayer Ophthalmic Research Award (€25.000) 'Classifying UM patients based on exosomal tumor DNA'
2017	Co-applicant Uitzicht Fund (€20.000) 'Exploring the use of exosomes as non-invasive biomarker'
2018	Co-applicant Uitzicht Fund(€40.000) 'Unravelling the multifactorial role of BAP1 in UM metastasis'

Other academic activities

2015 - 2019	Member PhD committee Erasmus MC
2017	Organizing committee Annual Meeting OOG
2018	Female Talent Class, Erasmus MC

Total ECTS	**48.4**

Chapter 6.4
List of publications

List of publications

Smit KN, Boers R, Vaarwater J, Boers J, Brands T, Mensink H. Novel DNA-methylation silenced tumor suppressor genes identified for BAP1-mediated uveal melanoma metastasis. Cell Oncol. *Submitted*

Smit KN, Jager MJ, de Klein A, Kilic E. Uveal melanoma: Towards a molecular understanding. Prog Retin Eye Res. 2019:100800.

Smit KN, Chang J, Derks K, Vaarwater J, Brands T, Verdijk RM, et al. Aberrant MicroRNA Expression and Its Implications for Uveal Melanoma Metastasis. Cancers (Basel). 2019;11(6).

Smit KN, van Poppelen NM, Vaarwater J, Verdijk R, van Marion R, Kalirai H, et al. Combined mutation and copy-number variation detection by targeted next-generation sequencing in uveal melanoma. Mod Pathol. 2018;31(5):763-71.

Yavuzyigitoglu S, Mensink HW, **Smit KN**, Vaarwater J, Verdijk RM, Beverloo B, et al. Metastatic Disease in Polyploid Uveal Melanoma Patients Is Associated With BAP1 Mutations. Invest Ophthalmol Vis Sci. 2016;57(4):2232-9.

Yavuzyigitoglu S, Drabarek W, **Smit KN**, van Poppelen N, Koopmans AE, Vaarwater J, et al. Correlation of Gene Mutation Status with Copy Number Profile in Uveal Melanoma. Ophthalmology. 2017;124(4):573-5.

van Poppelen NM, Yavuzyigitoglu S, **Smit KN**, Vaarwater J, Eussen B, Brands T, et al. Chromosomal rearrangements in uveal melanoma: Chromothripsis. Genes Chromosomes Cancer. 2018;57(9):452-8.

van Poppelen NM, Drabarek W, **Smit KN**, Vaarwater J, Brands T, Paridaens D, et al. SRSF2 Mutations in Uveal Melanoma: A Preference for In-Frame Deletions? Cancers (Basel). 2019;11(8).

Grosserichter-Wagener C, Radjabzadeh D, van der Weide H, **Smit KN**, Kraaij R, Hays JP, et al. Differences in Systemic IgA Reactivity and Circulating Th Subsets in Healthy Volunteers With Specific Microbiota Enterotypes. Front Immunol. 2019;10:341.

Drabarek W, Yavuzyigitoglu S, Obulkasim A, van Riet J, **Smit KN**, van Poppelen NM, et al. Multi-Modality Analysis Improves Survival Prediction in Enucleated Uveal Melanoma Patients. Invest Ophthalmol Vis Sci. 2019;60(10):3595-605.

Cunha Rola A, Taktak A, Eleuteri A, Kalirai H, Heimann H, Hussain R, Bonnett LJ, Hill CJ, Traynor M, Jager MJ, Marinkovic M, Luyten GPM, Dogrusöz M, Kilic E, de Klein A, **Smit KN**, van Poppelen NM, Damato BE et al. Multicenter External Validation of the Liverpool Uveal Melanoma Prognosticator online: An OOG Collaborative Study. Cancers (Basel). 2020; 12(2).

Chapter 6.5
Acknowledgements

Dankwoord

Na 5 jaar onderzoek te hebben gedaan ben ik dan eindelijk toegekomen aan het schrijven van mijn dankwoord! Ik had mijn proefschrift nooit kunnen afmaken zonder de hulp van veel verschillende mensen en daar wil ik op de laatste bladzijdes van mijn proefschrift graag even bij stilstaan.

Allereerst wil ik mijn begeleiders Dr. de Klein en Dr. Kiliç bedanken. Annelies, wat voel ik me vereerd dat ik als eerste onder jou mag promoveren! Ik kon altijd bij jou binnenlopen met vragen en als ik soms even niet wist hoe ik verder moest met mijn onderzoek kon jij altijd alles relativeren en had je direct een antwoord klaar. (Al geloof ik graag dat ik in mijn laatste jaar ook wel een aantal vragen heb weten te stellen, waar je niet direct een antwoord op had). Emine, ik ben ontzettend blij dat ik ook een klinische begeleider had, die ik altijd kon benaderen met vragen. Al vanaf het begin van mijn PhD heb ik met veel bewondering toegekeken hoe jij onderzoek en kliniek combineert (daarvoor was ik altijd in de veronderstelling dat deze combinatie onmogelijk was). Tijdens mijn gehele PhD heb je me gestimuleerd om als wetenschapper te groeien; je had genoeg vertrouwen in mij om mij nieuwe projecten te laten starten en betrok me bij de fondsaanvragen. Daarnaast heb ik het geluk om een derde vrouwelijke (co)-promoter te hebben; dr. Mensink. Hanneke, hartstikke bedankt dat je mijn co-promoter wil zijn! Ik denk dat de samenwerking met het OZR heel waardevol is. Zonder deze goede samenwerking hadden we een stuk minder materiaal gehad en had mijn PhD (nog) langer geduurd.

De leden van de kleine commissie; Prof.dr. Hofstra, Prof.dr. Martens en dr. Kiilgaard, wil ik graag bedanken voor de tijd die ze gestoken hebben in het lezen van mijn proefschrift en voor hun bereidheid om in mijn leescommissie plaats te nemen. Dr. Kiilgaard, dear Jens, when we were brainstorming about which international committee member we should ask, I immediately knew we had to ask the person that manages to ask difficult questions at every meeting of the OOG! Thank you for taking the time to be a part of my committee, I look forward to hearing your questions. Daarnaast wil ik graag Prof.dr. Vingerling, Prof. Dr. Zwarthoff en Prof.dr. Paridaens hartelijk bedanken voor hun deelname in mijn grote commissie.

Dan natuurlijk mijn twee paranimfen; Jolanda en Natasha! Jolanda, ik ben heel blij dat ik gedurende mijn gehele PhD jou achter me had zitten (letterlijk en figuurlijk). Als ik het even niet meer zag zitten, wist jij altijd alles in perspectief te zetten en mij gerust te stellen. Naast het feit dat we goed kunnen samenwerken, vond ik het ook altijd heel gezellig om met je praten over van alles en nog wat. Of we nou op een foute glitterpartyboot in Rusland zaten of hongerig waren tijdens een oneindige museumtour in Italië, overal konden we ons goed vermaken. Natasha, wat was ik blij toen jij in onze groep kwam werken. Er zijn maar weinig mensen op deze wereld, die na een wetenschappelijk praatje zich afvragen welk type bloedbuizen er gebruikt werd voor de isolatie van celvrij DNA en vervolgens zich daarna ook meteen afvragen waar degene die haar praatje hield haar laarzen zou hebben gekocht. Ik prijs mezelf gelukkig dat ik met zo'n breed geïnteresseerd persoon heb mogen samenwerken!

Marjolein, mijn researchproject bij de moleculaire genetica heeft mij niet alleen wetenschappelijke kennis opgeleverd, maar ook een hele goede vriendin! Ondanks dat we niet meer in hetzelfde ziekenhuis werken (al kom ik binnenkort achter je aan!), stond je altijd klaar om te helpen met nieuwe technieken of luisterde je mijn PhD-problemen geduldig aan. Dit was echt heel belangrijk voor mij, dus dankjewel hiervoor! Liza, alweer 7 jaar geleden ontmoeten wij elkaar tijdens de ESN-introductie dagen. Ik was heel blij dat ik een gezellige Brabantse naast me had tijdens mijn Master en mijn onderzoekstage bij de Immunologie. Heel veel succes met het afronden van je PhD en

ik hoop nog vele gezellige etentjes, borrels en koffie-dates met je te hebben!

De 16.10 groep; Wojtek, Daniel, Anass, Josephine, Jackelien, Jan-Roelof, Magda, Serdar en Annelien bedankt voor al jullie gezelligheid en hulp! Serdar, bedankt voor al je hulp tijdens de start van mijn PhD en voor alle levendige discussies. Wojtek, ik kan me voorstellen dat je het in het begin wat zwaar had in een groep met drie vrouwelijke collega's die allen een vrij sterke mening hadden en het vaak met elkaar eens waren. Maar je hebt je goed staande gehouden en je uiteindelijk als aberrant RNA-expert in de groep weten te ontwikkelen! (al was ik het meest jaloers op jouw expertise in Rotterdamse horeca). Anass, ik hoop dat je je niet al te eenzaam hebt gevoeld als enige niet-oogmelanoom onderzoeker in de groep! Heel veel succes met het afronden van je project! Daniel, jij hebt de eervolle taak gekregen om het niet-invasieve onderzoek in de groep voort te zetten. Ondanks dat ik wellicht een lichte vlaag van jaloezie zal ervaren, hoop ik oprecht dat jij het voor elkaar krijgt om dit project af te ronden! (ik kan mezelf altijd troosten met het feit dat ik sneller kan fietsen). Josephine, ik heb helaas niet heel lang met je mogen samenwerken maar ik wens je heel veel succes met je verdere onderzoek! Elisa, even though you only worked in our group for a couple of months, I will never forget about you because you are the only colleague that gave me cookies and wine after work (although I am still not fully convinced about that specific combination). I really enjoyed working together with you on the exosome project!

De andere helft van onze groep op 20 kan ik natuurlijk ook niet vergeten; Bert, Tom, Hannie, Frank, Beau en Evelien! Bedankt voor jullie hulp en gezelligheid tijdens meetings, etentjes en borrels. Evelien, ik weet uit ervaring dat het soms al best lastig is om op 2 afdelingen werkzaam te zijn, maar jij deed hier nog een stapje bovenop met 3 verschillende afdelingen. Bedankt dat je ons introduceerde in hippe vegan tentjes en voor alle gezelligheid. Heel veel succes met de laatste loodjes! Bert; bedankt voor al je hulp bij Filemaker-gerelateerde zaken! Ik hoop dat ik je niet te veel frustratie opgeleverd heb als ik weer eens vroeg om een extra veld zodat ik mijn plasmide DNA zonder reference genome kon invoeren. Tom, bedankt voor de enorme aantallen donut-plots die je voor mij gemaakt hebt! Frank; elke groep heeft een persoon nodig die orde schept in de chaos en ik denk dat wij heel veel geluk hebben met jou! Sinds jij in onze groep werkt hebben we flessen (en koelkasten!), die netjes gelabeld zijn en hebben we werkende templates. Bedankt hiervoor! Erwin, je zit niet fulltime op 20, maar je hoort natuurlijk wel bij onze groep! Het is jammer dat je pas in de laatste maanden van mijn PhD in onze groep bent gekomen, het is namelijk altijd fijn om iemand in de groep te hebben die veel labkennis heeft. Heel veel succes met het voortzetten van het oogmelanoom-onderzoek (en sorry dat ik het ML2 lab 'soms' vergat).

Ik wil daarnaast ook graag mijn studenten bedanken. Stanley, Emma en Begum jullie hadden allemaal nieuwe projecten, die vrij lastig waren (celvrij DNA, exosomen en CRISPR/Cas9), maar jullie hebben stug doorgewerkt en stuk voor stuk een mooi verslag ingeleverd! Heel veel succes met jullie toekomstige baan!

Dr. Verdijk, beste Rob, hartelijk dank voor al je hulp en expertise bij alle pathologie gerelateerde zaken! Dr. Dubbink en Ronald van Marion, bedankt voor al jullie hulp bij het schrijven van het Iontorrent paper. Dr. Naus, beste Nicole, dankzij jouw hulp vanuit de kliniek hadden we altijd meer dan genoeg samples voor ons onderzoek. Hartelijk dank hiervoor!

Collega's van de 20ste; bedankt voor jullie hulp bij onder andere het sequencen. Als ik op de 24ste vragen had over celkweek, qPCR en andere lab-gerelateerde zaken kon ik altijd even binnenlopen bij de functionele unit. Hannie, Mark, Leontine, Marianne en Peter;

dank voor al jullie advies!

I would also like to thank everybody from the 9th floor for adopting me in their lab! Guido, Bianca, Herma, Rachel, Lies-Anne; bedankt dat jullie me hielpen als ik weer eens iets niet kon vinden in het lab. Ofcourse all the colleagues from the Clinical Genetics; Laura, Fenne, Katherine, Rob, Elena, Maria, Chantal, Nynke, Roy, Anita, Alessandro, Eva, Rodrigo, Pablo, Mike, Laura, Atze, Ana, Yuying, Jonathan, Stijn, Fabio, Ellis, Daphne, Martyna, Saif; it was a privilege working with such fun, open, intelligent and motivated people! The MGC-workshops, lab-drinks and picnic in the park were always a lot of fun! Gerben, hartelijk dank voor je hulp bij het opzetten van mijn exosomen flow cytometry experimenten! Prof.dr. Willemsen, beste Rob, bedankt voor alle mooie EM plaatjes!

En natuurlijk ook de PhD-studenten en AIO's van de Oogheelkunde; de EMCRO is helaas een stille dood gestorven, maar het was altijd gezellig om even met jullie te kletsen als ik jullie tegen kwam op de poli, bij het koffiezetapparaat of in de gangen! Nicole van Basten, bedankt voor je hulp als er weer eens iets geregeld moest worden met PSA!

Veel projecten had ik niet kunnen uitvoeren zonder hulp vanuit andere afdelingen. Prof. dr. Joost Gribnau en Ruben, hartelijk dank voor jullie hulp bij het methylatie-project! Ik had in het begin geen idee wat ik met de data aan moest, maar dankzij jullie hulp begon ik steeds meer plezier te krijgen in de analyse en hebben we er mooie resultaten uit weten te halen! Fabian, thanks for all the help and advice you gave me during my PhD. I am convinced your PAX5 article will end up in a high impact journal! Kasper, Chang en Joris Pothof, thanks for helping me finish the neverending miRNA-manuscript! Prof.dr. Martine Jager, het duurde allemaal iets langer dan we gedacht hadden, maar ik denk dat we uiteindelijk een heel mooie review hebben weten te publiceren. Hartelijk dank voor al je input en hulp! Voor alle ICT-gerelateerde problemen kon ik altijd terecht op de 7de; bedankt hiervoor! Tom de Vries Lentsch; hartelijk dank voor je hulp bij de lay-out van mijn boekje.

Ofcourse I would also like to thank my colleagues from Sweden! Jan, thanks for giving me the opportunity to work in your lab. I was a complete newbie in the field of extracellular vesicles, but you were immediately enthusiastic about a collaboration and welcomed me in your lab. Taral, Su Chul, Cecilia, Ganesh, Aleksander, Rossella, Kristina, Nasibeh ! I have to admit that I definitely underestimated the Swedish winter (so cold and so dark!), but the fun I had at work and at conferences really made up for that. Taral, thanks for teaching me everything about exosomes (and for giving me the best Indian meal I had in my life!).

Steve, thanks for taking the time to correct my review. I am still very much impressed that an engineer knows the difference between RNA and DNA. Another engineer that now knows the difference between RNA and DNA; Pete! It took me five years to slightly understand cancer, but I am convinced you can solve it in less! Naomi en Amber, ik prijs mezelf gelukkig met twee van zulke slimme, leuke en lieve zussen! Jullie laten mij allebei zien dat het hebben van een gezin goed te combineren is met een carrière.

Lieve pap, mam jullie staan altijd voor mij klaar en tonen altijd interesse in mij (en soms zelfs ook in mijn onderzoek). Zonder jullie onvoorwaardelijke steun en vertrouwen was ik waarschijnlijk nooit zo ver gekomen. Ontzettend bedankt voor alles!